

Attempts Toward An Improved Synthesis of Aza-Dipyrrins

by

Rosinah Liandrah Gapare

Submitted in partial fulfilment of the requirements for
the degree of Doctor of Philosophy

at

Dalhousie University
Halifax, Nova Scotia
July 2023

Dalhousie University is located in Mi'kma'ki,
the ancestral and unceded territory of the
Mi'kmaq. We are all Treaty people.

© Copyright by Rosinah Liandrah Gapare, 2023

DEDICATION

To my children and all the African young women in a dark place with no hope of a better tomorrow. If I could do it, SO CAN YOU.

TABLE OF CONTENTS

DEDICATION	ii
LIST OF TABLES	v
LIST OF FIGURES	vi
LIST OF SCHEMES	viii
ABSTRACT	xi
LIST OF ABBREVIATIONS USED	xii
ACKNOWLEDGEMENTS	xv
Chapter 1 - Introduction	1
1.1- Pyrrole.	1
1.2 - Dipyrrins and Aza dipyrrins.	3
1.3 - <i>F</i> -BODIPYs and aza BODIPYs.	7
1.4 - Thesis Overview.	9
Chapter 2: Attempts Towards an Economic Synthesis of <i>F</i> -BODIPYS.	10
2.1 – Introduction.	10
2.2 – Synthetic strategy.	11
2.2 - Continuous flow process.	12
2.3 - Project Goals.	13
2.4 - Results and Discussion	14
2.4.1 - Reaction Optimization and Understanding of Batch Operation.	14
2.4.2 - Reaction Optimization in Flow Operation.	18
2.5 - Hydrogen fluoride scavengers	22
2.6 - Effect of solvent and temperature on the reaction.	26
2.7 - Conclusion.	31
2.8 – Experimental	32
Chapter 3 – Towards an Improved Synthesis of Aza Dipyrrins.	35
3.1 - Introduction.	35
3.2 - Synthesis of aza BODIPYs.	37
3.3 - Project goals	44
3.4 - Synthetic strategy for aza dipyrrins.	45
3.5 - Exploration of the proposed strategy.	48

3.6 - Future Work.....	62
3.7 - Experimental.....	62
Chapter 4 – Attempted PPh ₃ -Mediated C–N Coupling of Nitrosoarenes.	68
4.1 - Introduction	68
4.2 - Project Goals	73
4.3 - Results and Discussion.	74
4.3.1 - Attempted coupling of nitropyrroles with boronic acids using Radosevich catalyst.	74
4.3.2 - Attempted visible light and coupling of nitroso pyrroles.....	80
4.3.3 - Attempted PPh ₃ /NaI photochemical reduction of nitroso pyrroles under blue LED irradiation.....	85
4.3.4 - An alternative route to α -nitroso pyrroles.	91
4.4.1 - Conclusion.....	109
4.4.2 - Future work	110
4.5 - Experimental.....	112
Chapter 5 - Substitution at Boron in BODIPYs.	136
Chapter 6 – Conclusions.....	160
Chapter 2 - Conclusion.	160
Chapter 3 - Conclusion.	161
Chapter 4 - Conclusion.	161
Chapter 5 - Conclusion.	162
References.....	163
Appendix A.....	182
Appendix B: X-Ray Crystallographic Analysis Data.	183
Appendix C: NMR data for synthesized compounds.	188

LIST OF TABLES

Table 1: Batch process optimization.....	18
Table 2: Optimization of the continuous flow process.	20
Table 3: Synthesis of F-BODIPY in the presence of HF scavengers	24
Table 4: Screening of different reaction conditions for the synthesis of F-BODIPYs.	27
Table 5: Synthesis of F-BODIPYs using 1 equiv BF ₃ .OEt ₂	29
Table 6: Comparison of the synthesis of F-BODIPY	32
Table 7: Attempts to reduce the nitro group in nitrobutanone 3.27b.....	55
Table 8: Optimization of Nitrosylation reaction of 3.28 to 4.40..	94

LIST OF FIGURES

Figure 1: Structure and numbering of pyrrole.	1
Figure 2: Electrophilic addition of electrophiles to pyrrole and benzene.	2
Figure 3: Numbering system for dipyrrens (left) and aza dipyrren core (right).	4
Figure 4: Complexation of dipyrrens to different types of elements.	6
Figure 5: Structure and IUPAC labelling of F-BODIPYs.	7
Figure 6: A generic continuous flow set-up.	13
Figure 7: Stream-flow mechanism in a continuous flow operation.	14
Figure 8: ¹ H-NMR (CDCl ₃) spectra with benzene as an internal standard.	17
Figure 9: Lab-scale flow reactor setup.	19
Figure 10: Relationship between flow rate and product yield.	21
Figure 11: Structures of F-BODIPY, aza dipyrren and aza F-BODIPY cores.	36
Figure 12: Conformationally restricted β,β aza dipyrrens 3.7 and β,α aza dipyrren.	39
Figure 13: Chemical structure and photophysical properties.	41
Figure 14: Hypothetical exclusively alkyl-substituted aza dipyrren.	42
Figure 15: Target aza dipyrren for proof of concept via synthesis of imide.	48
Figure 16: ORTEP diagram of ester 3.31.	51
Figure 17: ORTEP diagram of ester alcohol.	54
Figure 18: ORTEP diagram of amide 3.35 with solvent.	57
Figure 19: Classic C-N coupling protocols.	70
Figure 20: Reductive C-N coupling (PIII/PV) redox catalysis.	71
Figure 21: Organophosphorus-Catalyzed Reductive C-N Coupling	72
Figure 22: Proposed coupling of nitropyrrole and boronic acid.	74
Figure 23: Proposed reaction sequence to form azoxy-bis pyrrole.	83
Figure 24: Synthesis of chalcones 4.42 (a-I)	97
Figure 25: Synthesis of nitrobutanones 4.43 (a-I) from chalcones 4.42.	98
Figure 26: Synthesis of pyrroles 4.44 from nitrobutanones 4.43.	99
Figure 27: Synthesis of aryl- nitroso pyrroles on a variety of pyrrole substrates.	100

Figure 28:: Failed attempted nitrosylation of pyrroles.	101
Figure 29: OTREP diagram of pyrrole 4.49..	104
Figure 30: ¹ H NMR spectrum of pyrrole 4.51.	105
Figure 31: ¹ H NMR spectrum of compound 4.54.....	107
Figure 32:TLC analysis of the reaction of 4.51.	108
Figure 33: Core frameworks of pyrrole, dipyrin, F-BODIPY and aza-dipyrin.	138
Figure 34: Two commercially available BODIPY probes used in molecular	140
Figure 35: ORTEP diagram of ester 3.31..	183
Figure 36: ORTEP diagram of alcohol.	184
Figure 37:	186

LIST OF SCHEMES

Scheme 1: Synthetic strategies to dipyrrens.....	5
Scheme 2: Synthetic strategies to F-BODIPYs.	8
Scheme 3: Addition of $\text{BF}_3 \cdot \text{Et}_2\text{O}$ (1 equivalent) to free-base 2.1 in toluene.....	11
Scheme 4: Synthesis of pyrrole 2.4.	15
Scheme 5: Synthesis of free base dipyrren 2.1.....	15
Scheme 6: Synthesis of aza dipyrrens 3.3a, 3.3b and aza BODIPY 3.4.....	37
Scheme 7: Synthesis of conformationally restricted aza dipyrrens.....	40
Scheme 8: Synthesis of alkyl-substituted aza BODIPY 3.19.	43
Scheme 9: Retrosynthetic analysis of tetraaryl aza dipyrren 3.3a.....	46
Scheme 10: Proposed synthesis of aza dipyrrens 3.3a via imide 3.22a.	48
Scheme 11: Attempted coupling of oxoacid and oxoamine to amide.	49
Scheme 12: Attempted protection of nitrobutanone 3.27b by the gen 3.29.	50
Scheme 13: Synthesis of active ester 3.31.....	51
Scheme 14: Attempted synthesis of amide.....	52
Scheme 15: Reduction of nitrobutanone to nitrobutanol and compound.	53
Scheme 16: Reduction of nitobutanone 3.27b to pyrroline 3.34.	56
Scheme 17: Attempted coupling of the nitrobutanone and active ester.	57
Scheme 18: Proposed route to 3.22b, with the late-stage installation of the ketone.	59
Scheme 19: Attempted coupling of nitrobutanol 3.32 and active ester 3.31.....	60
Scheme 20: Proposed strategy for the synthesis of amide.....	61
Scheme 21: Cyclization of acid chloride furanol.....	61
Scheme 22: Proposed synthesis of imide via coupling of phosphinimidic amide.....	62
Scheme 23: Suggested mechanistic pathway for the formation of aza dipyrrens.	69
Scheme 24: Synthesis of diphenyl nitropyrrole 4.7a.....	75
Scheme 25: Attempted coupling of diphenyl nitropyrrole and boronic acid.....	76
Scheme 26: Coupling of nitrobenzene 4.4 with boronic acid.....	77
Scheme 27: Reaction of boronic acids with nitro (hetero)arenes.	78

Scheme 28: Synthesis of N-methyl protected diphenyl nitroso-pyrrole 4.21.....	79
Scheme 29: Attempted coupling of N-methyl nitroso-pyrrole with boronic acid.	80
Scheme 30: A: Photochemical PPh ₃ -mediated coupling of nitrobenzene.	81
Scheme 31: Attempted photochemical PPh ₃ -mediated coupling of nitroso pyrrole.....	82
Scheme 32: TM-catalyzed reduction of nitroso pyrrole.	86
Scheme 33: A: NaI/PPh ₃ -mediated photochemically reductive amination.	87
Scheme 34: Synthesis of aza dipyrin via NaI/PPh ₃ -mediated amination.	88
Scheme 35: Attempted nitrosylation of alkyl-substituted pyrroles.	90
Scheme 36: Use of leaving groups for aryl nitrosylation using NOBF ₄	92
Scheme 37: Proposed nitrosylation of pyrroles using NOBF ₄ salt.....	92
Scheme 38: Attempted nitrosylation of dimethyl pyrrole 4.45.	102
Scheme 39: Synthesis of hydroxyl intermediate.	103
Scheme 40: Attempted protonation of hydroxyl intermediate 4.48.	103
Scheme 41: Attempted nitrosylation of pyrrole 4.51.....	104
Scheme 42: Attempted synthesis of aza dipyrin from the second addition.....	106
Scheme 43: Synthesis of N-hydroxyl intermediate 4.54.	107
Scheme 44: Attempted synthesis of aza-F-BODIPY 4.55 from 4.51.....	108
Scheme 45: The proposed pathway to the pyrrole-based azoxy compounds.	111
Scheme 46: Synthesis of the first F-BODIPYs.....	139
Scheme 47: Synthetic approaches to F-BODIPYs.	141
Scheme 48: Microwave-assisted deborylation of F-BODIPYs.	144
Scheme 49: Synthesis and use of Li dipyrinato salts.	145
Scheme 50: Synthesis of first dipyrinato boronium salts.....	147
Scheme 51: Synthesis of Cl-BODIPYs	148
Scheme 52: Chelated O-BODIPY utilizing Cl-BODIPY as a synthetic	150
Scheme 53: BCl ₃ -activated synthesis of COO-BODIPYs from F-BODIPY.....	151
Scheme 54: Synthesis of N-BODIPY via BCl ₃ activation of F-BODIPY.....	152
Scheme 55: Glycine-based N,O-aza-BODIPY via Cl-aza-BODIPY.	152
Scheme 56: BODIPY-sugar conjugates utilizing Cl-BODIPY as synthetic	153
Scheme 57: Deprotection of F-BODIPYs via Cl-BODIPYs.....	154

Scheme 58: Synthesis of prodigiosenes using F-BODIPYs as protected.....	155
Scheme 59: Activation and deprotection of F-BODIPYs using $\text{BF}_3 \cdot \text{OEt}_2$	157
Scheme 60: Synthesis and utility of Cl-aza-BODIPYs.	157

ABSTRACT

Compounds built on the 4,4-difluoro-4-bora-3a,4a-diaza-*s*-indacene (*F*-BODIPY) framework have a wide range of uses stemming from their highly tunable electronic properties. The versatility of this class of compound affords them applications as probes in biological systems and as dyes. Aza-dipyrrins and respective boron compounds (aza-BODIPYs) are direct analogues of BODIPYs in which a carbon *meso*-atom is replaced with nitrogen. This change leads to a large red-shift in their absorption spectra making these compounds effective for applications such as biological imaging and photodynamic therapy (PDT). This thesis aims to develop new methodologies for the effective, eco-friendly and cost-effective synthesis of *F*-BODIPYs and aza-BODIPYs. Attempts to avert the challenges faced by the current synthesis of *F*-BODIPYs are described. These involve using only 1 equiv. of $\text{BF}_3 \cdot \text{Et}_2\text{O}$ in a continuous flow operation. The design of alternative synthetic routes toward aza-dipyrrins is described, where the generation of unstable intermediates that render traditional methods inflexible are avoided. Details of preliminary experimentation to validate these methods are included, as are considerations for future development. Further attempts towards the synthesis of aza-dipyrrins are described. One new route takes advantage of the reductive power of tetravalent phosphorus reagents in C–N coupling. It also describes a new route towards the nitrosylation of pyrroles that is fast, effective and avoids the use of acidic conditions and can thus be potentially applied to less stable pyrroles.

LIST OF ABBREVIATIONS USED

AcOH	Acetic acid
Ar	Aromatic
BF ₃ •OEt ₂	Boron trifluoride diethyl etherate
BH ₃ •THF	Borane tetrahydrofuran
BODIPY	4-Bora-3a,4a-diaza-s-indacene
br s	Broad singlet
CDCl ₃	Chloroform
d	Doublet
DBU	1,8-Diazabicyclo[5.4.0]undec-7-ene
DDQ	2,2-Dichloro-5,6-dicyano-1,4-benzoquinone
DEATMS	N,N-Diethylamino trimethylsilane
DIPEA	N,N-Diisopropylethylamine
EDC.HCl	1-Ethyl-3-(3-dimethylaminopropyl)carbodiimide
Equiv	Equivalents
Et ₂ O	Diethyl ether
EtOAc	Ethyl acetate
EtOH	Ethanol
<i>F</i> -BODIPY	4,4-Difluoro-4-bora-3a,4a-diaza-s-indacene
g	Gram
GP	General procedure
h	Hour
HMDS	Hexamethyldisilazane
HRMS	High resolution mass spectrometry
Hz	Hertz

IUPAC	International Union of Pure and Applied Chemistry
<i>J</i>	Coupling constant
LiHMDS	Lithium hexamethyldisilazide
<i>m</i>	Multiplet
MeOH	Methanol
mg	Milligram
min	Minute
mL	Millilitre
NIR	Near infrared region
NMR	Nuclear Magnetic Resonance
°C	Degrees Celsius
<i>p</i> -chloranil	Tetrachloro-1,4-benzoquinone
PDT	Photodynamic therapy
Ph	Phenyl
PFP	Pentafluorophenylphenol
PFA	Perfluoroalkoxyalkane
<i>q</i>	Quartet
rt	Room temperature
R_f	Retention time factor
<i>s</i>	Singlet
sec	Second
<i>t</i>	Triplet
THF	Tetrahydrofuran
TLC	Thin-layer chromatography
TMSPa	Tris(trimethylsilyl)phosphate
t_R	Residence time

wt%	Weight percent
δ	Chemical shift
Δ	Heat
μL	Microlitre

ACKNOWLEDGEMENTS

Firstly, I would like to sincerely appreciate the SASEP scholarship committee for awarding me a fully funded scholarship to study here at Dalhousie and for bringing me from Zimbabwe to Canada. I would also like to express my sincere gratitude to my supervisor Prof. Alison Thompson. I would like to thank her for taking a chance on me and accepting me into her research group. Her dedication towards the research program and students is admirable and it has been a real privilege to observe and participate in. She allowed me to freely explore chemistry, to make mistakes and most importantly to learn. She has been an exceptional mentor, who has been supportive throughout this experience. It has been my pleasure to experience your creativity, enthusiasm and passion for chemistry and research. I would also like to sincerely thank my supervisory committee, Dr. Speed, Dr. Chitnis and Dr. Cozens for their time in reviewing my work throughout the years. Their support throughout is greatly appreciated. None of this work would have been possible without the excellent support of exceptional past and present group members of the Thompson laboratory. Their assistance, ideas and friendship will forever be cherished. To my family and friends who supported me morally during this journey, I thank you. Lastly to my husband Amos and my daughter Hailey, I would like to express my immense gratitude for holding my hand in the ups and downs of this journey. For pushing me and believing in me. Above all for coming halfway around the world with me so I can pursue my dream.

Chapter 1 - Introduction

1.1- Pyrrole.

This thesis is centred around the chemistry of pyrrole and pyrrole-containing compounds. Pyrrole is a heterocycle containing a nitrogen atom within the ring.¹ Due to the dominance of pyrrolic components in natural compounds and medicines,^{2,3} pyrrole (**Figure 1**) stands out as one of the most well-known heterocycles. Indeed, the biological significance of pyrrole and its derivatives cannot be overstated given that the pyrrolic motif constitutes part of many naturally occurring substances, for example, tetrapyrroles and porphyrins, which serve as active moieties in chlorophyll, heme, vitamin B12, bile pigments. Other examples involve the tripyrrolic prodigiosin skeleton,⁴ and many pyrrole-containing alkaloid natural products of varying complexity and biological activity.

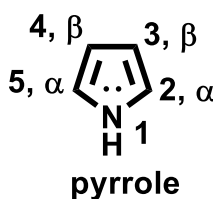


Figure 1: Structure and numbering of pyrrole.

A description of the various positions in the pyrrole ring is achieved either by the use of numbers or by the use of Greek letters as shown in **Figure 1**. The nitrogen atom is commonly referred to as the 1-position. The 2- and 5- positions are known as the α -positions. Positions 3- and 4 positions are referred to as the β -positions. The presence of the lone pair of electrons on the nitrogen atom of the pyrrole construct results in the delocalization of six π -electrons over five atoms such that pyrrole is classified as a π -excessive aromatic system.⁵ The pyrrolic system is thus susceptible to

electrophilic substitution reactions. In fact, pyrrole is more reactive than benzene in this respect² because the 5-membered 6π -system results in the stability of pentacyclic intermediate (δ -complexes) relative to the isoelectronic cyclopentadiene (**Figure 2**). The 6π system formed as a result of the conjugation of the nitrogen lone pair makes pyrrole aromatic as it follows the $4n + 2$ Huckle's rule of aromaticity.

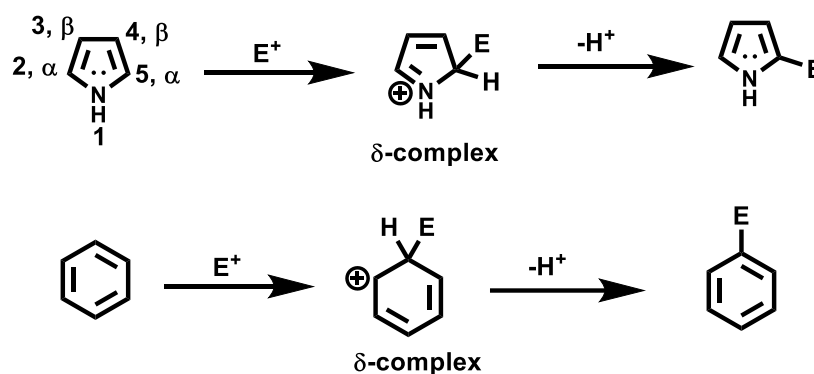


Figure 2: Electrophilic addition of electrophiles to pyrrole and benzene.

The delocalization of the nitrogen lone pair also gives rise to resonance forms bearing formal charges with significant electron density at both the α - and β -positions of pyrrole. As a result, electrophilic addition occurs at both the α - and β -positions, with the α -position strongly favoured as shown in **Figure 2**. This result can be explained by theoretical means through the calculation of electron densities,⁶ and through resonance stabilization and/or HOMO/LUMO coefficients, which reveal that electrophilic addition at the β -positions results in an intermediate that is cross conjugated.^{7,8}

1.2 - Dipyrrins and Aza dipyrrins.

The connection of two pyrrolic units by a methine bridge through the 2-positions results in a planar dipyrrin (**Figure 3**) that exhibits strong absorbance bands in the visible region of the electromagnetic spectrum. Dipyrrins are fully conjugated compounds with 12π electrons delocalized across the dipyrrin core. The conjugation is responsible for strong absorbance bands in the visible region of the electromagnetic spectrum; of these intensely coloured compounds.⁹ The IUPAC nomenclature used to label dipyrrins follows that used in pyrroles with the 1- and 9-positions known as the α -positions, and the 2-, 3-, 7- and 8-positions as the β -positions. The 5-position of the dipyrrins is known as the *meso*-position given that it is located centrally within the framework shown in **Figure 3**.¹⁰ Dipyrrins are prone to both electrophilic and nucleophilic attack on unsubstituted ring positions, such that the fully unsubstituted dipyrrin is unstable.¹¹ Enhanced stability is achieved with the presence of alkyl groups on the α - and β - positions about the dipyrrin core. Therefore, dipyrrins are typically isolated as their hydrobromide or hydrochloride salts both of which are more stable than the corresponding free bases.¹² However, aryl-substitution in the *meso*-position of the dipyrrin framework results in significantly enhanced stability and these dipyrrins can be isolated as the free bases under room conditions. A common modification to the dipyrrin framework is the replacement of the central carbon atom of the dipyrrin with a nitrogen atom. This yields a related but distinct class of compounds called aza dipyrrins (**Figure 3**).¹³ Although much less studied than dipyrrins on account of challenging synthetic approaches, aza dipyrrins are gaining interest due to their red-shifted absorptions compared to those of the parent dipyrrins.

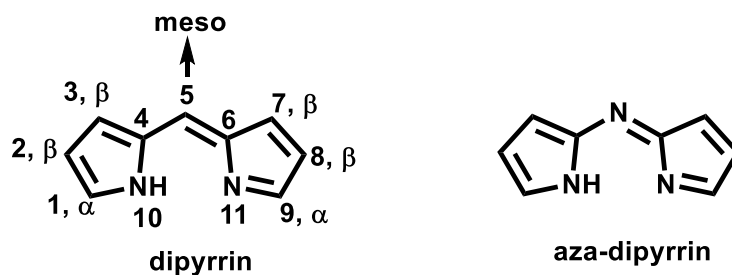
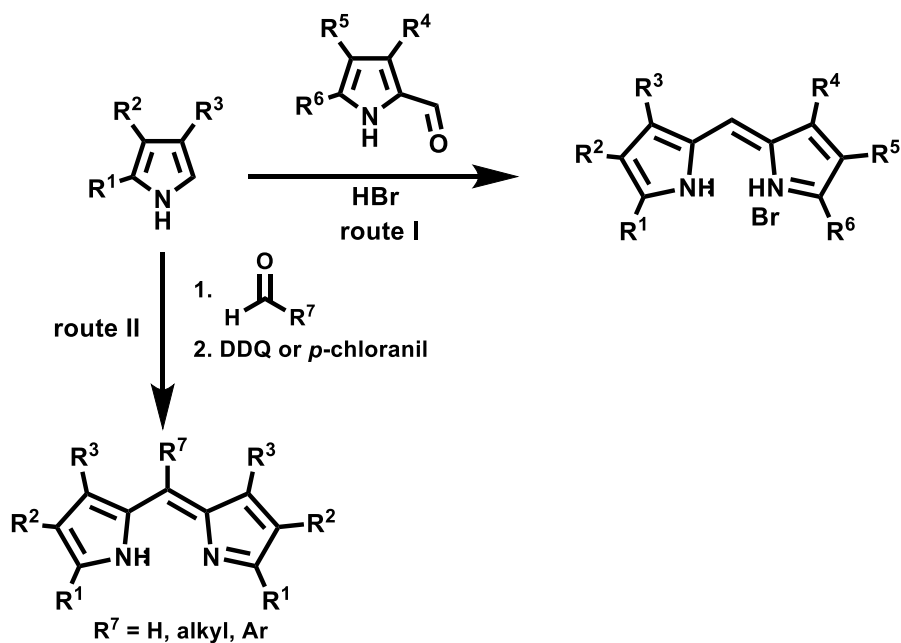


Figure 3: Numbering system for dipyrrius (left) and aza dipyrriu core (right).

Adopting from porphyrin chemistry, the construction of the dipyrriu framework can be achieved through one of several generalized methods. The first general approach (**Scheme 1, route I**) involves the condensation of an α -free pyrrole with an α -formyl pyrrole, under acidic conditions, and enables the formation of dipyrriu salts bearing different substituents about the two pyrrolic units.¹⁴ The other approach (**Scheme 1, route II**) involves condensation of two equiv. of an α -unsubstituted pyrrole with an aldehyde to provide a symmetric dipyrromethane. Oxidation then provides the dipyrriu. This route often utilizes aryl aldehydes, thus placing an aryl group in the *meso*-position, although alkyl variants are also known.¹⁵ A variation of this strategy utilizes a carboxylic acid¹⁴ or an acid chloride,^{16,17} rather than an aldehyde, thus generating the dipyrriu directly and negating the need for later oxidation across the *meso*-position.



Scheme 1: Synthetic strategies to dipyrins.

Oxidation of dipyrromethanes to dipyrins is achieved with 2,3-dichloro-5,6-dicyano-1,4-benzoquinone (DDQ) or the milder 2,3,5,6-tetrachloro-1,4-benzoquinone (*p*-chloranil), as indicated in **Scheme 1**. These oxidants were originally borrowed from the shelves of chemists familiar with the oxidation of cyclic tetrapyrroles to make porphyrins, with little variation published since that early work. The oxidation is typically a messy business and is further complicated by challenging chromatographic requirements. As such, incorporation of the -BF₂ moiety, chelating both nitrogen atoms, is often effected in situ as the formation of the apolar boron complex significantly improves the outlook for isolation of purified material. The so-formed BODIPYs are the subject of Chapter 2 in this thesis.

Dipyrrins and aza dipyrrins were traditionally used as synthetic intermediates for the construction of porphyrins and aza porphyrins (aka phthocyanines). However, recent interest in the dipyrrinato framework has since increased due to the ability of dipyrrins to act as metal-chelating ligands for various metal cations. This strategy has shown potential to form charge-neutral complexes with striking optical properties, as well as tunable functionality.¹⁴ The versatility of dipyrrinato ligands as chelating agents for various main group elements and in various applications also is well documented.¹⁸⁻²¹ Deprotonation of the dipyrrin gives a resonance-stabilized monoanionic ligand (**Figure 4**) allowing dipyrrins to act as bidentate chelating ligands which can easily be complexed with transition metal ions through the two nucleophilic nitrogen atoms to form isolable complexes of different conformations.¹⁴ As such complexes of dipyrrins with cations such as Ti(IV),²² Mn(III),²³ Fe(II),^{24,25} Co(III),²⁶ Rh(I),²⁷ Rh(III),²⁸ Ir(III),²⁸ Sn(IV),²² Pd(II)²⁹ etc. have been reported, along with their various optical, electronic and catalytic capabilities.

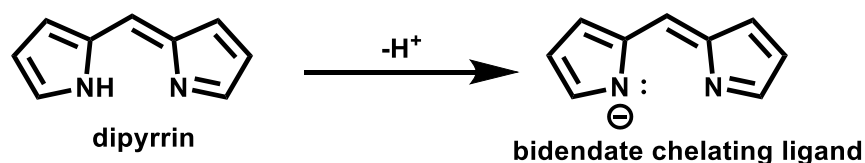


Figure 4: Complexation of dipyrrins to different types of elements via the nucleophilic nitrogens.

1.3 - *F*-BODIPYs and aza BODIPYs.

The most common and intensively studied dipyrinato complexes are the boron difluoride ($-\text{BF}_2$) chelated complexes known as *F*-BODIPYs (**Figure 5**).^{30,31} The generally highly fluorescent *F*-BODIPY framework was unintentionally discovered in 1968 by Treibs and Kreuzer but has since found increasing applications in a large variety of scientific fields.²⁰ The IUPAC numbering system for *F*-BODIPYs is different than dipyrrens, but the term α -, β - and *meso*-positions are utilized for both frameworks.³² Chelation of dipyrrens with $-\text{BF}_2$ facilitates tetrahedral geometry at boron. This essentially acts as the “glue” that restricts motion such that the typically non-fluorescent dipyrren skeleton is rigidified to result in sharp absorption and emission bands.^{33,34} Such (photo)electronic properties have been intensely studied, with fine-tuning resulting in highly capable BODIPYs, e.g. bespoke emission, redox properties and/or (photo)sensitization to generate singlet oxygen, and beyond. Many BODIPY-based fluorescent probes have been developed for use in fluorescence imaging.³⁵

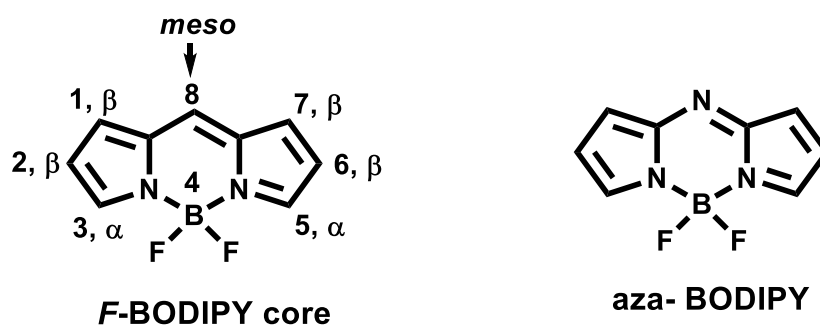
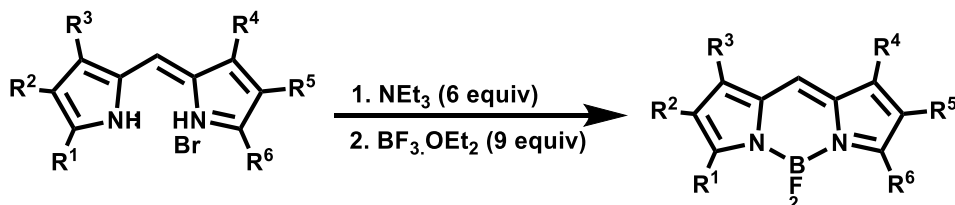


Figure 5: Structure and IUPAC labelling of *F*-BODIPYs (left) and the structure of aza BODIPY (right).

Beyond their use as fluorescent bioprobes, the electronic tunability of BODIPYs has led to utility as photosensitizers for photodynamic therapy³⁶ and in dye-sensitized solar cells for photovoltaic technology.³⁷ The planar core, facile functionalization and tunable HOMO–LUMO gap of BODIPYs offer significant promise in this regard.³⁸ Furthermore, the replacement of the carbon atom with a nitrogen atom at the meso-position forms the aza *F*-BODIPY framework (**Figure 5**). This change lowers the energy of both absorption and emission transitions by reducing the HOMO–LUMO energy gap compared to *F*-BODIPYs with similar substituents. As such, aza BODIPY dyes typically absorb and emit at 600–750 nm and beyond,³⁹ i.e. significantly red-shifted compared to their equivalent BODIPYs.

F-BODIPYs are synthesized from dipyrrens or aza dipyrrens by treatment with a base (triethylamine, DIEA, DBU etc.) and boron trifluoride diethyl etherate (BF₃•OEt₂) (**Scheme 2**). For meso aryl-substituted BODIPYs, the dipyrren is made in situ from the reaction of an aldehyde with excess pyrrole under acid conditions and subsequent oxidation with DDQ or p-chloranil as mentioned before (**Scheme 1**). Without being isolated, the dipyrren is often treated with excess base and boron trifluoride diethyl etherate to give the *F*-BODIPY (**Scheme 2**).



Scheme 2: General synthetic strategy to *F*-BODIPYs.

1.4 - Thesis Overview.

Considering the importance of $-BF_2$ complexes of the dipyrinato and aza dipyrinato units, economical and versatile access to these constructs is required. This thesis research aims to develop new methodologies for the effective, eco-friendly and cost-effective synthesis of *F*-BODIPYs and aza BODIPYs. Chapter 2 describes attempts to avert the challenges faced in the current synthesis of *F*-BODIPYs by using only 1 equiv of $BF_3 \cdot Et_2O$ in a continuous flow operation. Chapter 3 describes attempts towards a new synthetic route to aza dipyrins, precursors to aza BODIPYs. The route described is based on the use of acyclic precursors to the aza dipyrin construct that thus avoids the unstable intermediates encountered in the current synthesis of these compounds. Chapter 4 also describes attempts towards the synthesis of aza dipyrins, in this case via a new route that takes advantage of the reductive power of tetravalent phosphorus reagents in C–N coupling. Chapter 4 further describes a new route toward the nitrosylation of pyrroles that is fast, effective and avoids the use of acidic conditions. Chapter 5 of this thesis consists of a review⁴⁰ reproduced in its entirety and with permission (see Appendix A) from the Royal Society of Chemistry. This published review highlights the various approaches to effecting substitution at the boron atom of BODIPYs. The thesis concludes with Chapter 6 comprising of conclusions from Chapters 2-5.

Chapter 2: Attempts Towards an Economic Synthesis of *F*-BODIPYS.

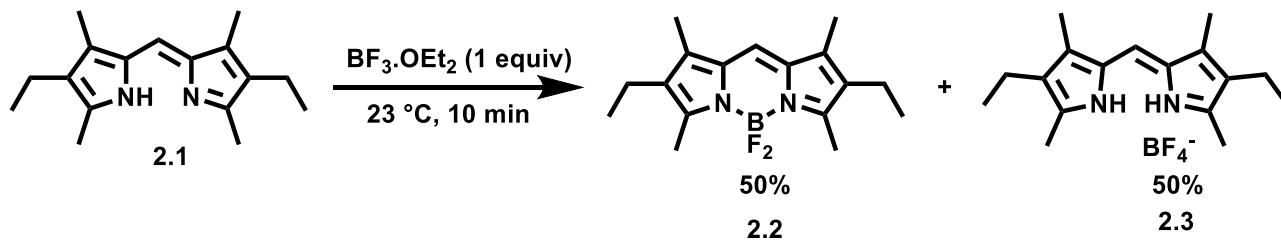
2.1 – Introduction.

This chapter describes efforts towards the synthesis of *F*-BODIPYS using 1 equiv. of $\text{BF}_3 \cdot \text{OEt}_2$. For decades, the chemistry of BODIPYS rested with *F*-BODIPYS via chelation of the dipyrin unit with $-\text{BF}_2$. Although new strategies^{41,42} have emerged for the synthesis of *F*-BODIPYS, the treatment of a solution of dipyrin, or its HX salt, with excess base (typically 6 equiv. NEt_3 or DIPEA) and $\text{BF}_3 \cdot \text{OEt}_2$ (typically 9 equiv.) has provided the traditional route to *F*-BODIPYS in generally quite high yields.⁴³ Despite the obvious excesses of reagents, yields generally decrease upon decreasing the stoichiometry.^{44,45} Furthermore, the yields vary significantly with the use of compromised “anhydrous” conditions. This is unsurprising, given the anticipated behaviour of $\text{BF}_3 \cdot \text{OEt}_2$ in the presence of alternative donors, yet to an extent implying complications beyond simple quenching and instead consequent to the complexity of various equilibria involving Lewis acidic boron in the presence of NEt_3 , H_2O , Et_2O and the chelating ligand. With the goal of simplifying synthetic protocol, a general method for *F*-BODIPY synthesis was published,⁴³ that involves a second aliquot of excess NEt_3 and $\text{BF}_3 \cdot \text{OEt}_2$ in an open-air environment (hydrous conditions).⁴³ While this synthesis of *F*-BODIPYS removes the need for anhydrous conditions, the use of further reagent excesses is far from ideal. Furthermore, the separation of the $\text{BF}_3 \cdot \text{NEt}_3$ byproduct from the desired *F*-BODIPY, on scale, is non-trivial.⁴³ These problems highlight the need for the development of a new synthetic approach to *F*-BODIPYS that is high-yielding and environmentally acceptable. Due to the favourable optical and physical properties inherent to *F*-BODIPYS, a staggering number of these compounds have been synthesized. Conversely, little investigative research has been performed examining the fundamental nature of dipyrin

complexation of boron. The work reported herein explores the stoichiometric addition of $\text{BF}_3 \cdot \text{Et}_2\text{O}$ to dipyrrens in the absence of a base.

2.2 – Synthetic strategy.

Exploration by a previous researcher in the Thompson Lab⁴⁶ attempted to synthesize the popular *F*-BODIPY **2.2** from the free base dipyrren **2.1** using just one equiv of $\text{BF}_3 \cdot \text{OEt}_2$, conducting the reaction in the absence of the base revealed that the ligation of the free-base dipyrren to $\text{BF}_3 \cdot \text{OEt}_2$ formally liberates fluoride ion, which presumably binds with the unreacted $\text{BF}_3 \cdot \text{OEt}_2$ resulting in 50% ratio of the desired *F*-BODIPY **2.2** and 50% ratio of non BF_2 complexed material of the dipyrren **2.3** (Scheme 3).⁴⁶ The F^- readily binds with the unreacted $\text{BF}_3 \cdot \text{OEt}_2$, generating anionic BF_4^- making $\text{BF}_3 \cdot \text{OEt}_2$ unavailable to react with the remaining free-base dipyrren to make the desired *F*-BODIPY. Although the yield of the *F*-BODIPY is lower than that achieved using some other approaches, these preliminary investigations offer a rationale for the synthetic work described in this chapter. While this new methodology represents a high atom economic use of the $\text{BF}_3 \cdot \text{OEt}_2$, the formation of the unwanted HBF_4 salt needs to be addressed in order for higher yields of the desired *F*-BODIPY to be attained.



Scheme 3: Addition of $\text{BF}_3 \cdot \text{Et}_2\text{O}$ (1 equivalent) to free-base **2.1** in toluene.

Importantly, the stoichiometric by-products of the reaction are a proton and fluoride. There is, therefore, a need to minimize contact between the ejected F^- and the unreacted $BF_3 \cdot OEt_2$. This encouraged the exploration of the use of a continuous flow process for this transformation, to prevent the produced fluoride from interacting with the as-yet unreacted $BF_3 \cdot OEt_2$. This strategy would hopefully minimize the formation of the non-complexed material and thus maximize the yield of the *F*-BODIPY.

2.2 - Continuous flow process.

Continuous flow processes involve performing chemical reactions in a tube or a pipe (reactor coil).⁴⁷ In a continuous flow set-up, reagents are continuously pumped through different streams, combined through the mixer upon passing into the reactor coil, and the product then continuously collected downstream. There is, therefore, no interaction between the incoming reagents (upstream) and the products formed downstream (**Figure 6**). Having such a setup, introducing the free base dipyrin **2.1** and $BF_3 \cdot OEt_2$ from different streams, would hopefully avoid the interaction of the ejected F^- with the unreacted BF_3 . The use of flow chemistry has been shown to improve control of reaction parameters such as heat and mass transfer, mixing and residence time which leads to improved robustness compared with related batch processes.⁴⁸ The overall time a chemical species spends in the reactor coil is equivalent to the total reaction time and is known as the residence time. The residence time can be fluctuated based on the flow rate of reagents and the internal volume of the reactor coil.

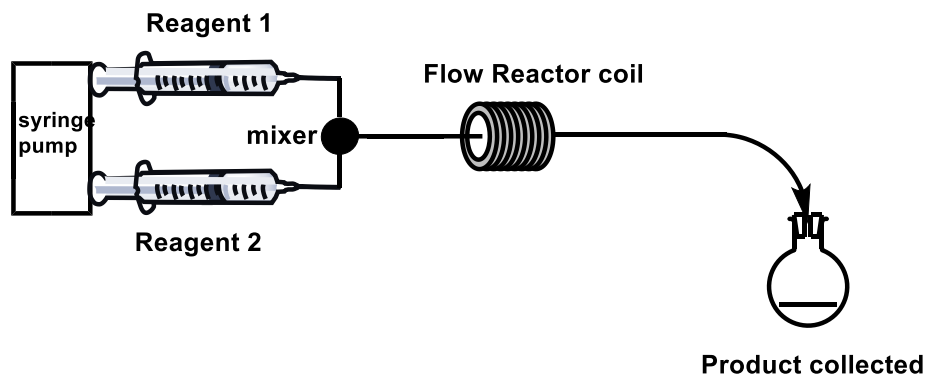


Figure 6: A generic continuous flow set-up.

2.3 - Project Goals.

This project aims to develop a new methodology for the synthesis of *F*-BODIPYs using a continuous flow setup that uses only one equiv of $\text{BF}_3 \cdot \text{OEt}_2$ and eliminates, reduces or optimizes the use of a base. As mentioned, in a continuous flow process, reagents are pumped from different streams and then mixed at a common point (T or Y mixer) before moving into the reactor coil where the reaction continues to form products which are then collected downstream (**Figure 7**). The hypothesis, therefore, is that using flow chemistry to pump the free base and the $\text{BF}_3 \cdot \text{OEt}_2$ through different streams would enable mixing at a common point, formation of the *F*-BODIPY and generation of fluoride and proton by-products. All would be continuously pumped downstream, thus divorcing the (by)products from the incoming $\text{BF}_3 \cdot \text{OEt}_2$. In this way, it was anticipated that the formation of the HBF_4 salt would be averted and, in turn, the yield of the desired *F*-BODIPY increased. This method will ideally increase the availability of $\text{BF}_3 \cdot \text{OEt}_2$ for reaction with the free-base dipyrin, thus potentially increasing the yield of the desired *F*-BODIPY product. The use of just one equiv of $\text{BF}_3 \cdot \text{OEt}_2$ in the absence of NEt_3 will avert the formation of Lewis adducts such as $\text{BF}_3 \cdot \text{NEt}_3$, enhancing purification procedures as well as product yields,

thereby producing an overall increase in efficiency thus addressing the challenges encountered in the traditional synthesis of *F*-BODIPYs.

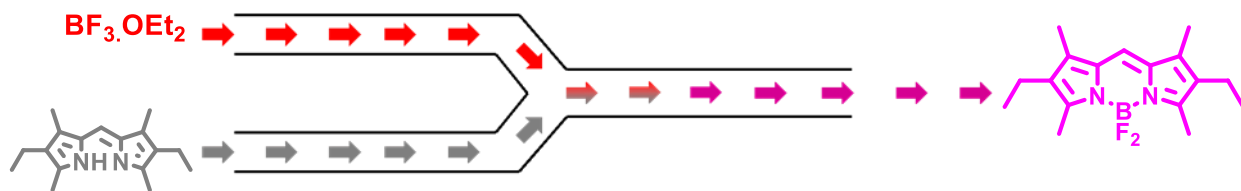
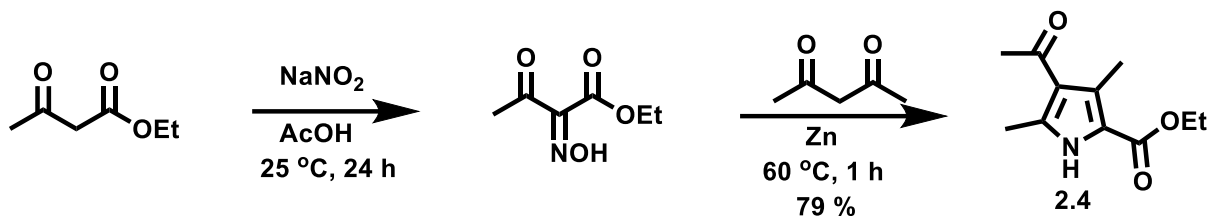


Figure 7: Stream-flow mechanism in a continuous flow operation.

2.4 - Results and Discussion.

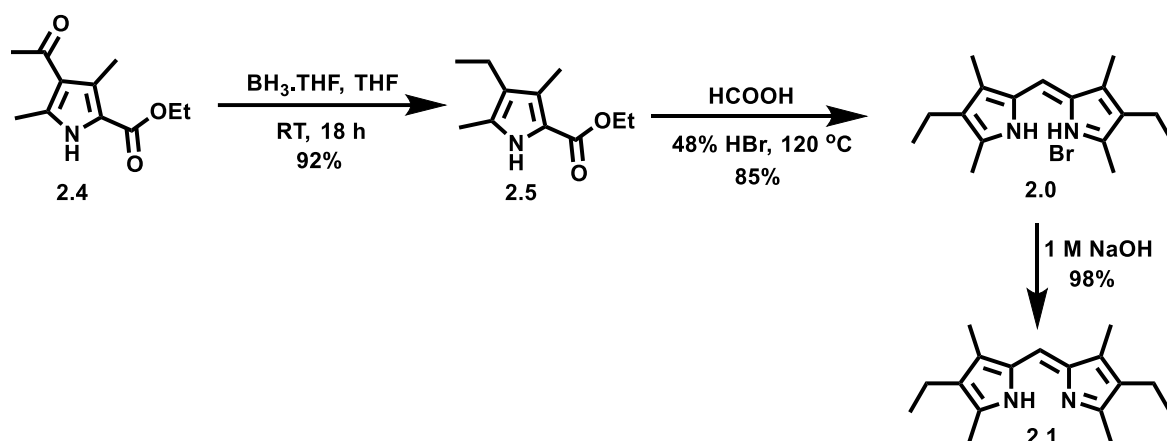
2.4.1 - Reaction Optimization and Understanding of Batch Operation.

Prior to performing the synthesis of an *F*-BODIPY using flow chemistry, there was a need to understand the synthesis using the batch method. As a first trial, the published conditions leading to the discovery of this reactivity were repeated.⁴⁶ Prior to performing the synthesis of the *F*-BODIPY, free dipyrin **2.1** was prepared from its HBr salt **2.0** as this is generally a more stable and isolable form of dipyrins.⁴⁹ To prepare the dipyrin salt **2.0**, pyrrole **2.4** was synthesized first. Following a published procedure, pyrrole **2.4** was prepared via the reaction of ethyl acetoacetate with sodium nitrite in the presence of acetic acid to produce ethyl 2-aminoacetoacetate which then reacted with 2,4-pentanedione to give ethyl 4-acetyl-3,5-dimethylpyrrole-2-carboxylate **2.4** as a white solid after recrystallization from ethyl acetate (**Scheme 4**).⁵⁰



Scheme 4: Synthesis of pyrrole 2.4.

Once isolated, pyrrole **2.4** was reduced with $\text{BH}_3 \cdot \text{THF}$ to yield pyrrole **2.5** as a white solid after purification by column chromatography.⁵¹ Dipyrin **2.0** was then synthesized in 85% isolated yield from pyrrole **2.5** via one-pot acid-catalyzed hydrolysis, decarboxylation, and condensation in the presence of formic acid and HBr (**Scheme 5**).⁵²



Scheme 5: Synthesis of free base dipyrin 2.1.

For each run, the bromide salt was dissolved in CH_2Cl_2 and washed with aqueous NaOH (1M). The organic layer was then dried over anhydrous Na_2SO_4 and the solvent was removed to yield dipyrin **2.1** as a brown, crystalline solid.⁹ With the desired substrate in hand, the formation of the *F*-BODIPY **2.2** on the bench top (batch mode) was explored by screening solvents, equivalents, temperature, and reaction time for the addition of 1 equiv of $\text{BF}_3 \cdot \text{OEt}_2$ to the free-base dipyrin in

the absence of base. For each entry, the free base dipyrin **2.1**, was dissolved in anhydrous toluene in a round bottom flask under a nitrogen atmosphere, and 1 equiv. of $\text{BF}_3 \cdot \text{OEt}_2$ was added with stirring. After stirring for 10 minutes, the reaction mixture was filtered over celite. The *F*-BODIPY **2.2** was collected first by flushing with hexanes in a 49% yield. The HBF_4 dipyrin salt **2.3**, was then collected in a 46% yield from the celite pad by flushing with CH_2Cl_2 followed by removal of the solvent in vacuo.

To minimize operations and to make future exploration more efficient by avoiding the need for work-up and isolation of the reaction products after each trial, ^1H NMR spectroscopic analysis of a crude reaction mixture was utilized to determine the amount of each component present in the reaction mixture after the completion of the reaction. To identify and/or quantify all the components of a given mixture, the amounts of specific (known) components were determined using an internal standard. Ideally, the internal standard must be present in a known amount and its spectrum must have at least one well-resolved assignable and integrable peak that does not overlap with other peaks in the spectrum of the sample.⁵³ Benzene was chosen for this investigation because it is soluble in the NMR solvent CDCl_3 and has a ^1H NMR resonance separate from those of the analyte being quantified.⁵⁴ To determine conversion, upon completion of the reaction according to TLC analysis, the reaction solvent was removed *in vacuo* and the crude material was dissolved in a known volume of deuterated chloroform (CDCl_3). A known volume of benzene was added. A known aliquot of the product mixture, now containing benzene, was added to an NMR tube, and then diluted with a known amount of CDCl_3 to reach a volume suitable for ^1H NMR analysis. Figure 8 compares ^1H NMR spectra for the *F*-BODIPY (**2.2**, middle), the HBF_4 salt (**2.3**, top) and the crude reaction mixture containing both the *F*-BODIPY and the dipyrin salt. The crude mixture clearly contains *F*-BODIPY and non-complexed material. The non-complexed material

presumably consists of an NMR-averaged mixture of starting dipyrin and dipyrin salts, including the BF_4^- salt of the protonated dipyrin.

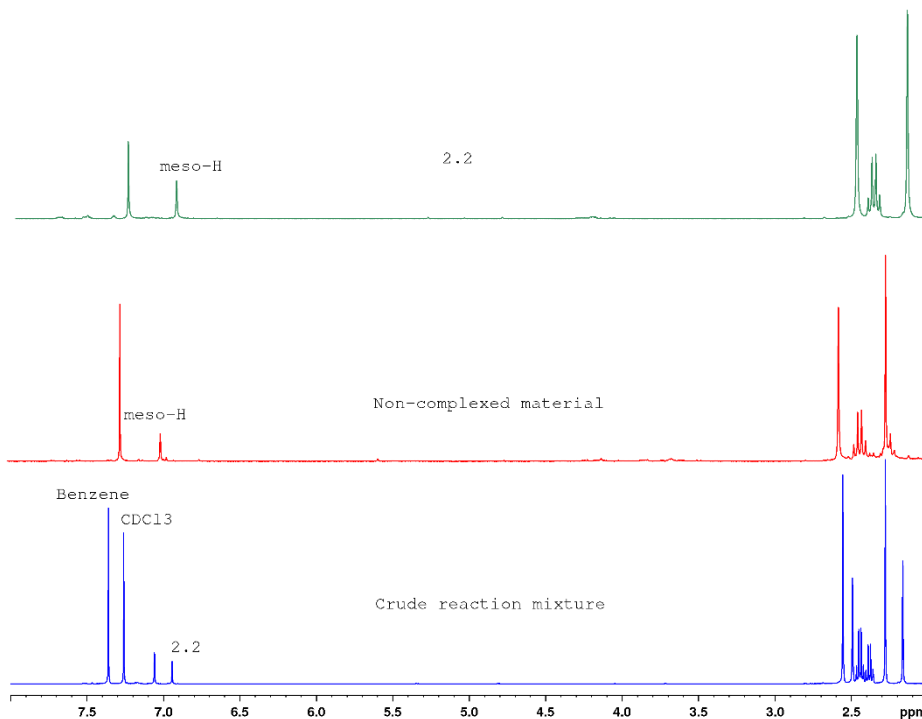


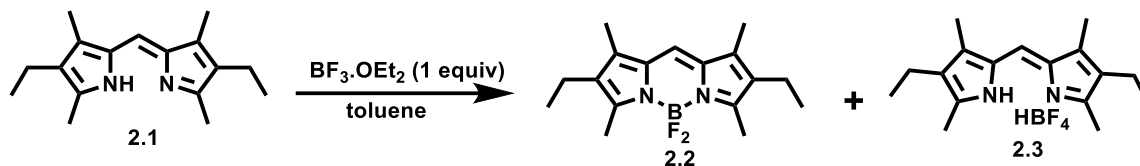
Figure 8: $^1\text{H-NMR}$ (CDCl_3) spectra of 2.2 (top), Non-complexed material (middle) and a crude mixture (bottom) with benzene as an internal standard.

By setting the integral of benzene to 6, the integral for the meso-H of the *F*-BODIPY and the non-complexed material were determined for the crude product mixture. Since a known amount of benzene had been added, the number of moles of benzene could, therefore, be calculated. The number of moles of each component present in the crude reaction mixture (analyte, **A**) was then calculated from the molar amount of internal standard and the molar ratio:

$$n_A = n_{IS} \times r_{A/IS}$$

The mass of the sample does not factor into the calculation because the method relies solely on the molar ratio of the internal standard to the compound to be determined. Once the number of moles

present at the end of the reaction are known, the percentage conversion for each product could be calculated using the initial number of moles of the free base **2.1** used in the reaction. After several rounds of optimization for the batch synthesis process, it was found that the highest yields and conversions of the desired *F*-BODIPY could be achieved using 3 mL (for 50 mg of free-base dipyrin) of toluene for 10 minutes at 23°C as shown in (Table 1, entry 1).



Entry	Volume (mL)	Time (min)	Temp (°C)	2.2 ^a	Non-complexed material ^a
1	3	10	23	49	46
2	30	60	23	20	65
3	3	5	150	34	48
4	30	18 h	23	17	74
5	3	24 h	23	0	75

Table 1: Batch process optimization. ^a ratio of 2.2 and non-complexed material present in the reaction mixture.

Based on these results, the conditions associated with entry 1 were selected for exploration in a continuous flow operation for the synthesis of the desired *F*-BODIPY **2.2**.

2.4.2 - Reaction Optimization in Flow Operation.

As mentioned before, in a continuous flow setup, reagents are introduced upstream and products are collected downstream. It was hypothesized that introducing the free base **2.1** from one stream

and the $\text{BF}_3 \cdot \text{OEt}_2$ from another stream would avert the reaction of the components of HF, supposedly produced downstream, from reacting with the unreacted BF_3 upstream. To study this concept, a rudimentary continuous flow setup was assembled from affordable and commercially available components to give the reactor shown in (Figure 9) harnessing two syringes to one syringe pump to allow the syringes to be pumped at the same rate.

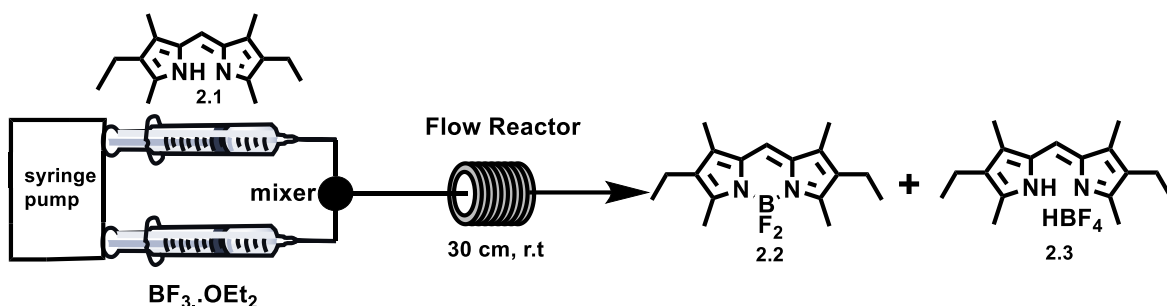


Figure 9: Lab-scale flow reactor setup.

To begin the study for the synthesis of *F*-BODIPY **2.2** using a flow method, the equivalents previously investigated in the batch method were used in the continuous flow reactor setup as shown in Figure 9. Solutions of starting materials were prepared just like in the batch syntheses i.e., 50 mg of **2.1** was placed in a pear-shaped flask, purged with nitrogen and then 3 mL of anhydrous toluene was added into the flask. In another pear-shaped flask, $\text{BF}_3 \cdot \text{OEt}_2$ was treated in the same manner. Each solution was loaded, under nitrogen, into a gas-tight syringe. Both syringes were then filled up with nitrogen to keep the reaction mixture anhydrous and ensure that the nitrogen gas pushes the reaction mixture through the flow reactor and thus no solution is left in the tubing. The solutions were pumped by a syringe pump, through a 0.02-inch internal diameter tee mixer into perfluoroalkoxyalkane (PFA) tubing also 0.02-inch internal diameter. The length of the reactor coil determines the length of time (residence time t_R) it takes for a fluid to pass through the reactor coil. Changing the flow rate of fluid through the reactor coil, or the length of the coil,

changes the residence time.⁵⁵ Since the hypothesis is that the reaction of the free base dipyrin and BF₃•OEt₂ is essentially spontaneous, the length of the PFA flow reactor loop was made short and kept constant at 30 cm. To test the hypothesis, the flow rate was varied to adjust the residence time (t_R). It was noted that when the two streams came into contact, an immediate colour change from orange to deep red was observed, indicating the formation of the *F*-BODIPY. The reaction mixture was collected in a vial downstream. The reaction was immediately quenched upon exit using a solution of saturated NaHCO₃. The solvent was removed in *vacuo* and the reaction mixture was placed under vacuum to remove residual solvent. To determine the reaction conversion, the crude reaction mixture was evaluated, just like for the batch reaction described above, using an internal standard and ¹H NMR spectroscopy. A total of five runs were performed and the results are shown in **Table 2**.

Entry	Flow Rate/mLmin ⁻¹	t _R /sec	T/°C	2.2 ^a	Non-complexed material ^a
1	0.2	18.3	0	29	71
2	0.5	7.31	0	41	59
3	1.0	3.65	0	39	61
4	2.0	1.83	0	40	60
5	5.0	0.73	0	24	76

Table 2: Optimization of the continuous flow process with a reactor coil of 30 cm. ^aratio of 2.2 vs non-complexed material.

The residence time (t_R) was calculated using the equation:

$$\text{Residence time} = \text{Reactor Volume} / \text{Flow Rate}$$

$$\text{And Reactor Volume} = \text{cross section} \times \text{Length}$$

$$\begin{aligned}
 &= \pi r^2 L \\
 &= 3.1416(0.0254 \text{ cm})^2 \times 30 \text{ cm} \\
 &= 0.061 \text{ cm}^3
 \end{aligned}$$

This reactor volume was constant for this investigation since the reactor length was kept constant at 30 cm. The residence time for each flow rate was calculated using the above equation. The flow rate was plotted against the percentage conversion for both the *F*-BODIPY **2.2** and the non-complexed material. It was observed that generally the complexation was always limited, suggesting that the $\text{BF}_3 \cdot \text{OEt}_2$ has a greater affinity for the F^- produced in situ than for the free base dipyrin coming through from a different stream. As the flow rate increases the residence time decreases and so does the yield of both the *F*-BODIPY. Furthermore, the 5 mL/min flow rate was too fast i.e. t_R was too short to achieve optimal conversion to the desired *F*-BODIPY, whilst the 0.5 mL/min (7.31-sec) gave the greatest conversion. Further decreasing the flow rate to 0.2 mL/min, thus increasing the residence time to 18.3 sec, resulted in a decrease in conversion to the desired *F*-BODIPY (**Figure 10**): this can be attributed to less efficient mixing when using lower flow rates.⁵⁶

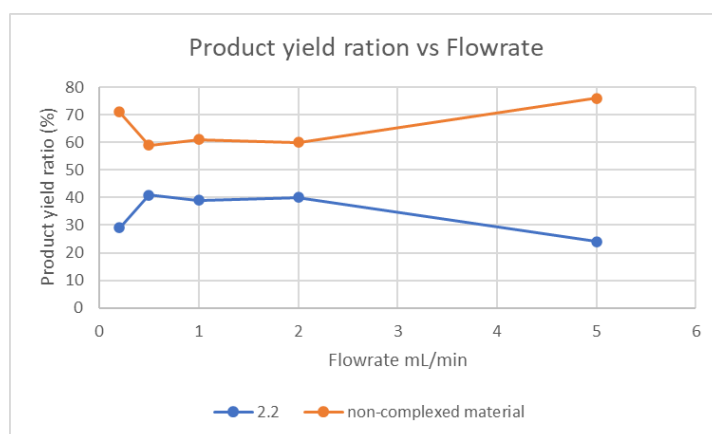


Figure 10: Relationship between flow rate and product yield.

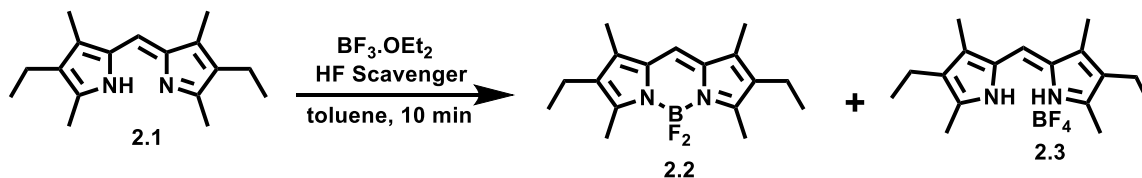
The results confirmed that the reaction is rapid as shown by the colour change of the free base dipyrin upon contact with $\text{BF}_3 \cdot \text{OEt}_2$. Both the results obtained in continuous flow and batch reactions did not vary significantly, with the formation of the non-complexed material limiting the yields of F-BODIPY. Also, when operating a continuous flow system using highly air-sensitive reagents, it should be noted that PFA tubing allows slow permeation of air and moisture, which could lead to poor yields.⁵⁵ These disappointing results encouraged us to return to exploring the reaction in batch in the presence of HF scavengers to attempt to mop up the proton and fluoride produced in situ.

2.5 - Hydrogen fluoride scavengers.

It was speculated that the moderate yield of the *F*-BODIPY **2.2** in both the batch and flow setups might be attributed to the HF reacting with unreacted $\text{BF}_3 \cdot \text{OEt}_2$ to form HBF_4 and thus the HBF_4 dipyrin salt. The continuous flow setup was ineffective at preventing HBF_4 dipyrin salt formation, and therefore the addition of a scavenger to the reaction mixture to mop up the proton and fluoride formally produced in situ was envisioned. HF scavengers⁵⁷ such as bases like Na_2CO_3 , K_2CO_3 and CaCO_3 have been reported to be effective in mopping up HF in reactions where the presence of HF could potentially interfere with the formation of the desired products. Furthermore, mopping up the HF produced will serve to drive the reaction equilibrium towards the product, and thus increase yields of the desired product.

Therefore, a quick and simple potential solution to avert the formation of HBF_4 salt was to add an organic or inorganic base (>1.0 equiv) to the reaction mixture to neutralize HF. Inorganic bases (K_2CO_3 ,⁵⁸ Na_2CO_3 , CaCO_3 ⁵⁹) were chosen as the first scavengers with hopes of producing an inorganic base-HF salt, potentially beneficial in that this approach to scavenge HF offered a

possible non-chromatographic approach to purify **2.2** from an inorganic base-HF salt. This is based on reports that solubilities of alkali-metal are very limited in organic solvents⁶⁰ The effectiveness of these scavengers, in the reaction of **2.1** with $\text{BF}_3 \cdot \text{OEt}_2$, was thus investigated. To this end, 1.5 equiv of each scavenger was added to a stirring solution of free base **2.1**. The mixture was then treated with 1 equiv $\text{BF}_3 \cdot \text{OEt}_2$ in a dropwise manner. In each run, the heterogeneous reaction mixture reached completion after 10 minutes, as monitored by TLC. After completion of the reaction, the reaction mixture was filtered, and the solvent was removed *in vacuo*. The resulting crude reaction mixture was dissolved in chloroform and the ^1H NMR spectrum recorded. As before, the ratio of integration of the meso-H peaks was used as a measure of conversion for the products shown in **Table 3** (entry 1-4). In all these runs, the yield of the non-complexed material was higher than that of the desired BODIPY **2.2**. This shows that the inorganic bases were unsuccessful at scavenging such as to improve desired yields.



Entry	HF Scavenger	2.2	Non-complexed material
1	K_2CO_3	28	72
2	NaCO_3	30	70
3	CaCO_3	27	73
4	CaCl_2	0	100
5	Calcium 2-ethylhexanoate	0	100
6 ^a	DEATMS	4	79

Entry	HF Scavenger	2.2	Non-complexed material
7	HMDS	28	72
8	TMSPa	39	0
9	2,6-Di-tert-butyl-4-methyl-pyridine	31	69
10	DABCO	Trace	100
11	DBU	Trace	100
12	<i>N,N</i> -dimethyl-1-naphthylamine	0	100
13 ^a	Proton sponge	34	56
14	BH ₃ •THF	35	65
15	Triethylborane	23	77
16	Triphenylborane	28	72
17	2,6-Lutidine	43	57

Table 3: Synthesis of F-BODIPY in the presence of HF scavengers, ^aIsolated yield

Attention was thus turned to the use of organic HF scavengers. In lithium-ion battery research, HF is notorious for causing the electrochemical decomposition of electrolytes by attacking cathode materials that contain transition metal components affording metal-fluoride species.^{61,62} This not only destroys the cathode structure but also seriously impedes the electrochemical reaction of the anode.^{63,64} To improve lifetime and decrease impedance build-up in lithium-ion batteries, several additives have been successfully introduced to scavenge HF and avoid undesired surface reactions. In light of this, attention was thus turned to the additives that have been shown to be effective in this regard. *N,N*-diethylamino trimethylsilane (DEATMS) and hexamethyldisilazane (HMDS) have the ability to form a strong Si-N bond which effects the H₂O/HF-scavenging.^{65,66} The basicity of the nitrogen atom and the fluorophilicity of the Si atom work in tandem to scavenge HF.⁶⁷ It

was anticipated that this matched chemical reactivity between the Si-N functional group and the HF species would be effective for reducing the HF concentration in the reaction of **2.1** and $\text{BF}_3 \cdot \text{OEt}_2$. Tris(trimethylsilyl)phosphate (TMSPa)⁶⁸ has also been used successfully in the scavenging of HF in Li batteries, with this ability attributed to the $-\text{SiMe}_3$ moieties. In all the runs performed, when the free-base **2.1** was treated with $\text{BF}_3 \cdot \text{OEt}_2$ in the presence of these HF scavenging additives, the formation of the desired *F*-BODIPY **2.2** occurred in trace amounts (**Table 3, entry 6 to 9**). These disappointing results encouraged the exploration of proton trapping approaches.

Triethylamine and DIPEA are nucleophilic bases used in the traditional synthesis of BODIPYs. Attention was therefore turned to the use of non-nucleophilic bases that are usually employed in proton scavenging with hopes of mopping up proton but not interfering with other functions in the reaction.⁶⁹ It was postulated that sterically hindered bases like DABCO, DBU, *N,N*-dimethyl-1-naphthylamine could be employed to trap the proton and suppress, if not eliminate, the reaction of HF with BF_3 to minimize the formation of the undesired non-complexed material. Thus, the stage was set to commence experimentation with proton traps, to determine whether the formation of BODIPY **2.2** was possible in the presence of sterically hindered bases. With the above thoughts, the free-base dipyrin was treated with $\text{BF}_3 \cdot \text{OEt}_2$ in the presence of the hindered bases. Unfortunately, only trace amounts of *F*-BODIPY were formed in the presence of the hindered bases, as confirmed by TLC (**Table 3, entries 10 to 13**). It was postulated that the presence of the bulky bases might also hinder the $\text{BF}_3 \cdot \text{OEt}_2$ from reacting with the free base and hence no product was formed. In the case of the proton sponge, 34% of the desired *F*-BODIPY was isolated, which is less than the yield obtained in the absence of HF scavengers. Attention was turned to an alternative approach.

According to previous studies,⁷⁰ the formation of *F*-BODIPY is initiated by the donor-acceptor interaction of the lone electron pair of the pyrroline nitrogen atom of the free base and the vacant orbital of the boron atom in BF₃, followed by the formation of a hydrogen bond between the hydrogen atom of the NH group of the free base and the nearest fluorine atom in BF₃ adduct. It is this bonding that promotes the formal elimination of HF in the last step of the synthesis of BODIPY. It was therefore speculated that having another boron source in the reaction mixture, which could scavenge the ejected fluoride, could potentially prevent the formation of non-complexed material and possibly increase the yield of the desired BODIPY **2.2**. In light of this, the use of boranes was explored (**entry 14 to entry 16**). The free base was reacted with the BF₃•OEt₂ in the presence of each borane but formation of the desired product **2.2** was not enhanced. Given the lack of success thus far, attention was turned to varying solvents and other reaction conditions for the *F*-BODIPY synthesis utilizing 1 equiv. of BF₃•OEt₂ in the absence of a base.

2.6 - Effect of solvent and temperature on the reaction.

To gauge the effect of the reaction solvent on the synthesis of BODIPY using 1 equiv of BF₃•OEt₂, the reaction according to **Table 1** was performed multiple times with variations in solvents and temperature in pursuit of securing the best yielding conditions. To this end, the free base **2.1** was dissolved in the anhydrous solvent and the solution was treated with 1 equiv of BF₃•OEt₂ for the allocated reaction time. The reaction solvent was removed *in vacuo* and the crude residue was analyzed using ¹H NMR spectroscopy in the presence of benzene as an internal standard. The *F*-BODIPY was formed in trace amounts in most of the solvents. However, 50% conversion was observed for the reaction conducted in toluene. However, when toluene was used, the TLC before

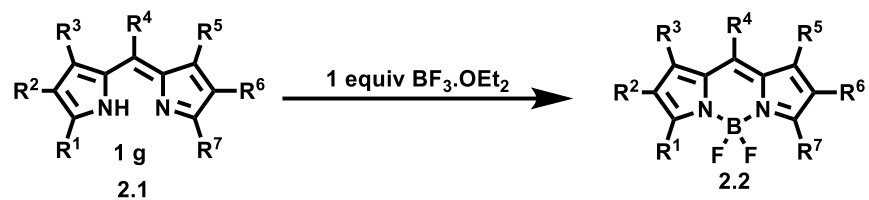
concentration in vacuo had a vibrant red/orange spot with a green hue that is typical for *F*-BODIPYs but after concentration in vacuo, the TLC analysis reviewed a much paler spot at the same r_f value. We speculated that because the toluene has a very high boiling point, the product was decomposing to the non-complexed material during evaporation of the solvent in vacuo. The suitability of other solvents and solvent mixtures for this reaction were thus explored (**Table 4**).

Entry	Solvent/s	Volume/mL	Time/min	Temp.	2.2 ^a	Non-complexed material ^a
1	CH ₂ Cl ₂	3	10	rt	21	79
2	Et ₂ O	3	10	rt	0	100
3	CH ₃ CN	3	10	rt	0	100
4	THF	3	10	rt	0	100
5	hexanes	3	10	30	33	67
6	CH ₂ Cl ₂ :THF	5:1	3	30	trace	88
7	CH ₂ Cl ₂ :hexanes	5:1	3	30	69	31
8	toluene:CH ₂ Cl ₂	5:1	60	30	25	75

Table 4: Screening of different reaction conditions for the synthesis of F-BODIPYs. ^aratio.

For the various reaction conditions screened, the use of hexanes (**Table 4, entry 5**) resulted in a, enhanced conversion, even though the free base **2.1** did not fully dissolve but was suspended in

the hexanes. This result was encouraging, hence it was speculated that the complete dissolution of the free base **2.1** would increase conversion to the desired *F*-BODIPY **2.2**. The free base (50 mg) was therefore dissolved in 1 mL of anhydrous CH₂Cl₂. Anhydrous hexanes (5 mL) was then added to this solution (**Table 4, entry 7**). Treatment of the reaction mixture with 1 equiv. of BF₃•OEt₂ gratifyingly resulted in the formation of the desired product in 69% yield and these conditions showed promise for the general synthesis of *F*-BODIPYs. To demonstrate the utility of these newly established conditions, a variety of *F*-BODIPYs with various substitution patterns were synthesized. The starting dipyrrens were synthesized as HBr salts and then deprotonated to their free bases by washing with aq. NaOH. The dipyrren substituted at the meso position with the tolyl substituent was isolated as its free base, as meso-aryl-substituted dipyrrens are generally isolated as such. In each case, the free base was subsequently dissolved in 1 mL of anhydrous CH₂Cl₂, and 5 mL of hexanes was then added. In each case, the reaction mixture was treated with 1 equiv. of BF₃•OEt₂ and stirred for 1-10 minutes, depending on the substrate. After completion of the reaction, as confirmed by TLC, the reaction mixture was then quenched with water and extracted with CH₂Cl₂. The organic layers were combined and dried with Na₂SO₄, concentrated in vacuo and the crude reaction mixture was dissolved in CH₂Cl₂ followed by filtration through a pad of silica to afford the desired *F*-BODIPY. After the BODIPY had been collected, the silica was then washed with ethyl acetate to afford the HBF₄ salt after removal of solvent from the resulting filtrate.



Entry	BODIPY Product	Yield
1		51
2		39, 58 ^a
3		21
4		25
5		38

Table 5: Synthesis of F-BODIPYs using 1 equiv $\text{BF}_3 \cdot \text{OEt}_2$, ^aIn the presence of 1 equiv NEt_3 .

The new method was tolerated by the alkyl-substituted substrates, for which *F*-BODIPYs were isolated in 51% and 39% yield, and the toluyl substituted dipyrin (**entry 5**) which was isolated in 38% yield. However, dipyrins containing alkanoate (**entry 3**) and conjugate ester (**entry 4**) functionalities were isolated in only 21% and 25 % yield, respectively. Although the yields were lower than for the traditional *F*-BODIPYs synthesis (9 equiv of $\text{BF}_3 \cdot \text{OEt}_2$ and 6 equiv of NEt_3) obtaining 20-50% yield of the product with just 1 equiv of BF_3 in the absence of base, accompanied by a facile purification and isolation of the free base starting material as its HBF_4 salt, is a satisfactory result. On a small scale, the traditional methodology for the synthesis of *F*-BODIPY and the hydrous method established in the Thompson lab⁴³ poses no problems as the workup and purification are somewhat simple. However, on a larger scale, above 1 g, the unwanted $\text{BF}_3 \cdot \text{NEt}_3$ adduct is formed in significant amounts, particularly considering the excess reagents used. As such, the workup becomes more difficult as complex emulsions are usually witnessed.⁷¹ Since the synthesis with 1 equiv of $\text{BF}_3 \cdot \text{OEt}_2$ does not include the use of a base, no unwanted adduct would be formed and thus the workup would be relatively simple and thereby making it a method of choice for larger-scale syntheses. To this end, the three methods were compared on a 1 g scale, making note of reaction time, the total amount of solvent required for workup and the total amount of waste solvent during purification. The use of 1 equiv of $\text{BF}_3 \cdot \text{OEt}_2$ in the absence of base proved to be advantageous as the reaction only took up to 10 minutes and the workup was also fast as no emulsions were observed – unlike for the other methods where mild emulsions were observed. Overall waste was the least for the method involving 1 equiv $\text{BF}_3 \cdot \text{OEt}_2$ in toluene, and the absence of base or scavenger, because purification only required filtration through a pad of silica, eluting with CH_2Cl_2 to provide the *F*-BODIPY product followed by elution with hexanes to obtain the HBF_4 dipyrin salt.

Method	Total reaction time			Total waste		2.2 yield
	Reaction/ hr	Work up/ min	Purification/ min	Work up/mL	Purification/ mL	
Traditional method (anhydrous) ³⁰	2.5	26	35	1440	358	53 ^a
Hydrous method ⁴³	2.5	37	58	1730	620	86 ^b
1 equiv method (developed herein)	10 min	23	19	1320	234	30 ^c

^aNEt₃, CH₂Cl₂, N₂ atmosphere, ^bNEt₃, CH₂Cl₂, air, ^cCH₂Cl₂:Hexanes (1:5), N₂ atmosphere

Table 6: Comparison of the synthesis of F-BODIPY using 9 equiv BF₃·OEt₂ and 6 equiv NEt₃ (anhydrous), 18 equiv BF₃·OEt₂ and 12 equiv NEt₃ (hydrous method) and 1 equiv BF₃·OEt₂ (1 equiv method).

2.7 - Conclusion.

We have investigated the synthesis of F-BODIPY in a continuous flow operation using 1 equiv of BF₃·OEt₂ in the absence of a base. The results confirmed that the reaction of the free-base dipyrin and BF₃·OEt₂ is rapid at the point of mixing. Indeed, by comparing results obtained in batch to those obtained in flow, it was found that there was no significant change in the yields obtained. This suggests that the continuous flow operation failed to eliminate the interaction between the HF produced in situ, with the unreacted BF₃·OEt₂ to form BF₄⁻ and thus the dipyrin HBF₄ salt. We then introduced HF scavengers in batch mode with the hope of counteracting the formation of the

HBF₄ salt and thus the desired *F*-BODIPY would be generated in higher yields. To this end, the use of a variety of additives was explored but none resulted in the generation of the desired product in high yields. Some additives, like TMSPa, resulted in the elimination of the HBF₄ salt but the yield of the BODIPY did not change. We then studied the reaction of the free-base dipyrin and 1 equiv of BF₃•OEt₂ in the presence of various solvents and at various temperatures to discover that the reaction performed moderately well in 1:5 CH₂Cl₂: hexanes at 30 °C. This was however only optimal for the alkyl-substituted *F*-BODIPYs, which were formed in moderate yields. A comparison of this new method with the traditional anhydrous method³⁰ and the hydrous method⁴³ on a 1 g scale of free base **2.1** showed that this new method is advantageous from an economic point of view as it requires only 1 equiv of BF₃ and reduced volume of solvent for purification. This method only takes 10 min for the reaction to reach completion, unlike for the other methodologies which take 2.5 and 3 hours.⁴³

2.8 – Experimental.

All chemicals were used as received unless otherwise indicated. All NMR spectra were recorded using 500 MHz or 300 MHz spectrometers. ¹H chemical shifts are reported in ppm relative to tetramethylsilane using chloroform solvent residual at $\delta = 7.26$ ppm as an internal standard. ¹³C spectra were recorded using UDEFT pulse sequence with chemical shifts reported in ppm referenced to CDCl₃ resonance at $\delta = 77.2$ ppm. Splitting patterns are indicated as follows: br, broad; s, singlet; d, doublet; t, triplet; q, quartet; m, multiplet. All coupling constants (*J*) are reported in Hertz (Hz). High-resolution mass spectra were obtained using TOFMS experiments operating in both positive and negative modes. Column chromatography, as indicated, was

performed using 230-400 mesh ultra-pure silica. Pyrrole **2.4**,⁵⁰ **2.5**,⁵¹ and dipyrin **2.0**,⁵² **2.1**,⁹ were prepared according to literature procedures.

General Procedure for the synthesis of *F*-BODIPY with 1 equiv. of BF₃•OEt₂ in a batch process (GP1).

The free-base dipyrin **2.1** (50 mg, 0.20 mmol) was dissolved in anhydrous toluene (3 mL) under a nitrogen atmosphere and BF₃•OEt₂ (25 μL, 0.20 mmol) was added to the solution. The reaction mixture was then stirred for 10 min at room temperature. The crude reaction mixture was quenched by the addition of H₂O, followed by an extraction with CH₂Cl₂ (30 mL, x 3). The combined organic fractions were then washed with aqueous NaHCO₃ (x 3), resulting in the dissolution of the crude product in the organic layer which was then dried over Na₂SO₄ and concentrated in vacuo. Hexane was added to the concentrated crude product to form a suspension which was then filtered over a pad of celite. Rinsing with excess hexanes and concentration of the resulting fraction in vacuo afforded the *F*-BODIPY **2.2** as a deep red solid. The celite pad was re-washed with excess CH₂Cl₂ and the resulting fraction was concentrated in vacuo to isolate the HBF₄ dipyrin salt **2.3** as a bright orange solid.

General Procedure for the synthesis of *F*-BODIPY with 1 eq. of BF₃•OEt₂ in a continuous flow process (GP2).

The free-base dipyrin **2.1** (50 mg, 0.20 mmol) was dissolved in anhydrous CH₂Cl₂ (1.5 mL) under a nitrogen atmosphere in a pear-shaped bottom flask. In another pear-shaped flask, BF₃•OEt₂ (25 μL, 0.20 mmol) was dissolved in anhydrous CH₂Cl₂ (1.5 mL) under a nitrogen atmosphere. The

solutions were each loaded into 3 mL syringes and nitrogen gas was then used to fill the extra volume of the syringe to keep the mixture under a nitrogen gas environment. This was done by pulling some of the nitrogen gas from the bottle of anhydrous solvent which was placed under a nitrogen gas environment. Both reagents were then pumped, at the same flow rate, and combined at a T-piece mixer. The combined stream was directed to a 30 cm (0.06 mL) PFA flow reactor coil at room temperature. The crude reaction mixture was quenched in H₂O followed by an extraction with CH₂Cl₂ (30 mL, x 3). The combined organic fractions were then washed with aqueous NaHCO₃ (x 3), resulting in the dissolution of the crude product in the organic layer which was then dried over Na₂SO₄ and concentrated *in vacuo*. The resulting residue was dissolved in CDCl₃ (4 mL), and benzene (4 mL) was added, with stirring. An aliquot (200 μL) of this solution was added to an NMR sample tube and then diluted with CDCl₃ (400 μL). A ¹H NMR spectrum of the sample was collected, and the NMR-based yield was determined.

Chapter 3 – Towards an Improved Synthesis of Aza Dipyrrins.

3.1 - Introduction.

As mentioned in Chapter 2, one essential requirement for fluorescence bioimaging/detection is a high-performance organic material (fluorophore) with good absorption and emission that is located in the red to deep red region of the electromagnetic spectrum (near-infra-red, NIR, 650–900 nm). When light enters body tissues it is either scattered or absorbed, and the extent of both processes depends on tissue type and wavelength of the light. The light absorption characteristics of tissues decrease with increasing wavelength, hence longer wavelengths of light penetrate more efficiently through tissue.^{72,73} The shorter wavelengths (<650 nm) have less tissue penetration and are mostly absorbed, resulting in a variety of physiological damage. Therefore, ideal tissue permeability of light occurs within the wavelength range of approximately 650-900 nm, known as the “phototherapeutic window”.⁷⁴ A good fluorophore should preferably have strong absorbance in this phototherapeutic window, where light penetration into the body tissue is maximized. Therefore for bio-imaging in living organisms, the BODIPY framework offers significant potential.^{75,76,77,78} Though BODIPY dyes are promising for use in bio-imaging, the absorption maxima of conventional BODIPY dyes are generally below 700 nm. For BODIPY dyes to be more useful as fluorescent probes and sensors in bioapplications, their absorption should lie in the near-infrared region (650-900 nm).^{79,80} In recent years, studies regarding the BODIPY family have enabled several promising strategies to efficiently push the absorption and emission of BODIPYs to the far-red and NIR regions. One such strategy involves increasing the extent of conjugation of the BODIPY core. Generally, increasing molecular conjugation enhances π -electron delocalization, which facilitates a shift of absorption and emission maxima into the NIR

regions.^{81,82} An alternative strategy to designing systems capable of absorbing in the NIR region involves the use of aza BODIPYs. Aza BODIPYs are a class of BODIPYs that derives from conventional BODIPYs by replacement of the *meso*-carbon with a nitrogen atom (N). Incorporation of the *meso*-nitrogen atom in aza BODIPYs results in a LUMO that is significantly stabilized compared to that in BODIPYs.^{83,39}

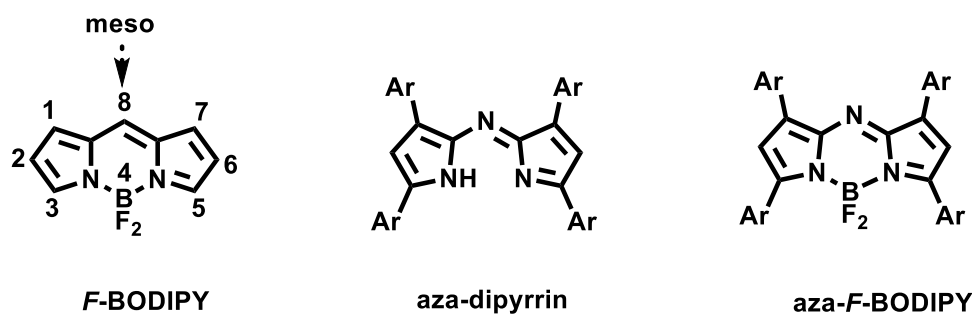
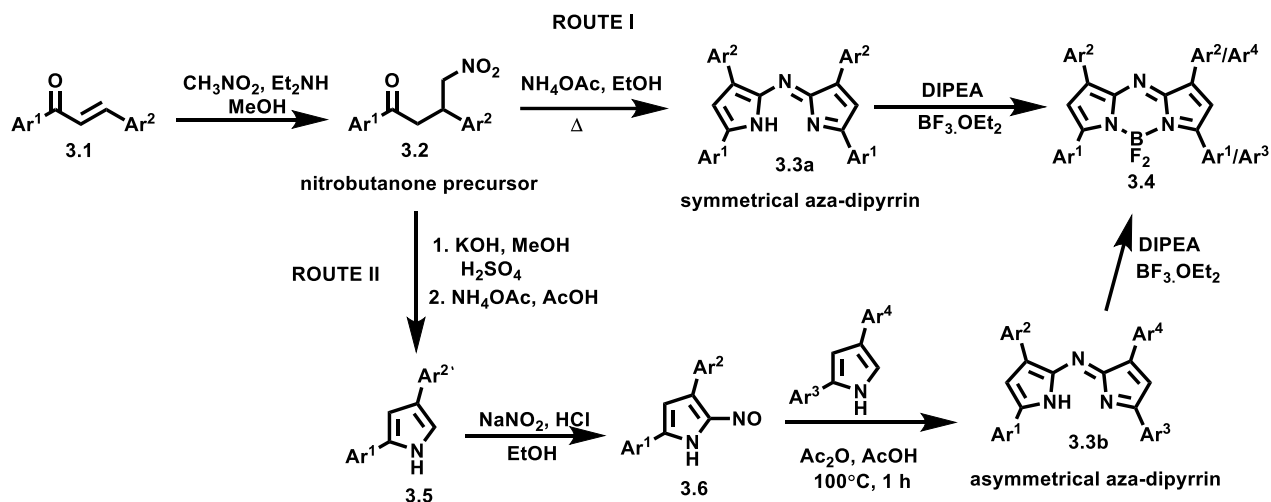


Figure 11: Structures of F-BODIPY, aza dipyrin and aza F-BODIPY cores.

The HOMO–LUMO energy gap in aza BODIPYs is significantly smaller than that in BODIPYs, which leads to absorption and emission at longer wavelengths. Indeed, aza BODIPYs generally absorb and emit bathochromically, with a significant increase of about 100 nm, compared to the parent BODIPY bearing an equivalent substitution pattern. Modest fluorescence quantum yields⁸⁴ and excellent photostability generally accompany these desirable properties of aza BODIPYs.^{33,85,86,87,13} Consequently, the aza BODIPY framework is promising for use in fluorescence bioimaging. Furthermore, the long absorption wavelengths and good photostability make aza BODIPYs suitable for use as sensitizers for photodynamic therapy (PDT) applications.⁸⁸ Photovoltaic applications also benefit from long wavelength absorbance, allowing for harvesting a large portion of solar energy.⁸⁹

3.2 - Synthesis of aza BODIPYs.

Applications utilizing aza BODIPYs rely on the availability of aza dipyrrens, which were first reported in 1943 as unexpected deep blue, coloured products.⁸⁹ There are two classes of aza dipyrrens, differing in their substitution patterns about the pyrrolic rings. The most common class features a tetra-aryl substitution pattern. The synthesis of aza dipyrrens bearing a tetra-aryl substitution pattern begins with the aldol condensation of benzaldehydes and acetophenones to form the chalcones **3.1** (Scheme 6).⁹⁰ Subsequent 1,4-Michael addition of nitromethane to chalcones yields the nitrobutanone derivatives **3.2**, which are the common precursors of the two known routes to this class of aza dipyrrens. The first route involves the condensation of the nitrobutanone derivatives **3.2** in the presence of an excess of an ammonium source (up to 40 equiv), heated at reflux temperature in ethanol for reaction times of up to 48 h resulting in the formation of the aza dipyrren **3.3a** (Scheme 6, Route I). Generally, the aza dipyrren precipitates from the reaction mixture and can be easily collected by filtration, or purified by chromatography. This route results in symmetrical aza dipyrrens with yields usually around 20-50%.⁹⁰



Scheme 6: Synthesis of aza dipyrrens **3.3a**, **3.3b** and aza BODIPY **3.4**.

To accommodate different functional groups in the aza dipyrin framework, for fine-tuning both spectroscopic and solubility properties of the compounds and allowing the introduction of specific functional groups for molecular sensors and bioconjugated analogs, the asymmetric route is often utilized (**Scheme 6, Route II**).⁹¹ In this approach, 2,4-diaryl pyrrole **3.5** is synthesized first from the same nitrobutanone precursor **3.2**, followed by a subsequent reaction with sodium nitrite in the presence of ethanolic HCl to form nitroso pyrroles **3.6** (**Scheme 6**). These conditions do not allow alkyl-substituted pyrroles to be nitrosylated. Cross-condensation of pyrroles **3.5** and nitroso pyrroles **3.6**, under elevated temperature in acetic acid and acetic anhydride, results in the formation of the asymmetric aza dipyrin **3.3b**. Prefunctionalization of the pyrroles offers access to both symmetrical and non-symmetrical aza dipyrins in moderate to high yields.⁹¹ The popular boron derivatives aza BODIPYs (**3.4**) can be synthesized from **3.3a** and **3.3b**, using boron trifluoride etherate in the presence of a base.⁸⁹ The two routes, I and II, have been widely employed to prepare tetra-aryl aza BODIPYs.

Another class of the aza dipyrin family is the β,β - (**3.7**) or β,α - (**3.8**) ring-fused annulated framework as shown in **Figure 12**. This type of aza dipyrin framework absorbs further bathochromically compared to the tetra-aryl aza dipyrins shown in **Scheme 6**.⁸¹ This is due to the higher coplanarity and higher rigidity, causing enhanced conjugation.¹³

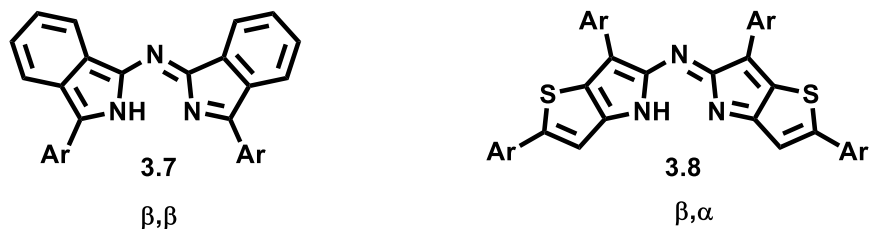
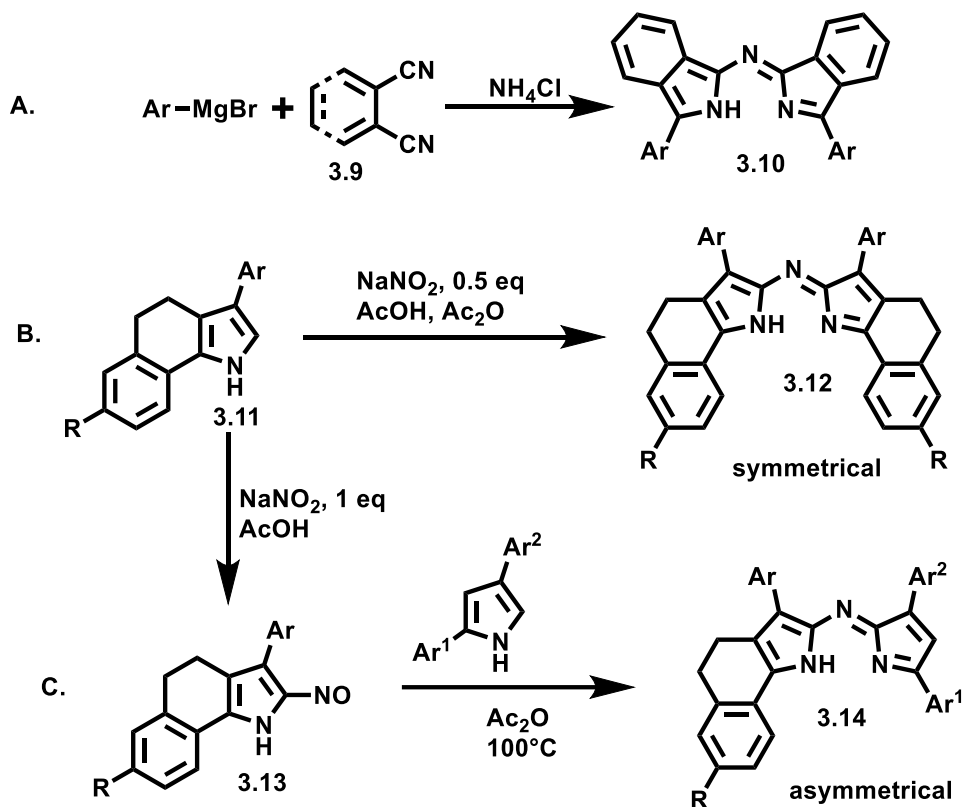


*Figure 12: Conformationally restricted β,β aza dipyrins **3.7** (left) and β,α aza dipyrin **3.8** (right).*

Synthesis of the annulated aza dipyrins **3.7** involves the addition of aryl Grignard reagents to dinitriles (phthalonitriles) **3.9** (Scheme 7, A),⁹² followed by the addition of excess aqueous ammonium chloride. This route is inefficient in most cases, leaving starting materials unconsumed, observation of complex mixtures of by-products, and low aza dipyrin yields.⁹³ An adaptation of the approach involving condensation of an α -free pyrrole and a nitroso pyrrole has been reported for producing conformationally restricted aza dipyrins,⁸⁴ e.g. symmetric aza dipyrin **3.12** and asymmetric aza dipyrin **3.14** (Scheme 7, B and C). For the synthesis of the symmetric aza dipyrin **3.12**, a one-pot reaction of the aryl-constrained pyrrole **3.11** with 0.5 eq of NaNO_2 in acidic media is utilized.⁹⁰ In this approach (Scheme 7, B), half of the pyrrole **3.11** is converted, under acidic conditions, to the nitrosopyrrole in situ, and then immediately condenses with the original pyrrole to yield the aza dipyrin **3.12**. On the contrary, the asymmetric synthesis of aza dipyrin **3.14** (Scheme 7, C), involves first the generation and isolation of nitrosopyrrole **3.13**, followed by the addition of a second pyrrole bearing different substituents.⁹⁰



Scheme 7: Synthesis of conformationally restricted aza dipyrins 3.10, 3.12 and 3.14.

Despite the growing importance of aza BODIPYs, all the synthetic methods to the parent aza dipyrins only support arylated systems.⁹⁴ Unfortunately, the presence of numerous aromatic rings in the aza BODIPYs causes aggregation. The presence of π -stacking in these multi-aryl systems results in poor water solubility that limits their application in bioapplications and clinical translation despite their good photochemical properties.⁸⁸ Indeed, the conventional aza BODIPY is hydrophobic. For use in biological systems, the size and hydrophilicity of aza BODIPYs need to be improved without significant loss of valuable photophysical characteristics.⁹⁴ The rotation of the bulky aryl groups in aza BODIPYs and BODIPYs, in the excited states results in the dissipation of energy via thermal relaxation. This leads to low fluorescent Φ_F values when compared with those of many conventional alkyl-substituted BODIPYs.⁹⁵ For instance, alkyl-substituted BODIPYs

such as **3.15** are well-known (**Figure 13**).⁹⁶ These emit strongly in the 510 nm region. However, complementary aryl-substituted BODIPYs **3.16** absorb at longer wavelengths (588-626 nm) (**Figure 13**) with extinction coefficients and the fluorescence quantum yields are significantly lower than that of the alkyl-substituted variant **3.15**. A possible rationale for the reduced quantum yields of the aryl-substituted variants such as **3.16** relative to the alkyl-substituted systems (**3.15**), is that energy is lost from the excited state via thermal pathways involving rotation of the aryl substituents. The ability to tune substitution about the dipyrin framework is highly advantageous for improving the applicability of the aza BODIPYs. For instance, introducing the alkyl substitution to the aza BODIPY framework will reduce the thermal relaxation pathways brought about by the free rotation of the aryl substituents, and reduce π -stacking which would serve to reduce the aggregation and solubility problems.

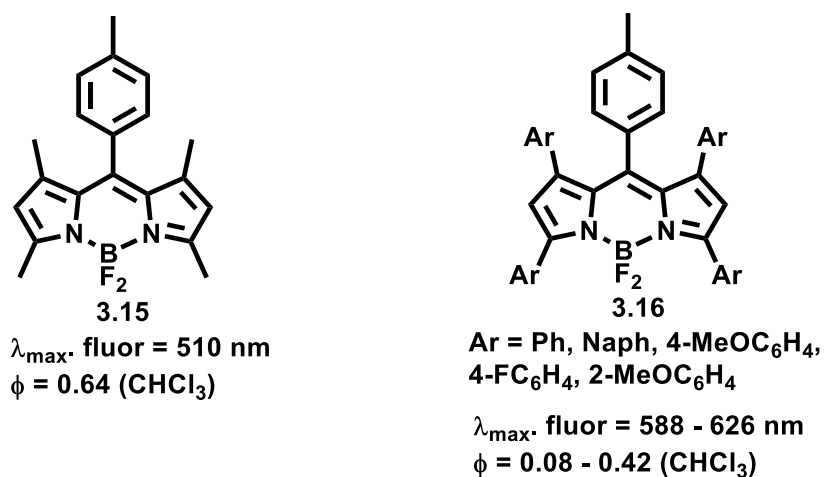


Figure 13: Chemical structure and photophysical properties of representative BODIPYs 3.15 and 3.16.

Attempts to synthesize alkyl-substituted aza dipyrins such as **3.17** (**Figure 14**) have been reported though all have been unsuccessful.⁹⁷ Polyalkylated aza dipyrins cannot be synthesized by any known methods. There is only one reported aza dipyrin that is not exclusively aryl-substituted. It

features methyl groups on the β -positions of the pyrrolic units **3.18** (**Figure 14**) and phenyl rings on the α -positions, as demanded by synthetic routes. Leaving the α -positions unsubstituted or with non-aryl substituents results in the failure of the aldol condensation that is key to the synthesis of aza dipyrins (**Scheme 6**).⁹⁷

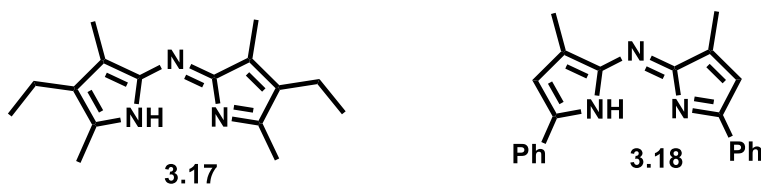
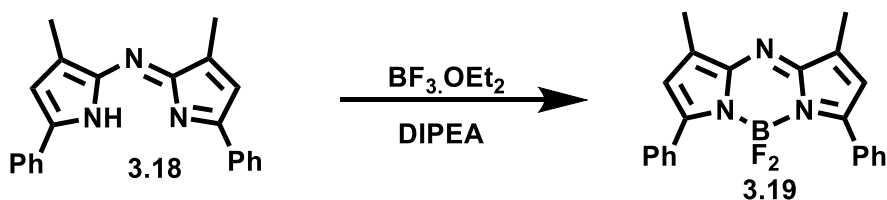


Figure 14: Hypothetical exclusively alkyl-substituted aza dipyrin 3.17 (left) and β,β methyl-aza dipyrin 3.18 (right).

The lack of derivatives beyond the extensively arylated aza dipyrins, a consequence of the limited synthetic approaches, substantially limits the applications of aza BODIPYs in bioapplications. The installation of the *meso* aza N atom is a major challenge. The high temperatures and acidic media along with long reaction times and excess ammonia used in the described approaches (**Scheme 6** and **Scheme 7**), only allow for aryl substituted starting materials, particularly on the α -positions. Furthermore, the α -nitrogenated pyrrole intermediates lack stability, potentially leading to unproductive pathways that are most detrimental in the very reactive alkyl-substituted pyrroles. A new pathway, that avoids the generation of these unstable α -nitrogenated pyrroles for the installation of the *meso* N-atom, is highly desirable. Ideally, a new pathway would allow for variation of substitution about the pyrrolic units of the aza dipyrin.

Taken together, the methods described above (**Scheme 6** and **Scheme 7**) provide a foundation for synthesizing the majority of aza dipyrin derivatives with the preferred route being the condensation of nitrobutanones with excess ammonium acetate (**Scheme 6, Route I**). A comprehensive mechanistic study⁹⁸ of this route indicates the formation of a mixture of mono-, di-

, and tri-labeled species representative of a more complex process which has been shown to be non-viable in alkyl-substituted aza dipyrrens. Furthermore, the high-yielding route to aza dipyrrens through nitroso pyrroles and α -free pyrroles, though simple, cannot be translated to alkyl-substituted pyrroles as the acid-mediated nitrosylation is only successful in pyrroles bearing aryl substituents. However, and as motivation for this thesis, complexation of the alkyl-bearing aza dipyrren **3.18** (Scheme 8) with $\text{BF}_3 \cdot \text{OEt}_2$ and *N,N*-diisopropylethylamine (DIPEA) in CH_2Cl_2 led to aza BODIPY **3.19** with improved solubility and excellent NIR photophysical properties in organic and aqueous solutions compared to its all aryl-substituted counterparts. These results are encouraging indications that alkyl-substituted aza BODIPYs could be adapted for in vitro and in vivo NIR fluorescence imaging.⁸⁷ Development of synthetic routes to enable the preparation of aza dipyrrens with a wide variety of substitution patterns is therefore desirable.



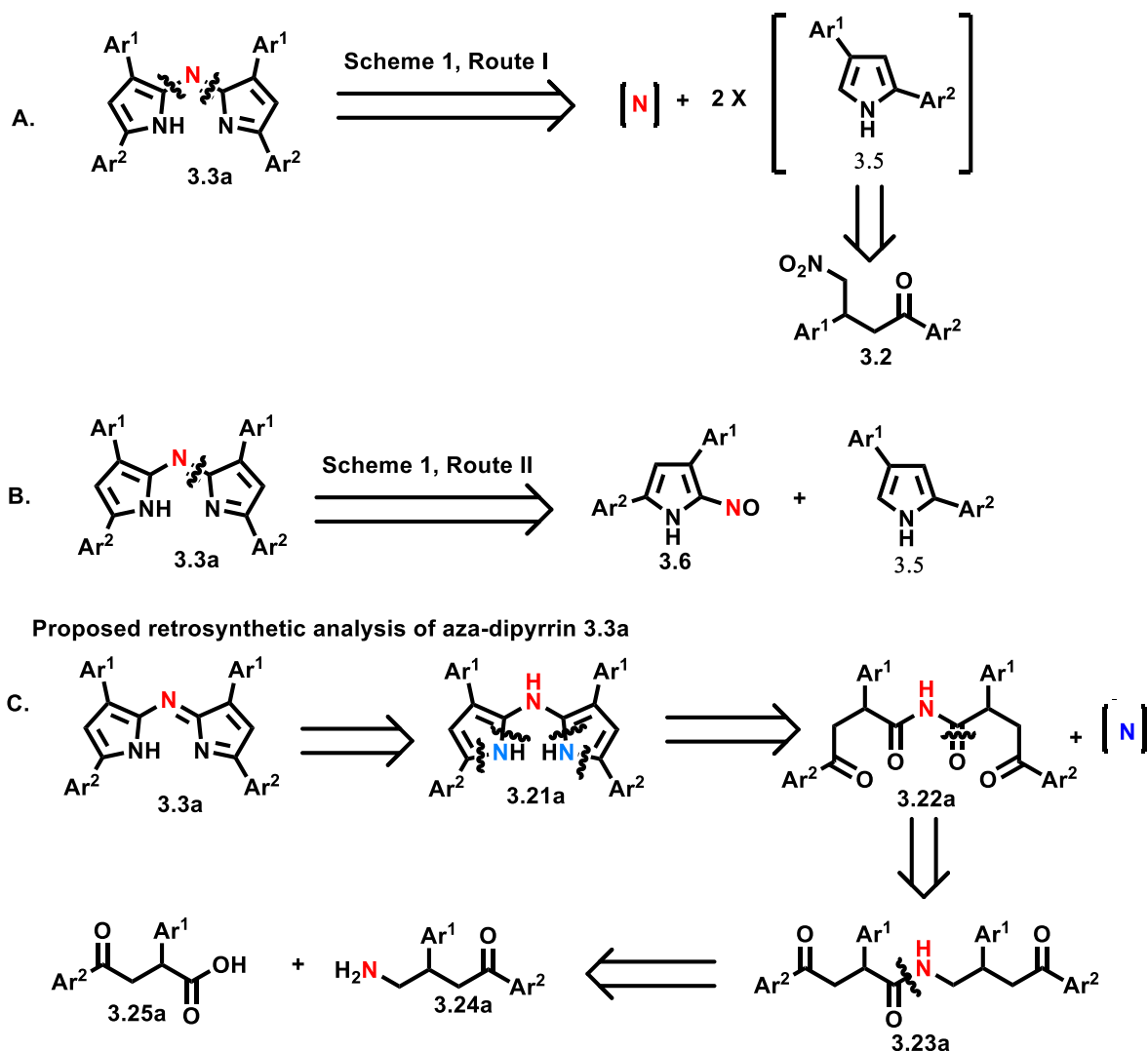
Scheme 8: Synthesis of alkyl-substituted aza BODIPY 3.19.

3.3 - Project goals.

This project aims to explore synthetic routes toward aza dipyrrens that accommodate the introduction of a variety of substituents about the pyrrolic units. This study focuses on the development of synthetic methodology toward aza dipyrrens with a particular interest in less and non-arylated aza dipyrrens i.e. alkyl-substituted aza dipyrrens. If successful, this study will provide a route for the synthesis of aza dipyrrens of various substitution patterns which will then be used to synthesize aza BODIPY complexes. Photophysical properties of these aza BODIPYs will then be investigated, including solubility, aggregation, and optical properties and the suitability thereof for future clinical translation.

3.4 - Synthetic strategy for aza dipyrrens.

Retrosynthetic analysis of the tetraaryl aza dipyrrens through the routes shown in **Scheme 6** reveals that the *meso*-N atom is installed onto already-made pyrroles in- or ex-situ. In the approach described in **Scheme 6, Route I**, two molecules of the nitrobutanone **3.2** undergo intramolecular cyclization in situ to form pyrroles. Ammonia from NH₄OAc (the source of the *meso*-N atom) and an α -free pyrrole (**Scheme 9, A**) react to produce the amino pyrrole **3.20**, which reacts with another equivalent of the α -free pyrrole to furnish the aza dipyrren.⁹⁸ On the other hand, in **Scheme 6, Route II**, the nitrobutanone **3.2** also undergoes intramolecular cyclization to form pyrrole, which is then isolated and separately reacted with NaNO₂ to install the *meso*-N via the isolated α -nitrogenated nitrosopyrrole **3.6** (**Scheme 9, B**). The nitrosopyrrole then reacts with another equivalent of α -free pyrrole to afford the aza dipyrren. Clearly, the late-stage installation of the *meso*-N atom, after pyrrole formation, is a limitation in these routes to aza dipyrrens. The conditions required to produce unstable α -nitrogenated pyrroles are harsh and non-selective, and cannot be translated to non-aryl substitution patterns. Preinstallation of the *meso*-N atom before the formation of the pyrrolic units offers an alternative approach to the synthesis of aza dipyrrens.

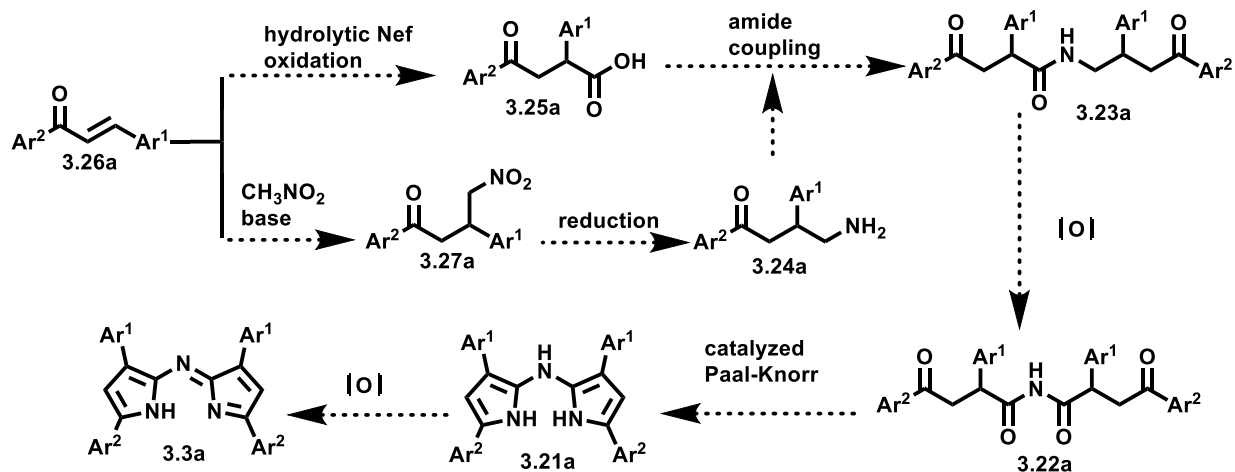


Scheme 9: Retrosynthetic analysis of tetraaryl aza dipyrin 3.3a.

Cognizant of this possibility, a previous researcher in the Thompson group proposed a strategy wherein an appropriately substituted 4,4'-diketomide **3.22a** (Scheme 9, C), prepared from the oxoacid **3.25a** and oxoamine **3.24a**, might be converted to a dipyrrolamine **3.21a** via a double Paal-Knorr cyclization. The dipyrrolamine **3.21a** could then be oxidized to aza dipyrin **3.3a**, either in air or via the use of a supplementary oxidant such as DDQ or *p*-chloranil. Using this disconnection strategy, strategic insertion of the meso-N atom would be achieved prior to the formation of the

pyrrolic framework courtesy of imide **3.22a**. This strategy takes advantage of the Paal- Knorr cyclization, an extremely robust method already demonstrated to convert almost all 1,4-diketones to their corresponding heterocycles.^{99,100} In this strategy, the source of the meso-N atom is the central imide within **3.22a** (**Scheme 9, C**), therefore, avoiding the unstable α -nitrogenated pyrroles that currently limit the pathways to aza dipyrrens. Furthermore, the two halves of the imide may be functionalized separately and then coupled to result in asymmetric aza dipyrrens.

There are several possible routes to imides depending on the desired substitution patterns. Synthetically, **3.24a** and **3.25a** become targets. For the synthesis of **3.24a** and **3.25a** (**Scheme 10**), diaryl chalcone **3.26a** was chosen as the starting point, given reports⁹¹ of successful hydrolytic Nef oxidation and Micheal addition chemistry. As discussed in section **3.2**, chalcones are readily prepared by an aldol/dehydration reaction of the corresponding benzaldehyde and acetophenone.⁹⁰ As shown in **Scheme 10**, the chalcone **3.26a** can readily undergo oxidation to the oxoacid **3.25a** and nitromethylation gives nitrobutanone **3.27a**. For the disconnection in **Scheme 9, C** to be feasible, nitrobutanone **3.27a** might then be reduced to oxo-amine **3.24a**. The oxoacid **3.25a** and the oxo-amine **3.24a** could then be coupled to give the amide **3.23a**, then oxidized to the target imide **3.22a**.^{101,102} The imide **3.22a** might then be cyclized under Paal-Knorr conditions to produce the dipyrrolamine **3.21a**, ready for oxidation to provide the target aza dipyrren **3.3a**.



Scheme 10: Proposed synthesis of aza dipyrins 3.3a via imide 3.22a.

3.5 - Exploration of the proposed strategy.

To investigate the viability of this proposed strategy, the initial target was the stable tetraphenyl-substituted aza dipyrin **3.3b** (Figure 15), so that the new route could be explored without fear of product instability hampering success.

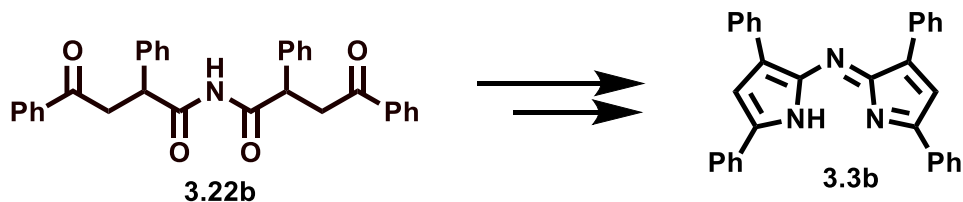
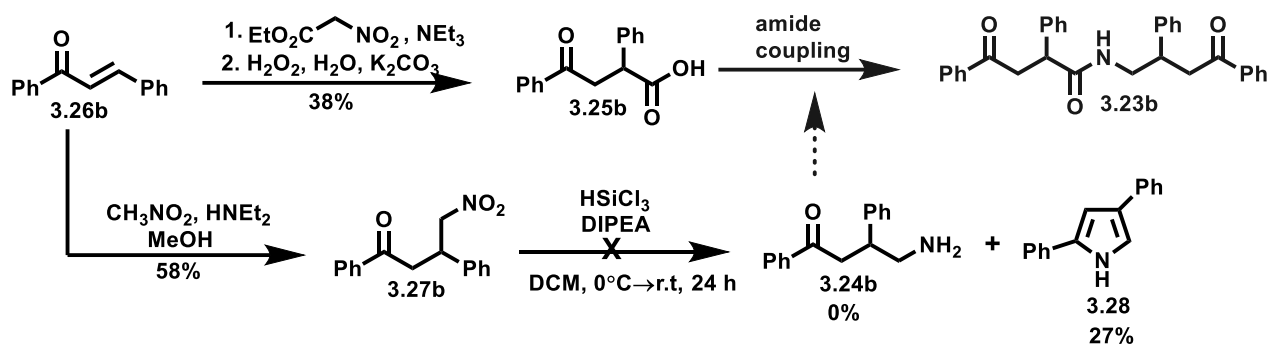


Figure 15: Target aza dipyrin 3.3b for proof of concept via synthesis of imide 3.22b.

To prepare the target imide **3.22b** according to the proposed route in **Scheme 10**, the starting point was chalcone **3.26b** (**Scheme 11**). Chalcone **3.26b** was smoothly converted to oxoacid **3.25b** via the Michael addition of ethyl nitroacetate followed by Nef oxidation under hydrolytic conditions.¹⁰³ The oxoacid was isolated in a 38% yield as a white solid, and characterized

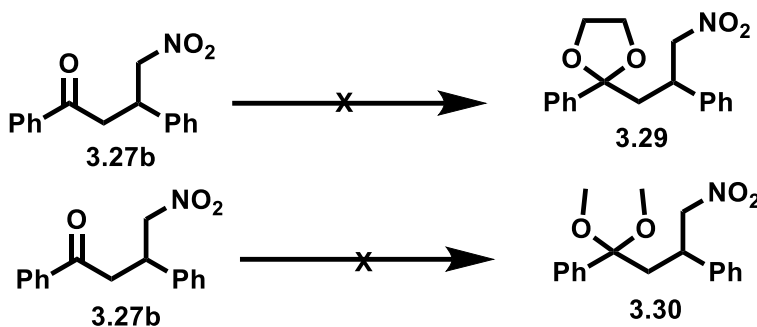
according to ^1H NMR spectroscopic analysis. The chalcone **3.26b** was then converted to nitrobutanone **3.27b**, via the Michael addition of nitromethane, and was isolated in a 58% yield. The next step required the reduction of nitrobutanone **3.27b** to oxoamine **3.24b**. For this reduction, the mild, metal-free, HSiCl_3 -mediated protocol presented by Orlandi et al., was chosen as this was reported to be successful and highly selective for aliphatic nitro compounds.¹⁰⁴ However, treatment of nitrobutanone **3.27b** with HSiCl_3 in the presence of DIPEA did not result in the formation of the desired oxoamine **3.24b**.



Scheme 11: Attempted coupling of oxoacid **3.25b** and oxoamine **3.24b** to amide **3.23b**.

Instead, the reaction resulted in a complex mixture with no spectroscopic evidence of the presence of the desired oxo-amine. Further analysis of the mixture showed the presence of 2,4-diphenyl pyrrole **3.28** (Scheme 11), which was isolated in a 27% yield. The presence of 2,4-diphenyl pyrrole suggested that the nitro group was indeed reduced to the desired oxoamine **3.24b**, and that this material underwent in-situ intramolecular cyclization to provide the pyrrole. To avoid this intramolecular cyclization, attempts were made to protect the ketone of **3.27b** before the reduction of the nitro group. Attempts to form the propylene glycol acetal **3.29** (Scheme 12), catalyzed by hydrochloric acid or triethyl orthoformate/tetrabutyl ammonium tribromide,¹⁰⁵ and attempts to

form dimethyl acetal **3.30** using methanol and *p*-toluenesulfonic acid, were unfruitful and instead resulted in the recovery of starting material. The protection of the ketone was unsuccessful, presumably because the ketone is insufficiently electrophilic.¹⁰⁵

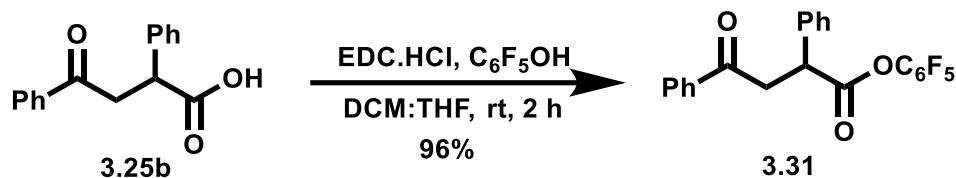


*Scheme 12: Attempted protection of nitrobutanone **3.27b** by the generation of the acetal **3.29** and dimethyl acetal **3.30**.*

Given that the oxoamine **3.24b** could not be isolated, the proposed strategy (**Scheme 11**) wherein the oxoacid **3.25b** is coupled with the oxoamine **3.34b** could not be pursued. Therefore, a new strategy was proposed wherein the oxoamine **3.24b** would be trapped in situ by a more reactive carboxylic acid surrogate, such as an activated ester, thus avoiding intramolecular cyclization to form the pyrrole. Various carboxylic acid surrogates have been used as acylating substrates to enhance the atom- and step-economies of amidation.^{106,107} Among them, activated aryl esters are common since they are often crystalline stable materials, and more electrophilic towards amines, than are the parent carboxylic acids, producing fewer side reactions during coupling.¹⁰⁷ To evaluate this strategy, the pentafluorophenyl (PFP) active ester **3.31** (**Scheme 13**) was chosen, as it is readily synthesizable, stable, has good organic solubility and has been useful for making amides (**Scheme 13**).^{108,109,110} The presence of active ester **3.31** in the reaction mixture undergoing reduction of nitrobutanone **3.27b** would hopefully limit intramolecular cyclization to form pyrrole **3.28**.

instead, **3.27b** which would react in situ, with excess active ester **3.31** to form amide **3.23b**, thus potentially outcompeting the unproductive intramolecular cyclization.¹⁰⁹

The desired pentafluorophenyl-activated ester **3.31** (**Scheme 13**) was synthesized by treatment of oxoacid **3.25b** with EDC.HCl and pentafluorophenol.¹¹¹ Ester **3.31** was isolated in a 96% yield after purification via column chromatography. The colourless oil solidified to a white solid upon standing,. Confirmation of structure was achieved by NMR analysis and X-ray crystallography. The crystal structure of the active ester is shown in **Figure 16**, clearly demonstrating incorporation of the pentafluoro moiety.



Scheme 13: Synthesis of active ester 3.31.

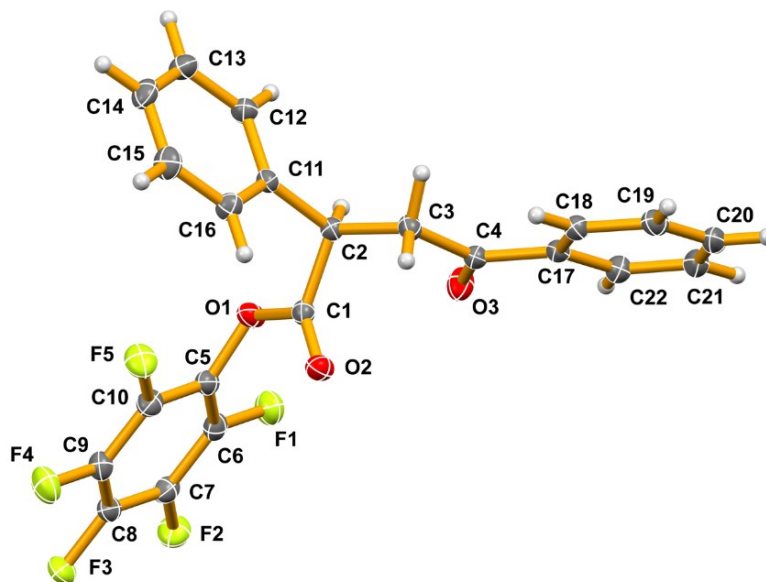
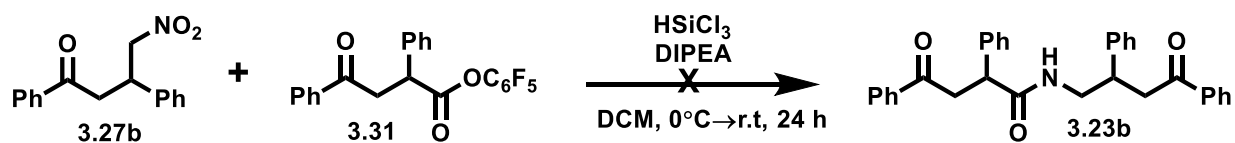


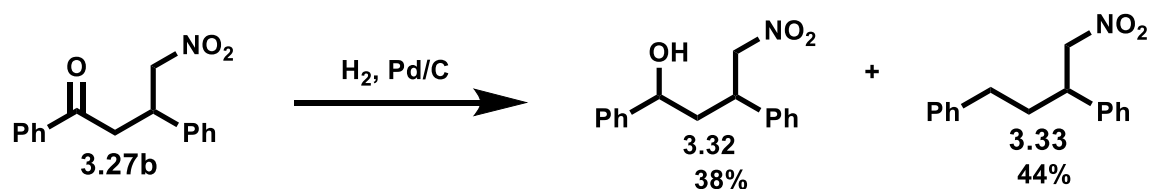
Figure 16: ORTEP diagram of ester 3.31. Thermal ellipsoids are shown at 50% probability.

The reduction of nitrobutanone **3.27b** was repeated, this time in the presence of the active ester **3.31**. Reduction using HSiCl_3 conditions was again employed, given that these conditions had been successful in reducing the nitrobutanone **3.27b** to the oxoamine **3.24b** (Scheme 11), even though intramolecular cyclization was observed. The reaction of nitrobutanone **3.27b** (Scheme 14) with HSiCl_3 in the presence of the active ester **3.31** resulted in partial consumption of both starting materials, as observed by TLC analysis. A new vibrant yellow spot was observed on the baseline of the TLC plate when stained with bromocresol green. A white precipitate was formed upon quenching the reaction mixture with NaHCO_3 , and this was affiliated with the aqueous layer during work-up. The white precipitate was collected via filtration. Efforts to identify this material were unsuccessful because this solid was not soluble in common organic solvents (CH_2Cl_2 , CDCl_3 , DMSO, CH_3CN , MeOH, EtOAc, and Et_2O). The filtrate was concentrated and purified by column chromatography to recover both the starting materials **3.27b** and **3.31** in 93% and 38% yield, respectively. It was hypothesized that the use of HSiCl_3 was the likely source of the white solid, possibly a polysiloxane, presumably by reaction with the active ester **3.31** and hence the 38% recovery of this active ester. Polysiloxanes are generally insoluble in organic solvents, thereby explaining the insolubility of the isolated white solid.¹¹² The nitrobutanone was recovered quantitatively, suggesting that the HSiCl_3 was not available to react with the nitrobutanone **3.27b**.



Scheme 14: Attempted synthesis of amide 3.23b by coupling of nitrobutanone 3.27b and active ester 3.31.

The consumption of the active ester **3.31** under the HSiCl_3 reduction conditions, suggests that the active ester is not stable under the reduction conditions. Given this challenge, a new system was required in order to perform the chemoselective reduction of nitrobutanone **3.27b** in the presence of other functional groups. To this end, a range of alternative conditions for the selective reduction of the nitro group were screened. Identification of a useful reduction protocol, even if accompanied by cyclization of the resulting oxoamine and formation of the corresponding pyrrole, would enable further attempts to trap the oxoamine with the active ester. Firstly, the reduction of nitrobutanone **3.27** was attempted using hydrogenation in the presence of 10% palladium on carbon, as successfully utilized for the reduction of other nitro groups.¹¹³ Under these conditions, starting material was consumed and the presence of two new spots as confirmed by TLC analysis. Filtration and purification of the reaction mixture afforded two white solids which, upon analysis, were not any of the expected products. The first spot (with a lower R_f relative to the second spot) stained vibrant dark purple with vanillin. Following quenching and workup, the compound corresponding to the first spot was isolated via column chromatography on silica. After analysis via ^1H NMR spectroscopy, the isolated compound was characterized as alcohol **3.32** (Scheme 15). Interestingly, instead of reduction of the nitro group of nitrobutanone **3.27b**, the ketone was partially reduced to an alcohol, generating nitrobutanol **3.32** in a 38% yield.



Scheme 15: Reduction of nitrobutanone 3.27b to nitrobutanol 3.32 and compound 3.33.

A crystal of compound **3.32** was submitted for X-ray crystallography. The structure is shown in **Figure 17**, confirming the presence of the hydroxyl moiety in the compound.

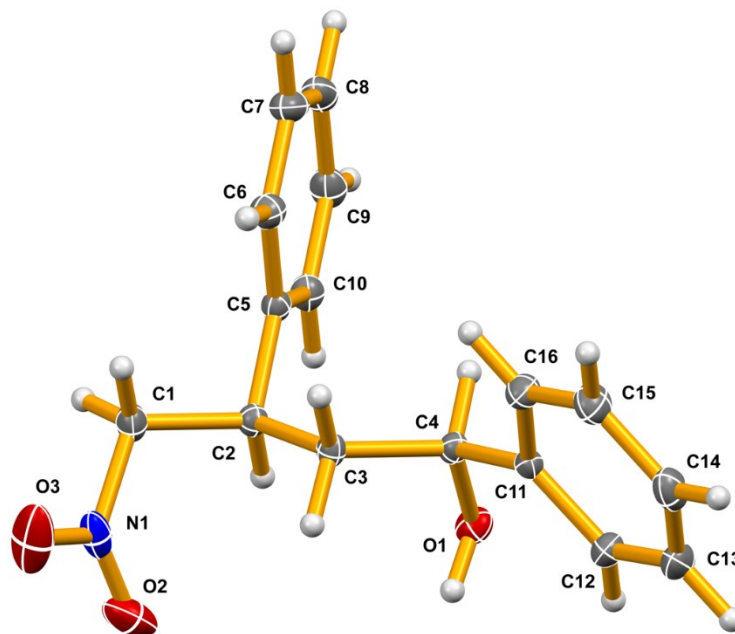
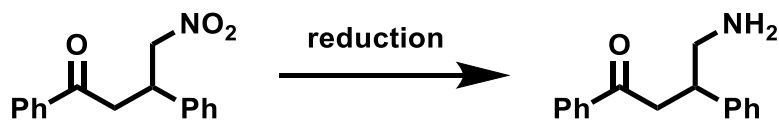


Figure 17: ORTEP diagram of ester alcohol. Thermal ellipsoids are shown at 50% probability.

Analysis of the material corresponding to the second spot (with a higher R_f relative to the first spot) with ^1H NMR spectroscopy and MS spectrometry, revealed compound **3.33** (**Scheme 15**). Interestingly, this was formed through the complete reduction of the ketone. The ortho hydrogen atoms on the phenyl group adjacent to the ketone moiety in **3.2b** are the most deshielded in the ^1H NMR spectrum, but in the isolated product **3.33**, these are less deshielded. Furthermore, the chemical shift for two hydrogen atoms adjacent to the nitro group stayed consistent in the starting material **3.27b** (4.64-4.82 ppm) and the product **3.33** (4.53-4.60 ppm).¹¹⁴ The complete reduction of the ketone was also confirmed by MS spectrometry. Clearly, the ketone was chemoselectively reduced, rather than the nitro group, despite evidence to the contrary. This is not overly surprising

as catalytic hydrogenation using transition metals, though it has received high interest, can exhibit limited selectivity in the presence of other reducible functional groups.¹¹³

Due to the lack of selectivity of the hydrogenation for the nitro group, the reduction of the nitrobutanone **3.27b** was then attempted under other conditions that have been successfully utilized in the chemoselective reduction of nitro in the presence of ketones (**Table 7**).

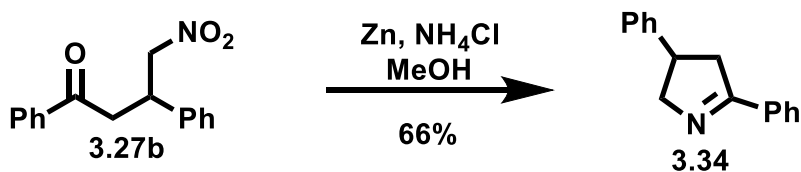


Conditions	Solvent	Time/ h	Temperature/°C	Outcome
Fe, CaCl ₂ ¹¹⁵	EtOH	6	60	No conversion
SnCl ₂ .2H ₂ O ¹¹⁶	EtOAc	24	50	No conversion
Na ₂ S ₂ O ₄ ¹¹⁷	DMF	5	90	No conversion
NH ₂ -NH ₂ ¹¹⁸	EtOH	6	78	No conversion

Table 7: Attempts to reduce the nitro group in nitrobutanone 3.27b.

However, most of these attempts did not result in the consumption of starting materials and/or did not result in the formation of any of the expected products. However, the protocol involving the use of elemental zinc powder in the presence of ammonium chloride as a proton source (**Scheme 16**), did result in reactivity. Chemoselectivity for this protocol is impressively high, with the conversion of aliphatic nitro compounds to amines.^{119,120} Reaction of nitrobutanone **3.27b** with zinc and ammonium chloride in MeOH resulted in the complete consumption of nitrobutanone **3.27b**. A single new product was formed, according to TLC analysis. Workup and column

chromatography of the resulting reaction mixture furnished a white product characterized as the pyrroline **3.34** (Scheme 16).¹²¹

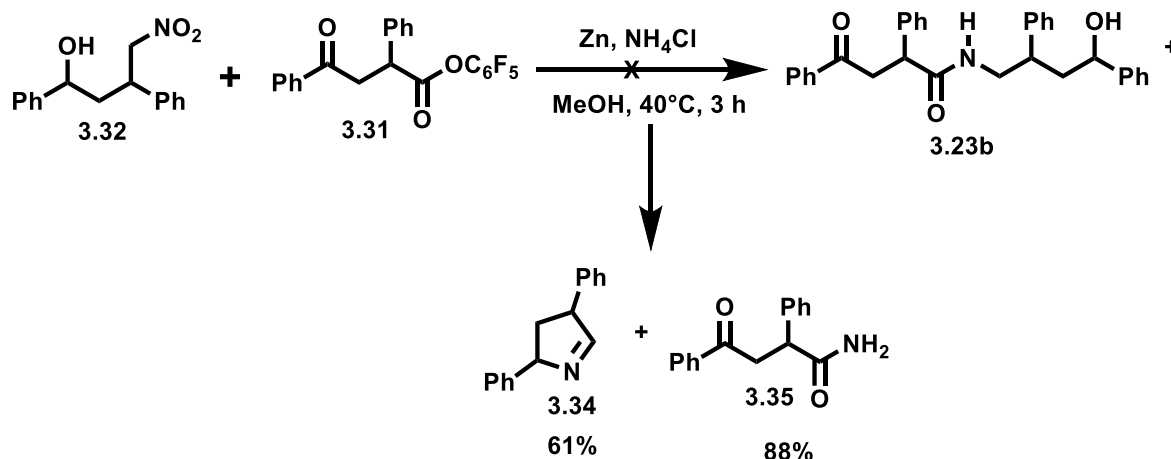


Scheme 16: Reduction of nitobutanone 3.27b to pyrroline 3.34.

This result suggests that nitobutanone **3.27b** was indeed reduced to oxoamine **3.24b**, which subsequently underwent intramolecular cyclization, generating pyrroline **3.34** in a 66% yield. The reduction of the nitro group in Michael adducts, using zinc and ammonium chloride, has been reported to produce pyrrolines and in some cases pyrroline-N-oxides through the formation of hydroxylamine.^{121,122,123} The reaction of pyrroline-N-oxides in acidic media has been reported to result in the formation of pyrrole.^{124,125} However, the reduction protocol using zinc results in the formation of only the pyrroline **3.34** which does not undergo oxidation to form pyrrole under these conditions.¹²⁵ This contradicts the results for the HSiCl₃-mediated reduction of **3.27b** (Scheme 11), where pyrrole was isolated. Presumably, in this case (Scheme 16), the nitro group is reduced to hydroxylamine, which undergoes intramolecular cyclization to the pyrroline-N-oxide. The HSiCl₃ then undergoes nucleophilic substitution at silicon, forming a strong bond with oxygen resulting in the formation of silanol and then the pyrroline-N-oxide forms the pyrrole.¹²⁵

The success of the reductive cyclization promoted conditions to explore the viability of trapping nitobutanone **3.27b** with active ester **3.31** to provide the amide **3.23b** according to Scheme 14. In light of this, the nitobutanone **3.27b** and the active ester **3.31** were treated with zinc dust and

NH₄Cl at 60 °C (**Scheme 17**). However, analysis of the product mixture revealed the presence of pyrroline **3.34**, as before, and a new compound that was characterized as amide **3.35** (**Scheme 17**). The formation of amide **3.35** suggests that the active ester **3.31** reacted with NH₄Cl generating the corresponding primary amide **3.35**. A crystal of the amide suitable for X-ray analysis was obtained from the slow evaporation of a solution of this material in CH₂Cl₂ and pentane. The resulting crystal structure diagram for the amide is shown in **Figure 18**, confirming the presence of the -NH₂ moiety in the compound.



Scheme 17: Attempted coupling of the nitrobutanone 3.27b and active ester 3.31.

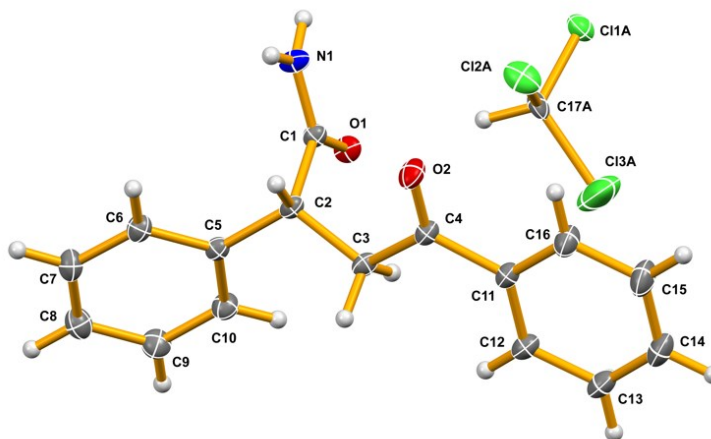
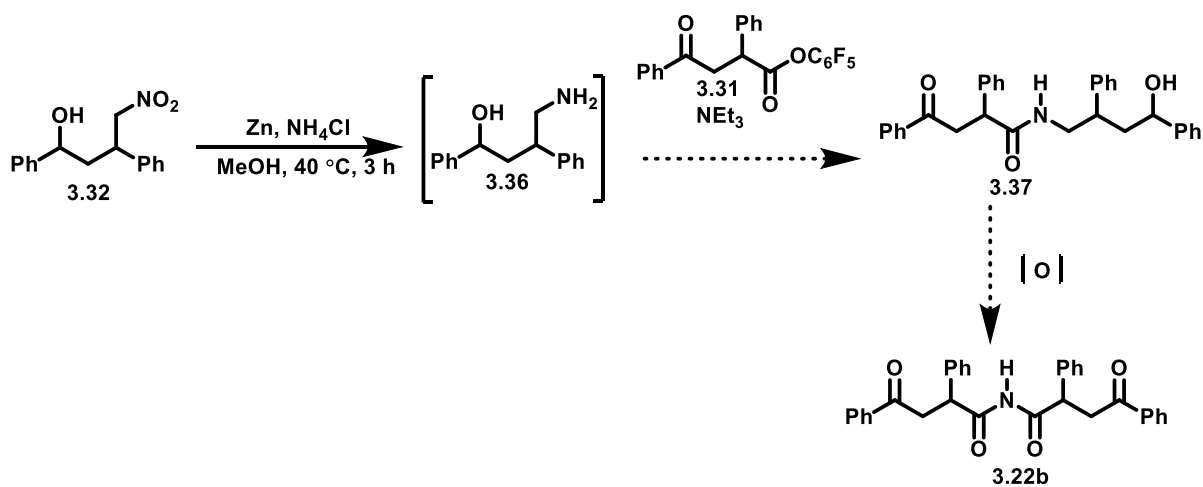


Figure 18: ORTEP diagram of amide 3.35 with solvent. Thermal ellipsoids are shown at 50% probability.

The trapping of the nitrobutanone with the active ester was unsuccessful as the active ester reacted with an ammonia equivalent present in the solution, and was thus unavailable to couple with the formed oxoamine. The reduction itself was however successful, as indicated by the isolation of the pyrroline **3.34**. Cognizant of these results, the use of ammonium chloride for the reduction of the nitrobutanone **3.27b** needed to be avoided and the use of zinc powder maintained to avoid the conversion of the active ester **3.31** to the amide **3.35**.

Rather than ammonia providing the hydrogen atoms, the reduction of nitro groups with zinc can be achieved in acidic media, though yield and chemoselectivity are often compromised.¹²⁰ This protocol is familiar as it is frequently utilized within the Thompson lab for the Knorr pyrrole synthesis.⁷⁷ The Knorr pyrrole synthesis involves a zinc-induced exothermic reduction of ethyl 2-aminoacetoacetate to form an α -amino ketone, which immediately reacts in situ to form pyrrole, as discussed in Chapter 1. Given the instability of the active ester **3.31** in the presence of NH_4Cl , the Knorr pyrrole synthesis conditions were mimicked for the reduction of **3.25**, with hopes of avoiding the conversion of the active ester to its primary amide **3.35**. However, when nitrobutanone **3.27b** was reacted with the active ester **3.31** in the presence of zinc in AcOH, the expected amide product (**3.23b**) was not formed. Instead, the active ester **3.31** was recovered in an 89% yield and the pyrroline **3.34** was again isolated. This result suggests that the reduction of nitrobutanone **3.27b** to oxoamine **3.24b** was successful under these conditions. Intramolecular cyclization of the oxoamine **3.24b** to the pyrroline **3.34** is, however, again favoured over coupling with the active ester. Therefore, the proposed trapping of the oxoamine with the active ester was unsuccessful.

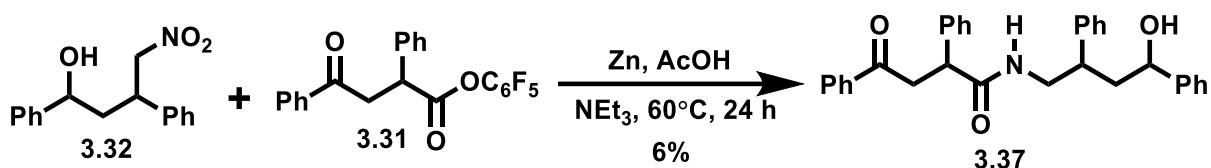
Given that the oxoamine trapping strategy was unsuccessful, a new strategy was explored wherein the nitrobutanol **3.32** obtained from the hydrogenation of nitrobutanone **3.27b** (Scheme 15), could be subjected to the Zn/NH₄Cl conditions for the reduction of the amine **3.36** (Scheme 18). The desired carbonyl functionality would then be installed from the alcohol later in the approach. Without the carbonyl moiety, the nitro group would hopefully be reduced without intramolecular cyclization, to afford the amine **3.36**. The amine **3.36** could then be coupled with the active ester **3.31** to yield the amide **3.37**. Oxidation would then install the desired ketone in **3.22b** (Scheme 18). With this amide in hand, the pathway would be anticipated to continue as proposed in Scheme 10 to yield the desired aza dipyrin **3.3a**.



Scheme 18: Proposed route to 3.22b, with the late-stage installation of the ketone.

The nitrobutanol **3.32** was therefore dissolved in AcOH and subjected to reduction with zinc dust in the presence of an excess of active ester **3.31** (Scheme 19). Following workup and purification via column chromatography, active ester **3.31** was recovered in an 85% yield together with two new compounds. Gratifyingly, the product corresponding to the spot with the lowest R_f on the TLC

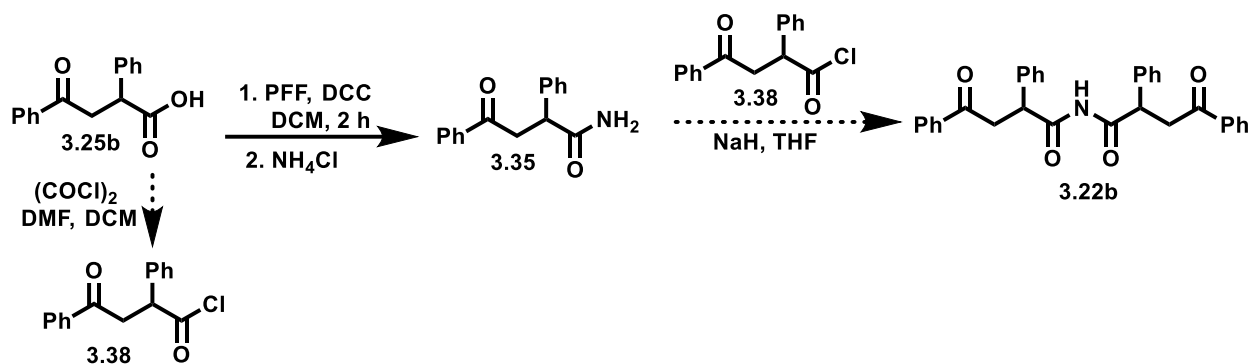
plate was characterized as the desired amide **3.37** by analysis of the ^1H NMR spectrum and with support from mass spectrometry. The identity of the other compound isolated (spot with higher R_f on the TLC), has not been successfully elucidated. The success in synthesizing **3.37**, despite the 6%, crude yield, is exciting and still warrants further development to determine the viability of this pathway. The isolated product was not clean according to TLC and ^1H NMR spectroscopy.



Scheme 19: Attempted coupling of nitrobutanol 3.32 and active ester 3.31.

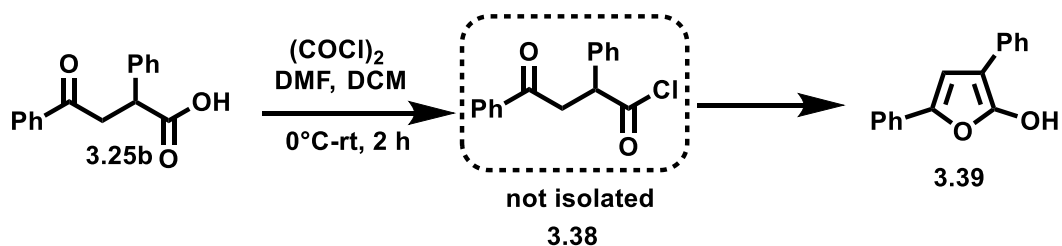
The focus thus returned to the amide **3.35** in

Scheme 17. A method of formation of imides was explored wherein an acid chloride is coupled with an amide in the presence of sodium hydride.¹²⁶ Since the primary amide **3.35** was available, coupling with the acid chloride **3.38** would hopefully provide the desired amide **3.22b** (Scheme 20).¹²⁶



Scheme 20: Proposed strategy for the synthesis of amide 3.22b via acid chloride 3.38.

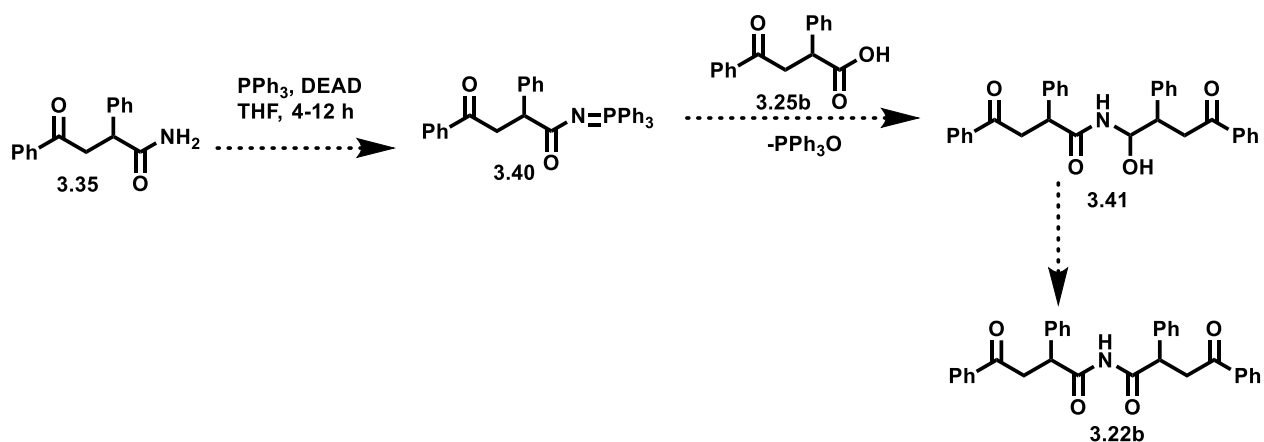
To this end, oxoacid **3.25b** was reacted with oxalyl chloride in the presence of catalytic amounts of DMF. The mixture was stirred at 0 °C for 10 min, and then at room temperature for two hours. The solvent and excess oxalyl chloride were removed *in vacuo*. Analysis of the spectral data revealed furanol **3.39** (Scheme 21). The presence of this product suggested that the desired acid chloride **3.38** indeed formed under the reaction conditions but underwent intramolecular cyclization to generate product **3.39** (Scheme 21). This cyclization was a major drawback and meant that we could not proceed with the proposed pathway in Scheme 20.



Scheme 21: Cyclization of acid chloride 3.38 to furanol 3.39.

3.6 - Future Work.

The hint of success from the formation of amine **3.23b** (**Scheme 19**) from the reaction of nitrobutanone **3.27b** and active ester **3.31**, though in a low yield, means we can undertake optimization of this reaction to further investigate this method for the synthesis of aza dipyrrens. Another possible alternative to synthesize aza dipyrrens might involve the use of the amide **3.35** (**Scheme 17**) which can be converted to phosphinimidic amide **3.40** (**Scheme 22**) by treatment with stoichiometric quantities of phosphines and diethyl azodicarboxylate (DEAD).^{127,128} The phosphinimidic amide **3.40** might then be coupled with the oxoacid **3.25b** to give the hydroxyl amide **3.41**, ready for oxidation to the desired imide **3.22b** enabling the pathway to continue as proposed in **Scheme 10**.



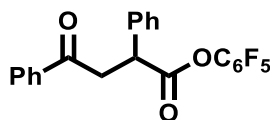
Scheme 22: Proposed synthesis of imide 3.22b via coupling of phosphinimidic amide 3.40 and oxoacid 3.25b.

3.7 - Experimental.

All chemicals were used as received unless otherwise indicated. All NMR spectra were recorded using 500 MHz or 300 MHz spectrometers. ^1H chemical shifts are reported in ppm relative to tetramethylsilane using chloroform solvent residual at $\delta = 7.26$ ppm as an internal standard. ^{13}C spectra were recorded using UDEFT pulse sequence with chemical shifts reported in ppm

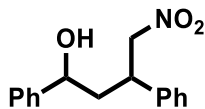
referenced to CDCl_3 resonance at $\delta = 77.2$ ppm. Splitting patterns are indicated as follows: br, broad; s, singlet; d, doublet; t, triplet; q, quartet; m, multiplet. All coupling constants (J) are reported in Hertz (Hz). High-resolution mass spectra were obtained using TOFMS experiments operating in both positive and negative modes. Column chromatography, as indicated, was performed using 230-400 mesh ultra-pure silica. 4-Oxo-2,4-diphenylbutanoic acid **3.25b**¹⁰³ and 4-Nitro-1,3-diphenylbutanone **3.27b**⁹¹ were synthesized according to reported procedures.

4-Oxo-2,4-diphenylbutanoic acid pentafluorophenyl ester, (3.31).



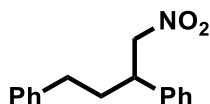
4-Oxo-2,4-diphenylbutanoic acid **3.25b** (9.6 mmol, 1 equiv.), EDC.HCl (1.25 equiv.) and pentafluorophenol (1.25) were dissolved in THF: CH_2Cl_2 1:1 (2 mL) and stirred at room temperature for 2 hours. The reaction was diluted to 10 mL with CH_2Cl_2 and washed with water and brine. The organics were dried over Na_2SO_4 and concentrated in vacuo. Purification over silica eluting with 17% EtOAc/hexanes gave **3.31** as a white solid (3.86g, 96%). ^1H NMR (500 MHz; CDCl_3) δ : 8.00 (d, $J = 7.28$ Hz, 2H), 7.56-7.60 (m, 1H), 7.41.-7.48 (m, 6H), 7.35-7.38 (m, 1H), 4.65-4.68 (dd, $J = 3.9, 10.2$ Hz, 1H), 3.98-4.05 (m, 1H), 3.45-3.49 (dd, $J = 3.9, 10.6$ Hz, 1H). ^{13}C NMR (CDCl_3) δ : 196.7, 169.6, 136.5, 136.0, 133.5, 129.2, 128.7, 128.3, 128.1, 127.9, 46.1, 42.8, 4 carbon signals missing. ^{19}F NMR (471 MHz, CDCl_3) δ : -152.0 (d, $J = 17.7$ Hz, 2F), -158.7 (t, $J = 21.6$ Hz, 1F), -162.6 (dt, $J = 4.7, 17.7$ Hz, 2F). NMR data were found to be in accordance with literature.¹²⁹

4-Nitro-1,3-diphenylbutan-1-ol, (3.32).



A mixture of **3.27b** (300 mg, 1.11 mmol), 10% Pd/C (30 mg), and NEt₃ (few drops) was dissolved in THF (0.08 M). Following repeated evacuation under vacuum and re-filling the atmosphere with nitrogen, the reaction vessel was again evacuated and then placed under an atmosphere of hydrogen. The reaction mixture was stirred under an atmosphere of hydrogen for 24 h. Upon completion of the reaction, the mixture was flushed with nitrogen and then filtered over a pad of Celite, flushing with THF. Concentration of the solution *in vacuo* gave the crude product. Purification of the crude product over silica eluting with 5% EtOAc/hexanes gave **3.32** as a white solid (108 mg, 36%). ¹H NMR (500 MHz; CDCl₃) δ: 7.30-7.35 (m, 4H), 7.24-7.29 (m, 2H), 7.20-7.23 (m, 2H), 7.14-7.16 (m, 2H), 4.53-4.62 (m, 2H), 4.48-4.52 (m, 1H), 3.34-3.40 (m, 1H), 2.23-2.29 (m, 1H), 2.06-2.11 (m, 1H), OH (br, 1.82). ¹³C NMR (CDCl₃) δ: 143.1, 139.1, 129.1, 128.8, 128.2, 127.8, 127.6, 126.2, 80.4, 72.1, 41.6, 40.9. HRMS-ESI (*m/z*): [M+Na]⁺ calc'd for C₁₆H₁₇NNaO₃: 294.1101, found 294.1089.

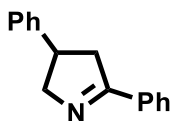
1,1'-(4-Nitrobutane-1,3-diyl)dibenzene, (3.33).



Nitrobutanone **3.27b** (300 mg, 1.11 mmol), 10% Pd/C (30 mg), and NEt₃ (few drops) were dissolved in THF (0.08 M). Following repeated evacuation under vacuum and re-filling the atmosphere with nitrogen, the reaction vessel was again evacuated and then placed under an atmosphere of hydrogen. The reaction mixture was stirred under an atmosphere of hydrogen for

24 h. Upon completion of the reaction, the mixture was flushed with nitrogen and then filtered over a pad of Celite flushing with THF. Concentration of the solution *in vacuo* gave the crude product. Purification of the crude material over silica eluting with 5% EtOAc/hexanes gave **3.33** as a colourless oil (125 mg, 44%). ¹H NMR (500 MHz; CDCl₃) δ: 7.36-7.39 (m, 2H), 7.25-7.32 (m, 3H), 7.18-7.23 (m, 3H), 7.09 (d, *J* = 7.28 Hz, 2H), 4.52-4.59 (m, 2H), 3.45-3.51 (m, 1H), 2.44-2.57 (m, 2H), 2.01-2.06 (m, 2H). ¹³C NMR (CDCl₃) δ: 140.9, 139.0, 129.1, 128.5, 128.3, 127.8, 127.7, 126.2, 80.9, 43.8, 34.5, 33.0. HRMS-ESI (*m/z*): [M+Na]⁺ calc'd for C₁₆H₁₇NNaO₂: 278.1151; found 278.1151.

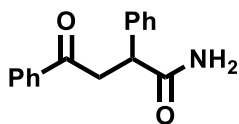
3,5-Diphenyl-3,4-dihydro-2H-pyrrole, (3.34).



Nitrobutanone **3.27b** (50 mg, 0.19 mmol) and NH₄Cl (41 mg, 0.76 mmol) were dissolved in MeOH. Zinc dust (38 mg, 0.57 mmol) was added portion-wise over 30 min and the mixture was stirred at 60°C for 3 h. Upon completion, the reaction mixture was allowed to cool to room temperature then diluted to 15 mL with water and extracted with CH₂Cl₂. The organic layer was washed with brine, dried over Na₂SO₄ and the solvent was removed *in vacuo* to give the crude product. Purification of the crude product over silica eluting with 20% EtOAc/hexanes gave **3.34** as a white solid (27 mg, 66%). ¹H NMR (500 MHz; CDCl₃) δ: 7.87-7.89 (m, 2H), 7.42-7.50 (m, 3H), 7.31-7.34 (m, 2H), 7.23-7.26 (m, 3H), 4.51-4.57 (m, 1H), 4.10-4.15 (m, 1H), 3.65-3.71 (m, 1H), 3.46-3.52 (m, 1H), 3.08-3.13 (m, 1H). ¹³C NMR (CDCl₃) δ: 174.2, 144.1, 133.2, 131.3, 128.8,

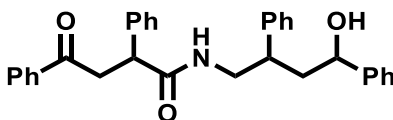
128.6, 128.0, 126.7, 68.3, 44.3, 42.4, 1 signal missing. HRMS-ESI (m/z): $[M+H]^+$ calc'd for $C_{16}H_{16}N$ 222.127726, found 222.127962.

4-Oxo-2,4 diphenylbutanamide, (3.35).



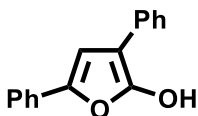
Oxoacid **3.25b** (50 mg, 0.19 mmol) and NH_4Cl (41 mg, 0.76 mmol) were dissolved in MeOH. Zinc dust (38 mg, 0.57 mmol) was added portion-wise over 30 min and the reaction was stirred at $60^\circ C$ for 3 h. Upon completion, the reaction mixture was allowed to cool to room temperature and then diluted to 15 mL with water and extracted with CH_2Cl_2 . The organics were washed with brine, dried over Na_2SO_4 and the solvent was removed *in vacuo* to give the crude product. Purification of the crude product over silica eluting with 40% EtOAc/hexanes gave **3.35** as a white solid (29 mg, 58%). 1H NMR (500 MHz; $CDCl_3$) δ : 7.95-7.97 (m, 2H), 7.52-7.55 (m, 1H), 7.41-7.45 (m, 2H), 7.38-7.40 (m, 2H), 7.32-7.36 (m, 2H), 7.26-7.29 (m, 1H), 5.59-5.68 (d, $J = 46.7$ Hz, 2H), 4.22-4.25 (m, 1H), 4.02-4.08 (m, 1H), 3.19-3.24 (m, 1H). ^{13}C NMR ($CDCl_3$) δ : 198.1, 174.9, 139.5, 136.6, 133.2, 129.0, 128.5, 128.1, 127.9, 127.6, 47.2, 42.5. HRMS-ESI (m/z): $[M+Na]^+$ calc'd for $C_{16}H_{15}NNaO_2$ 276.0995; found 276.0986.

N-(2-Hydroxy-4-phenylbutyl)-4-Oxo-2,4-diphenylbutanamide, (3.37).



Nitrobutanol **3.32** (388 mg, 1.43 mmol), NEt₃ (200 μL, 1.43 mmol) and active ester **3.31** (3.58 mmol) were dissolved in 3 mL of AcOH and the mixture stirred at 60°C. Zinc dust was added slowly over 30 min and the reaction mixture was stirred for 3 h. After **3.32** was consumed as monitored by TLC, the reaction mixture was cooled to room temperature. The mixture was then filtered over a pad of celite and the resulting mixture was extracted with CHCl₃. The organic layer was dried over anhydrous Na₂SO₄ and concentrated *in vacuo* to give the crude product. Purification over silica gave **3.37** as a brown oil (6 mg, 1%). ¹H NMR (500 MHz; CDCl₃) δ: 8.01 (d, 2H), 7.61 (t, 3H), 7.50 (m, 3H), 7.31-7.43 (m, 14H), 4.57-4.70 (m, 3H), 4.36-4.39 (m, 1H), 3.93-3.99 (m, 1H), 3.43-3.47 (m, 1H), 3.31-3.36 (m, 1H), 2.27-2.38 (m, 2H), 2.14-2.19 (m, 1H). HRMS-ESI (*m/z*): [M+Na]⁺ calc'd for C₃₂H₃₁NNaO₃ 500.2196; found 500.2189.

3,5-Diphenyl-2-furanol, (3.39).

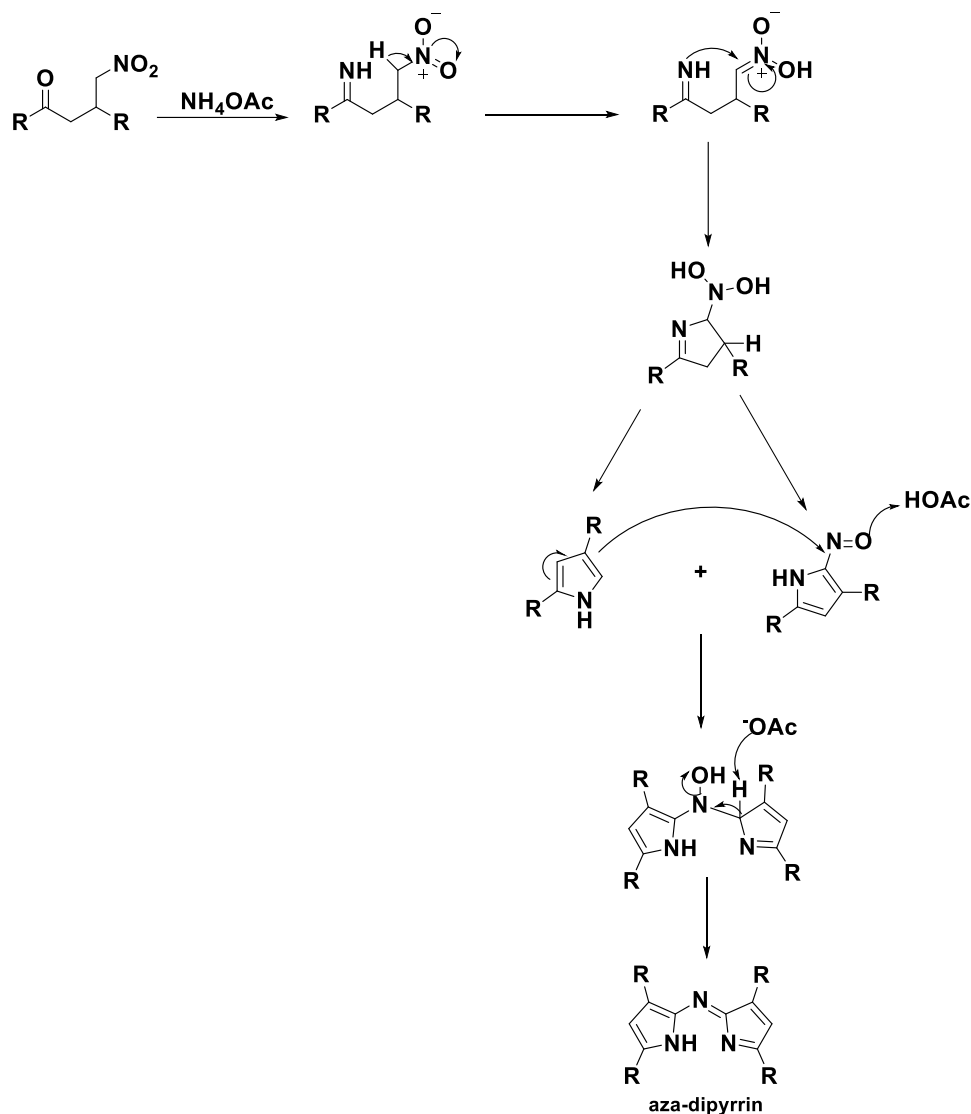


Oxoacid **3.25b** (1 g, 3.93 mmol) was dissolved in anhydrous CH₂Cl₂ (15 mL) and the resulting solution cooled to 0 °C. Oxalyl chloride (4.72 mmol, 1.2 equiv.) was added dropwise followed by the addition of a drop of DMF. The mixture was stirred at 0 °C, coming to room temperature over 2 h. The solvent and excess oxalyl chloride were removed *in vacuo* to give a yellow oil. The yellow oil was dissolved in a small amount of CH₂Cl₂ and excess hexanes to effect precipitation. The resultant white crystalline solid was collected by filtration, (890 mg, 96%). ¹H NMR (500 MHz; CDCl₃) δ: 7.89-7.91 (m, 2H), 7.63 (d, *J* = 2.14 Hz, 1H), 7.39-7.44 (m, 6H), 3.73-3.75 (m, 2H), 6.03-6.03 (m, 1H). ¹³C NMR (CDCl₃) δ: 171.7, 147.3, 134.8, 130.9, 129.5, 129.2, 128.7, 127.1, 126.6, 81.5. HRMS-ESI (*m/z*): [M+Na]⁺ calc'd. for C₁₆H₁₂NaO₂ 259.0730; found 259.0728.

Chapter 4 – Attempted PPh₃-Mediated C–N Coupling of Nitrosoarenes.

4.1 – Introduction.

The work in Chapter 3 aimed to form aza dipyrins in an acyclic manner through the preinstallation of the linking C-N bond, before the formation of the pyrrolic rings, but to no avail. Perhaps exploring other methods for the installation of the C-N bond in pyrroles would provide a desirable synthesis of aza dipyrins. As mentioned in Chapter 3, the most direct synthetic route for the generation of aza dipyrins involves heating nitrobutanones with an ammonium source, in alcohol. Despite the practical simplicity, the reaction pathway(s) for this conversion is complex. However, the proposed mechanism (**Scheme 23**) for this transformation suggests, first, the multi-step generation of a nitroso pyrrole. This material then, upon reaction with an α -free pyrrole, condenses to form the aza dipyrin. Given the large number of steps, many of which are likely reversible, no wonder the yields for this route are low and typically less than 50%.¹³⁰ Another strategy for the synthesis of aza dipyrins, again leveraging early-stage C-N bond formation, is the use of nitroso-pyrroles as described in Chapter 3. The reported⁹¹ route to nitroso pyrroles involves the reaction of an α -free pyrrole with NaNO₂ in acidic media, but this cannot be applied to the more electron-rich alkyl-substituted pyrroles. This warrants the need to consider other C-N bond formation strategies in pyrrolic systems.⁹¹ Perhaps, the most viable alternative for the synthesis of aza dipyrins, that can hopefully be applied to non-aryl substituted starting materials, requires exploration of other, mild, C-N bond formation strategies.



Scheme 23: A suggested mechanistic pathway for the formation of aza dipyrins from nitrobutanones.

Most prevailing C-N bond-forming strategies involve transition metal (TM) catalysis.¹³¹ TM-catalyzed C-N cross-coupling involves an electrophile-nucleophile approach, characterized by the Buchwald-Hartwig^{132,133} and Ullmann-Goldberg^{134,135} reactions in which aryl halides react with an amine or amide using stoichiometric or catalytic amounts of a Cu promoter (**Figure 19, A**). This has since been overshadowed by developments in Pd (**Figure 19, A**) catalysis due to low yields and harsh conditions.¹³⁴ Pd-catalyzed C-N cross-coupling, one of the primary methods used for

catalytic C-N bond formation from aryl (pseudo)halides, still has persistent limitations. These include the requirement for elevated temperatures, strong bases, and expensive Pd (pre)catalysts.¹³⁶ Improved turnover, and the advantages of a reduced cost of base metal, encouraged the development of Ni-catalyzed C-N cross-coupling^{137,138} (**Figure 19, A**) but these still face limitations such as the use of air-sensitive Ni(0) catalysts or customized ligand systems. An alternative approach to TM-catalyzed C-N bond formation involves the oxidative copper-catalyzed intermolecular C-N cross-coupling of N-nucleophiles with aryl-boron reagents (**Figure 19, B**)¹³¹ In addition to the synthetic simplicity, this approach is supported by an impressive catalogue of aryl-boron derivatives now available both commercially and synthetically.¹³⁹ This protocol requires only mild reaction conditions, generally inexpensive reagents and tolerates a vast scope of coupling partners.

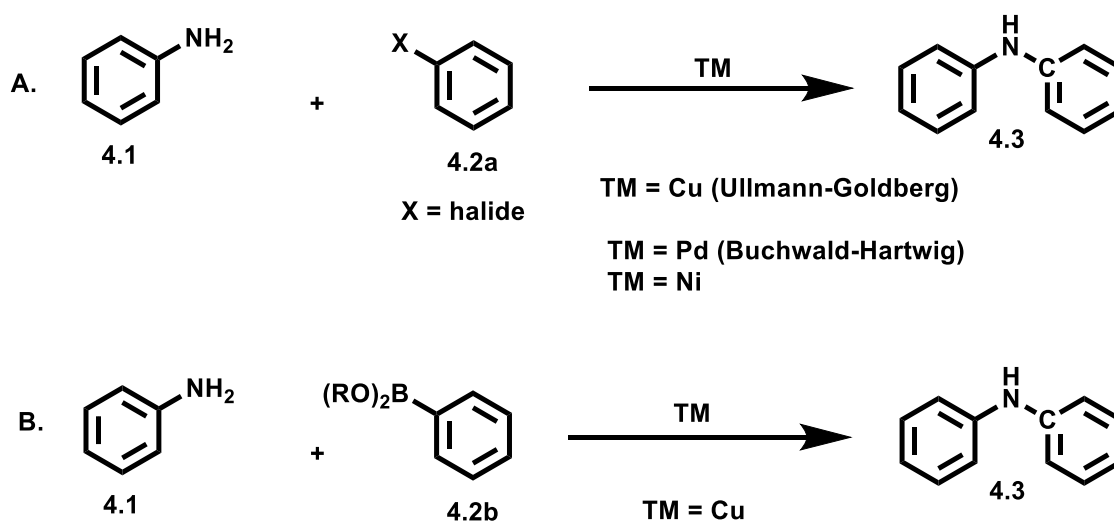


Figure 19: Classic C-N coupling protocols.

While these strategies allow for facile C-N bond formations, replacing to an extent harsher methods (Goldberg reaction, nucleophilic aromatic substitution, etc.),¹³⁵ and significantly expanding the repertoire of C-N bond formation, transition metal-based catalysts are often toxic, costly to make and/or require complicated ligands. Their removal from the final product can be cumbersome. Therefore, metal-free routes to C-N bond formation for application to the synthesis of aza dipyrrens are more desirable.

Recently, the Radosevich group reported a reductive strategy for C-N coupling that does not rely on transition metals, thereby enabling a complementary route from readily accessible nitro compounds and boronic acids (**Figure 20**).¹⁴⁰ Specifically, this organophosphorus-based strategy relies on an all-main-group system composed of an organophosphorus P(III)/P(V) redox catalyst and hydrosilane as a reducing agent. This protocol requires in situ activation of the phosphine(V) oxide to form an active P(III) intermediate, which reacts with nitro substrates and regenerates phosphine(V) oxide. This method uses nitroarene substrates that are distinct from, but generally no less accessible than, those used in established C-N cross-coupling methods. The method also offers unique chemoselectivities and functional group tolerance.¹⁴¹

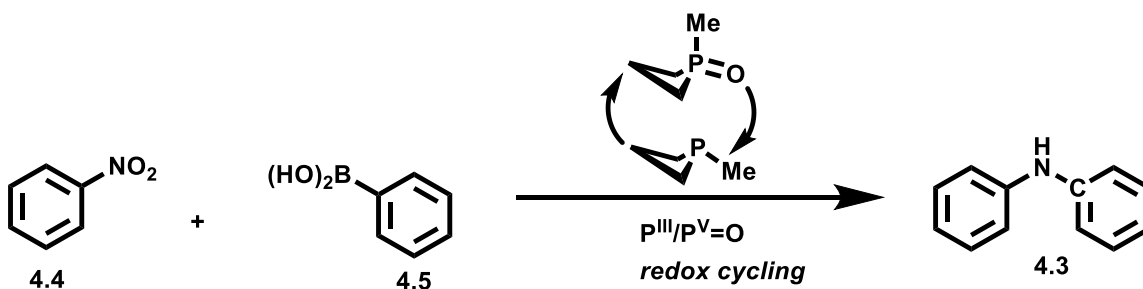


Figure 20: Reductive C-N coupling (P(III)/P(V) redox catalysis).

Given the challenges described in Chapter 3 involving the intramolecular cyclization of oxoamines in the attempted synthesis of the 4'4-diketoimides (**3.22b**), this P(III)/P(V) redox catalysis (**Figure 21, A**) presented an attractive approach for pyrroles. Synthesis of aza dipyrrens was envisioned via the phosphorus-based catalyst C-N coupling of α -nitro pyrroles and 2-pyrrole-boronic acids (**Figure 21, B**) in the presence of the silane reductant as reported by the Radosevich group.¹⁴⁰

The hope was that the corresponding amino bispyrrole would undergo facile oxidation to form the desired aza dipyrin. This approach is attractive as it relies on the availability of α -nitro pyrroles. These can be accessed via the reaction of an α -free pyrrole with nitric acid/sulfuric acid, with a variety of functionalized pyrroles. Similarly, aryl-boronic acids are generally bench-stable reagents that can be handled with no special precautions against air or humidity. Their toxicity is low, they present limited documented environmental issues and produce boric acid upon consumption in the Radosevich chemistry. Furthermore, there are lots of reported methods for their preparation.¹⁴²

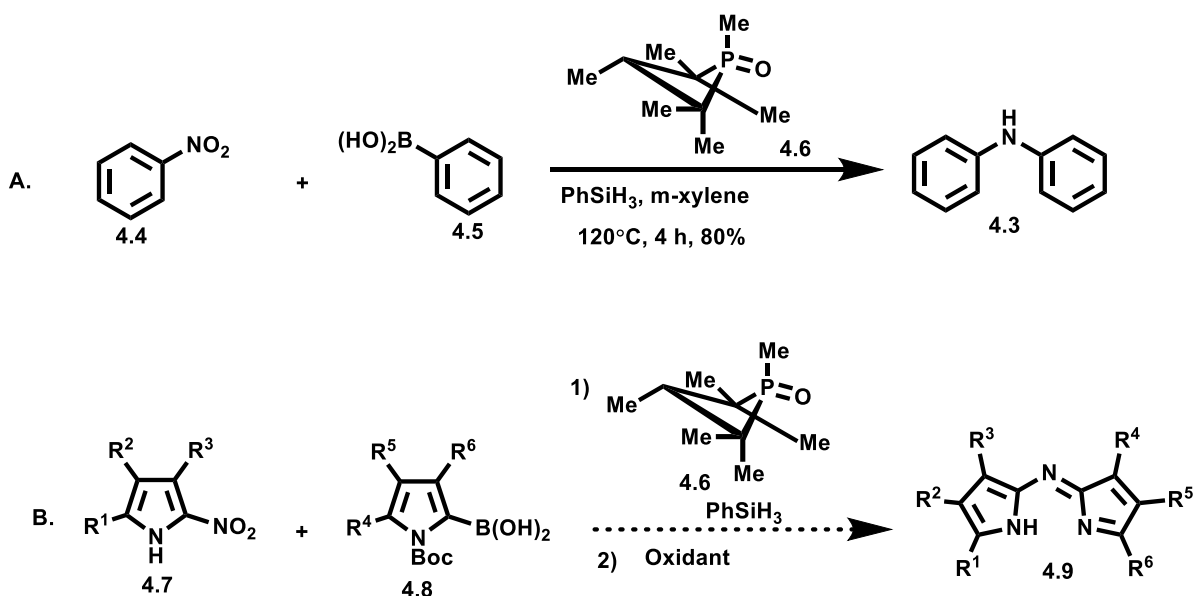


Figure 21: Organophosphorus-Catalyzed Reductive C–N Coupling of nitro aryls and boronic acids.

4.2 - Project Goals.

This project aims to develop a new method for the synthesis of aza dipyrins by making use of Radosevich-inspired C-N phosphine-based catalysis, using nitropyrroles and 2-pyrrole boronic acids. The proposed coupling is mild, with no use of acid or excess reagents, and thus should offer potential with non-aryl-substituted pyrroles for the synthesis of novel non-aryl-substituted aza dipyrins.

4.3 - Results and Discussion.

4.3.1 - Attempted coupling of nitropyrroles with boronic acids using Radosevich catalyst.

To investigate the viability of the proposed Radosevich-inspired C-N coupling for the synthesis of aza dipyrrens, diphenyl nitropyrrole **4.7a** (Figure 22) was chosen, as diphenyl pyrrole precursor can be readily synthesized. Boronic acid **4.8a** was chosen as the coupling partner, as it is commercially available. Successful coupling of these partners, followed by oxidation, would result in the formation of the aza dipyrren **4.10a** (Figure 22).

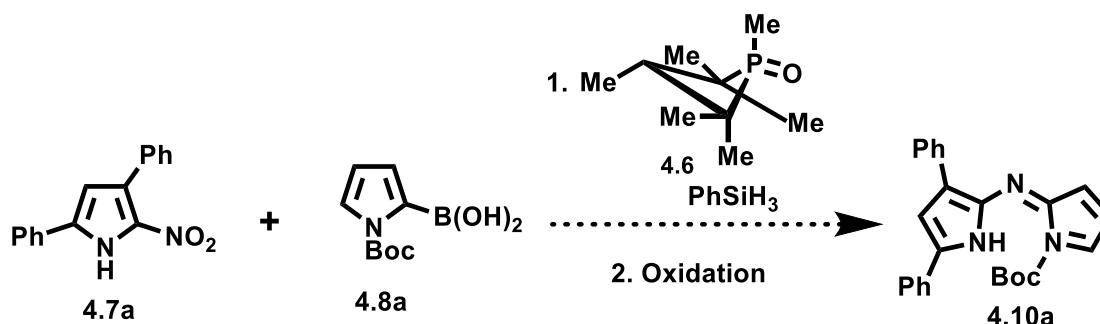
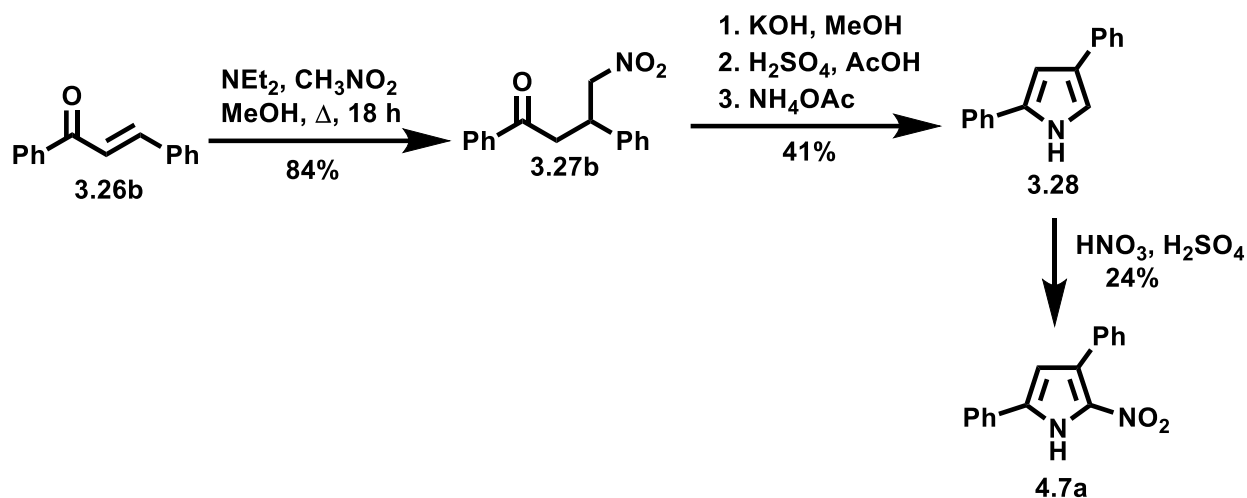


Figure 22: Proposed coupling of nitropyrrole **4.7a** and boronic acid **4.8a** to aza dipyrren **4.10a**.

In order to synthesize the nitro-substituted pyrrole **4.7a**, the previously described chalcone chemistry was utilized.⁹¹ To this end, the chalcone **3.26b** was converted, via Micheal addition of nitromethane, to nitrobutanone **3.27b**. This transformation proceeds via deprotonation of nitrobutanone **3.27b** with KOH in MeOH to generate a nitro-stabilized anion. Hydrolysis in the presence of H₂SO₄ gave the 1-keto-4-dimethyl acetal intermediate, which was converted directly to the diphenyl pyrrole **3.28** using NH₄OAc.¹⁴³ The pyrrole was isolated in a 41% yield (Scheme 24). Nitration of diphenyl pyrrole **3.28** was then accomplished by reaction with nitric acid and sulfuric acid¹⁴⁴ to afford **4.7a** in a 24% yield.¹² Isolation and purification of the nitropyrrole was

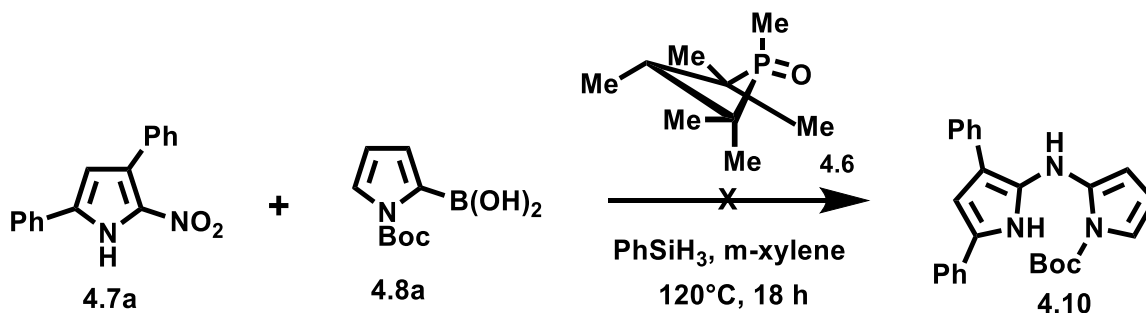
difficult as nitration also occurred on the phenyl rings, providing a somewhat complex product mixture that requires careful chromatography in order to achieve the desired purity of product. Despite the low yield, the successful isolation of **4.7a** enabled the exploration of the proposed strategy.



Scheme 24: Synthesis of diphenyl nitro-pyrrole 4.7a.

To evaluate the utility of the Radosevich chemistry, the diphenyl nitro-pyrrole **4.7a** was dissolved in *m*-xylene, then subjected to the coupling conditions with N-boc-2-pyrrole boronic acid **4.8a** in the presence of the phosphorus catalyst **4.6** (which was obtained from Dr. Speed's lab) and PhSiH₃ as reductant (**Scheme 25**). According to the literature method, the reaction mixture was stirred for 18 hours at 120 °C, using an oil bath. Disappointingly, analysis of the reaction mixture by TLC revealed a mixture consisting of multiple components. Further analysis of the reaction mixture using MS analysis did not show evidence of dipyrrolic materials. The anticipated C-N coupling of the diphenyl-nitro pyrrole **4.7a** with the N-boc-2-pyrrole boronic acid **4.8a** was thus deemed unsuccessful under these conditions. It was speculated that stirring pyrroles at such high temperatures for long periods would likely result in decomposition, and hence the complex

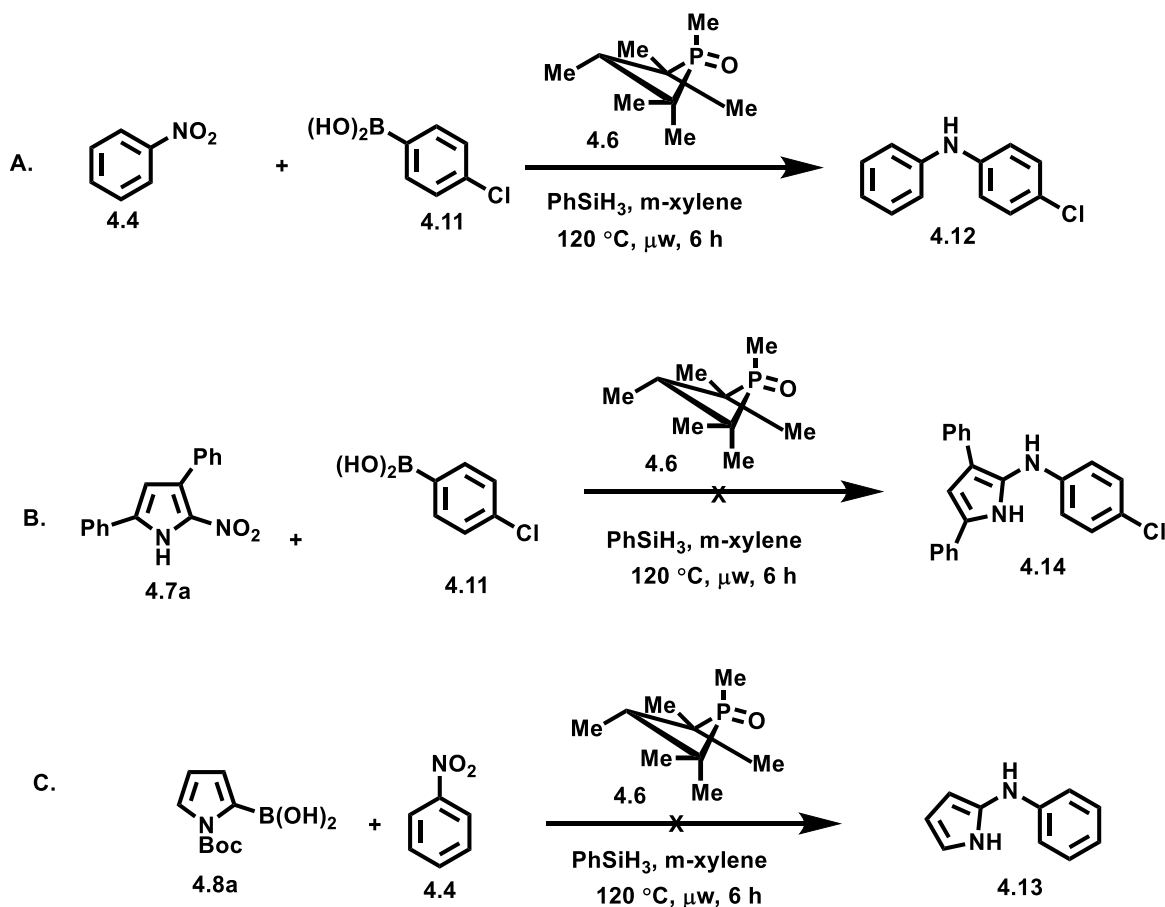
mixtures obtained. To enable further exploration of this phosphorus-based coupling, extending it to pyrroles, further work turned to heating using microwave irradiation in order to shorten the reaction times.



Scheme 25: Attempted coupling of diphenyl nitropyrrole 4.7a and N-boc-2-pyrrole boronic acid 4.8a.

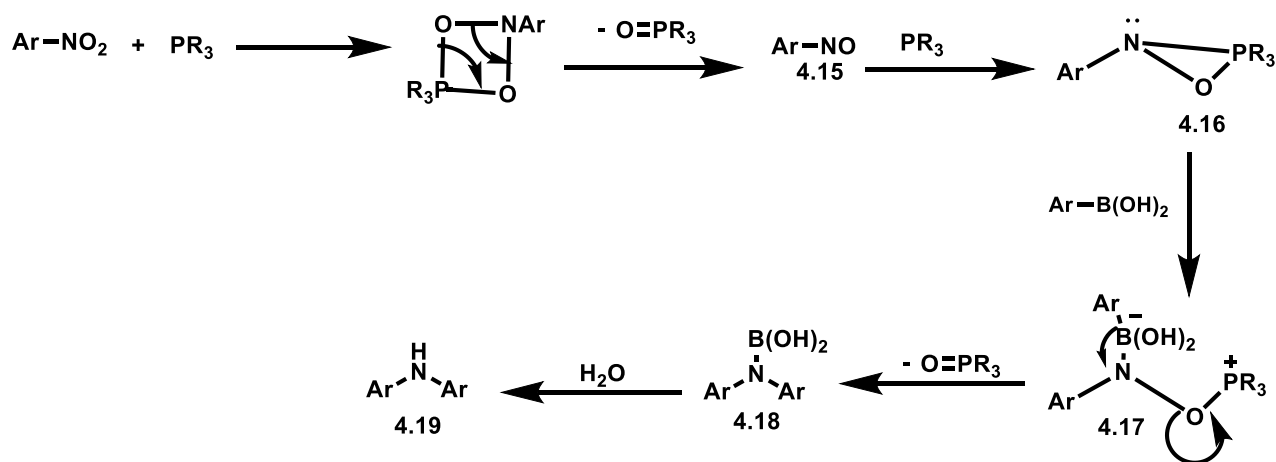
Furthermore, given the failed C-N coupling involving two pyrrolic substrates, the procedure was repeated with phenyl substrates as reported by Radosevich's group,¹⁴⁰ so as to both confirm the feasibility of the original chemistry in our hands and to evaluate the feasibility of using microwave-promoted heating. To this end, nitrobenzene **4.4** and 4-chloro-phenylboronic acid **4.11** (**Scheme 26, A**) were subjected to C-N coupling in the presence of the phosphorus catalyst **4.6** and PhSiH₃. The reaction was heated using microwave irradiation. Analysis using TLC revealed the complete disappearance of starting material after 2 hours. Reassuringly, the desired arylamine **4.12** was successfully formed as the major product as shown by the formation of a single product according to analysis using TLC. Analysis of the crude reaction mixture using MS confirmed that the singular product was the expected material. Given that the method was successful for the synthesis of arylamine **4.12**, efforts returned to the incorporation of pyrroles. To that end, the coupling partners were varied so as to investigate the ability of diphenyl nitropyrrole (**4.7a**) to react with 4-chloro-phenylboronic **4.11** (**Scheme 26, B**) under the phosphorus-catalyzed conditions. The ability of the

N-boc-2-pyrrole boronic acid (**4.8a**) to act as a coupling partner with nitrobenzene was also explored **4.4** (**Scheme 26, C**). However, when either of the pyrrole-based substrates was subjected to the C-N coupling conditions with the corresponding phenyl substrate, the desired product was not identified via MS analysis of the reaction mixture. The reactions resulted in complex reaction mixtures with no evidence of expected products,



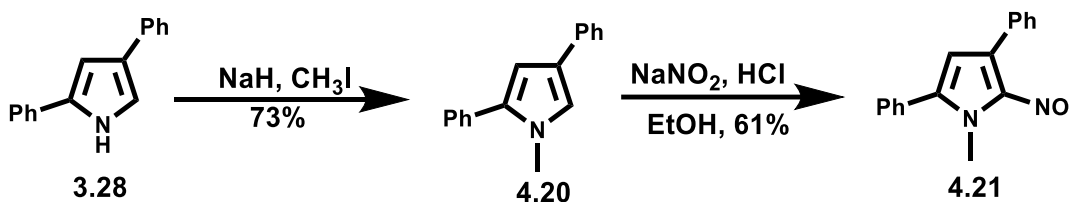
Scheme 26: (A) Coupling of nitrobenzene 4.4 with boronic acid 4.11. (B) Attempted coupling of nitropyrrole 4.7a and boronic acid 4.11. (C) Attempted coupling of nitrobenzene 4.4 and boronic acid 4.8a.

Based on these results it was concluded that these pyrrole-based substrates could not participate in the C-N coupling using Radosevich's catalyst **4.6**. This result was a major setback that prompted us to explore alternate organophosphorus compounds for the catalysis of this transformation. Tervalent organophosphorus compounds (PR_3) are potent nucleophiles that are used as catalysts in many reactions and react with a wide variety of oxygen-containing compounds to yield the corresponding quinquevalent derivatives ($\text{O}=\text{PR}_3$).¹⁴⁵ The major driving force behind these reactions is the great strength of the $\text{P}=\text{O}$ bond formed.¹⁴³ Furthermore, experimental, spectroscopic, and computational data¹⁴¹ suggest that $\text{P(III)/P(V)}=\text{O}$ catalysis results in the reductive deoxygenation of nitro substrates to the corresponding nitroso compound in the first catalytic cycle (**Scheme 27**). Once formed, nitrosylated material **4.15** then undergoes a reaction with PR_3 to give an oxazaphosphirane intermediate **4.16**. This is postulated to coordinate with the boronic acid, followed by 1,2-migration of the organoboron residue to nitrogen, and final hydrolysis to afford the coupling product **4.19** (**Scheme 27**).¹⁴¹



Scheme 27: Reaction of boronic acids with nitro (hetero)arenes.

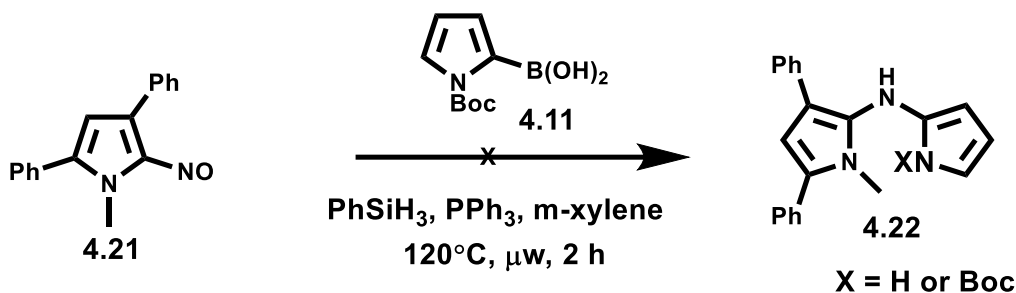
The realization that the nitro-aryl substrate shown in **Scheme 27** undergoes reduction, in the first catalytic cycle, to form a corresponding nitroso compound was beneficial because aryl nitroso pyrroles can be synthesized in much higher yield and with easier purification than their nitro-counterparts. Using nitroso pyrroles as starting materials would eradicate the first catalytic cycle and hopefully shorten the reaction time as nitroso compounds are deoxygenated by phosphines and phosphites much more rapidly than nitro compounds.¹⁴⁶ The protection of the N-atom of the nitroso pyrrole was deemed necessary before commencing the coupling. In this way, the reactivity of the N-atom could not interfere with the desired coupling chemistry. To prepare the nitroso-pyrrole, the pyrrole precursor was protected before the installation of the nitroso group. To this end, diphenyl-pyrrole **3.28** was reacted with iodomethane in the presence of sodium hydride¹⁴⁷ to yield the N-methyl pyrrole **4.20** in a 73% yield (**Scheme 28**). The N-methyl pyrrole **4.20** was then subjected to nitrosylation via treatment with NaNO₂ in ethanolic HCl to afford the novel N-methyl nitroso pyrrole **4.21** as a green solid in a 61% yield (**Scheme 28**).¹⁴⁸



Scheme 28: Synthesis of N-methyl protected diphenyl nitroso-pyrrole 4.21.

Triphenylphosphine (PPh₃) was chosen for the first exploration of phosphorus(III)-based catalysts since it has been reported¹⁴⁹ to aid the deoxygenative coupling of nitroarenes and boronic acids. The N-methylated nitroso pyrrole **4.21** was therefore subjected to attempted deoxygenative C-N coupling with N-Boc-2 pyrrole boronic acid **4.11** using PPh₃ as the catalyst in the presence of

PhSiH₃ as reductant (**Scheme 29**). The reaction was stirred at 120 °C under microwave irradiation. Sequential analysis of the reaction mixture after heating for 10 minutes to 1 hour did not show any change in the reaction mixture. However, analysis of the reaction mixture after heating for 2 hours did not show consumption of nitrosopyrrole **4.21** but did reveal the disappearance of the boronic acid **4.11** and the generation of a new spot. Further analysis of the compound corresponding to the new spot revealed the presence of N-H pyrrole. It was speculated that the very high temperatures utilized might be causing the boronic acid **4.11** to decompose and hence exploration of alternative energy sources was deemed necessary.

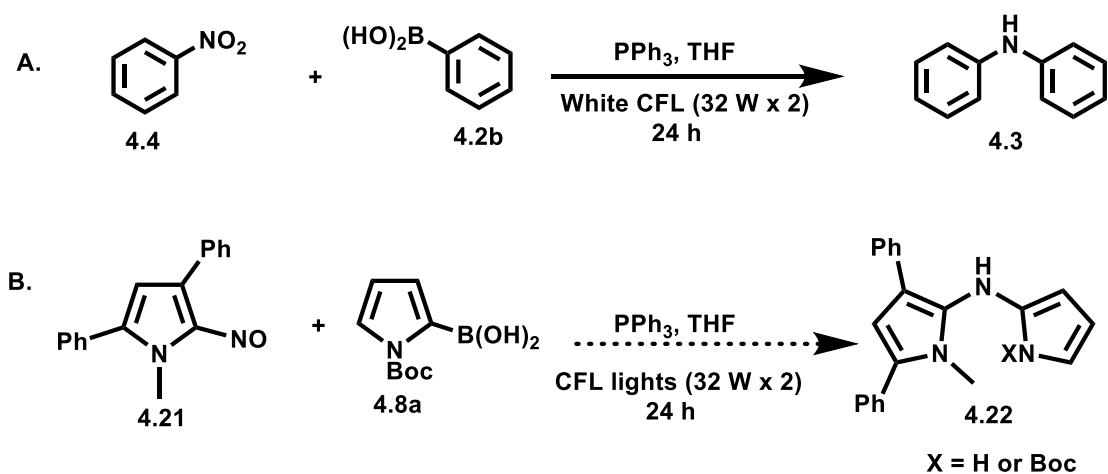


Scheme 29: Attempted coupling of N-methyl nitroso-pyrrole 4.21 with boronic acid 4.11.

4.3.2 - Attempted visible light and coupling of nitroso pyrroles with boronic acids.

Given that the N-boc-2-pyrrole boronic acid **4.8a** decomposed under the phosphorus-based catalysis conditions, other non-heat energy sources were considered for activation of the desired transformation. Recently, Manna and coworkers reported¹⁵⁰ a metal-free, visible-light-mediated reductive amination between nitroarenes and boronic acids involving triphenylphosphine (**Scheme 30, A**). This approach is performed at ambient temperature without any photocatalyst. In this synthesis, the nitroarenes are activated under the irradiation of visible light facilitating

deoxygenation through single-electron oxidation of triphenylphosphine. A nitroso-arene is formed that is readily converted to a nitrene intermediate which subsequently engages in C-N coupling with boronic acids.¹⁵⁰ Given that this approach does not require heating of the starting materials, it presents an attractive approach to aza dipyrroles via coupling of α -nitroso pyrroles and 2-pyrroleboronic acids (Scheme 30, B) under CFL light irradiation. The hope was that, without heat, the boronic acid **4.8a** would survive and thus couple with the nitroso substrate **4.21** to form the desired amino bispyrrole **4.22**.

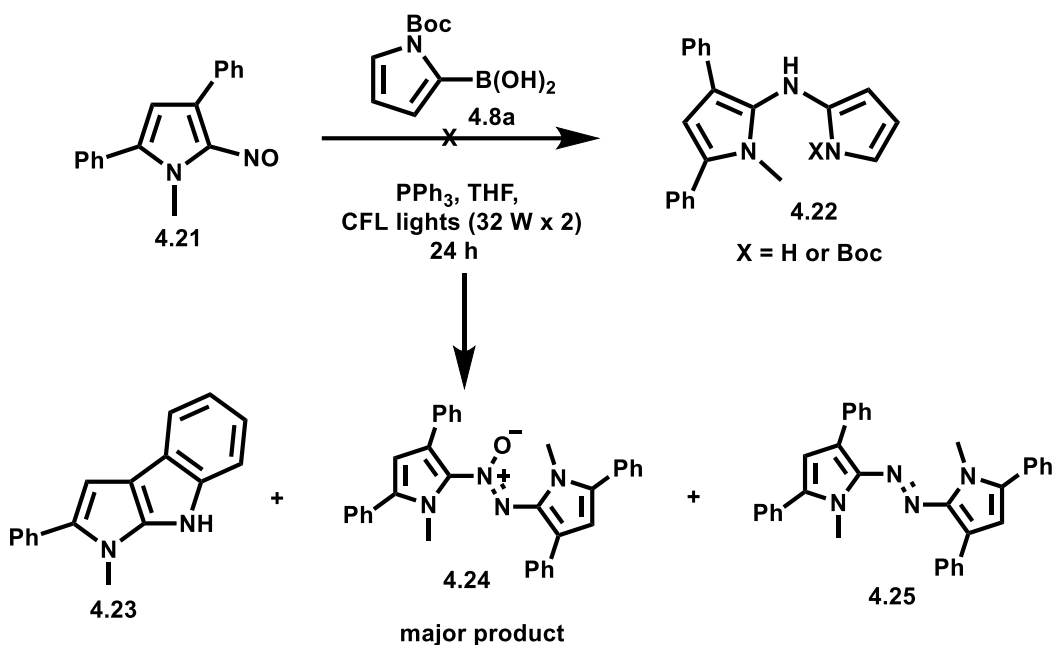


Scheme 30: A: Photochemical PPh₃-mediated coupling of nitrobenzene and phenylboronic acid. B: Proposed photochemical PPh₃-mediated coupling of nitrosopyrrole and boronic acids.

To evaluate the utility of this photochemistry in a pyrrole-based system, diphenyl-nitroso pyrrole **4.21** and N-boc-2 pyrrole boronic acid **4.8a** were dissolved in dry THF in the presence of PPh₃ and the reaction mixture placed under a nitrogen atmosphere. Irradiation with 64 W (2 × 32 W) CFL lamps for 24 hours (Scheme 31) and analysis of the reaction mixture using TLC after, revealed the complete consumption of the nitroso substrate and formation of three new spots. However, the boronic acid was not consumed based on the TLC analysis and was recovered quantitatively.

Spectroscopic analysis of the compounds corresponding to the three compounds formed suggested the carbazole-type product **4.23**, azoxy-type product **4.24** and azo dye **4.25** (Scheme 31). It was speculated that upon photoirradiation with the CFL lights, the nitroso substrate **4.21** undergoes reductive deoxygenation by reaction with the PPh_3 to form a nitrene intermediate which reacts differently forming the three obtained compounds.

One of the compounds formed is a carbazole type of product **4.23**. Research into this class of compounds revealed they are a known product of the Cardogan cyclization reaction of 2-nitrophenyl derivatives in the presence of suitable organophosphorus reagents.¹⁴⁵



*Scheme 31: Attempted photochemical PPh_3 -mediated coupling of nitroso pyrrole **4.21** and boronic acids **4.8a**.*

It was speculated that the formation of **4.23** is a result of a nitrene insertion into the proximal C-H position on the adjacent phenyl ring, rather than coupling with the boronic acid partner **4.8a**.^{151–153}

Based on this hypothesis, we postulated that to avoid the formation of the carbazole product **4.23**

and form the desired product **4.22**, the boronic acid **4.8a** should be present in excess. However, when the reaction was repeated in the presence of excess boronic acid **4.8a**, the carbazole product was still observed and the boronic acid was recovered quantitatively with no evidence of the desired product.

Another reaction product observed during the reaction of diphenyl-nitroso pyrrole **4.21** with PPh₃ under CFL light irradiation is the azoxy-type product **4.24**, analogous to azoxybenzenes (also known as N-oxides of azo compounds).¹⁵⁴ This type of product has been shown as an intermediate in the reduction of nitrobenzene to aniline with an unexpected level of stability.¹⁵⁵ The formation of this product suggests a reduction of nitroso pyrrole **4.21** to hydroxylamine **4.26** (Figure 23), which condenses with another molecule of nitroso pyrrole **4.21** to form the novel azoxytetraphenylpyrrole **4.24**.¹⁵⁶

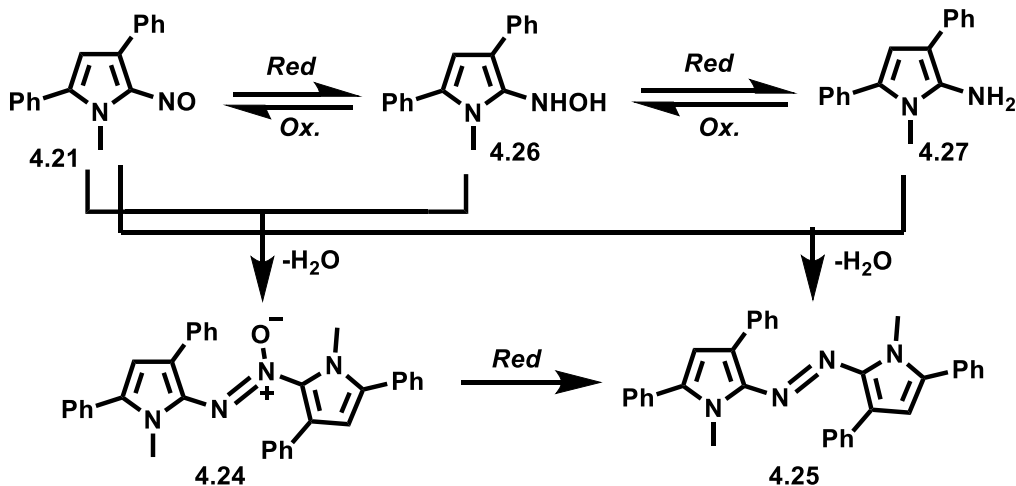


*Figure 23: Proposed reaction sequence to form azoxy-bis pyrrole **4.24** and azo bispyrrole **4.25** via hydroxylamine pyrrole **4.26** and amino pyrrole **4.27**.*

Compounds containing an azoxy functionality are known to have broad applications in industry such as for dyeing and reducing agents,^{157,158} chemical stabilizers,¹⁵⁹ chemical intermediates,¹⁶⁰

polymerization inhibitors,¹⁶¹ and therapeutic agents.¹⁶² Traditional industrial syntheses of azoxy compounds are often costly, inefficient, and environmentally unfriendly.^{154,163} The discovery of these pyrrole-based azoxy compounds **4.24** can complement and meet the need for new sustainable azoxy compounds in industry.

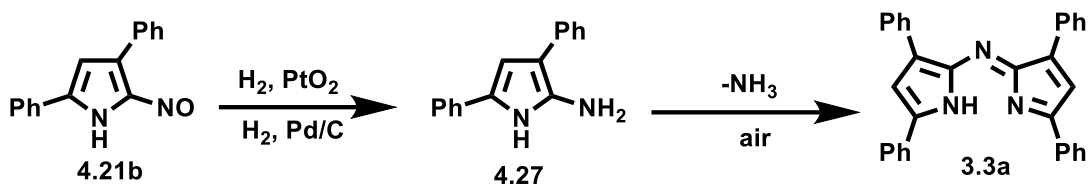
The third product formed from the reaction of the nitroso pyrrole with boronic acid **4.8a** in the presence of PPh₃ and irradiation with white CFL lights appeared as an intense non-polar red spot upon analysis via TLC. The spot displayed bright orange fluorescence under long-wave ultraviolet light. A small amount of the red material was collected from the crude reaction mixture following chromatographic separation. Spectroscopic analysis of the red material and the LRMS-ESI⁺ showed a [M+ H]⁺ peak at *m/z* =493.23 The NMR data further suggested that the red material was diphenyl-azo bispyrrole **4.25** (Scheme 31). It was speculated that the hydroxylamine **4.26** (Figure 23) undergoes further reduction to form the amino pyrrole **4.27**, which then condenses with another nitroso pyrrole **4.21** forming the azo bis pyrrole **4.25**. Azo bispyrroles were accidentally discovered¹²⁹ in the Thompson lab by a previous researcher in their attempt to synthesize aza dipyrins. These featured rotationally constrained β-aryl substituents and were prepared using NH₄OAc in glacial acetic acid under microwave irradiation. However, the yields for these syntheses of azo bispyrroles are very low. Another researcher from the Thompson group attempted⁴⁶ the development of a methodology to afford azo bispyrroles with improved yields, following the traditional way through which azo dyes are made i.e., via diazonium salts.¹⁶⁴ This traditional route demanded the use of amino pyrrole **4.27** which is very unstable and is notoriously known for self-condensing to the aza dipyrin.⁹⁰ This resulted in the adoption of stringent anhydrous conditions for this synthesis with no ultimate reaction of the diazonium salts to the azo bispyrroles. The discovery of azo bispyrroles from the reductive deoxygenation of nitroso pyrroles

with PPh₃ under CFL light irradiation provides an alternative route to these pyrrole-based azo-dyes. The azo dye features the substitution pattern of the starting materials, presumably enabling the synthesis of variously substituted azo dyes. This will in turn allow further solid-state absorbance and emission studies on these compounds. Azo dyes often display spectacular photophysical properties and are key to dyes such as methyl orange, commonly known as the pH indicator and so have earned utility in textile, food, rubber, and plastic industries.¹⁶⁵ Besides their characteristic colouring function, azo compounds are reported²⁰ as antibacterial, antiviral, antifungal and cytotoxic agents. They can be used as drug carriers and are currently being screened for their potential biomedical use, including cancer diagnosis and therapy.¹⁶⁶

Despite the exciting discovery of new classes of pyrrolic compounds, the aim of this project is to find an improved alternative synthesis of aza dipyrins. Given the unsuccessful attempts thus far, other alternative conditions were thus explored.

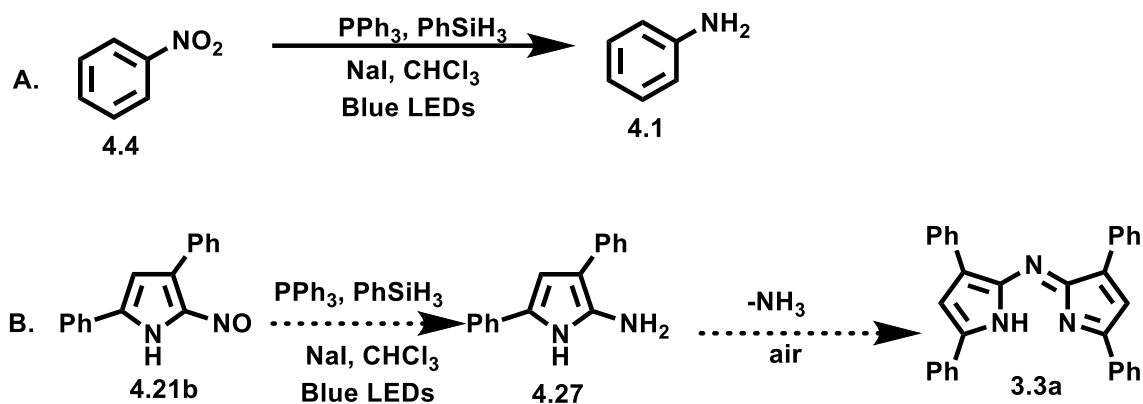
4.3.3 - Attempted PPh₃/NaI photochemical reduction of nitroso pyrroles under blue LED irradiation.

Given the recovery of boronic acid **4.8a** in the attempted coupling with nitroso pyrrole **4.21** under photo irradiation with CFL lights, it was concluded that N-boc-2-pyrrole boronic acid **4.8a** is not reactive under these conditions. Therefore, efforts focused in the use of the nitroso pyrroles **4.21b**. Nitroso pyrroles are known to undergo reduction with Adams catalyst or by hydrogenation with palladium on carbon catalyst to provide amino pyrrole **4.27** which undergoes dimerization upon exposure to air to form aza dipyrins, with loss of ammonia, in very low yield.^{90,98,167}



Scheme 32: TM-catalyzed reduction of nitroso pyrrole 4.21b to amino pyrrole 4.27 and condensation of 4.27 to aza dipyrin 3.3a.

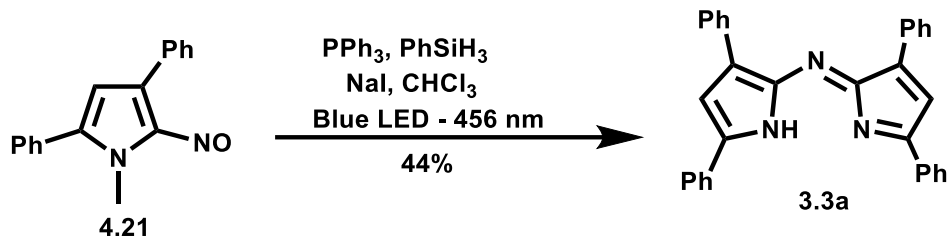
Recently, Qu and co-workers reported¹⁶⁸ a mild, highly selective transition-metal-free photo redox system based on the combination of NaI and PPh₃ for the reduction of nitroarenes (**Scheme 33, A**). In this system, the combination of nitroarenes with NaI and PPh₃ was found to generate an electron-donor-acceptor (EDA) complex under blue LED light irradiation. This EDA complex absorbs photons to enable reductive hydrogenation of nitroarenes with a variety of functional groups. Mechanistic insight on this NaI/PPh₃-mediated reduction of nitroarenes suggested the reduction of nitrosoarenes to the nitroso intermediate and then the hydroxylamine intermediate which is then decomposed by the EDA complex to provide the amine product.¹⁶⁹ From this system, a new pathway to the aza dipyrins using the NaI/PPh₃ mediated reduction of nitroso pyrroles under blue LED light irradiation was envisioned (**Scheme 33, B**).



Scheme 33: A: NaI/PPh₃-mediated photochemically reductive amination of nitrobenzene 4.4. B: Proposed synthesis of aza dipyrin 3.3a via NaI/PPh₃-mediated photochemically reductive amination of nitroso pyrrole 4.21b.

The hope was that the nitroso pyrrole **4.21b** would undergo reduction under the blue LED light irradiation to form the amino pyrrole **4.27** in situ. The amino pyrrole would then dimerize to form the desired aza dipyrin **3.3a**. To evaluate the feasibility of this proposed hydrogenative amination approach, nitroso pyrrole **4.21b**, PPh₃, NaI and PhSiH₃ were dissolved in anhydrous CHCl₃ and the reaction mixture was stirred under blue LED irradiation for 18 hours (**Scheme 34**). Pleasingly, the reaction mixture changed from the green nitroso colour to a vibrant blue colour typical for aza dipyrins. The crude reaction mixture showed two spots on TLC analysis and when the crude sample was submitted for MS analysis, it revealed that the spots were that of the aza dipyrin and the pyrrolehydroxylamine **4.26**. The blue compound was isolated by column chromatography in a 44% yield and ¹H NMR showed that it was indeed the tetraphenyl aza dipyrin **3.3a**. This was a satisfying result which meant that a new method for the synthesis of aza dipyrin was successfully developed, with a comparative yield to the current chalcone route towards aza dipyrins.⁹⁰ The disappearance of the methyl group in the final product is baffling as it is a rigid protecting group

for pyrroles, we hypothesized that the presence of triphenylphosphine might have led to the deprotection of pyrrole. Attempts to isolate the pyrrolehydroxylamine **4.26** were unfruitful as it



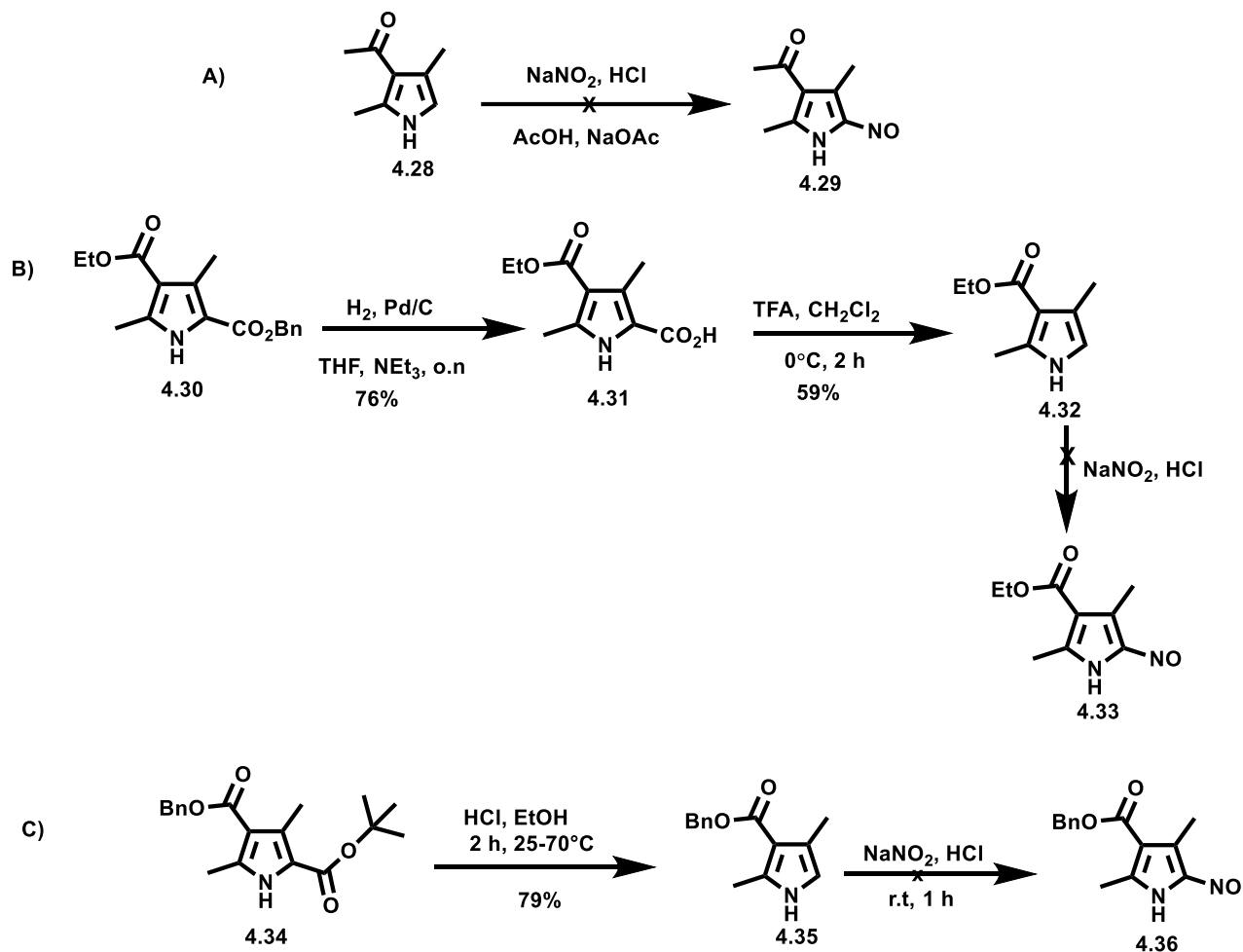
Scheme 34: Synthesis of aza dipyrin 3.3a via NaI/PPh₃-mediated photochemical reductive amination of nitroso pyrrole 4.21.

decomposed upon exposure to air. The presence of the pyrrole hydroxylamine provides evidence that the NaI/PPh₃ reductive amination under blue LED irradiation indeed follows the mechanism described by Qu and co-workers¹⁶⁸ where the nitroarenes are reduced to the nitroso intermediate, which is then reduced to the hydroxylamine intermediate which is further reduced to the aminopyrrole, which dimerizes to the aza dipyrin. Based on this hypothesis, we speculated that the addition of excess PhSiH₃ would prompt the full conversion of hydroxylamine **4.26** to amino pyrrole **4.27** and hence lead to an increase in the yield of the aza dipyrin **3.3a**. However, repeating the reaction in the presence of excess PhSiH₃ resulted in the complex reaction mixture based on TLC analysis and a drastic decrease in the yield of the desired aza dipyrin **3.3a**.

Given the salient features of the present reduction protocol including no need for transition-metal catalysts, mild reaction conditions, ample potential substrate scope with broad functional group tolerance, and high chemoselectivities. Application to non-aryl substituted pyrroles for the synthesis of particularly alkyl-substituted aza dipyrins was envisioned. With the established reductive amination by the blue LED irradiation-induced NaI/PPh₃ catalytic system, it was

postulated that other substrates, including alkyl-substituted nitroso pyrroles, would survive under these conditions. In order to explore the tolerance of the reaction when utilizing alkyl-substituted nitroso pyrroles, the starting materials were to be synthesized. Nitroso pyrroles are generally synthesized by the direct nitrosylation of pyrroles using sodium nitrite in ethanolic HCl. Even though reports¹⁷⁰ show that this approach cannot be applied to alkyl-substituted pyrroles, a decision was made to try this nitrosylation in our own hands. To this end, pyrroles stabilized by electron-withdrawing groups were chosen ahead of any attempts to synthesize nitroso pyrroles bearing exclusively alkylated substitution. To start, dimethyl acetal-pyrrole **4.28** (**Scheme 35, A**) was subjected to a reaction with NaNO₂ in ethanol in the presence of concentrated HCl following reported conditions.¹⁴⁸ Analysis of the reaction with TLC showed a complex product mixture with multiple spots. MS results for the reaction mixture did not show the peak for the desired product **4.29**. Faced with this challenge another substrate was chosen. The Knorr-type pyrrole **4.30** (**Scheme 35, B**), featuring a benzyl ester and an ethyl ester in the 2- and 3-positions, respectively, is prepared in large quantities within the Thompson group and is hence readily available for use. In order to prepare the α -free pyrrole **4.32**, first the benzyl ester was cleaved to the carboxylic acid **4.31** via hydrogenolysis. Decarboxylation of **4.31**, facilitated by the treatment with TFA, generated the α -free pyrrole **4.32**(**Scheme 35, A**). The α -free pyrrole was then subjected to nitrosylation conditions with NaNO₂ in ethanolic HCl. Just as with the previous substrate, the desired nitroso product **4.33** was not identified in the reaction mixture, based on the MS results of the crude reaction mixture. Before giving up on the nitrosylation of alkyl-substituted pyrroles, another substrate was chosen. The pyrrole **4.34** also available in the Thompson group, was deprotected by reaction with HCl in ethanol to provide the α -free pyrrole **4.35** which was subjected to nitrosylation conditions with NaNO₂ but to no avail (**Scheme 35, C**). The reaction resulted in a complex mixture

as with the previous substrates. At this point, it was concluded that alkyl-substituted pyrroles could not be nitrosylated using the current method used for the aryl-substituted pyrroles.¹⁴⁸



Scheme 35: Attempted nitrosylation of alkyl-substituted pyrroles.

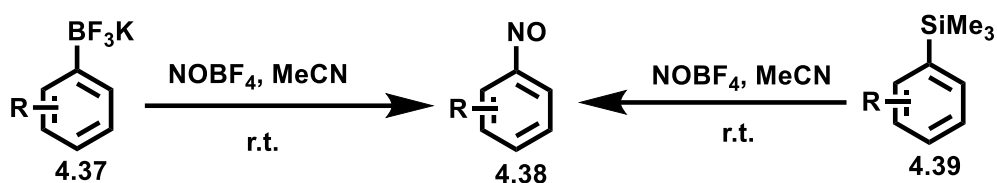
While this approach has been well-established for aryl-substituted pyrroles, the nitrosylation of alkyl-substituted pyrroles clearly remains a challenge.^{148,171} Possibly the acidic conditions induce polymerization of the highly reactive alkyl-substituted pyrroles.¹⁷² This necessitates the development of an efficient and selective method for the nitrosylation of non-aryl-substituted pyrroles for the synthesis of non-aryl-substituted aza dipyrrens.

4.3.4 - An alternative route to α -nitroso pyrroles.

The encountered challenges in the synthesis of non-aryl substituted nitroso pyrroles warrant the need for the development of a new approach requiring only mild and preferably non-acidic conditions. A common route to α -nitroso pyrroles, as mentioned before, involves the *in situ* generation of nitrosonium ions by treatment of α -free pyrroles with sodium nitrite under acidic conditions.¹⁷³ Evidently, this method for the nitrosylation of pyrroles cannot be applied to non-aryl substituted derivatives. The first nitroso compound to be synthesized was nitrosobenzene published by Baeyer over a century ago.¹⁷⁴ Since then, several methods have been published for the synthesis of nitrosoarenes¹⁷³ via nitrosonium ions generated in-situ from salts with different counterions (e.g. BF_4 , PF_6 , HSO_4 , ClO_4 etc). Starting materials e.g. NO_x , N_2O_3 , N_2O_4 , nitrites and prefunctionalized ionic liquids, and reactions involve numerous protocols.¹⁷³

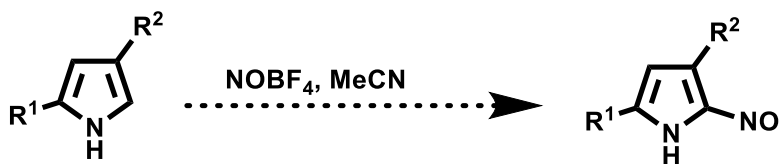
Attention was thus turned to the use of nitrosonium salts, rather than NaNO_2 , for nitrosylation. Nitrosonium salts are generally inexpensive, stable and safe in handling, which makes them attractive reagents in organic chemistry. Molender et al.¹⁷⁵ showed that nitrosoarenes can be synthesized by a mild direct nitrosylation procedure using the NOBF_4 nitrosonium salt (**Scheme 36, left**). In this synthesis, the authors used the potassium trifluoroborate aryl system **4.37** with the trifluoroboryl moiety acting as a directing group for the introduction of the nitroso electrophile at the ipso-position. The procedure led to the formation of a nitrosoarenes **4.38** with defined regioselectivity and with compatibility with various functional groups including challenging heteroarenes.¹⁷⁵ Hilt et al.¹⁷⁶ also reported the use of NOBF_4 as a nitrosylating reagent for the synthesis of nitrosobenzene derivatives from trimethylsilyl-substituted benzene derivatives **4.39** (**Scheme 36, right**). The synthesis was shown to be effective for both electron-rich, electron-deficient and bulky starting materials.¹⁷⁶ A shared feature of both methods is the fast reaction rate,

with the formation of products occurring within the first few minutes. According to the proposed mechanism for the two approaches, a shared pathway for the nitrosylation exists. This involves initial electrophilic ipso addition of nitrosyl and subsequent loss of $-\text{BF}_3$ or $-\text{SiMe}_3$ moieties. While these methods have been efficient for nitrosylation of other heteroarenes such as substituted pyridines, they have not been demonstrated in heteroaromatics such as pyrrole.



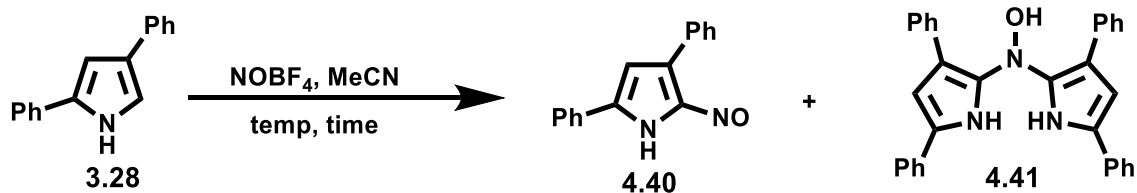
Scheme 36: Use of leaving groups for aryl nitrosylation using NOBF_4 .

Based on the simplicity of this protocol it was desirable for application in pyrroles, particularly alkyl-substituted pyrroles. Pyrroles are known as electron-rich heterocycles, and functionalization of the pyrrole core generally occurs at the α -position.^{7,8} Based on this reactivity, it was hypothesized that pyrroles would react directly with NOBF_4 for the introduction of the nitroso group on the α -position (**Scheme 37**).



Scheme 37: Proposed nitrosylation of pyrroles using NOBF_4 salt.

To evaluate the utility of the proposed nitrosylation of pyrroles using NOBF₄, diphenyl-pyrrole **3.28** was chosen as the model substrate given that the corresponding product **4.40** is stable and well described.^{90,91} Pyrrole **3.28** was synthesized according to a reported procedure.¹⁴⁸ The investigation of the nitrosylation of **3.28** with NOBF₄ was evaluated under various conditions (via varying solvents, temperature, equivalents and order of addition) as shown in **Table 8**. Initially, the reaction was carried out open to air in MeCN at room temperature (**Table 8, entry 1**), stirring the reaction mixture at room temperature as described by Molander et al.¹⁷⁵ Unfortunately, the desired product **4.40** was not detected. However, all starting material was consumed, as confirmed by TLC analysis and MS spectrometry data corresponding to the reaction mixture. Instead, a complex mixture was obtained. Repeating the attempted reaction at a reduced temperature of 0°C did not result in the detection of the expected product, nor did stirring for 24 hours (**Table 8, entry 2**). Fortunately, the portion-wise addition of NOBF₄ to the solution of **3.28** in MeCN under nitrogen at 0°C proved to be efficient for this transformation, affording the required nitroso product **4.40** in a 30% (**entry 3**). A by-product was also isolated. This material was characterized by ¹H NMR spectroscopy and MS spectrometry as compound **4.41**, which is an intermediate to the tetraphenyl aza dipyrin **3.3a** (**Table 8, entry 4**). Attempts to obtain a crystal structure for compound **4.41** were unfruitful as it forms the tetraphenyl aza dipyrin **3.3a** upon sitting for a few days. It was speculated that the occurrence of this intermediate could be a result of the reaction of the desired nitroso pyrrole product **4.40** with some unreacted starting material **3.28**, a known reaction of nitroso compounds.^{90,173} The reduced temperature was thus advantageous to formation of the desired nitroso pyrrole.



Run	NOBF_4 (equiv)	Temp ($^{\circ}\text{C}$)	Time (min)	Base	3.28 ^a	4.40 ^a	4.41 ^a
1 ^b	1.5	rt	120	none	ND	Trace	ND
2 ^b	1.5	0	24 h	none	ND	9%	ND
3	1.5	0	5	none	42%	30%	18%
4	2	0	5	none	ND	31%	29%
5	2	0	60	none	ND	40%	ND
6 ^c	2	0	5	none	ND	17%	ND
7	1.8	-5	10	none	10%	65%	ND
8	1	-5	24 h	none	8	40%	ND
9	0.9	-5	5	none	ND	60%	ND
10	0.5	r.t	6 h	none	57%	27%	13%
11	1.8	-5	4 h	none	trace	59%	18%
12	1.8	-5	5	NaHCO_3	None	49%	trace
13	1.8	-5	5	Et_3SiH	None	61%	trace
14	1.8	-5	5	NaH	None	58%	trace
15 ^d	1.8	-5	15	None	None	52%	ND

Table 8: Optimization of Nitrosylation reaction of 3.28 to 4.40. ^aIsolated yield, ^bOpen to air, ^c Addition of pyrrole to the NOBF_4 in MeCN, ^d 1 g scale.

In an attempt to further increase the yields of the nitroso pyrrole, the order of addition was reversed. Thus the pyrrole was added to a solution of NOBF₄ in anhydrous MeCN. Unfortunately, this resulted in a reduction in the yield of the desired nitroso product (**Table 8, entry 6**), suggesting that the nitroso product **4.40** is not stable in the presence of excess NOBF₄. Therefore, all reactions that followed were performed with the addition of the NOBF₄ to the solution of **3.28** in MeCN, to limit exposure of the product to NOBF₄. To improve the yields of the nitroso product and reduce the production of the intermediate **4.41**, the equivalents of the NOBF₄ were increased. However, this did not change the yield of the desired product, even when the reaction mixture was stirred for longer times (**entry 5**). Further screening revealed that a reduction in temperature to the -5 to -10°C range, by using a combination of an ice bath and acetone, is essential in slowing down if not eradicating the formation of the intermediate **4.41** (**Table 8, entry 8**). This makes sense as nitroso pyrroles have been reported to react with α -free pyrroles to generate the aza dipyrrens at elevated temperatures.⁹¹ Furthermore, because the reaction of α -free pyrroles and NOBF₄ results in the formation of HBF₄, a strong acid, the use of additives (**entry 12 to entry 15**) to quench the HBF₄ was explored. Unfortunately, the use of bases to quench the HBF₄ did not have a positive effect on the yield of the nitroso product. In all the runs conducted, traces of the tetraphenyl aza dipyrren **3.3a** were observed. And so I settled on utilizing 50 mg of **3.28** and 1.8 equiv of NOBF₄ in the absence of additives for all optimizations. When the reaction was scaled up from 50 mg to 1 g scale, the desired product was isolated in a 52% yield as shown in **Table 8 (entry 14)**. Although the yield is within the same margin as the original NaNO₂/HCl protocol, the new NOBF₄-mediated nitrosylation is faster as the latter requires three steps that run for over 2 hours.⁹¹ Furthermore, the NOBF₄ approach does not involve the use of acidic conditions and requires simple workup and purification procedures.

Although a marginally improved yield was obtained using 1.8 equiv of NOBF₄ at -5°C using an ice bath and acetone as shown in **Table 8 (entry 8)**, the use of 0.9 equiv (**Table 8, entry 9**) was selected for application in other pyrrole derivatives based on stoichiometric reasons, and the desire to not promote dinitrosylation and to limit exposure of the nitroso product to excess NOBF₄. With the selected optimization conditions in hand (**Table 8, entry 9**), the protocol was extended to other pyrroles. Firstly, the generality of this transformation with respect to aryl-substituted pyrroles was evaluated. To do this, pyrroles with a variety of aryl-substitutions were synthesized to enable the study of how different functional groups behave under the new nitrosylation conditions. The synthesis of the pyrroles started with the synthesis of the chalcones **4.42(a-l)**, prepared from the corresponding benzaldehydes and acetophenones utilizing reported⁹⁰ conditions. The chalcones prepared are shown in **Figure 24**.

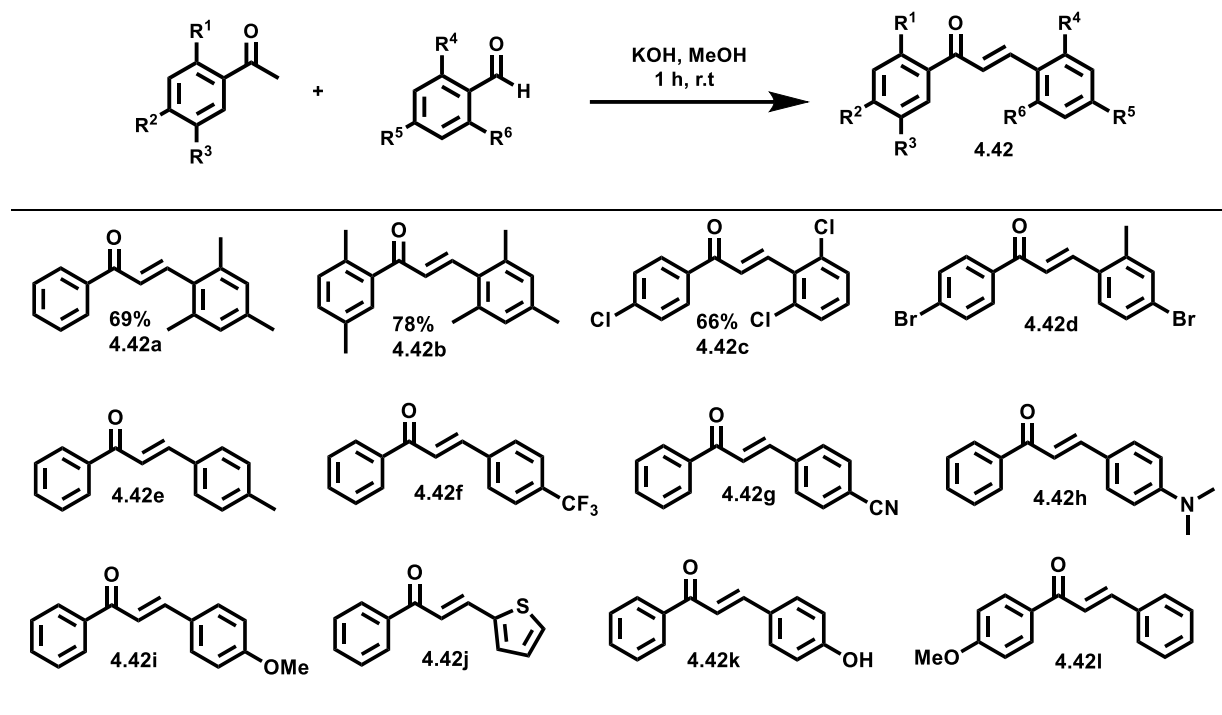


Figure 24: Synthesis of chalcones 4.42 (a-l)

The chalcones **4.42(a-l)** were then reacted with nitromethane under basic conditions and the reaction mixture was stirred at reflux temperature for 1h (**Figure 25**). In each case, the reaction mixture was then quenched via the addition of 1M HCl until pH 2 was achieved. At pH 2, each product precipitated as a white solid and was then isolated via filtration. In order to purify the white solids, each precipitate was dissolved in minimal dichloromethane and an excess of 20% ethyl acetate/hexane was added, and the resulting mixture was allowed to stand until a precipitate formed. The precipitate was then isolated via filtration and dried to afford the nitrobutanones **4.43 (a-l)**. Although a literature procedure was used as a template for this synthesis,¹⁴⁸ DBU was identified as a superior alternative to diethylamine which was the reported base for this Michael

addition. Nitrobutanones **4.43(f-i)** were prepared with the help of Jacob Campbell, Emily brown and Adil Alkas from the Thompson group.

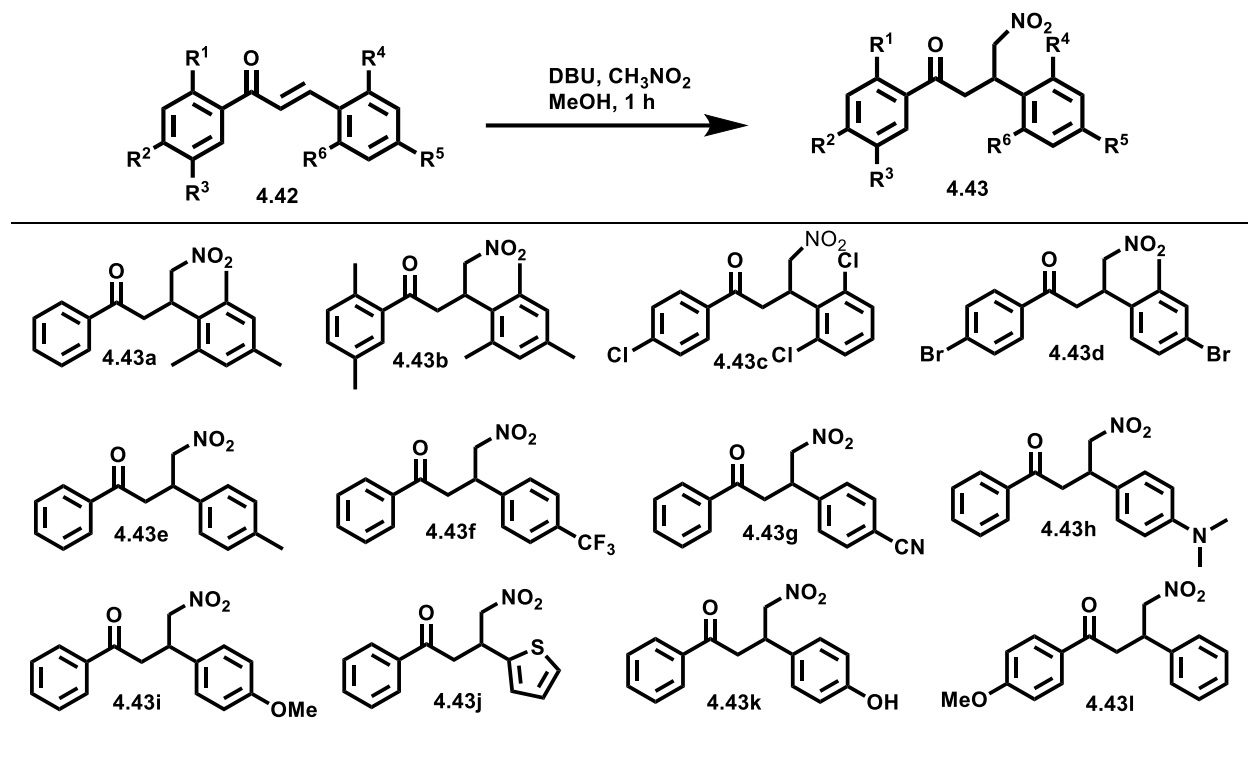


Figure 25: Synthesis of nitrobutanones **4.43 (a-l)** from chalcones **4.42**.

Following a published procedure,¹⁴⁸ the nitrobutanones were converted into pyrroles via a three-step procedure (**Figure 26**). Thus, the nitrobutanones **4.43(a-l)** were treated with a solution of KOH in anhydrous MeOH. The reaction mixture was stirred at room temperature for 1h and then the colourless solution was added dropwise into a solution of concentrated H₂SO₄ in anhydrous MeOH at 0°C. The reaction mixture was then allowed to slowly warm up to room temperature and further stirred for 1h. The reaction was quenched by the addition of water and ice, then neutralized to pH 7 with 4M NaOH. The mixture was then filtered, and the white solid thus obtained was dissolved in acetic acid and NH₄OAc was then added. The mixture was stirred at reflux

temperature (100°C) for 1h. The mixture was cooled, poured over ice, and neutralized to pH 7 with 4M NaOH. The resulting precipitate was isolated via filtration and then dried. The solid was dissolved in minimal dichloromethane and upon the addition of excess cold pentane, a solid precipitated which was isolated via filtration and washed with cold pentane and dried to afford the pyrroles **4.44(a-l)** as a free flowing-solids (**Figure 26**). Pyrroles **4.44(f-l)** were prepared with the help of members from the Thompson group.

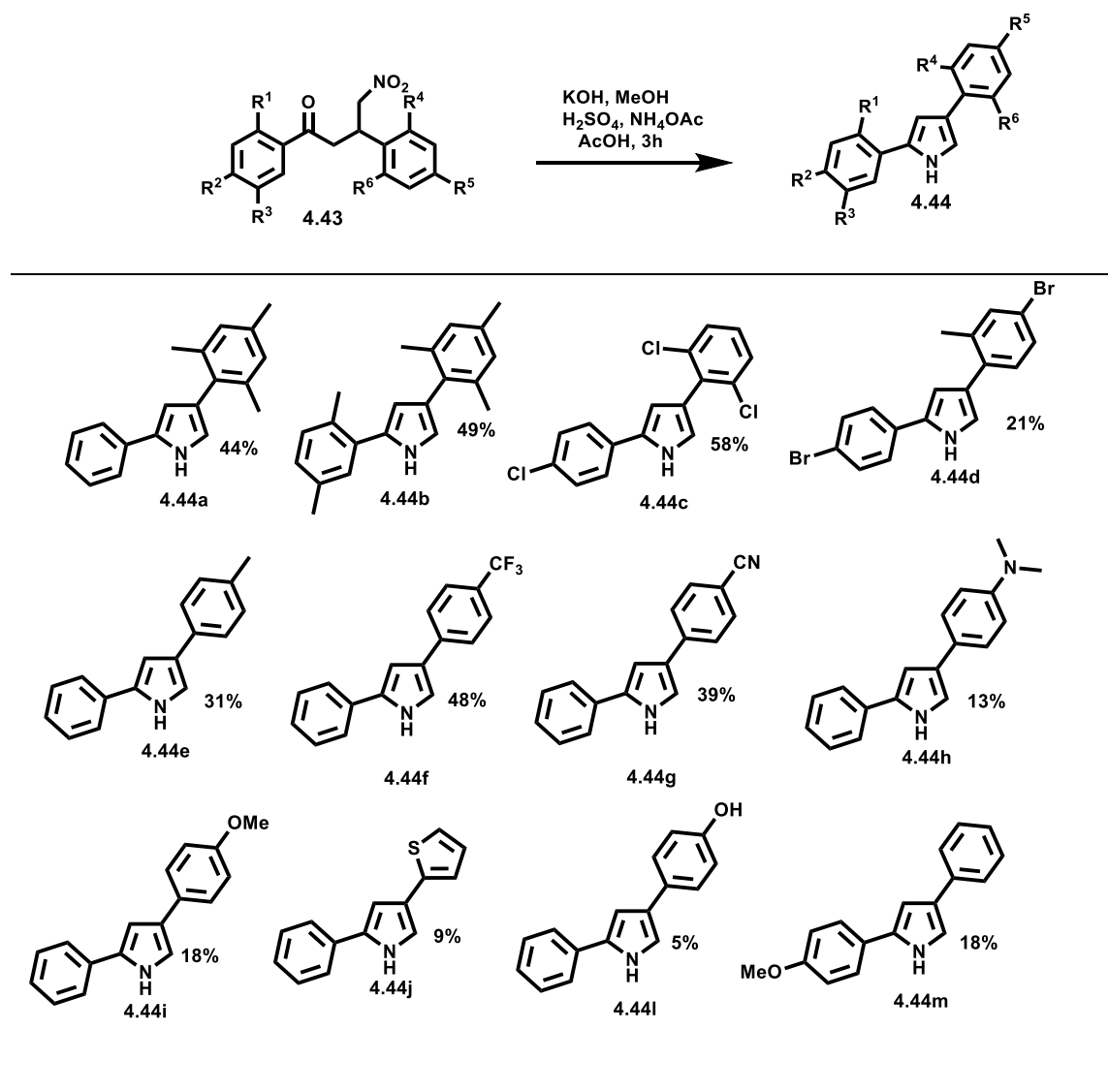


Figure 26: Synthesis of pyrroles 4.44 from nitrobutanones 4.43.

With the pyrroles in hand, the newly established nitrosylation conditions using NOBF₄ were applied to other pyrrole derivatives. To this end, the aryl-substituted pyrroles **4.44(a-l)** containing a wide array of substrates were each dissolved in anhydrous MeCN under a nitrogen atmosphere at -5 to -10°C (achieved using an ice/acetone bath). Solid NOBF₄ (0.9 eq) was then added in 3 portions. The resulting solution was stirred for 5-10 minutes, in the cold bath, at which point all starting material was consumed according to analysis by TLC. The reaction mixture was added to water and extracted into CH₂Cl₂. The combined organic fractions were dried over anhydrous Na₂SO₄ and then concentrated *in vacuo*. The resulting solid was purified using column chromatography to afford the desired 2-nitroso pyrroles. Pyrroles **4.44(a-h)** reacted successfully under the nitrosylation conditions to form each nitroso pyrrole in satisfactory yields (46-79%, **Figure 27**). These yields are within the same range as those obtained using NaNO₂/HCl.⁹⁰

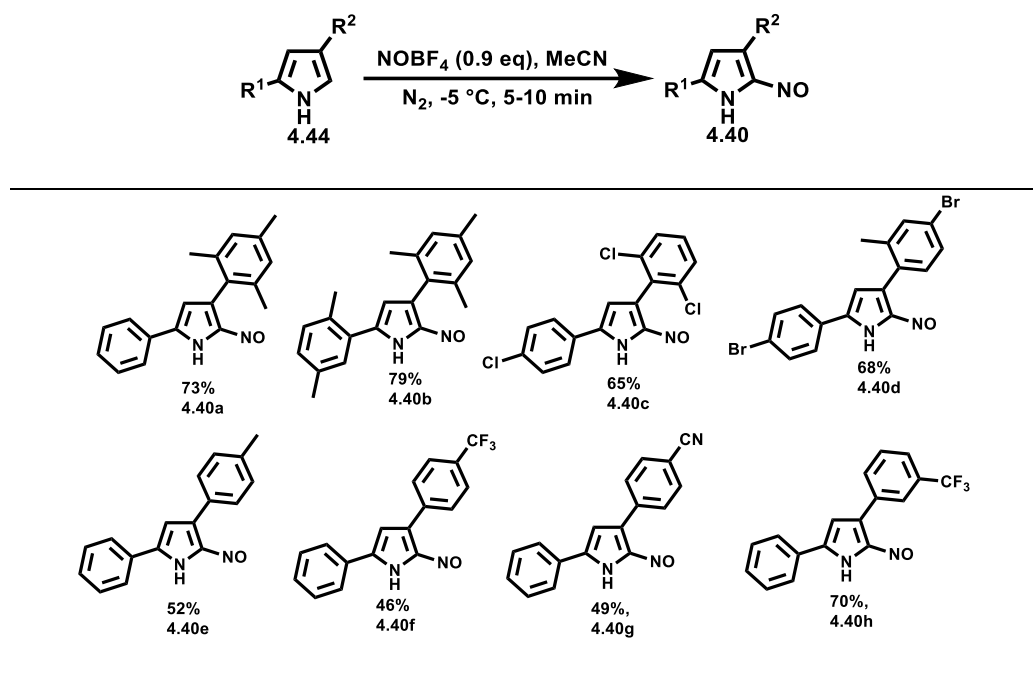


Figure 27: Synthesis of aryl-nitroso pyrroles on a variety of pyrrole substrates.

Despite success with pyrroles 4.44(a-h), analogues **4.44(i-m)** did not form the desired nitroso product under the optimal conditions for nitrosylation using NOBF₄ (**Figure 28**). These pyrroles all bear some electron-donating groups on the aryl rings.

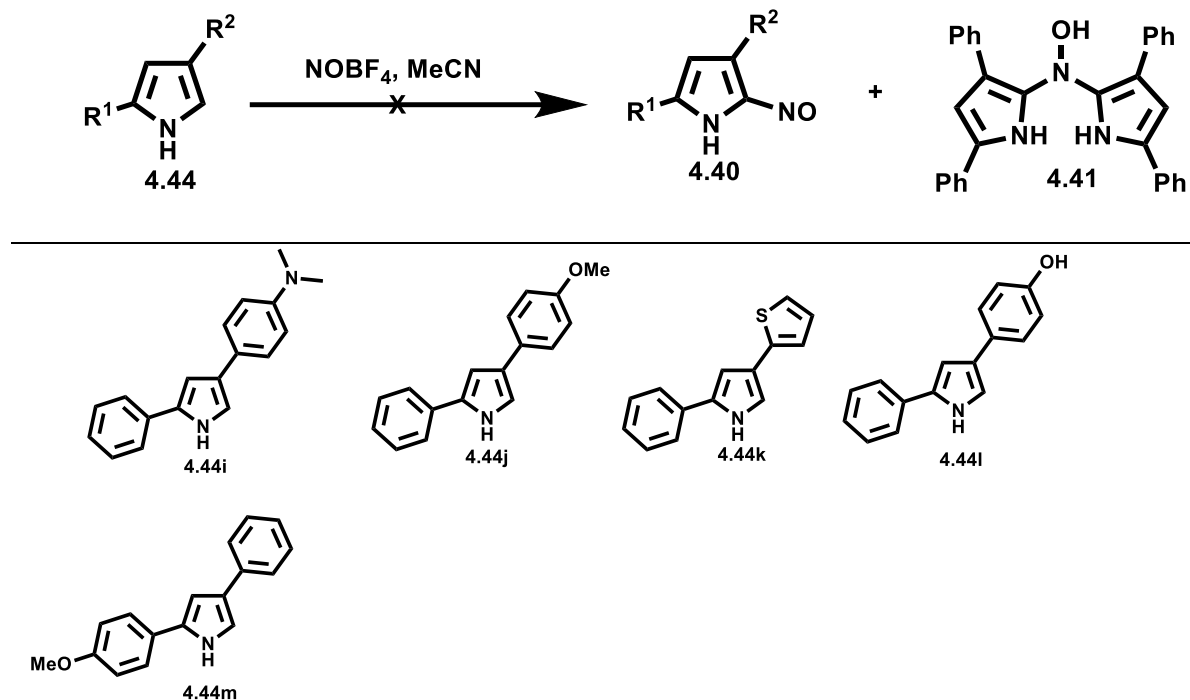
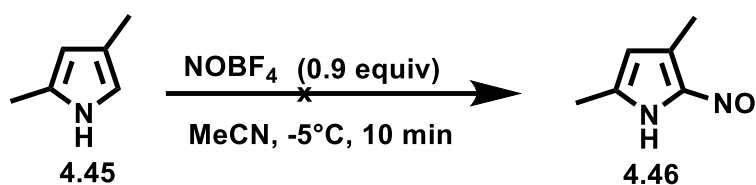


Figure 28: Failed attempted nitrosylation of pyrroles bearing electron-donating groups on the phenyl rings.

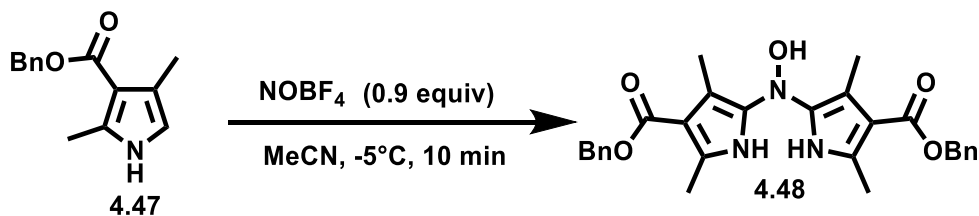
Although expending no efforts to isolate the material, based on MS analysis of the crude reaction mixtures the mass for the N-hydroxyl intermediate **4.41** was found in all runs, particularly for substrates bearing substituents featuring electron donating groups (**Figure 28**). Based on this observation, it was hypothesized that the increased electron density prompts the α -free pyrrole still present in the solution to immediately attack the nitroso pyrrole once formed to form the N-hydroxyl intermediate **4.41**. This is a positive result for the ultimate goal of the project which is the synthesis of aza dipyrrens, as the N-hydroxyl intermediate **4.41** is only one step away from the

aza dipyrin. Based on this hypothesis and having established a broad scope for aryl-substituted pyrroles, attention was then turned to alkyl-substituted pyrroles. Attempts towards the nitrosylation of the dimethylpyrrole **4.45** (**Scheme 38**), using the optimal protocol involving NOBF₄, resulted in a complex reaction mixture, based on TLC and ¹H NMR analysis of the crude reaction mixture. The desired nitroso product was not detected. The stoichiometry was reduced to as low as 0.5 equiv NOBF₄, given the electron-rich nature of the pyrrole, yet without detection of the desired product.



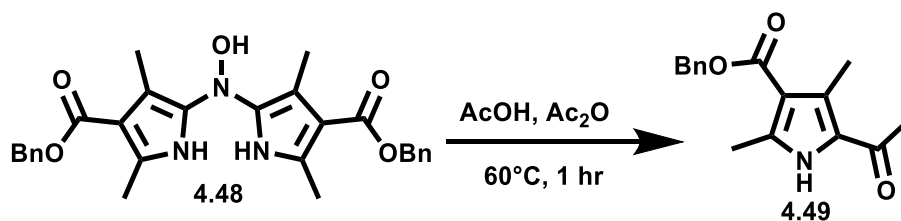
Scheme 38: Attempted nitrosylation of dimethyl pyrrole 4.45.

It was reasoned that since the pyrrole has two potential reactive sites that can potentially be nitrosylated, coupled with the high reactivity of alkyl-substituted pyrroles, it might be over-nitrosylated and/or prompt further reaction of the nitroso product with components of the reaction mixture. With this in mind, efforts turned to the evaluation of stabilized alkyl-substituted pyrrole **4.47** (**Scheme 39**), i.e. those bearing electron-withdrawing groups and with only one reactive position. In this way, it was anticipated that any potential side reactions would be minimized. Subjecting **4.47** to the optimal NOBF₄ conditions resulted in the formation of product **4.48** (**Scheme 39**), which was isolated after column chromatography in a 53% yield, verified by NMR and MS analysis. This result was particularly pleasing as it suggests that the desired nitroso product did form but immediately reacted with the unreacted α -free pyrrole to make the hydroxyl intermediate **4.48**. Leaving product **4.48** in an open-air environment for a couple of days did not result in the formation of the aza dipyrin as observed with the diphenyl nitroso pyrrole reaction.



Scheme 39: Synthesis of hydroxyl intermediate 4.48 from the nitrosylation of pyrrole 4.47.

According to the proposed mechanism by Loudet et al. (Scheme 23)¹³⁰ for the formation of aza dipyrins involving the condensation of a nitroso pyrrole and another α -free pyrrole, the hydroxyl aza dipyrin intermediate is protonated by acetic acid, losing a molecule of water to produce an aza dipyrin.¹⁷⁷ In light of this mechanism, it was hypothesized that subjecting **4.48** to acidic media would result in the formation of the alkyl-substituted aza dipyrin. However, when **4.48** was stirred in acetic acid/acetic anhydride at 60°C, the desired aza dipyrin was not detected. Instead, product **4.49** (Scheme 40) was isolated. Presumably, compound **4.40b** dissociated under the acidic conditions to make α -free pyrrole which reacted with a molecule of acetic anhydride to form pyrrole **4.49**. The X-ray structure of **4.49** is shown in Figure 29.



Scheme 40: Attempted protonation of hydroxyl intermediate 4.48.

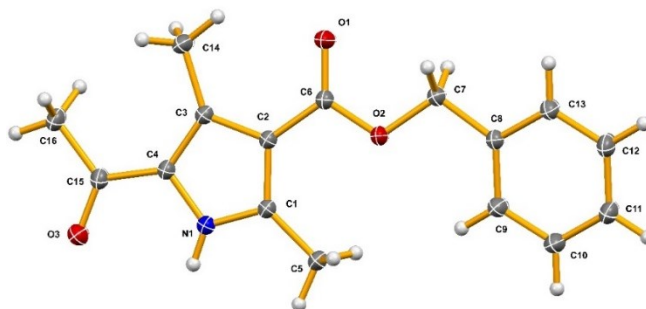
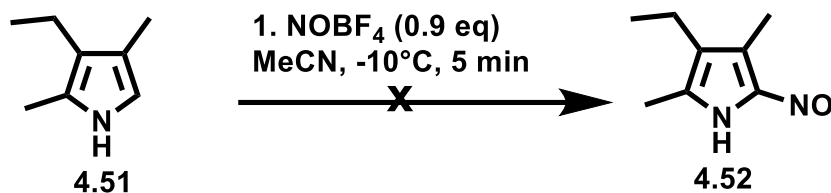


Figure 29: OTREP diagram of pyrrole 4.49. Thermal ellipsoids are shown at 50% probability.

The formation of the hydroxyl intermediate **4.48** prompted the evaluation of the protocol on an exclusively alkylated substrate **4.51** (Scheme 41). When **4.51** was treated with NOBF_4 , the starting material disappeared 5 minutes after the addition of NOBF_4 , according to TLC analysis. However, when subjected to aqueous workup, the colour of the crude reaction mixture changed from light brown to green, and then to black upon evaporation of the solvent in *vacuo*.



Scheme 41: Attempted nitrosylation of pyrrole 4.51

Analysis of the crude product mixture using TLC, after the workup, revealed many new spots and the corresponding NMR spectrum did not exhibit any peaks characteristics of the expected product. To avoid the aqueous workup and heat, the solvent (MeCN) was removed under a high vacuum. The sample was submitted for NMR spectroscopy. Although shimming was challenging due to the product methyl peaks lying under the MeCN solvent peak, the spectrum shows that the α -proton of the starting material **4.51** disappeared, indicating the presence of another species other

than a proton on the α -position of the pyrrole. Furthermore, the peaks in the product slightly shifted compared to the starting material **4.51** as shown in **Figure 30**.

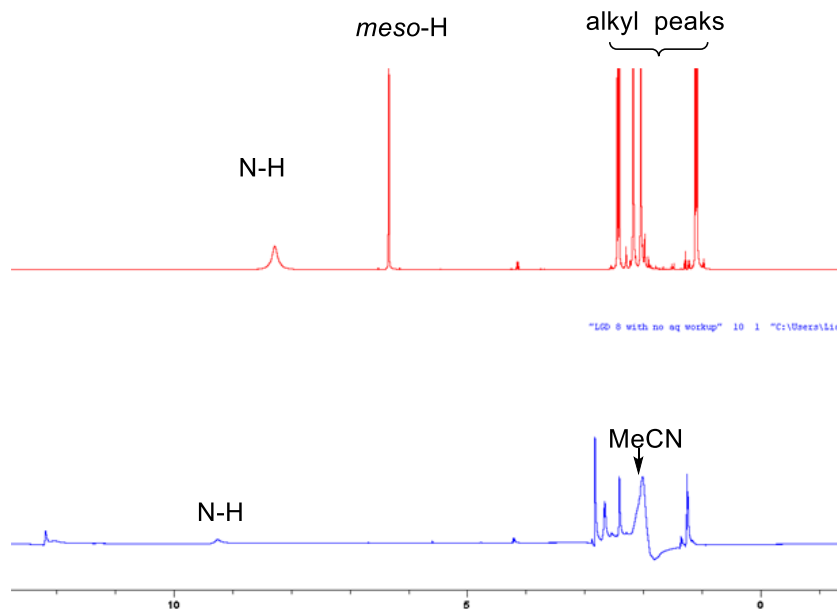
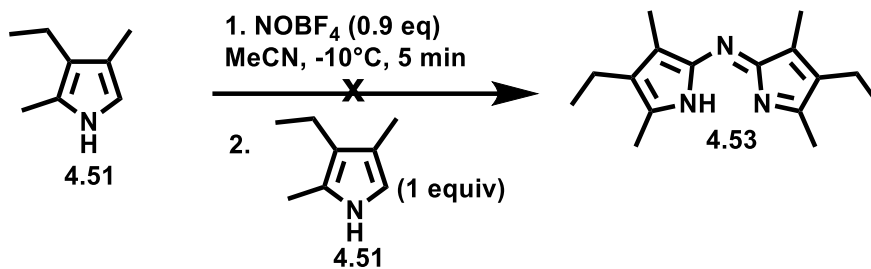


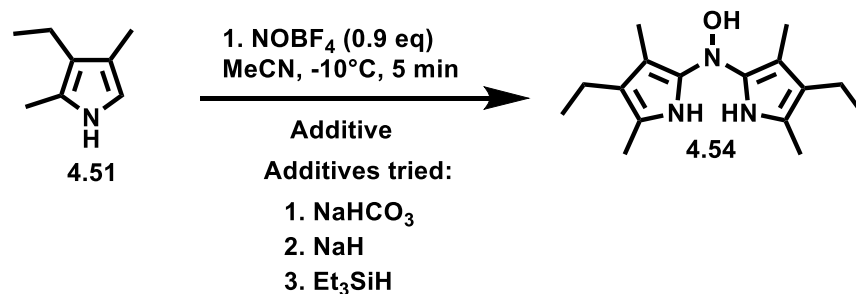
Figure 30: Top: ¹H NMR spectrum of pyrrole **4.51**. Bottom: ¹H NMR of the reaction mixture in MeCN showing disappearance of meso-H peak.

The desired nitroso product was detected by MS analysis. This, together with the NMR data, suggests that the nitroso product forms under these nitrosylation conditions but is not stable in aqueous conditions and under heat. Based on this result, it was hypothesized that if the nitroso product formed, the addition of a second equivalent of **4.51** to the reaction mixture upon consumption of starting material, would result in the formation of the aza dipyrin **4.53** (**Scheme 42**). However, the addition of a second equivalent of **4.51** resulted in a complex reaction mixture.



Scheme 42: Attempted synthesis of aza dipyrin 4.53 from the second addition of 4.51 to a solution of 4.51 and NOBF₄.

Given the intense reactivity of the pyrrole **4.51**, it was hypothesized that the formation of HBF₄ would interfere with **4.51**, and/or with reaction products. Therefore, *in-situ* quenching of HBF₄ could potentially irradiate any side reactions. To quench the HBF₄, a variety of additives (**Scheme 43**) were added to the solution of pyrrole before the addition of NOBF₄. Addition of Et₃SiH and NaH still resulted in complicated reaction mixtures but, interestingly, the addition of NaHCO₃ to the reaction mixture resulted in the formation of the N-hydroxyl intermediate **4.54** (**Scheme 43**), confirmed by MS and ¹H NMR analysis. The corresponding ¹H NMR spectrum is shown in **Figure 31**, showing the sets of peaks for the product **4.54**. However, attempts toward acquiring a carbon NMR for **4.54** were unfruitful as the material decomposed.



Scheme 43: Synthesis of N-hydroxyl intermediate 4.54 in the presence of additives to quench HBF₄ in situ.

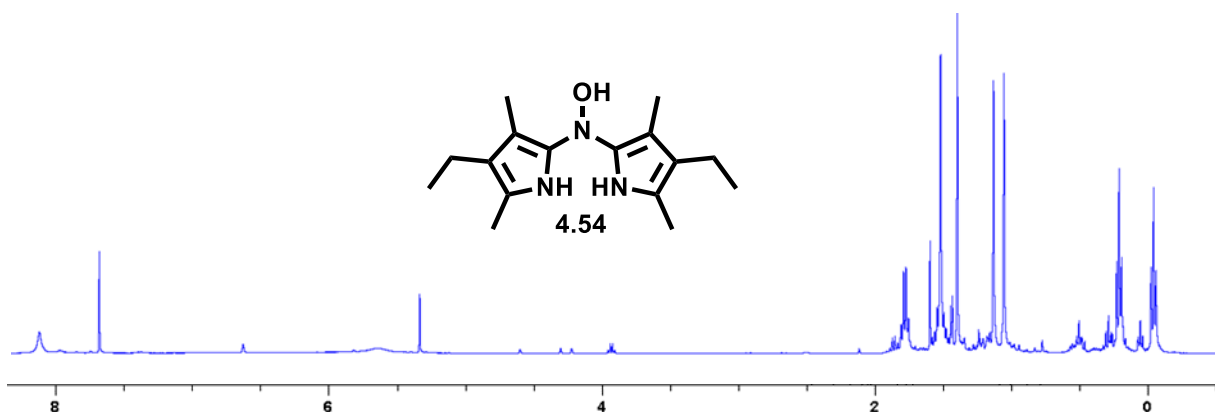
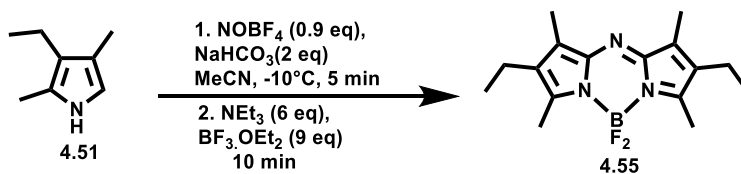


Figure 31: ¹H NMR spectrum of compound 4.54.

With the insight that product **4.54** was presumably being formed, but is not stable, it was hypothesized that trapping this material as an *F*-BODIPY **4.55** would enhance stability and allow further study and/or manipulations of this compound. To this end, pyrrole **4.51** was reacted with NOBF₄ in the presence of NaHCO₃. Instead of quenching the reaction, 6 equivalents of anhydrous NEt₃ were added and the reaction mixture was allowed to stir for 10 minutes before the addition of 9 equivalents of BF₃•OEt₂ (**Scheme 44**). A drastic colour change from brown to a deep purple fluorescent hue was observed upon addition of BF₃•OEt₂. TLC analysis of the reaction mixture showed the disappearance of the starting material after about 5 minutes of stirring, and the presence of a significant baseline spot plus two very fluorescent spots as shown in (**Figure 32, left**). The reaction was quenched with water and extracted with CH₂Cl₂. TLC analysis of the crude product

mixture showed the presence of multiple new spots. Purification to obtain the two compounds corresponding to the spots was achieved using column chromatography. The two isolated materials were submitted for NMR and MS analysis. The spectra obtained were complex but the boron and fluorine NMR spectra suggested the presence of a $-\text{BF}_2$ moiety in the two samples. Efforts toward the characterization of the fluorescent species obtained from this study are underway. The TLC plate shows a red fluorescent spot: although isolated, the amount was insufficient to allow for characterization.



Scheme 44: Attempted synthesis of aza-F-BODIPY 4.55 from 4.51.

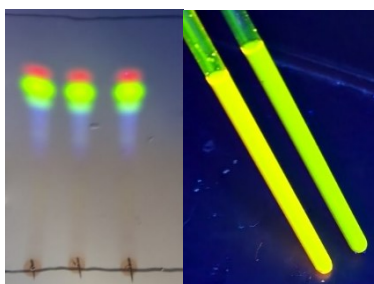


Figure 32: TLC analysis of the reaction of 4.51 with NEt_3 and $\text{BF}_3\cdot\text{OEt}_2$ before work-up (left), NMR samples for the two fluorescent compounds isolated (right).

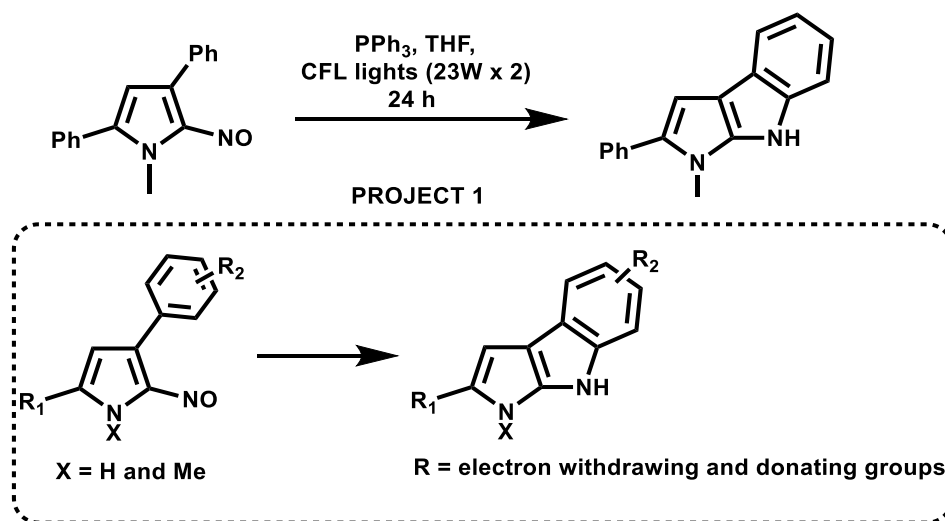
The incorporation of a $-\text{BF}_2$ moiety into the dipyrin and aza-dipyrin framework causes these compounds to fluoresce. The evidence of the presence of the $-\text{BF}_2$ moiety, according to NMR analysis, and the fluorescence is an exciting indication of some kind *F*-BODIPY formed. However, pyrrole **4.51** might not have reacted in the expected way, as the expected products were not detected via MS analysis of the product materials.

4.4.1 - Conclusion.

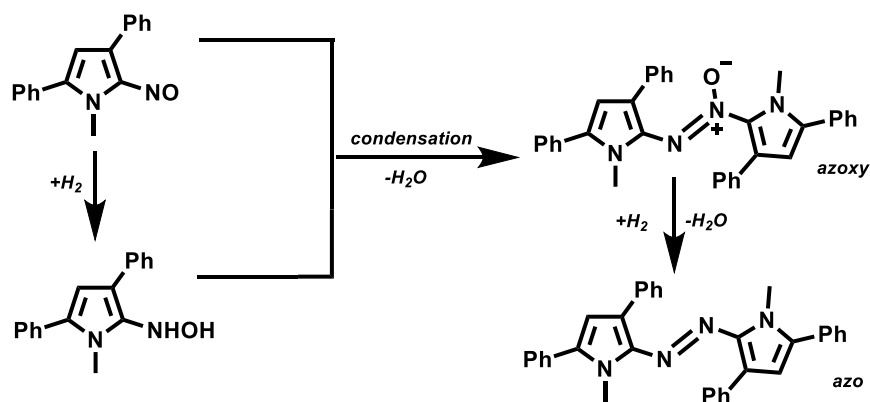
This chapter discusses the development of a potential alternative route to the synthesis of aza dipyrins, ideally to overcome limitations in the current methods of synthesis. Several pathways have been proposed herein wherein α -nitro or α -nitroso pyrroles bearing desired substituents are synthesized and then coupled with 2-boc-pyrrole boronic acid **4.11** under catalysis with tetravalent phosphorus reagents in the presence of phenylsilane as a reductant. Investigations of this coupling revealed multiple challenges, with complex mixtures obtained. This prompted the reaction of nitroso pyrroles with 2-boc-pyrrole boronic acid **4.11** under light-promoted triphenylphosphine-induced catalysis. The use of blue LED lights resulted in the formation of the desired aza dipyrin in a 44% yield, an achievement comparable to the current routes to aza dipyrins.⁹⁰ Given this success, attempts to synthesize alkyl-substituted nitroso-pyrroles for subjection to the blue LED-mediated methods using the nitrosylation conditions with NaNO₂ in ethanolic HCl were unsuccessful. This prompted the exploration of alternative nitrosylation conditions for pyrroles. The reaction of α -free pyrroles with NOBF₄ in acetonitrile resulted in the formation of nitroso pyrroles and several novel nitroso pyrroles were synthesized in reasonable yields. Application of this nitrosylation to alkyl-substituted systems did not proceed as expected but provided evidence for the formation of N-hydroxyl intermediates. This provides intriguing evidence that aza-dipyrins are possibly just a step away. Further development is necessary to determine the viability of the pathway.

4.4.2 - Future work.

The synthesis of the fluorescent material from the reaction of the alkyl-substituted pyrrole with NOBF_4 and subsequently with $\text{BF}_3 \cdot \text{OEt}_2$ in the presence of NEt_3 , excitingly suggests the presence of incorporation of the $-\text{BF}_2$ moiety within the product compounds. Efforts towards elucidation and characterization of the fluorescent compounds should be pursued. If successfully characterized, a possible mechanism for the reactivity of alkyl pyrrole derivatives with NOBF_4 can be proposed. This will allow further study of the reactivity of alkyl-substituted pyrroles in the synthesis of aza dipyrrens. The discovery of the new pyrrole-based carbazole provides a new class of pyrrolic compounds. Varying the substitution around the pyrrolic frame will allow for the synthesis of a variety of novel compounds of this kind. Solid-state absorbance and emission spectra of the compounds should then be studied and their optical properties elucidated.



The azoxy class of compounds carries uncommon 1,3-dipolar O=N=N linkage with charges distributed over the three-atom set which is a valuable building block in the preparation of dyes and pigments, potential for drug delivery,¹⁷⁸ and promising anticancer activities. The discovery of a pyrrole-based azoxy compound can complement and meet the needs of new azoxy compounds and potentially provide a sustainable option as the traditional industrial syntheses of azoxy compounds are often costly, inefficient, and environmentally unfriendly.^{160,163} It follows that practical, accessible methods for the synthesis of azoxybenzene and functional azoxy derivatives are urgently needed. We speculate that azoxy pyrrole was formed as a result of the condensation of the nitroso pyrroles and hydroxyl pyrrole formed as a result of the reduction of nitrosopyrrole with the PhSiH₃ reductant.^{179,180} This work should give a strong impulse to new research efforts for this important transformation. Broadening the range of substitution about the pyrrolic rings will allow for the synthesis of novel azoxypyrroles which will stimulate further investigation into this unique and interesting class of products.



Scheme 45: The proposed pathway to the pyrrole-based azoxy and azo compounds.

The presence of azo dyes suggests that the further reduction of the azoxy compound and loss of water results in the formation of the azobispyrrole. The low yields suggest that this process is a slow process or less amount of reductant was used there was not enough reductant to reduce all the azoxy compound to the azo dye. Further optimization of the transformation of the azoxy compound to the azobispyrrole is needed to provide a new route to the azobispyrroles which are a new class of azo compounds. The current route being explored for the synthesis of these compounds relies on harsh reaction conditions, such as high temperature and excess amounts of ammonium reagents (up to 35 equiv) that lead to the formation of hazardous or undesirable byproducts following the over oxidation/reduction of the starting materials and the competing formation of aza dipyrins.¹⁸¹ With an optimized, efficient route to azobispyrroles from the azoxypyrroles, azobispyrroles can be synthesized in higher amounts enough for characterization.

4.5 - Experimental.

All ¹H NMR (500 MHz), ¹³C NMR (125 MHz) and ¹¹B NMR (160 MHz) spectra were recorded using a Bruker AV 500 MHz spectrometer. All ¹⁹F NMR (282 MHz) spectra were recorded using a Bruker AV 300 MHz spectrometer. ¹H chemical shifts are reported in ppm relative to tetramethylsilane using chloroform solvent residual at $\delta = 7.26$ ppm as an internal standard. ¹³C spectra were recorded using the UDEFT pulse sequence with chemical shifts reported in ppm referenced to CDCl₃ resonance at $\delta = 77.2$ ppm. Splitting patterns are indicated as follows: br, broad; s, singlet; d, doublet; t, triplet; q, quartet; m, multiplet. All coupling constants (*J*) are reported in Hertz (Hz). High-resolution mass spectra were obtained using TOFMS experiments with electrospray ionization operating in both positive and negative modes as indicated eg. [M + H]⁺, [M - H]⁻. Column chromatography was performed in glass tubes using 230-400 mesh ultra

pure silica or via a Biotage chromatograph. Chalcones were prepared according to literature procedures,^{90,95,182} except for **4.42b**, **4.42c**, and **4.42d**. Nitrobutanones were prepared according to literature procedures except for **4.43b**, **4.43c**, and **4.43d**. Nitroso pyrrole **4.21**¹⁴⁸ was synthesized according to a reported procedure.

4.5.1 - General procedure 1 (GP1) for the synthesis of chalcones, 4.42b-d

Following a published procedure¹⁴⁸ for the synthesis of aza-BODIPYs, to synthesize the chalcones **4.42b-d**, KOH (2.5 equiv.) was added to a stirring solution of a benzaldehyde (23.3 mmol, 1 equiv.) and acetophenone (23.3 mmol, 1 equiv.) in MeOH (20 mL). The reaction mixture was stirred at r.t. for 1 h. The precipitate formed was isolated via filtration, washed with MeOH and cold pentane, and then dried under vacuum to afford the desired chalcone.

4.5.2 - General procedure 2 (GP2) for the synthesis of nitrobutanones, 4.43a-d

To a solution of chalcone, **4.42a-d** (6 mmol, 1 equiv.) in MeOH (20 mL) was added 1,8-diazabicyclo(5.4.0)undec-7-ene (DBU) (30 mmol, 5 equiv.) and nitromethane (30 mmol, 5 equiv.). The mixture was heated at reflux temperature for 1 h, then allowed to cool to room temperature. The solution was acidified to pH 2 with 1 M HCl and then extracted with CH₂Cl₂ (2 x100 mL). The combined organics were washed with water (100 mL) and brine (100 mL), then dried over Na₂SO₄. The solvent was removed in vacuo, and the resulting oil was purified by column chromatography on silica (5→100% ethyl acetate/hexanes) to provide the desired product.

4.5.3 - General procedure 3 (GP3) for the synthesis of 2,4-diaryl-1Hpyrroles, 4.44a-d

To a solution of KOH (40 mmol) in MeOH (124 mL) was added nitrobutanone **4.43a-d** (8 mmol) and the mixture was stirred for 1 h at room temperature. The mixture was then added dropwise to a solution of conc. H₂SO₄ (12 mL) in MeOH (20 mL) at 0 °C. The solution was allowed to warm to room temperature and then stirred for a further 1 h. Water (100 mL) and ice (100 mL) were added, and the mixture was neutralized with aqueous 4 M NaOH and then extracted with CH₂Cl₂ (2 x 250 mL). The combined organics were washed with water (100 mL) and brine (50 mL), then dried over Na₂SO₄. The solvent was removed *in vacuo* to provide a crude oil, which was carried into the next stage without further purification. To the intermediate compound was added acetic acid (27 mL) and NH₄OAc (40 mmol), and the resulting mixture was heated at 100 °C for 1 h. The reaction mixture was allowed to cool to room temperature, and ice (100 mL), was then added. The mixture was carefully neutralized with aqueous 4 M NaOH to result in the generation of a precipitate which was isolated by filtration. The crude product was further purified by the dissolution of the solid in a small amount of CH₂Cl₂, followed by the addition of pentane and isolation of the resulting precipitate *via* filtration.

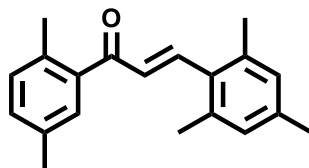
4.5.4 - General procedure 4 (GP4) for the synthesis of nitroso pyrroles 4.21a-h

To a stirred solution of pyrrole **4.44a-h** (50 mg) in anhydrous MeCN (5 mL) under a nitrogen atmosphere at -5 to -10°C (achieved using an ice/acetone bath) was added solid NOBF₄ (0.9 eq) in 3 portions, with a flow of nitrogen maintained during the additions. The resulting solution was stirred for 5-10 minutes, in the cold bath, at which point all pyrrole starting material was consumed

according to analysis by TLC. The reaction mixture was added to water (20 mL) at room temperature, and extracted into CH₂Cl₂ (2 x 20 mL). The combined organics were dried over Na₂SO₄, then concentrated *in vacuo*. The resulting solid was dry-loaded onto a silica chromatography column, aided by dissolution in CH₂Cl₂, and purified using a gradient of ethyl acetate/hexanes (0→60% ethyl acetate) as eluent to afford the desired 2-nitroso pyrrole as a green solid that stained orange on silica TLC plates visualized with vanillin stain and heat.

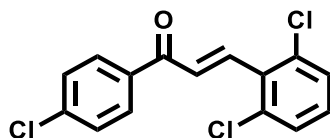
4.5.5 - Synthesis of compounds

(2E)-1-(2,5-Dimethylphenyl)-3-(2,4,6-trimethylphenyl)prop-2-en-1-one, (4.42b).



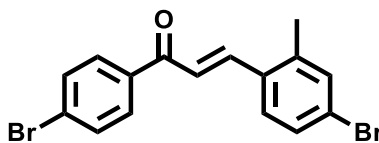
The title compound was synthesized from 2,4,6-trimethylbenzaldehyde and 2,5-dimethylacetophenone according to **GPI** and was isolated as a yellow solid (5.1 g, 78%). ¹H NMR (500 MHz, CDCl₃) δ: 7.65 (d, *J* = 17 Hz, 1H), 7.29 (s, 1H), 7.15-7.19 (m, 2H), 6.90 (s, 2H), 6.76 (d, *J* = 16 Hz, 1H), 2.43 (s, 3H), 2.35 (s, 3H), 2.34 (s, 6H), 2.29 (s, 3H). ¹³C NMR δ: 197.1, 144.8, 139.2, 138.9, 137.3, 135.3, 134.1, 132.1, 131.5, 129.6, 129.0, 21.5, 21.4, 21.2, 20.1, 2 carbon signals missing. HRMS-ESI (*m/z*): [M+Na]⁺ calc'd for C₂₀H₂₂NaO 301.1563, found 301.1559.

(2E)-1-(4-Chlorophenyl)-3-(2,6-dichlorophenyl)prop-2-en-1-one, (4.42c).



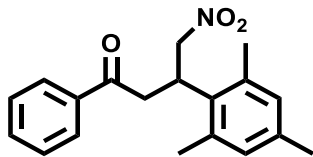
The title compound was synthesized from 2,6-dichlorobenzaldehyde and 4-chloroacetophenone according to **GP1** and was isolated as a yellow solid (4.79 g, 66%). ^1H NMR (CDCl_3): δ = 7.95 (m, 2H), 7.85 (d, J = 16 Hz, 1H), 7.61 (d, J = 16 Hz, 1H), 7.47 (d, J = 10 Hz, 2H), 7.38 (d, J = 10 Hz, 2H), 7.21 (t, J = 5.0 Hz, 1H); ^{13}C NMR (CDCl_3) δ : 188.9, 139.6, 138.3, 135.9, 135.2, 132.4, 130.1, 129.9, 129.0, 128.8, 1 carbon signal missing. HRMS-ESI (m/z): $[\text{M}+\text{Na}]^+$ calc'd for $\text{C}_{15}\text{H}_9\text{Cl}_3\text{NaO}$ 332.9617, found 332.9611.

(2E)-3-(4-Bromo-2-methylphenyl)-1-(4-bromophenyl)prop-2-en-1-one, (4.42d).



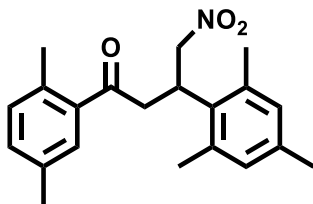
According to a modified version of **GP1**, the title compound was synthesized from 4-bromo-2-methylbenzaldehyde (5.02 mmol) and 4-bromoacetophenone (5.02 mmol), and was isolated as a yellow solid (1.71 g, 89%). ^1H NMR (CDCl_3) δ : 8.03 (d, J = 15 Hz, 1H), 7.64-7.88 (dd, J = 110 Hz, 7.0 Hz, 4H), 7.54 (d, 8.1 Hz, 1H), 7.37-7.40 (m, 3H), 2.45 (s, 3H). ^{13}C NMR δ : 189.2, 141.9, 140.5, 139.1, 136.9, 134.0, 132.8, 132.2, 130.2, 129.7, 128.0, 124.8, 123.0, 19.8. HRMS-ESI (m/z): $[\text{M}+\text{Na}]^+$ calc'd for $\text{C}_{16}\text{H}_{12}\text{Br}_2\text{NaO}$ 400.9147, found 400.9150.

4-Nitro-1-phenyl-3-(2,4,6-trimethylphenyl)butan-1-one, (4.43a).



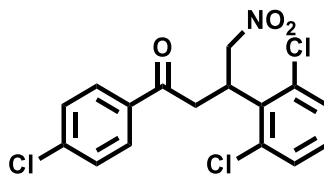
The title compound was synthesized from **4.42a**, according to **GP2**, and was isolated as an orange oil (1.37 g, 74%). $^1\text{H NMR}$ (CDCl_3) δ : 7.95 (d, $J = 7.6$ Hz, 2H), 7.55-7.58 (m, 1H), 7.44-7.47 (m, 2H), 6.86 (s, 2H), 4.85-4.96 (m, 2H), 4.77 (m, 1H), 3.49-3.59 (m, 2H), 2.47 (s, 6H), 2.26 (s, 3H). $^{13}\text{C NMR}$ (CDCl_3) δ : 197.2, 136.8, 136.4, 133.4, 132.9, 131.3, 129.9, 128.7, 128.1, 78.2, 40.5, 33.9, 21.3, 20.6, in accordance with literature.⁹⁵

1-(2,5-Dimethylphenyl)-4-nitro-3-(2,4,6-trimethylphenyl)butan-1-one, (4.43b).



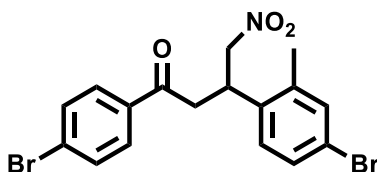
The title compound was synthesized from **4.42b**, according to **GP2**, and was isolated as a white crystalline solid (1.28 g, 63%). $^1\text{H NMR}$ (CDCl_3) δ : 7.31 (s, 1H), 7.18 (d, $J = 7.9$ Hz, 1H), 7.10 (d, $J = 8.1$ Hz, 1H), 6.82 (s, 2H), 4.83-4.86 (m, 1H), 4.75-4.80 (m, 1H), 4.68-4.72 (m, 1H), 3.36-3.46 (m, 2H), 2.41 (s, 3H), 2.33 (s, 3H), 2.29 (s, 3H), 2.25 (s, 3H), 2.22 (s, 3H). $^{13}\text{C NMR}$ (CDCl_3) δ : 201.3, 137.6, 137.0, 135.7, 135.3, 135.2, 132.2, 131.9, 131.2, 129.8, 128.7, 78.1, 43.3, 34.4, 21.5, 21.0, 20.8, 20.6, 20.3. HRMS-ESI (m/z): $[\text{M}+\text{Na}]^+$ calc'd. for $\text{C}_{21}\text{H}_{25}\text{NNaO}_3$: 362.1724; found 362.1727.

3-(2,6-Dichloro-phenyl)-4-nitro-1-(4-chloro-phenyl)-butan-1-one, (4.43c).



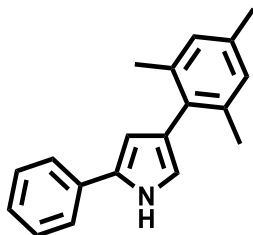
The title compound was synthesized from **4.42c**, according to **GP2**, and was isolated as a yellow solid (1.51 g, 67%). ^1H NMR (CDCl_3) δ : 7.86-7.88 (m, 2H), 7.41-7.43 (m, 2H), 7.37-7.38 (d, $J = 8.6$ Hz, 1H), 7.27-7.29 (d, $J = 9.0$ Hz, 1H), 7.14 (t, $J = 6.0$ Hz, 1H), 5.26-5.31 (m, 1H), 4.95-5.05 (m, 2H), 2.68 (d, $J = 7.9$ Hz, 2H). ^{13}C NMR (CDCl_3) δ : 195.3, 140.1, 137.0, 134.4, 134.2, 130.0, 129.4, 129.3, 129.0, 76.2, 38.9, 35.3, 1 carbon signal missing. HRMS-ESI (m/z): $[\text{M}+\text{Na}]^+$ cal'd for $\text{C}_{16}\text{H}_{12}\text{Cl}_3\text{NNaO}_3$: 393.9772; found 393.9775.

3-(2-Methyl-4-bromo-phenyl)-4-nitro-1-(4-bromo-phenyl)-butan-1-one, (4.43d).



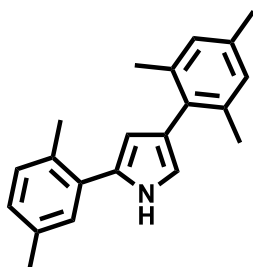
The title compound was synthesized from **4.42d**, according to **GP2**, and was isolated as a yellow oil (1.69 g, 64%). ^1H NMR (CDCl_3) δ : 7.76 (d, $J = 8.5$ Hz, 2H), 7.60 (d, $J = 8.5$ Hz, 2H), 7.35 (s, 1H), 7.28-7.31 (m, 1H), 7.02 (d, $J = 7.1$ Hz, 1H), 4.71-4.75 (m, 1H), 4.58-4.62 (m, 1H), 4.42-4.48 (m, 1H), 3.31-3.43 (m, 2H), 2.45 (s, 3H). ^{13}C NMR (CDCl_3) δ : 195.7, 139.1, 136.4, 135.0, 134.2, 132.3, 129.8, 129.6, 129.2, 127.1, 121.6, 78.9, 41.5, 34.1, 19.6. HRMS-ESI (m/z): $[\text{M}-\text{H}]^-$ calc'd. for $\text{C}_{17}\text{H}_{14}\text{Br}_2\text{NO}_3$: 437.9346; found 437.9333.

2-Phenyl-4-(2,4,6-trimethylphenyl)-1H-pyrrole, (4.44a).



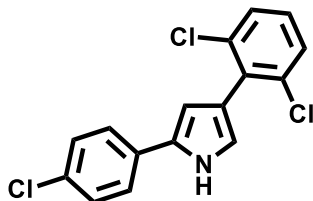
The title compound was synthesized from **4.43a**, according to **GP3**, and was isolated as a purple solid (920 mg, 44%). ¹H NMR (CDCl₃) δ: 8.45 (br, 1H), 7.55-7.56 (m, 2H), 7.42-7.45 (m, 2H), 7.26-7.29 (m, 1H), 7.02 (s, 2H), 6.71-6.72 (m, 1H), 6.48-6.50 (m, 1H), 2.39 (s, 3H), 2.26 (s, 6H). ¹³C NMR (CDCl₃) δ: 137.6, 136.1, 133.1, 132.7, 131.6, 128.9, 127.9, 126.0, 123.9, 123.5, 117.5, 107.7, 21.1, 21.0. HRMS-ESI (*m/z*): [M+H]⁺ calc'd. for C₁₉H₂₀N: 262.1590; found 262.1591.

2-(2,5-Dimethylphenyl)-4-(2,4,6-trimethylphenyl)-1H-pyrrole, (4.44b).



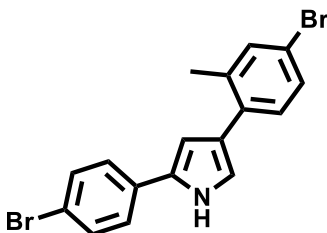
The title compound was synthesized from **4.43b**, according to **GP3** and was isolated as a purple solid (1.13 mg, 49%). ¹H NMR (CDCl₃) δ: 8.52 (br, 1H), 7.52-7.53 (m, 1H), 7.45-7.62 (d, *J* = 8.5 Hz, 1H), 7.30-7.32 (d, *J* = 8.6 Hz, 1H), 7.25 (s, 2H), 6.95-6.96 (m, 1H), 6.52-6.53 (m, 1H), 2.74 (s, 3H), 2.66 (s, 6H), 2.52 (s, 6H). ¹³C NMR (CDCl₃) δ: 137.6, 136.0, 135.4, 133.4, 132.7, 131.8, 131.1, 130.9, 128.0, 127.9, 127.3, 123.0, 116.4, 110.7, 21.2, 21.1, 20.9, 1 signal missing. HRMS-ESI (*m/z*): [M+H]⁺ calc'd. for C₂₁H₂₄N: 290.1903, found 290.1903.

4-(2,6-Dichloro-phenyl)- 2-(4-chloro-phenyl)-1H-pyrrole, (4.44c).



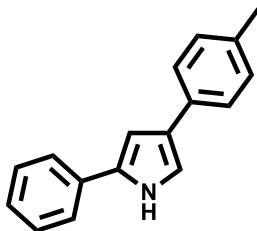
The title compound was synthesized from **4.43c**, according to **GP3**, and was isolated as a purple solid (1.31 g, 51%). ^1H NMR (CD_3NO_2) δ : 8.22 (br, 1H), 7.95 (d, $J = 7.1$ Hz, 2H), 7.44 (m, 1H), 7.32 (d, $J = 7.1$ Hz, 2H), 7.16 (m, 1H), 7.06 (m, 1H), 6.94 (m, 1H), 6.69 (m, 1H). ^{13}C NMR (CDCl_3) δ : 137.6, 136.0, 135.4, 133.4, 132.7, 131.8, 131.1, 130.9, 128.0, 127.9, 127.3, 123.0. HRMS-ESI (m/z): $[\text{M}+\text{H}]^+$ calc'd. for $\text{C}_{16}\text{H}_{11}\text{Cl}_3\text{N}$: 323.6130; found 323.3133.

4-(4-Bromo-2-methylphenyl)-2-(4-bromophenyl)-1H-pyrrole, (4.44d).



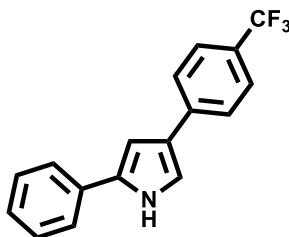
The title compound was synthesized from **4.43d**, according to **GP3**, and was isolated as a purple solid (657 mg, 21%). ^1H NMR (CDCl_3) δ : 8.49 (br, 1H), 7.54 (d, $J = 9.4$ Hz, 2H), 7.43-7.44 (m, 1H), 7.41 (d, $J = 8.9$ Hz, 2H), 7.35-7.37 (m, 1H), 7.28 (s, 1H), 6.97-6.98 (m, 1H), 6.66-6.67 (m, 1H), 2.46 (s, 3H). ^{13}C NMR (CDCl_3) δ : 137.6, 133.4, 132.2, 131.5, 131.2, 130.8, 129.0, 128.1, 127.7, 125.5, 120.2, 120.0, 118.3, 107.4, 21.4. HRMS-ESI (m/z): $[\text{M}+\text{H}]^+$ calc'd. $\text{C}_{17}\text{H}_{14}\text{Br}_2\text{N}$ for 389.9488, found 389.9499

4-(4-Methylphenyl)-2-phenyl-1H-pyrrole, (4.44e).



The title compound was synthesized from **4.43e**, according to a literature procedure,¹⁸³ and was isolated as a crystalline silver solid (490 g, 31%). ¹H NMR (CDCl₃) δ: 8.32 (br, 1H), 7.52 (d, *J* = 6.9 Hz, 2H), 7.47 (d, *J* = 8.3 Hz, 2H), 7.39 (t, *J* = 6.9 Hz, 2H), 7.24 (t, *J* = 6.9 Hz, 1H), 7.18 (d, *J* = 8.3 Hz, 2H), 7.12 (bs, 1H), 6.80 (bs, 1H), 2.36 (s, 3H). ¹³C NMR (CDCl₃) δ: 135.5, 133.1, 132.8, 132.7, 129.5, 129.1, 126.8, 126.6, 125.3, 124.0, 115.4, 104.1, 21.3. NMR data were found to be in accordance with literature.¹⁸³

2-Phenyl-4-[4-(trifluoromethyl)phenyl]-1H-pyrrole, (4.44f).

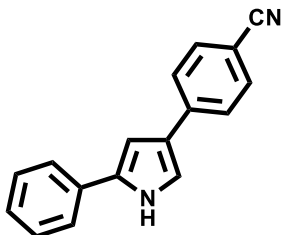


The title compound was synthesized from **4.43f**, according to a literature procedure,¹⁸⁴ and was isolated as an off white crystalline solid (0.54 g, 48%). ¹H NMR (400 MHz, CDCl₃) δ: 8.54 (bs, 1H), 7.66 (d, *J* = 8.0 Hz, 2H), 7.60 (d, *J* = 8.0 Hz, 2H), 7.53 (dd, *J* = 7.7, 1.3 Hz, 2H), 7.41 (t, *J* = 7.7 Hz, 2H), 7.27 (t, *J* = 7.7 Hz, 1H), 7.20-7.23 (m, 1H), 6.82-6.85 (m, 1H). ¹⁹F {¹H} NMR (377 MHz, CDCl₃) δ: -62.2 (s). ¹³C NMR (CDCl₃) δ: 139.2, 133.8, 133.0, 129.2, 127.0, 126.0, 125.8,

125.7, 125.4, 125.2, 124.1, 116.5, 104.1. NMR data were found to be in accordance with literature.

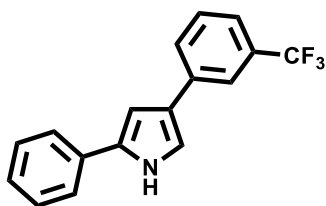
184

4-(4-Cyanophenyl)-2-phenyl-1H-pyrrole (4.44g)



The title compound was synthesized from **4.43g** according to a literature procedure¹⁸⁵ and was isolated as a yellow solid (190 mg, 39%). ¹H NMR (DMSO-d₆) δ: 11.69 (s, 1H), 7.81 (d, *J* = 8 Hz 2H), 7.75 (d, *J* = 8.1 Hz 2H), 7.69 (d, *J* = 7.3 Hz 1H), 7.58 (dd, *J* = 3.2, 1.7 Hz, 1H), 7.39 (t, *J* = 7.2 Hz, 2H), 7.20 (t, *J* = 7.1 Hz, 1H), 7.09 (dd, *J* = 2.7, 1.7 Hz, 1H), 1 signal missing. ¹³C NMR (DMSO-d₆) δ: 140.7, 133.0, 132.6, 132.3, 128.8, 126.1, 124.8, 123.6, 123.1, 119.5, 118.9, 106.7, 103.5. NMR data were found to be in accordance with literature.¹⁸⁵

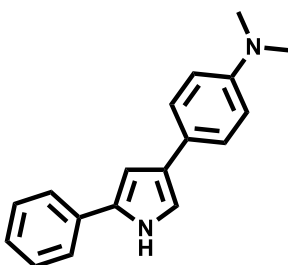
2-Phenyl-4-[3-(trifluoromethyl)phenyl]-1H-pyrrole, (4.44h).



According to an amended version of **GP3**, nitrobutanone **4.43h**,¹⁸⁶ (7.09 mmol) was reacted with KOH (35.6 mmol) in MeOH (60 mL). After 1 hour, the mixture was then added dropwise to a solution of conc. H₂SO₄ (9.3 mL) in MeOH (50 mL) at 0 °C. After the mixture was neutralized with aqueous 4 M KOH, the intermediate product was isolated by filtration and dried overnight in

a vacuum desiccator. To the intermediate compound was added acetic acid (27 mL) and NH_4OAc (17.7 mmol), and the resulting mixture was heated at 100 °C for 1 h. After the mixture was neutralised with aqueous 4 M KOH, the crude material was extracted with CH_2Cl_2 (50 mL) and the organics were later washed with water and brine, and then dried over Na_2SO_4 . The solvent was removed *in vacuo*, and the resulting material was purified by dissolution in a small amount of CH_2Cl_2 , followed by the addition of hexanes and isolation of the precipitate *via* filtration to provide the desired compound as a crystalline silver solid (0.27 g, 13%). ^1H NMR (CDCl_3) δ : 8.52 (br, 1H), 7.80 (s, 1H), 7.73 (d, $J = 6.1$ Hz, 1H), 7.53 (d, $J = 6.3$ Hz, 2H), 7.37-7.50 (m, 4H), 7.27 (t, $J = 6.1$ Hz, CDCl_3 shoulder), 7.16-7.22 (m, 1H), 6.81-6.87 (m, 1H). ^{19}F NMR (CDCl_3) δ : -62.7 (s). ^{13}C NMR (CDCl_3) δ : 136.5, 133.7, 132.3, 131.3, 131.0, 129.2, 128.4, 126.9, 125.5, 124.1, 123.2, 122.4, 121.9, 116.1, 104.0.

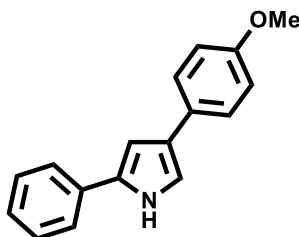
N,N-Dimethyl-4-(5-phenyl-1H-pyrrol-3-yl)benzenamine, (4.44i).



The title compound was synthesized according to an a literature procedure¹⁸² and was isolated as a crystalline silver solid (80 mg, 18%). ^1H NMR (400 MHz, CDCl_3) δ : 8.39 (br, 1H), 7.51 (d, $J = 7.3$ Hz, 2H), 7.47 (d, $J = 7.9$ Hz, 2H), 7.38 (t, $J = 7.9$ Hz, 2H), 7.22 (t, $J = 7.4$ Hz, 1H), 7.03-7.07 (m, 1H), 6.84 (br, 2H), 6.75-6.78 (m, 1H), 2.98 (s, 6H). ^{13}C NMR (CDCl_3) δ : 132.9, 132.8, 129.0,

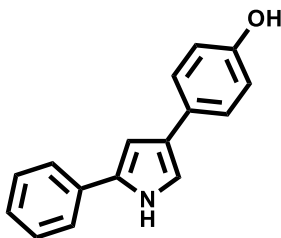
127.0, 126.4, 126.3, 123.9, 114.6, 113.6, 103.9, 41.2, 2 signals missing. NMR data were found to be in accordance with literature.¹⁸²

4-(4-Methoxyphenyl)-2-phenyl-1H-pyrrole, (4.44j).



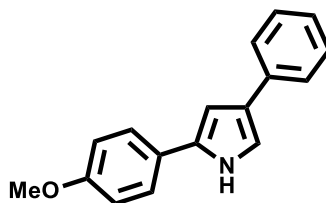
The title compound was synthesized from **4.43j** according to a literature procedure,^{183 62} and was isolated as a crystalline silver solid (0.15 g, 9%). ¹H NMR (DMSO-*d*₆) δ : 11.33 (bs, 1H), 7.67 (d, *J* = 8.0 Hz, 2H), 7.52 (d, *J* = 9.1 Hz, 2H), 7.36 (t, *J* = 8.0 Hz, 2H), 7.20-7.23 (m, 1H), 7.16 (t, *J* = 8.0 Hz, 1H), 6.90 (d, *J* = 9.1 Hz, 2H), 6.85-6.88 (m, 1H), 3.75 (s, 3H). ¹³C NMR (DMSO-*d*₆) δ : 157.1, 132.7, 132.0, 128.7, 128.4, 125.5, 124.6, 123.3, 115.7, 114.0, 103.0, 55.0 (one signal missing). NMR data were found to be in accordance with literature.¹⁸³

4-(4-Hydroxyphenyl)-2-phenyl-1H-pyrrole, (4.44l).



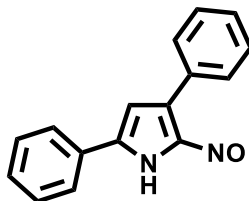
The title compound was synthesized from **4.43l** according to **GP3**, and was isolated as a light yellow solid (90 mg, 5%). ¹H NMR (DMSO-*d*₆) δ: 11.27 (s, 1H), 9.17 (s, 1H), 7.66 (d, *J* = 7.1 Hz, 2H), 7.40 (d, *J* = 8.5 Hz, 2H), 7.26 (t, *J* = 7.8 Hz, 2H), 7.19-7.12 (m, 2H), 6.82 (dd, *J* = 2.7, 1.7 Hz, 1H), 6.73 (d, *J* = 8.6 Hz, 2H). ¹³C NMR (DMSO-*d*₆) δ: 155.6, 133.3, 132.3, 129.1, 127.3, 126.1, 126.0, 125.5, 123.8, 115.8, 115.7, 103.4. HRMS-ESI⁻ *m/z* [M⁺ - H] calc'd for C₁₆H₁₂NO: 234.0924; found 234.0918.

2-(4-Methoxyphenyl)-4-phenyl-1H-pyrrole, (4.44m).



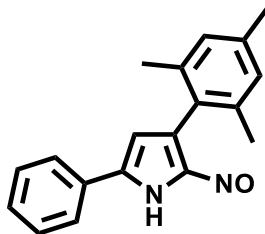
The title compound was synthesized from **4.43m** according to a literature procedure,¹⁸³ and was isolated as a crystalline silver solid (0.37 g, 18%). ¹H NMR (DMSO-*d*₆) δ: 11.28 (br, 1H), 7.56-7.64 (m, 4H), 7.31 (t, *J* = 7.7 Hz, 2H), 7.25-7.28 (m, 1H), 7.11 (t, *J* = 7.7 Hz, 1H), 6.95 (d, *J* = 8.9 Hz, 2H), 6.78-6.82 (m, 1H), 3.77 (s, 3H). ¹³C NMR (DMSO-*d*₆) δ: 157.6, 135.9, 132.3, 128.5, 125.6, 124.9, 124.8, 124.5, 124.4, 115.7, 114.2, 102.0, 55.1. NMR data were found to be in accordance with literature.¹⁸³

2-Nitroso-3,5-diphenyl-1H-pyrrole, (4.40).



The title compound was synthesized from **3.28b** according to **GP4** and was isolated as a green solid (37 mg, 65%). ¹H NMR (CDCl₃) δ: 8.16-8.19 (m, 2H), 7.80-7.83 (m, 2H), 7.47-7.51 (m, 6H), 7.14 (s, 1H). ¹³C NMR (CDCl₃) δ: 162.7, 147.6, 141.8, 132.1, 131.2, 130.2, 129.8, 129.5, 129.3, 129.0, 2 signals missing. HRMS-ESI (*m/z*): [M+Na]⁺ calc'd for C₁₆H₁₂N₂NaO: 271.0843; found 271.0842. NMR data were found to be in accordance with literature.¹⁸²

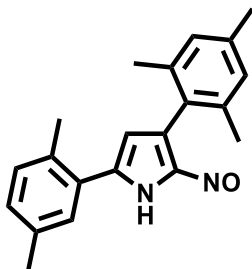
2-Nitroso-5-phenyl-3-(2,4,6-trimethylphenyl)-1H-pyrrole, (4.40a).



The title compound was synthesized from **4.44a** according to **GP4** and was isolated as a green solid (41 mg, 73%). ¹H NMR (CDCl₃) δ: 7.85 (m, 2H), 7.44-7.51 (m, 3H), 7.0 (s, 2H), 6.84 (s,

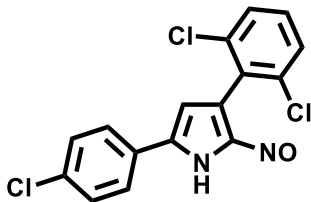
1H), 2.35 (s, 3H), 2.23 (s, 6H). ¹³C NMR (CDCl₃) δ: 163.0, 143.8, 138.1, 137.1, 131.2, 129.3, 128.8, 128.3, 126.9, 116.4, 21.1, 21.0, 2 signals missing. HRMS-ESI (*m/z*): [M+Na]⁺ calc'd. for C₁₉H₁₈N₂NaO: 313.1309; found 313.1311.

5-(2,5-Dimethylphenyl)-2-nitroso-3-(2,4,6-trimethylphenyl)-1H-pyrrole, (4.40b).



The title compound was synthesized from **4.44b** according to **GP4** and was isolated as a green solid (43 mg, 79%). ¹H NMR (CDCl₃) δ: 7.35 (s, 1H), 7.18-7.22 (m, 2H), 7.01 (s, 2H), 6.62 (s, 1H), 2.48 (s, 3H), 2.37 (s, 3H), 2.35 (s, 3H), 2.25 (s, 6H). ¹³C NMR (CDCl₃) δ: 137.6, 137.1, 135.8, 135.3, 135.2, 132.3, 132.2, 131.9, 131.2, 129.9, 128.7, 78.2, 43.4, 34.4, 20.9, 3 signals missing. HRMS-ESI (*m/z*): [M+Na]⁺ calc'd. for C₂₁H₂₂N₂NaO: 341.1621; found 341.1624.

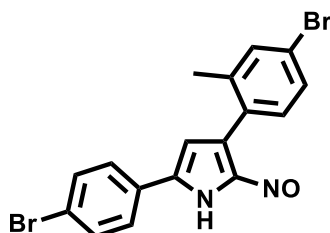
2-Nitroso-3-(2,6-dichlorobenzene)-5-(4-chlorobenzene)-1H-pyrrole, (4.40c).



The title compound was synthesized from **4.44c** according to **GP4** and was isolated as a green solid (35 mg, 65%). ¹H NMR (CDCl₃) δ: 8.16-8.19 (m, 2H), 7.80-7.83 (m, 2H), 7.47-7.51 (m, 2H), 7.14 (s, 1H), 6.77-6.78 (m, 1H), 1 signal missing. ¹³C NMR (CDCl₃) δ: 147.6,

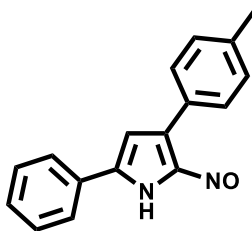
145.0, 139.4, 137.4, 136.7, 134.8, 133.4, 132.7, 131.1, 130.9, 128.0, 127.9. HRMS-ESI (m/z): $[M+H]^+$ calc'd. for $C_{16}H_{10}Cl_3N_2O$: 352.;6110 found 352.6113.

3-(4-Bromo-2-methylphenyl)-5-(4-bromophenyl)-2-nitroso-1H-pyrrole, (4.40d).



The title compound was synthesized from **4.44d** according to **GP4** and was isolated as a green solid (37 mg, 68%). 1H NMR ($CDCl_3$) δ : 7.71 (d, $J = 7.9$ Hz, 2H), 7.61 (d, $J = 7.9$ Hz, 2H), 7.50-7.52 (m, 2H), 7.43-7.45 (m, 1H), 6.94 (s, 1H), 2.45 (s, 3H), 1 signal missing. ^{13}C NMR ($CDCl_3$) δ : 163.0, 142.4, 139.0, 133.5, 133.2, 132.7, 130.4, 128.9, 128.4, 128.2, 126.1, 123.3, 20.9, 2 signals missing. HRMS-ESI (m/z): $[M+H]^+$ calc'd. for $C_{17}H_{13}Br_2N_2O$: 418.9390; found 418.9389.

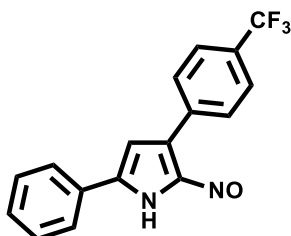
3-(4-Methylphenyl)-2-nitroso-5-phenyl-1H-pyrrole, (4.40e).



The title compound was synthesized from **4.44e** according to **GP4** and was isolated as a green solid (38 mg, 68%). 1H NMR ($CDCl_3$) δ : 8.01 (d, $J = 8.52$ Hz, 2H), 7.78-7.80 (m, 2H), 7.50-7.52

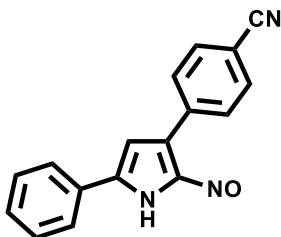
(m, 3H), 7.30 (d, $J = 8.47$ Hz, 2H), 7.12 (s, 1H), 2.43 (s, 3H). ^{13}C NMR (CDCl_3) δ : 135.5, 133.1, 132.8, 132.7, 129.5, 129.1, 126.8, 126.6, 125.3, 124.0, 115.4, 104.1, 21.3. HRMS-ESI (m/z): $[\text{M}+\text{H}]^+$ calc'd. for $\text{C}_{17}\text{H}_{15}\text{N}_2\text{O}$ 263.1179, found, 263.1187.

2-Nitroso-5-phenyl-3-[4-(trifluoromethyl)phenyl]-1H-pyrrole, (4.40f).



The title compound was synthesized from **4.44f** (80 mg) according to **GP4**, and was isolated as a green solid (41 mg, 46%). ^1H NMR (CDCl_3) δ : 8.30 (d, $J = 8.1$ Hz, 2H), 7.78-7.85 (m, 2H), 7.75 (d, $J = 8.2$ Hz, 2H), 7.49-7.55 (m, 3H), 7.19 (s, 1H). ^{13}C NMR (CDCl_3) δ : 162.5, 135.3, 131.5, 131.4, 129.8, 129.6, 128.9, 126.8, 125.8, 125.7, 125.4, 113.0, 1 signal missing. ^{19}F NMR (CDCl_3) δ : 62.77. HRMS-ESI (m/z): $[\text{M}^+ - \text{H}]$ calc'd for $\text{C}_{17}\text{H}_{10}\text{F}_3\text{N}_2\text{O}$: 315.0751; found 315.0740.

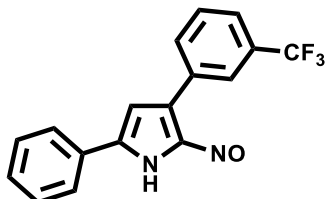
2-Nitroso 4-(4-Cyanophenyl)-2-phenyl-1H-pyrrole, (4.40g).



The title compound was synthesized from **4.44g** according to **GP4** and was isolated as a green solid (38 mg, 68%). ^1H NMR (MeCN) δ : 8.32 (d, $J = 8$ Hz, 2H), 7.78-7.81 (m, 3H), 7.52-7.55 (m, 3H), 7.28 (s, 1H), 7.20 (s, 1H), 1 signal missing. ^{13}C NMR (DMSO-d_6) δ : 140.7, 133.0, 132.6,

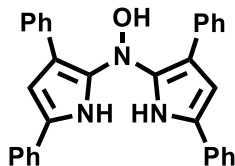
132.3, 128.8, 126.1, 124.8, 123.6, 123.1, 119.5, 118.9, 106.7, 103.5. HRMS-ESI (m/z): $[M+H]^+$ calc'd. for $C_{17}H_{12}N_3O$ 274.0975, found 274.0984.

2-Nitroso-5-phenyl-3-[3-(trifluoromethyl)phenyl]-1H-pyrrole, (4.40h).



The title compound was synthesized from **4.44h** according to **GP4** and was isolated as a green solid, (39 mg, 70%). 1H NMR ($CDCl_3$) δ : 8.44 (d, $J = 8.0$ Hz, 1H), 8.37 (s, 1H), 7.78-7.84 (m, 2H), 7.72 (d, $J = 7.6$ Hz, 1H), 7.63 (t, $J = 8.0$ Hz, 1H), 7.49-7.57 (m, 3H), 7.19 (s, 1H), 1 signal missing. ^{13}C NMR ($CDCl_3$) δ : 133.0, 132.6, 131.8, 131.6, 131.4, 130.2, 129.6, 129.4, 128.9, 126.8, 126.1, 126.0, 125.8, 125.9. ^{19}F NMR ($CDCl_3$) δ : 62.67. HRMS-ESI (m/z): $[M-H]^-$ cal'd. for $C_{17}H_{10}F_3N_2O$ 315.0751, found 315.0741.

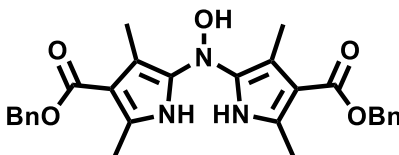
***N*-(3,5-diphenyl-1H-pyrrol-2-yl)-*N*-hydroxy-3,5-diphenyl-1H-pyrrol-2-amine, (4.41).**



The title compound was synthesized as a by-product from **3.28b** (50 mg) and $NOBF_4$ (1 equiv), according to **GP4**, and was isolated as a green solid, (18 mg, 34%). 1H NMR ($CDCl_3$) δ : 8.84 (br, 1H), 7.50-7.52 (m, 5H), 7.34-7.38 (m, 5H), 7.28-7.30 (m, 5H), 7.18-7.15 (m, 5H), 6.75 (s, 1H),

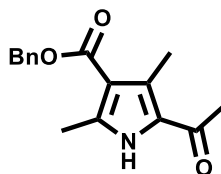
6.56-6.58 (m, 1H), 6.24 (br, 1H), 1 signal missing. ^{13}C NMR (CDCl_3) δ : 171.4, 135.5, 133.1, 132.5, 131.8, 131.3, 129.6, 129.6, 129.4, 129.2, 129.0, 128.9, 128.6, 128.2, 126.8, 126.5, 125.7, 125.2, 123.9, 115.5, 104.0, 3 signals missing. HRMS-ESI (m/z): $[\text{M}+\text{H}]^+$, calc'd for $\text{C}_{32}\text{H}_{26}\text{N}_3\text{O}$ 468.2070, found 468.2071.

Dibenzyl 5-(hydroxyamino)-2,4-dimethyl-1*H*-pyrrole-3-carboxylate, (4.48).



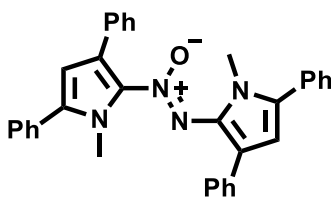
The title compound was synthesized from **4.47** (100 mg) and NOBF_4 (1.8 equiv), according to **GP4**, and was isolated as a white solid, (50 mg, 47%). ^1H NMR (CDCl_3) δ : 8.12 (br, 1H), 7.31-7.42 (m, 2H), 7.33-7.37 (m, 2H), 7.29-7.33 (m, 4H), 7.18-7.20 (m, 2H), 5.61 (br, 1H), 5.26 (s, 2H), 5.20 (d, $J = 11.3$ Hz, 1H), 5.08 (d, $J = 11.3$ Hz, 1H), 2.35 (s, 3H), 2.19 (s, 3H), 2.13 (s, 3H), 1.86 (s, 3H), 1 signal missing. ^{13}C NMR (CDCl_3) δ : 165.9, 163.3, 157.1, 141.7, 139.2, 137.1, 135.3, 134.6, 128.8, 128.5, 128.3, 128.2, 127.9, 124.3, 118.7, 111.8, 66.9, 65.4, 26.6, 14.2, 11.0, 10.9 2 signals missing. HRMS-ESI (m/z): $[\text{M}+\text{H}]^+$ calc'd for $\text{C}_{28}\text{H}_{30}\text{N}_3\text{O}_5$ 488.2180, found 488.2179.

Benzyl 5-acetyl-2,4-dimethyl-1*H*-pyrrole-3-carboxylate, (4.49).



To a solution of pyrrole **4.47** (100 mg) in AcOH (1 mL) and Ac₂O (1mL) under a nitrogen atmosphere was added solid NOBF₄ (1.8 equiv) in three portions. The mixture was stirred at 100°C for 1 h. The mixture was added to a saturated NaHCO₃ solution (10 mL), and extracted into CH₂Cl₂ (2 x 10 mL). The combined organics were dried over Na₂SO₄, then concentrated *in vacuo*. The resulting solid was dry-loaded onto a silica chromatography column, aided by dissolution in CH₂Cl₂, and purified using a gradient of ethyl acetate/hexanes (20→60% ethyl acetate) as eluent to afford the desired product as a brown solid (21 mg, 18%). ¹H NMR (CDCl₃) δ: 9.48 (br, 1H), 7.41-7.43 (m, 2H), 7.35-7.39 (m, 2H), 7.32-7.34 (m, 1H), 5.30 (s, 2H), 2.62 (s, 3H), 2.49 (s, 3H), 2.47 (s, 3H). ¹³C NMR (CDCl₃) δ: 188.0, 165.3, 140.5, 136.6, 130.2, 128.7, 128.3, 128.2, 113.8, 65.7, 28.6, 14.8, 13.0, 1 signal missing. HRMS-ESI (m/z): [M+Na]⁺, calc'd for C₁₆H₁₇NNaO₃ 294.1101, found 294.1104.

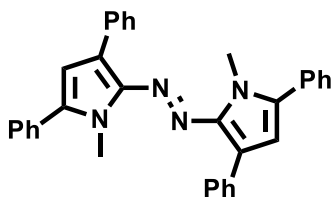
2,2'-diazenediyl-oxide-bis(3,5-diphenyl-1-methyl-pyrrole), (4.24).



A 2 dram vial was charged with pyrrole **4.21** (30 mg, 1 equiv.) and PPh₃ (1.2 equiv.) under a nitrogen atmosphere. The mixture was then dissolved in anhydrous THF (2 mL). The resulting mixture was stirred for 22 h under irradiation with 2 x 23 W CFL lamps. The reaction was monitored by TLC. When pyrrole **4.21** was fully consumed, the reaction was diluted with 10 mL of EtOAc and washed with 10 mL of water. The organics were combined and dried over Na₂SO₄ and concentrated *in vacuo*. The crude material was purified on the Biotage using 40%

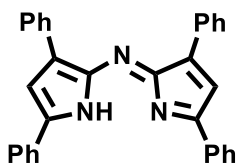
CH₂Cl₂/Hexanes to afford the desired product as a purple solid (14 mg, 24%). ¹H NMR (CDCl₃) δ: 7.55-7.57 (m, 2H), 7.45-7.51 (m, 8H), 7.35-7.38 (m, 6H), 7.18-7.21 (m, 2H), 7.08 (s, 2H), 6.55 (s, 2H), 3.73 (m, 6H). ¹³C NMR (CDCl₃) δ: 135.7, 133.6, 133.1, 128.9, 128.6, 128.4, 128.3, 126.9, 124.6, 120.5, 2 signals missing.

2,2'-Diazenediyl]bis(3,5-diphenyl-1-methyl-pyrrole), (4.25).



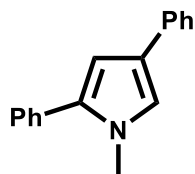
The reaction and work-up used to provided **4.24** also afforded **4.25** as a red solid (20 mg, 19%). ¹H NMR (CDCl₃) δ: 8.06 (d, *J* = 6.4 Hz, 4H), 7.95 (d, *J* = 6.4 Hz, 4H), 7.52-7.56 (m, 4H), 7.41-7.44 (m, 6H), 7.34-7.37 (m, 2H), 7.21 (s, 2H), 3.69 (s, 3H). HRMS-ESI (*m/z*): [M+H]⁺, calc'd for C₃₄H₂₉N₄ 493.238673, found 493.237809.

N-(3,5-Diphenyl-2H-pyrrol-2-ylidene)-3,5-diphenyl-1H-pyrrol-2-amine 2 (3.3a)



A 2 dram vial was charged with nitroso pyrrole **4.21** (52 mg, 1 equiv.), NaI (0.5 equiv.), and PPh₃ (1 equiv.) under a nitrogen atmosphere. The mixture was then dissolved in 2 mL of anhydrous CHCl₃. To this was added PhSiH₃ (2 equiv.). The resulting mixture was stirred for 18 h under irradiation with a 456 nm blue LED lamp. The reaction was monitored by TLC. When nitroso pyrrole **4.21** was fully consumed, the reaction was quenched with saturated Na₂CO₃ (10 mL) and extracted with CH₂Cl₂ (3 x 10 mL). The organics were combined and dried over Na₂SO₄ and concentrated *in vacuo*. The crude material was purified on the Biotage using 40% CH₂Cl₂/Hexanes to afford the desired product as a blue solid (20 mg, 44%). ¹H NMR (CDCl₃) δ: 8.06 (d, *J* = 7.4 Hz, 4H), 7.96 (d, *J* = 7.5 Hz, 4H), 7.57-7.51 (m, 4H), 7.50-7.41 (m, 6H), 7.39-7.34 (m, 2H), 7.21 (s, 2H), 1 signal missing. NMR data were found to be in accordance with literature.⁹⁸

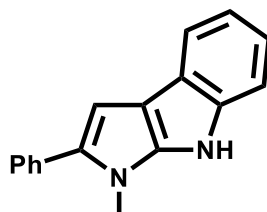
1-Methyl-2,4-diphenyl-1*H*-pyrrole, (**4.20**).



To a solution of pyrrole **3.28** (1.88 g, 1 equiv) in THF (18 mL) was added NaH (2 equiv.) and CH₃I (3 equiv.). The resulting mixture was stirred at 0°C overnight. When pyrrole **3.28** was fully consumed, the reaction mixture was diluted with EtOAc (10 mL) and washed with saturated NaCl (10 mL), then with water (10 mL). The organics were then dried over Na₂SO₄ and concentrated *in vacuo*. The crude material was dissolved in MeOH in which the desired product precipitated and was collected as a pale purple solid after filtration (1.14 g, 57%). ¹H NMR (CDCl₃) δ: 7.53 (d, *J* = 8.1 Hz, 2H), 7.40-7.46 (m, 4H), 7.32-7.35 (m, 3H), 7.15-7.18 (m, 1H), 7.01 (m, 1H), 6.53 (m, 1H),

3.97 (s, 3H). ^{13}C NMR (CDCl_3) δ : 135.6, 133.1, 128.7, 128.6, 128.4, 127.0, 125.4, 125.0, 124.3, 120.4, 106.6, 35.2, 1 signal missing.

1-Methyl-2-phenyl-1,8-dihydropyrrolo[2,3-*b*]indole, (4.23).



A 2 dram vial was charged with pyrrole **4.21** (30 mg, 1 equiv.) and PPh_3 (1.2 equiv.) under a nitrogen atmosphere. The mixture was then dissolved in anhydrous THF (2 mL). The resulting mixture was stirred for 22 h under irradiation with 2 x 23 W CFL lamps. The reaction was monitored by TLC. When pyrrole **4.21** was fully consumed, the reaction was diluted with EtOAc and washed with water. The organics were combined and dried over Na_2SO_4 and concentrated *in vacuo*. The crude material was purified on the Biotage instrument using 40% CH_2Cl_2 /Hexanes to afford the desired product as a yellow oil (3.1 mg, 11%). ^1H NMR (CDCl_3) δ : 7.60-7.62 (m, 2H), 7.43-7.49 (m, 3H), 7.28-7.33 (m, 4H), 6.47 (s, 1H), 3.68 (s, 3H), 1 signal missing. Sample too small to acquire a carbon spectrum. HRMS-ESI $^-$ (m/z): $[\text{M} + \text{H}]^+$, calc'd for $\text{C}_{17}\text{H}_{15}\text{N}_2$ 247.1230, found 247.1236.

Chapter 5 - Substitution at Boron in BODIPYs.

The material in this chapter was published as a peer-reviewed invited article in the journal *Chemical Communications*.⁴⁰ Copyright information is included in the Appendix of this thesis. Liandrah Gapare's contributions to this published review include the completion of a thorough literature review regarding substitution at the boron atom of BODIPYs, collation of all relevant material, creating the first draft for all sections, and working with Dr. Alison Thompson (graduate supervisor) to effect edits prior to submission.

The chemistry of boron has a long history, from its elemental isolation in the early nineteenth century to modern-day utility with an impact that transcends all the chemical disciplines.^{187,188} Boron is used extensively in synthesis, playing a key functional role in organic transformations ranging from classic hydroboration-oxidation to modern metal-catalyzed coupling reactions.¹⁸⁹ The utility of boron stems from the electronic properties of this Group 3 element, with its ground-state electronic configuration of $1s^2 2s^2 2p^1$. The study of boron, which adopts sp^2 hybridization and trivalency in compounds such as boron trifluoride (BF_3), presents an informative learning experience at all educational levels. The electron-deficient (six valence electron) atom, with its empty p-orbital, accepts electrons from donors to enable sp^3 hybridization at boron. In this way, boron readily interconverts between generally neutral sp^2 trigonal planar and charged sp^3 tetrahedral hybridization states upon coordination to heteroatoms such as oxygen and nitrogen and halogens. This apparently simple interconversion is at the heart of a wide range of applications across synthesis, materials science, sensing probes and drug discovery.^{190,191,192} Boronic acid $B(OH)_3$ was used as a component in a mild antiseptic in the early twentieth century.¹⁹³ However, perhaps on account of unwarranted toxicity concerns, it took more than five decades for boron to

be unreservedly adopted by the medicinal chemistry community. It is conceivably this same concern regarding toxicity that was responsible for the slow development of synthetic methods by which to manipulate boron-containing compounds and/or that exploit the reactivity offered by compounds containing this element. However, since the discovery of Suzuki–Miyaura coupling, the developing interest in organoboron chemistry has led to boron now being seen as mainstream across catalysis and structural modification. In 2003, FDA approval of the first boron-containing medicine (Bortezomib, marketed as Velcade® for the treatment of cancer) paved the way for the development of new boron-containing drugs.^{194,195}

Our adventures with boron in the Thompson group at Dalhousie University in Halifax, Canada originate with the chemistry of pyrroles. Given that Hans Fischer's unveiling of pyrrole as the major building block for porphyrins arguably constituted one of the first complete works of synthetic chemistry, this heterocycle is perhaps one of the most-studied.^{196,197} The work discussed herein focuses on molecular scaffolds composed of two pyrrolic units, namely dipyrrens and the corresponding 4,4-disubstituted-4-bora-3a,4a-diaza-*s*-indacene complexes of boron known as BODIPYs. **Figure 33** shows the IUPAC numbering of these systems. The structural similarities of BODIPYs and *s*-indacenes is at the origin of the numbering system used for BODIPYs. In keeping with journal guidelines, this Feature article highlights our contributions to this area, melding our published results with applications across a wider context. Readers interested in a comprehensive review of dipyrrens and/or BODIPYs should explore works dedicated to extensive content reviews.^{198,199,200,201,202,203,204}

Connection of two pyrrolic units through the 2-positions by a methine bridge results in a fully conjugated, planar dipyrren that exhibits strong absorbance bands in the visible region of the electromagnetic spectrum. Aza-dipyrrens and aza-BODIPYs, whereby the central carbon atom of

the dipyrin skeleton is replaced by nitrogen, also feature two pyrrolic units (**Figure 33**).²⁰⁵ Although much less studied than dipyrins on account of challenging synthetic approaches, and although not a focus of this review, aza-dipyrins are gaining interest due to their red-shifted absorptions compared to the parent dipyrins. The versatility of dipyrinato ligands as chelating agents for various main group elements and in various applications is well documented.^{206,207,208,209}

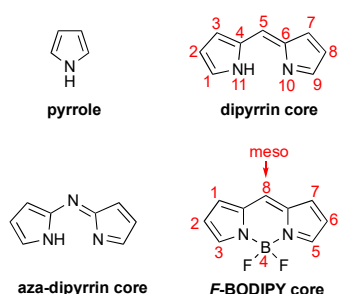
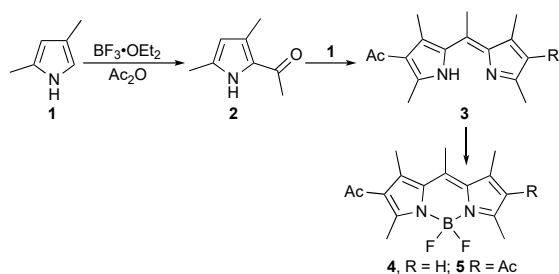


Figure 33: Core frameworks of pyrrole, dipyrin, *F*-BODIPY and aza-dipyrin.

The most common and intensively studied dipyrinato complexes are the boron difluoride ($-\text{BF}_2$) chelated complexes known as *F*-BODIPYs. Boron-dipyrinato complexes with oxygen-based substitution at boron are often denoted as *O*-BODIPYs, with variants featuring carbon substitution at boron referred to as *C*-BODIPYs. However, adherence to these naming conventions is far from absolute and the term “BODIPYs” is often used without consideration of the nature of the substituent at boron. The generally highly fluorescent *F*-BODIPY framework was unintentionally discovered in 1968 by Treibs and Kreuzer upon attempts to acylate 2,4-dimethylpyrrole with excess acetic anhydride in the presence of boron trifluoride as the Lewis acid catalyst. Instead of the desired 2-acyl-pyrrole **2** (**Scheme 46**), the two brightly coloured compounds **4** and **5** were isolated in $< 10\%$ yields.²¹⁰ Chelation of dipyrin **3** with $-\text{BF}_2$ facilitates tetrahedral geometry at boron. This essentially acts as the “glue” that restricts motion such that the typically non-fluorescent dipyrinato skeleton is rigidified to result in sharp absorption and emission bands.^{199,211}

Such (photo)electronic properties have been intensely studied, with fine-tuning resulting in highly capable BODIPYs, e.g. bespoke emission, redox properties and/or (photo)sensitization to generate singlet oxygen and beyond.



Scheme 46: Synthesis of the first F-BODIPYs.

Visualization of cellular biochemical activity is critical to understanding fundamental biology, with fluorescence imaging serving as an integral tool for labelling and for probing intracellular change. Fluorescence imaging relies upon the interplay of the probe (fluorophore) and the detection technique. In the presence of a desired interaction in the biological system, or upon occurrence of a biochemical change of interest, an ideal probe must itself exhibit a property, or a change in property, that is measurable by the detection method in use. The ideal probe should have optimal chemical and physical characteristics such as absorption and fluorescence emission in the visible or near-infrared (NIR) region, a large Stokes shift, high fluorescence quantum yield, useful lipophilicity, facile structural tunability and accessible synthesis. Given these requirements, many BODIPY-based fluorescent probes have been developed.²¹² Some of the commercially available probes are, just to mention a few, LysoTrackerTM Red DND-99,²¹³ which is selective for acidic organelles, and BODIPYTM FL-C₅,²¹⁴ used for label primary amines (R-NH₂) of proteins, amine-modified oligonucleotides and other amine-containing (bio)molecules (**Figure 34**)^{215,216,217} While these BODIPY-based probes are used for labelling, others report on intracellular events such as

hypoxia, a common feature of solid cancer tumours. As approx. 30% of cancer deaths are related to late diagnosis, accurate and early monitoring may be the most accessible route to increasing cancer survival rates thus lending urgency to the development of robust diagnostic probes.^{218,219,220}

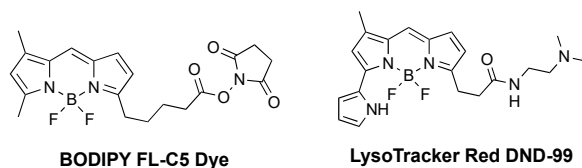


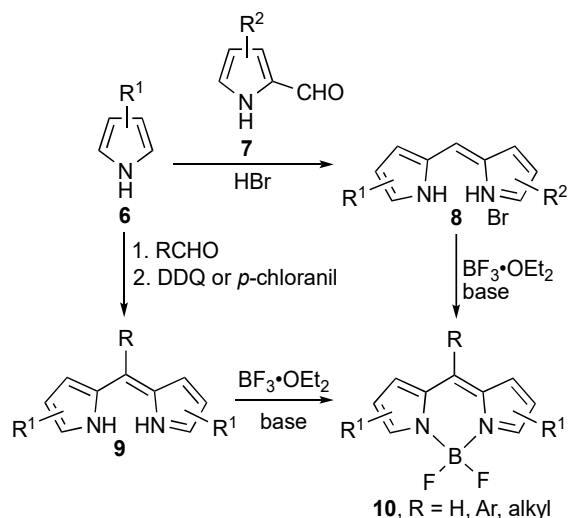
Figure 34: Two commercially available BODIPY probes used in molecular biology.

Beyond their use as fluorescent bioprobes, the electronic tunability of BODIPYs has led to utility as photosensitizers for photodynamic therapy²²¹ and in dye-sensitized solar cells for photovoltaic technology.²²² The planar core, facile functionalization and tunable HOMO-LUMO gap of BODIPYs offer significant promise in this regard.²²³ Furthermore, the presence of nitrogen at the meso-position of the aza-*F*-BODIPY framework lowers the energy of both absorption and emission transitions by reducing the HOMO–LUMO energy gap compared to *F*-BODIPYs with similar substituents. As such aza-BODIPY dyes typically absorb and emit at 600-750 nm and beyond.²²⁴

The tunability of dipyrrens is courtesy of the ability to vary substitution. Building on the various approaches by which to vary substitution about the dipyrrolic core, many of which require variation of the starting material pyrroles, work in our group has focussed on substitution at boron.

Construction of the boron-containing BODIPY framework necessitates prior synthesis of the corresponding dipyrrolic core, achieved through one of two generalized approaches. One approach (**Scheme 47**) involves the condensation of an α -free pyrrole **6** with an α -formyl pyrrole **7**, under

acidic conditions, and enables formation of dipyrroin salts **8** bearing different substituents about the two pyrrolic units.²⁰⁰ The other approach involves condensation of two equiv of an α -unsubstituted pyrrole **6** with an aldehyde to provide a symmetric dipyrromethane. Oxidation then provides the dipyrroin **9**. This route often utilizes aryl aldehydes, thus placing an aryl group in the meso position, although alkyl variants are also known.²²⁵ A variation of this strategy utilizes a carboxylic acid²⁰⁰ or an acid chloride,^{226,227} rather than an aldehyde, thus generating the dipyrroin directly and negating the need for later oxidation across the meso-position.



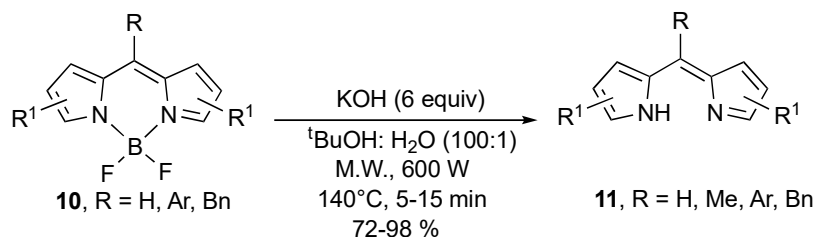
Scheme 47: Synthetic approaches to F-BODIPYs.

Oxidation of dipyrromethanes to dipyrroins is achieved with 2,3-dichloro-5,6-dicyano-1,4-benzoquinone (DDQ) or the milder 2,3,5,6-tetrachloro-1,4-benzoquinone (*p*-chloranil), as indicated in **Scheme 47**. These oxidants were originally borrowed from the shelves of chemists familiar with the oxidation of cyclic tetrapyrroles to make porphyrins, with little variation published since that early work. The oxidation is typically a messy business, and is further complicated by challenging chromatographic requirements. As such, $-\text{BF}_2$ incorporation is often effected in situ as the formation of the apolar boron complex significantly improves the outlook

for isolation of purified material. For decades, the chemistry of BODIPYs rested with *F*-BODIPYs via chelation of the dipyrinato unit with $-\text{BF}_2$. Although new strategies^{228,229} have emerged for the synthesis of *F*-BODIPYs, the treatment of a solution of dipyrin, or its HX salt, with excess base (typically 6 equiv NEt_3 or DIPEA) and $\text{BF}_3 \cdot \text{OEt}_2$ (typically 9 equiv) has provided the traditional route to *F*-BODIPYs in generally quite high yields (**Scheme 47**).²³⁰ Despite the obvious excesses of reagents, yields generally decrease upon decreasing the stoichiometry.^{231,232} Furthermore, the yields vary significantly with compromised “anhydrous” conditions. This is unsurprising, given the anticipated behaviour of $\text{BF}_3 \cdot \text{OEt}_2$ in the presence of alternative donors, yet to an extent implying complications beyond simple quenching and instead consequent to the complexity of various equilibria involving Lewis acidic boron in the presence of NEt_3 , H_2O , Et_2O and the chelating ligand. With the goal of simplifying synthetic protocol, we published a general method for *F*-BODIPY synthesis utilizing a hydrous, open-air environment and involving a second aliquot of excess NEt_3 and $\text{BF}_3 \cdot \text{OEt}_2$.²³⁰ While this synthesis of *F*-BODIPYs removes the need for anhydrous conditions, the use of further reagent excesses is far from ideal.

While synthesis of dipyrins is often facile the free-bases are typically unstable, especially when lacking substituents in the meso-position. For this reason dipyrins are commonly isolated as the brick-red hydrobromide (or sometimes hydrochloride) salts, which are more stable than the corresponding free-bases. The instability of free-base dipyrins is problematic when derivatizing the dipyrinato core. As such, consideration of the $-\text{BF}_2$ unit of *F*-BODIPYs as a protecting group for dipyrins holds considerable appeal. However, the reliability of deprotection is key to the utility of all potential protecting groups. Our unsuccessful attempts to remove the $-\text{BF}_2$ moiety from *F*-BODIPYs had, again borrowing from porphyrin chemistry, involved harsh treatments with strong acids. The premise of this approach was to protonate the N atoms of the dipyrinato unit,

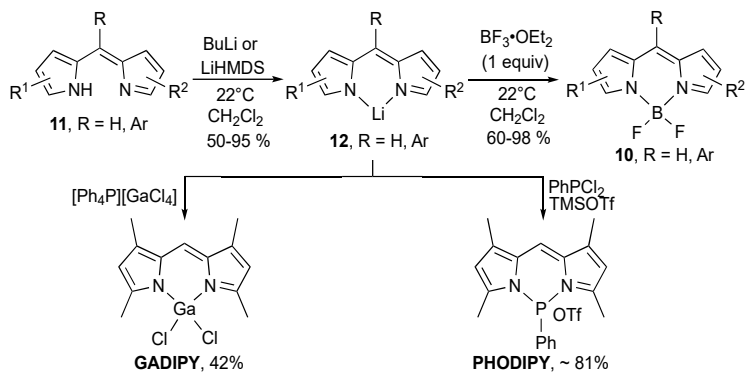
akin to the method used to demetallate porphyrins. We then instead leaned on the chemistry of boron, and relied on the strength of the B–O bond as a driving force for deprotection. Indeed, it is well documented that treatment of *F*-BODIPY with methoxide under forcing conditions results in substitution of fluoride to generate the corresponding *O*-BODIPY featuring two methoxy groups at boron.²³³ We hypothesized that B–O bond formation could be achieved with *tert*-butoxide, with steric bulk preventing formation of the corresponding bis-*tert*-butoxy *O*-BODIPY analogue and instead resulting in decomplexation at boron. Heating *F*-BODIPYs in wet *t*-BuOH under microwave irradiation in the presence of KOH, thus generating *t*-BuOK in situ, resulted in removal of the –BF₂ moiety and liberation of the deprotected dipyrins in generally high-quantitative yields, although lower for systems bearing electron-withdrawing groups such as acyl (**Scheme 48**).^{231,234} During optimization of this work, a small amount of the intermediate 4-*tert*-butoxide-4-fluoro-BODIPY was isolated, supporting the anticipated role of *tert*-butoxide as a bulky nucleophile at boron and providing our first glimpse of the ability to activate, and thereby derivitise, BODIPYs at boron. Similarly, treatment of *F*-BODIPYs with KOⁱPr provided the corresponding di(isopropoxy) *O*-BODIPYs. The dihydroxy *O*-BODIPY was also isolated in the course of this work. There are limited reports of boron complexes of this type, in which the boron atom bears two hydroxyl substituents, as decomposition to boric acid prevails under aqueous/acidic conditions.^{235,236,237,227} Observation of the dihydroxy *O*-BODIPY inspired subsequent development of the Lewis acid-activated deprotection of *F*-BODIPYs and *Cl*-BODIPYs discussed later in this article.



Scheme 48: Microwave-assisted deborylation of F-BODIPYs using tertbutoxide.

Returning to the synthesis of *F*-BODIPYs from dipyrrens, the use of excess base and BF_3 reagents inevitably results in unwanted boron-containing by-products such as $\text{BF}_3 \cdot \text{Et}_3\text{N}$, a material that results in the formation of emulsions during extractive work-up procedures, and complicates purification/isolation on a large scale. To improve upon this environmentally and economically unfavourable approach, we developed methodology that utilises stoichiometric quantities of $\text{BF}_3 \cdot \text{OEt}_2$. To do so, we relied upon our synthesis of lithium dipyrinato salts²³² (**Scheme 49**, top left) through treatment of dipyrrens with LiHMDS or *n*BuLi). We also investigated sodium and potassium salts, identifying complementary reactivity of the dipyrinato unit and the ability to generate heteroleptic metal complexes of transition metals.^{238,239} Lithium salts have since been used to generate the first gallium and phosphorus dipyrinato complexes²⁴⁰ (**Scheme 49**, bottom). The isolation of the lithium dipyrinato salt **12**, followed by treatment with $[\text{PPh}_4][\text{GaCl}_4]$, gave the corresponding GADIPY. Furthermore, the reaction of PhPCl_2 and TMSOTf produced a $[\text{PhPOTf}]^+$ fragment which then reacted with the lithium dipyrinato salt **12** to give the thermally unstable phenylphosphenium (PHODIPY). The alkali dipyrinato salts were key to extending the range of dipyrinato complexes reported, as it is challenging to imagine success such as that depicted in **Scheme 49** if limited to using the previous approach to dipyrinato complexes which essentially involved stirring HBr salts of dipyrrens with metal chloride/other salts.²⁰⁰ As a caution,

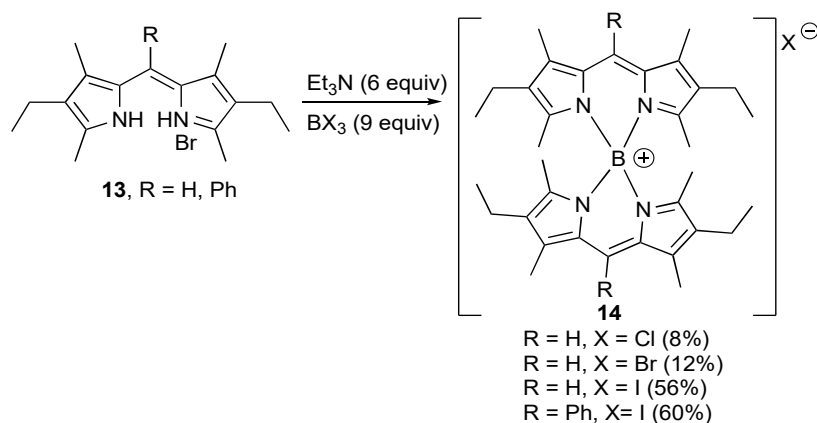
we note that the tetramethyl free-base dipyrin starting material for the GADIPY and PHODIPY shown in **Scheme 49** is a potent sternutator with the ability to sensitize users to its presence in even trace amounts.



Scheme 49: Synthesis and use of Li dipyrinato salts.

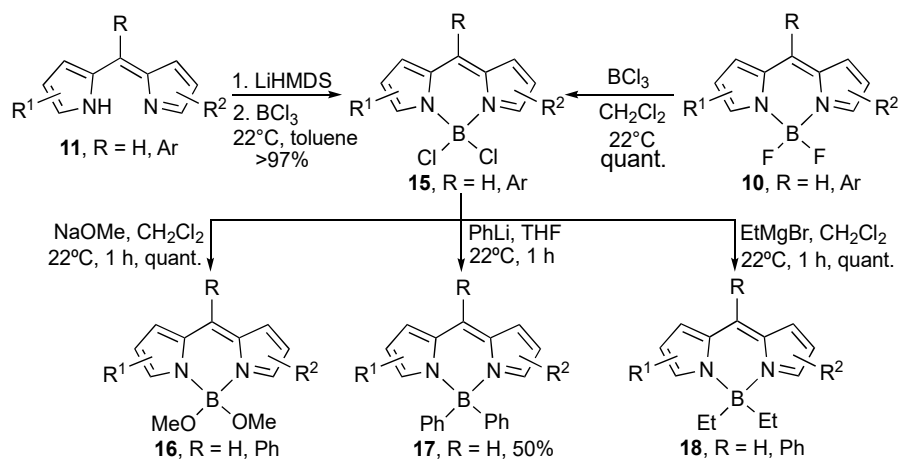
Given the success of lithium dipyrinato salts as synthetic precursors, we extended their reactivity to complexation with boron with hopes of developing a route to *F*-BODIPYs that utilised stoichiometric amounts of reagents. The free-base dipyrin was thus treated with 1.1 equiv LiHMDS, resulting in formation of the corresponding Li salt which then reacted in situ with 1 equiv $\text{BF}_3 \cdot \text{OEt}_2$ to give the *F*-BODIPY in 60-98% yields (**Scheme 49** (top)).²³² This method proved equally effective in averting the use of $\text{NEt}_3/\text{DIPEA}$ and excess $\text{BF}_3 \cdot \text{OEt}_2$, and eases purification challenges by avoiding the formation of unwanted Lewis adducts. A variety of *F*-BODIPYs, including both meso-H and meso-aryl substituents, were synthesized in quantitative yields. *F*-BODIPYs involving various pyrrolic substitution patterns, including a-free, b-free and fully unsubstituted dipyrins, as well as conjugated alkanate esters, were synthesized in this way. Furthermore, bis(*F*-BODIPYs) that had proven elusive via traditional approaches using $\text{NEt}_3/\text{DIPEA}$ and $\text{BF}_3 \cdot \text{OEt}_2$ were obtained via treatment of the corresponding bis(lithium

dipyrrinato) salts with a stoichiometric amount of $\text{BF}_3 \cdot \text{OEt}_2$.²³² Although many transition metal dipyrrinato complexes have been synthesized, BODIPYs featuring halogens other than fluoride at boron had yet to be reported: certainly the traditional route to *F*-BODIPYs involving excess $\text{NEt}_3/\text{DIPEA}$ and $\text{BF}_3 \cdot \text{OEt}_2$ was unsuited for reactions involving the more reactive boron trihalides. Furthermore, although the stability of *F*-BODIPYs provides a thermodynamic driving force for reaction success, this could not be relied upon for desired dipyrrinato products involving B–Cl, B–Br and/or B–I bonds. Nevertheless, to explore the possibility of non-fluoro *X*-BODIPYs, we treated dipyrrins **13** with 6 equiv NEt_3 and 9 equiv of either BCl_3 , BBr_3 or BI_3 (**Scheme 50**). Characterization of the resultant products did not reveal *X*-BODIPYs but instead provided the first dipyrrinato salts **14** featuring a boronium cation isolated with a counter-anion corresponding to the boron trihalide used. The yield of the boronium cations increased as the size of the halogen increased, corresponding to the improved leaving group ability and the susceptibility of the boron centre to nucleophilic attack. Of note, dipyrrinato-based boronium cations are large, and have the potential to be rendered (homo)chiral.



Scheme 50: Synthesis of first dipyrinato boronium salts.

Failure of this approach to form *X*-BODIPYs ($X = \text{halogen where } X \neq \text{F}$) fueled our consequent exploration of a salt metathesis approach to *Cl*-BODIPYs **15**. This approach was highly successful, with treatment of lithium dipyrinato complexes with 1 equiv BCl_3 providing *Cl*-BODIPYs in very high yields (**Scheme 51**, top left).²⁴¹ The quantum yields for *Cl*-BODIPYs are unsurprisingly lower than those of the corresponding *F*-BODIPYs, yet still exhibit considerable fluorescence (e.g. $\phi_{\text{F}} \approx 0.4$ vs. 0.9). These *Cl*-BODIPYs were unstable to moisture, thereby regenerating dipyrrens and indicating complementary reactivity for *Cl*- and *F*-BODIPYs.



Scheme 51: Synthesis of Cl-BODIPYs – synthetic intermediates for substitution at boron.

Although attempts to isolate *Br*-BODIPYs and *I*-BODIPYs using this methodology were unsuccessful we speculated that these compounds do form, as evident by the deep red colour and hints of fluorescence associated with addition of BBr_3 and BI_3 to lithium dipyrinato salts. However, these BODIPYs are presumably insufficiently stable, under the conditions we explored, to enable isolation. There are reports of the reactions of the dipyrinato motif with BCl_3 ²⁴² and BBr_3 .²⁴³ In these reports, the heavy atom BODIPYs were not isolated but were used as intermediates and underwent substitution with alkoxides, demonstrating their reactivity under ambient conditions. As a consequence of sequentially reacting bis(dipyrrins) with BF_3 and then BCl_3 in attempts to prepare unsymmetrical bis(BODIPYs), we established that *F*-BODIPYs can be smoothly converted into *Cl*-BODIPYs upon treatment with 1 equiv BCl_3 (Scheme 51, top right).²⁴⁴ As well as providing another reliable route to *Cl*-BODIPYs, this discovery prompted a mechanistic investigation. Through labelling the boron in *F*-BODIPYs, achieved via derivitisation of isotopically labeled $\text{B}(\text{OMe})_3$, halogen exchange (rather than $-\text{BX}_2$ exchange) was confirmed

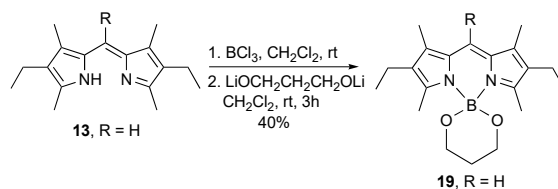
upon treatment of *F*-BODIPYs with BCl_3 .²⁴⁵ At first sight the loss of the strong B–F bond, and formation of the weaker B–Cl bond, in the BODIPY unit seems to conflict with thermodynamic principles,²⁴⁶ but a more thorough analysis reveals BClF_2 as the formal byproduct. Given somewhat rapid exchange in BX_3 Lewis acids,²⁴⁷ formation and loss of uncoordinated BClF_2 and BF_3 from the system is envisaged to drive the quantitative transformation of *F*-BODIPYs into *Cl*-BODIPYs. A *Br*-BODIPY was isolated using this strategy,²⁴⁸ i.e. treatment of *F*-BODIPY with BBr_3 , as confirmed via ^{11}B NMR spectroscopy. Although the weaker Br–B bond offers intriguing reactivity, the reactivity of *Br*-BODIPYs was not extensively investigated.

With halogen exchange at boron now firmly established, we turned our attention to other forms of substitution at boron and thus explored the reactivity of the new *Cl*-BODIPYs. We postulated that the weaker B–Cl bond would allow for more facile substitutions at the boron centre than had been possible when *F*-BODIPYs were the only starting materials available. To investigate this hypothesis, isolated *Cl*-BODIPYs were treated with alkoxides, aryl lithium reagents and Grignard reagents (**Scheme 51**, bottom).²⁴¹ Nucleophilic substitution at the boron center was found to be facile providing dialkoxy (*O*-BODIPYs), dialkyl and diaryl BODIPYs (*C*-BODIPYs) in high yields using stoichiometric amounts of reagents and under mild reaction conditions. Such substitution compares favourably to the harsh conditions and long reaction times necessary to effect the same substitution at boron in *F*-BODIPYs. For example, conversion of *F*-BODIPYs into the corresponding dimethoxy *O*-BODIPY had typically required reflux temperatures and reaction times reaching 18 h. Recent improvements demonstrated the use of other Lewis acids such as AlCl_3 to promote substitution at boron.^{235,237}

Uniting the ability to prepare *Cl*-BODIPYs, through halogen exchange of *F*-BODIPYs, with the facile substitution of *Cl*-BODIPYs at boron provided opportunities for substitutions beginning

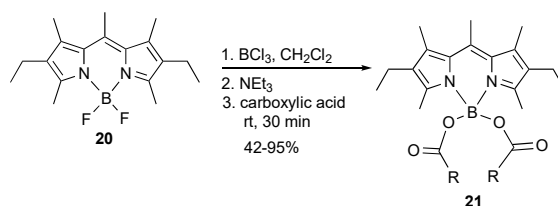
with the air-/moisture-stable *F*-BODIPYs. This one-pot approach utilizes *Cl*-BODIPY as a synthetic intermediate for substitution at boron. *F*-BODIPYs were treated with 1 equiv BCl_3 at room temperature. After 1 h, solid NaOMe was added to the solution under inert conditions to give *O*-BODIPYs in quantitative yield.²⁴⁴ Successful synthesis of *O*-BODIPYs via this route contrasts with the trace amounts observed when *F*-BODIPYs are treated directly with NaOMe under the same mild conditions. Similarly, in situ generation of *Cl*-BODIPYs and treatment with Grignard reagents provides *C*-BODIPYs in quantitative yield from *F*-BODIPYs.

The advantages of using *Cl*-BODIPYs as situ intermediates were also demonstrated through the synthesis of **19** (Scheme 52). Such spirocyclic-at-boron *O*-BODIPYs had previously proven to be elusive when *F*-BODIPYs were reacted with alcohols in the presence of AlCl_3 . This approach, proceeding via in situ formation of a B-F-Al-F chelate, had resulted in a range of *O*-BODIPYs and demonstrated the ability to activate the B-F bond through treatment with Lewis acid.²³⁷ However, under these conditions, attempted substitution of the fluoro substituents with 1,3-propanediol did not provide the corresponding spirocyclic derivative. Our methodology involving in situ generation of *Cl*-BODIPY, followed by treatment with the lithium dienolate of 1,3-propanediol in a stoichiometric amount and under mild conditions, provided the desired *O*-BODIPY **19**.



Scheme 52: Chelated *O*-BODIPY utilizing *Cl*-BODIPY as a synthetic intermediate.

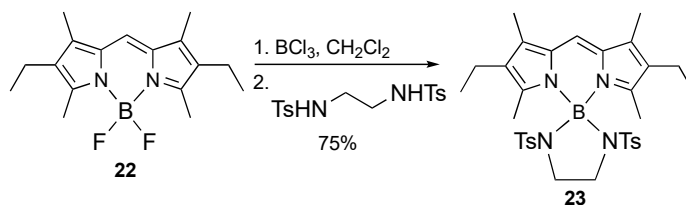
The BCl₃-mediated route to substitution of *F*-BODIPYs at boron has gained some popularity. For example, BODIPYs bearing carboxyl functionality at boron are of interest for use in biological settings as they can be rendered much less lipophilic than the corresponding *F*-BODIPYs and can be modified to present a red-shifted sharp emission band with rich fluorescence properties. The first such *COO*-BODIPYs were synthesized in low-moderate yields through treatment of *F*-BODIPYs at 90°C for 40 h with a pre-mixed solution containing TMSCl and acetic acid: the authors proposed the presence of TMSOAc, generated in situ, to be responsible for reactivity at boron.²⁴⁹ More recently, a milder and higher yielding synthesis of *COO*-BODIPYs was reported (**Scheme 53**).²⁵⁰ This involved activation of *F*-BODIPYs with BCl₃, and was applied to a range of mono- and bis-carboxylic acids. This approach enabled chiral auxiliaries to be appended at boron, leading to *COO*-BODIPYs that exhibited circularly polarized luminescence in the visible region.^{251,252,253} This Lewis-acid mediated approach offers considerable convergency and improved yields.



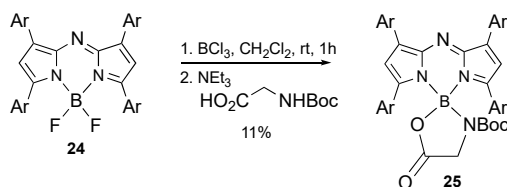
Scheme 53: BCl₃-activated synthesis of *COO*-BODIPYs from *F*-BODIPY.

Activation of *F*-BODIPYs through treatment with BCl₃ was also used for the synthesis of *N*-BODIPYs **23** (**Scheme 54**),²⁵⁴ with the Lewis donicity of the chelating diamines tempered through their incorporation as sulfonamides: use of simple amines such as ethylenediamine failed to produce *N*-BODIPYs. BODIPYs and aza-BODIPYs featuring both carboxyl and amino-functionality at boron, e.g. aza-BODIPY **25** (**Scheme 55**), were obtained via treatment of *Cl*-(aza)-

BODIPYs, prepared in situ from the corresponding *F*-(aza)-BODIPYs, with glycines protected with a variety of carbonyl-based electron-withdrawing protecting groups (PG) at nitrogen.^{255,256} In this way, water-soluble BODIPYs bearing amino acids at boron have been prepared, and investigated as regards cellular uptake and cytotoxicity.²⁵⁷



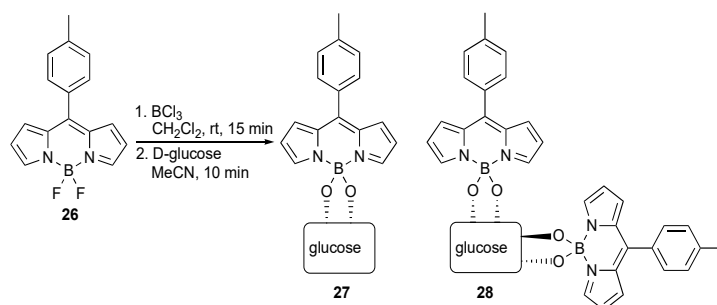
Scheme 54: Synthesis of *N*-BODIPY via BCl_3 activation of *F*-BODIPY.



Scheme 55: Glycine-based *N,O*-aza-BODIPY via *Cl*-aza-BODIPY.

Applying the utility of *Cl*-BODIPYs led to the first *O*-BODIPY:glucose conjugates featuring sugar moieties attached at the boron atom through covalent B–O–C bonds.²⁵⁸ Treatment of the meso-aryl *F*-BODIPY **26** with BCl_3 generated the corresponding *Cl*-BODIPY, which was used as the precursor for three fluorescent BODIPY-glucose conjugates: i.e., 1:1 α -glucofuranose BODIPY **27**, alongside 1:2 α -glucofuranose and 1:2 α -glucoseptanose BODIPYs which are both shown schematically as **28** (Scheme 56). Complexation between the boron atom of the BODIPYs and the C1, C2 *cis*-1,2 diol sites of glucose was observed, with binding to the C3, C5 1,3-diol most likely for the second BODIPY unit in the 1:2 constructs. This synthetic route melds the capabilities of the BODIPY and boronic acid moieties to enable *O*-BODIPY–sugar binding to occur: given the harsh conditions and extended reaction times necessary for substitution at boron in *F*-BODIPYs,

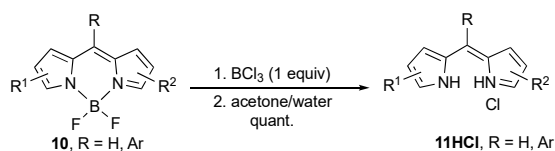
the reactivity of the newly available *Cl*-BODIPY motif must surely have been critical to this early success. More recent work conjugating BODIPYs to sugars through complexation at boron used *O*-BODIPYs bearing methoxy groups at boron, themselves prepared from the corresponding *Cl*-BODIPYs. Use of the *O*-BODIPYs provided only methanol as by-product, rather than production of HCl when *Cl*-BODIPYs were used. These milder conditions enabled improved yields courtesy of the increased stability of fragile sugar-BODIPY conjugates of glucose, xylose and ribose under these less acidic reaction conditions.²⁵⁹ Other Lewis acids have been used to activate *F*-BODIPYs. For example, AlCl₃ activates *F*-BODIPYs to enable substitution at boron with perfluoro-alkoxy groups.²⁶⁰



Scheme 56: BODIPY-sugar conjugates utilizing *Cl*-BODIPY as synthetic intermediate.

Our adventures modifying substituents at the boron atom of BODIPYs had led us to understand that the reactivity of the integral X–B bond could be tuned. While seemingly obvious in retrospect, we must remember that BODIPYs were celebrated for several decades in only their difluoro form. Such *F*-BODIPYs were applauded for their desirable photophysical properties and, critically, for their stability, i.e. their ability to tolerate a broad range of chemical and physiological conditions. With our new knowledge regarding substitution of boron in BODIPYs we realized that deprotection (i.e., removal of the -BF₂ unit from *F*-BODIPYs) could be revisited. Whilst the

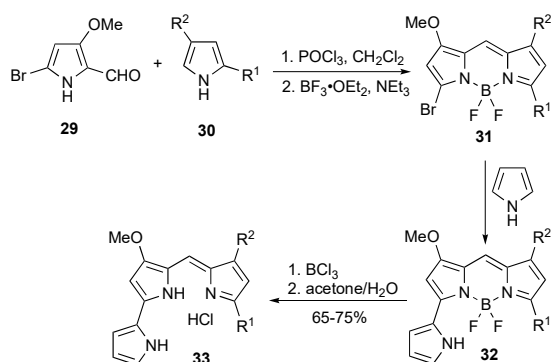
alkoxy-promoted deprotection of *F*-BODIPYs was successful (**Scheme 48**), the use of these basic conditions to remove the -BF₂ motif was less than ideal. However, as previously mentioned, we had learned that the Cl-B bonds within *Cl*-BODIPYs are susceptible to attack by water such as to generate the dihydroxy *O*-BODIPY – which decomposes to provide boric acid and the parent dipyrin as its stable HCl salt.²³⁴ Combined with the newly discovered and reliable transformation of *F*-BODIPYs into *Cl*-BODIPYs, this reactivity provided a new strategy for the deborylative deprotection of *F*-BODIPYs. Indeed, the reaction of *F*-BODIPYs with 1 equiv BCl₃, and subsequent dissolution in excess acetone: water (10:1), afforded a quantitative yield of the dipyrin salt (**Scheme 57**). This approach was demonstrated using *F*-BODIPYs featuring unsubstituted, alkyl-substituted and keto-substituted pyrrolic units. Similarly, meso-H and meso-aryl *F*-BODIPYs were successfully deprotected. Treatment of *F*-BODIPYs with BBr₃ was equally successful, with reaction of the corresponding *Br*-BODIPY with wet acetone providing the parent dipyrin as its HBr salt.²⁴⁸ Alternative methods for deprotection of *F*-BODIPYs, including via use of other Lewis acids,^{261,262} Brønsted acids²⁶³ and via treatment with methylboronic acid and TFA are also known.²⁶⁴ This approach has been key to generating prodigiosene-type complexes whereby a pyrrolide flanks the dipyrinato unit to create an effective chelation pocket.^{265,266}



Scheme 57: Deprotection of *F*-BODIPYs via *Cl*-BODIPYs.

Deprotection of *F*-BODIPYs via *Cl*-BODIPYs has proven to be reliable, gaining use such as in the synthesis of some tripyrrolic natural products. For example, a concise metal-free method for

the facile synthesis of synthetic and natural prodigiosenes utilized the $-BF_2$ unit as a protective motif for the dipyrinato construct **31**, enabling isolation of these stable and non-polar synthetic intermediates. Deprotection at boron via hydrolysis of the corresponding *Cl*-BODIPYs provided the desired prodigiosenes **33** as their HCl salts with purification merely requiring crystallisation (**Scheme 58**).²⁶⁷ Removal of the $-BF_2$ unit was also achieved with *tert*-butoxide to give the required prodigiosene as its free base, but in a reduced yield and after necessary chromatography.

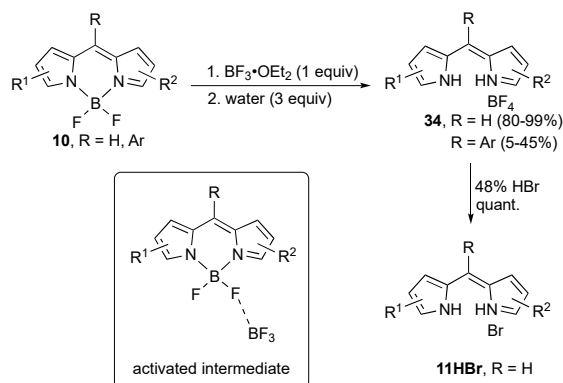


Scheme 58: Synthesis of prodigiosenes using *F*-BODIPYs as protected dipyrrens.

Returning to the synthesis of *F*-BODIPYs, we found ourselves in an ideal position to probe the somewhat capricious yields obtained when applying the traditional synthetic conditions involving treatment of dipyrrens, and/or their HX salts, with base (typically 6 equiv NEt_3 or DIPEA) and $BF_3 \cdot OEt_2$ (typically 9 equiv).²³⁰ One rationale for the variation in BODIPY yields rests with interactions between the Lewis acid BF_3 and adventitious water which may be present if strict anhydrous conditions are not adhered to. Indeed, even trace amounts of water can cause significant reductions in product yield. However, the effect of water on yields seems to go beyond simple deactivation of BF_3 .²⁶⁸ Our insight gained from reacting *F*-BODIPYs with Lewis acids such as BCl_3 and BBr_3 led us to question whether treatment with $BF_3 \cdot OEt_2$ would similarly result in

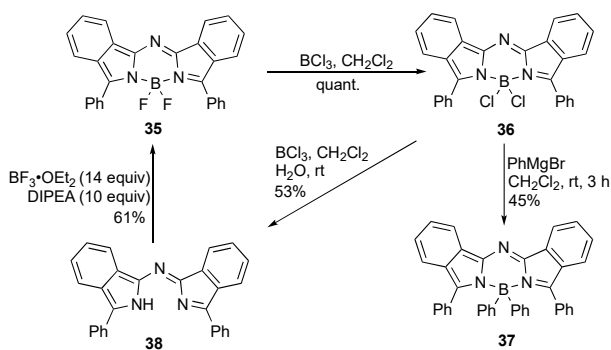
activation. If so, we envisaged that treatment with water may serve to effect nucleophilic attack at the boron atom of BODIPYs and thereby lead to ultimate formation of boric acid and liberated dipyrin. We were encouraged by published work that showed that BODIPYs were activated at boron through treatment with Lewis acids such as SnCl₄, enabling substitution of ¹⁹F for radioactive ¹⁸F at boron.²⁶⁹ In our investigations, we mixed *F*-BODIPYs with 1 equiv BF₃•OEt₂ and were delighted to observe new ¹⁹F and ¹¹B NMR signals c.f. the starting materials.²⁴⁸ This activated intermediate (**Scheme 59**), featuring reversible interaction of the fluoro substituents of the *F*-BODIPY with the Lewis acidic boron of the added BF₃•OEt₂, presents an opportunity to achieve direct substitution at the boron atom of *F*-BODIPYs.

Treatment of the activated intermediate with excess water, such as would be encountered during a typical aqueous /work-up, returned the original *F*-BODIPY in quantitative yields.²⁴⁸ Presumably, the added BF₃•OEt₂ is quenched in the presence of excess water. In contrast, upon the addition of just 3 equiv water to the activated intermediate, the boron atom of the BODIPY is nucleophilically attacked to form first the hydroxy O-BODIPY, followed by complete hydrolysis to liberate boric acid and the parent dipyrin isolated as its HBF₄ salt **34** (**Scheme 59**). These salts are intensely crystalline, although subject to loss of BF₃ over extended periods of time in air, and easily converted to the corresponding HBr salts. This deprotection strategy was successful for several *F*-BODIPYs bearing alkyl-substituted pyrrolic units. However, the incorporation of an aryl substituent at the meso-position resulted in significantly reduced yield for the deprotection, and suggests opportunities for chemoselective removal of the -BF₂ unit from *F*-BODIPYs. The use of 3 equiv water is critical to hydrolysis at the boron atom of the *F*-BODIPY, with the use of excess water instead quenching the F---B interaction involving the added BF₃•OEt₂ and thus quenching the activated intermediate.



Scheme 59: Activation and deprotection of *F*-BODIPYs using BF_3 .

to the corresponding HBr salts. This deprotection strategy was successful for several *F*-BODIPYs bearing alkyl-substituted pyrrolic units. However, the incorporation of an aryl substituent at the meso-position resulted in significantly reduced yield for the deprotection, and suggests opportunities for chemoselective removal of the $-\text{BF}_2$ unit from *F*-BODIPYs. The use of 3 equiv water is critical to hydrolysis at the boron atom of the *F*-BODIPY, with the use of excess water instead quenching the $\text{F} \cdots \text{B}$ interaction involving the added $\text{BF}_3 \cdot \text{OEt}_2$ and thus quenching the activated intermediate.



Scheme 60: Synthesis and utility of *Cl*-aza-BODIPYs.

Alkali salts of the aza-dipyrrinato complex²⁷⁰ enabled substitution at boron, as perhaps rationalized through appreciation of the donicity of the dipyrin and aza-dipyrrin constructs, deduced via ¹³C NMR spectroscopy.²⁷¹ Furthermore, the archetypal aza-dipyrrin subtypes were found to successfully undergo complexation to -BCl₂ when treated with BCl₃ (**Scheme 60**). For example, formation of the *Cl*-aza-BODIPYs **36** occurs through stepwise halogen exchange and a mixed halogen BODIPY intermediate featuring a -BClF unit.²⁷² *Cl*-aza-BODIPYs such as **36** were found to be unstable after a few days of exposure to air, decomposing to the aza-dipyrrin HCl salts. The utility of the *Cl*-aza-BODIPY scaffold, as contained within the subphthalocyanine motif,²⁷³ extends to substitution at boron under mild conditions through treatment with aryl Grignard reagents, courtesy of the lability of the B–Cl bond. Unlike in *F*-BODIPYs, the addition of a nucleophile immediately after in situ formation of the *Cl*-aza-BODIPY **36** from the *F*-aza-BODIPY **35** failed to effect B-substitution, and instead returned either the *F*-aza-BODIPY or the parent free-base (i.e., deborylated) dipyrin **38**. Rather, removal of the solvent and by-products such as BF₂Cl, prior to addition of the nucleophile, is essential to quenching the halogen exchange reaction and achieving complete substitution at boron. As for *F*-BODIPYs, *F*-aza-BODIPYs are also amenable to deprotection through formation of the corresponding *Cl*-aza-BODIPY. The chemistry of boron in aza-BODIPYs remains largely unexplored.

Conclusions

In conclusion, we have highlighted the utility and reactivity of boron in our work with BODIPYs and, briefly, with aza-BODIPYs. Installation of the -BR₂ moiety offers enhanced rigidity to the conjugated dipyrinato framework and therefore highly desirable photophysical properties. We have explored the reactivity at boron within BODIPYs such as to enable convergent substitution

at this position, as well as render the $-BX_2$ unit ($X = \text{halogen}$) effective as a useful protecting group that can be removed under highly specific conditions.

Chapter 6 – Conclusions.

Chapter 2 - Conclusion.

This chapter discusses the investigation of the synthesis of *F*-BODIPY in a continuous flow operation using 1 equiv of $\text{BF}_3 \cdot \text{OEt}_2$ in the absence of a base. The results confirmed that the reaction of the free-base dipyrin and $\text{BF}_3 \cdot \text{OEt}_2$ is rapid at the point of mixing. Indeed, by comparing results obtained in batch to those obtained in flow, it was found that there was no significant change in the yields obtained. This suggests that the continuous flow operation failed to eliminate the interaction between the HF produced in situ, with the unreacted $\text{BF}_3 \cdot \text{OEt}_2$ to form BF_4^- and thus the dipyrin HBF_4 salt. We then introduced HF scavengers in batch mode with the hope of counteracting the formation of the non-complexed material and thus the desired *F*-BODIPY would be generated in higher yields. To this end, the use of a variety of additives was explored but none resulted in the generation of the desired product in high yields. Some additives, like TMSPa, resulted in the elimination of the HBF_4 salt but the yield of the BODIPY did not change. We then studied the reaction of the free-base dipyrin and 1 equiv of $\text{BF}_3 \cdot \text{OEt}_2$ in the presence of various solvents and at various temperatures to discover that the reaction performed moderately well in 1:5 CH_2Cl_2 : hexanes at 30 °C. This was however only optimal for the alkyl-substituted *F*-BODIPYs, which were formed in moderate yields. A comparison of this new method with the traditional anhydrous method³⁰ and the hydrous method⁴³ on a 1 g scale of free base **2.1** showed that this new method is advantageous from an economic point of view as it requires only 1 equiv of BF_3 and reduced volume of solvent for purification. This method only takes 10 min for the reaction to reach completion, unlike for the other methodologies which take 2.5 and 3 hours.⁴³

Chapter 3 - Conclusion.

This chapter discusses the development of potential alternative syntheses of aza dipyrins wherein an acyclic diketimide is synthesized, then converted to dipyrrolamine via Paal-knorr cyclization then oxidation to aza dipyrin. Preliminary investigation of this pathway revealed challenges with undesired side reactions. However, the hint of success from the formation of amine **3.23b** from the reaction of nitrobutanone **3.27b** and active ester **3.31**, though in a low yield, means further optimization and development of this method is possible to determine the viability of this method for the synthesis of aza dipyrins.

Chapter 4 - Conclusion.

This chapter discusses the development of a potential alternative route to the synthesis of aza dipyrins, ideally to overcome limitations in the current methods of synthesis. Several pathways have been proposed herein wherein α -nitro or α -nitroso pyrroles bearing desired substituents are synthesized and then coupled with 2-boc-pyrrole boronic acid **4.11** under catalysis with tetravalent phosphorus reagents in the presence of phenylsilane as a reductant. Investigations of this coupling revealed multiple challenges, with complex mixtures obtained. This prompted the reaction of nitroso pyrroles with 2-boc-pyrrole boronic acid **4.11** under light-promoted triphenylphosphine-induced catalysis. The use of blue LED lights resulted in the formation of the desired aza dipyrin in a 44% yield, an achievement comparable to the current routes to aza dipyrins.⁹⁰ Given this success, attempts to synthesize alkyl-substituted nitroso-pyrroles for subjection to the blue LED-mediated methods using the nitrosylation conditions with NaNO₂ in ethanolic HCl were unsuccessful. This prompted the exploration of alternative nitrosylation conditions for pyrroles. The reaction of α -free pyrroles with NOBF₄ in acetonitrile resulted in the formation of nitroso

pyrroles and several novel nitroso pyrroles were synthesized in reasonable yields. Application of this nitrosylation to alkyl-substituted systems did not proceed as expected but provided evidence for the formation of N-hydroxyl intermediates. This provides intriguing evidence that aza-dipyrrins are possibly just a step away. Further development is necessary to determine the viability of the pathway.

Chapter 5 - Conclusion.

This chapter highlighted the utility and reactivity of boron in our work with BODIPYs and, briefly, with aza-BODIPYs. Installation of the $-BR_2$ moiety offers enhanced rigidity to the conjugated dipyrriato framework and therefore highly desirable photophysical properties. We have explored the reactivity at boron within BODIPYs such as to enable convergent substitution at this position, as well as render the $-BX_2$ unit ($X = \text{halogen}$) effective as a useful protecting group that can be removed under highly specific conditions.

References.

- (1) *Comprehensive Heterocyclic Chemistry: The Structure, Reactions, Synthesis and Uses of Heterocyclic Compounds*, 1st ed.; Katritzky, A. R., Rees, C. W., Eds.; Pergamon Press: Oxford [Oxfordshire]; New York, 1984.
- (2) Konar, D.; kumar, K. Recent Synthetic and Medicinal Perspectives of Pyrroles: An Overview. **2017**.
- (3) Jolicoeur, B.; Chapman, E.; Thompson, A.; Lubell, W. Pyrrole Protection. *Tetrahedron* **2006**, *62*, 11531–11563. <https://doi.org/10.1016/j.tet.2006.08.071>.
- (4) Object, object. Stereochemistry and Chiroptic Properties of Pheophorbides and Related Compounds.
- (5) Jones, R. A.; Bean, G. P. *The Chemistry of Pyrroles: Organic Chemistry: A Series of Monographs, Vol. 34*; Academic Press, 2013.
- (6) Delaere, D.; Pham-Tran, N.-N.; Nguyen, M. T. Ab Initio Study of Spectral and Thermochemical Properties of 1H-Phospholes. *J. Phys. Chem. A* **2003**, *107* (38), 7514–7523. <https://doi.org/10.1021/jp035405v>.
- (7) Seo, M.-K.; Kim, J.-B.; Seong, S.; Shim, Y. Molecular Orbital Calculations for the Reactions of 2,5-Dimethyl Pyrrole with Phenylsulfonyl Chloride. **5**.
- (8) Clayden, J.; Greeves, N.; Warren, S. G. *Organic Chemistry*, 2nd ed.; Oxford University Press: Oxford; New York, 2012.
- (9) Groves, B. R.; Cameron, T. S.; Thompson, A. Deuteration and Tautomeric Reactivity of the 1-Methyl Functionality of Free-Base Dipyrrins. *Organic and Biomolecular Chemistry* **2017**, *15* (37), 7925–7935. <https://doi.org/10.1039/c7ob01278k>.
- (10) Moss, G. P. Nomenclature of Tetrapyrroles (Recommendations 1986). *Pure and Applied Chemistry* **1987**, *59* (6), 779–832. <https://doi.org/10.1351/pac198759060779>.
- (11) van Koevinge, J. A.; Lugtenburg, J. Novel Pyrrromethenes. 1-Oxygen and 1-Sulfur Analogues; Evidence for Photochemical Z-E Isomerization. *Recueil des Travaux Chimiques des Pays-Bas* **1977**, *96* (2), 55–57. <https://doi.org/10.1002/recl.19770960209>.
- (12) *Dolphin: The Porphyrins V7: Biochemistry, Part B - Google Scholar*. https://scholar-google-com.ezproxy.library.dal.ca/scholar_lookup?hl=en&publication_year=1978&author=J.+B.+Paineauthor=D.+Dolphin&title=The+Porphyrins (accessed 2021-08-31).
- (13) Shi, Z.; Han, X.; Hu, W.; Bai, H.; Peng, B.; Ji, L.; Fan, Q.; Li, L.; Huang, W. Bioapplications of Small Molecule Aza-BODIPY: From Rational Structural Design to in Vivo Investigations. *Chem. Soc. Rev.* **2020**, *49* (21), 7533–7567. <https://doi.org/10.1039/D0CS00234H>.
- (14) Wood, T. E.; Thompson, A. Advances in the Chemistry of Dipyrrins and Their Complexes. *Chem. Rev.* **2007**, *107* (5), 1831–1861. <https://doi.org/10.1021/cr050052c>.
- (15) Laha, J. K.; Dhanalekshmi, S.; Taniguchi, M.; Ambroise, A.; Lindsey, J. S. A Scalable Synthesis of Meso-Substituted Dipyrrromethanes. *Org. Process Res. Dev.* **2003**, *7* (6), 799–812. <https://doi.org/10.1021/op034083q>.
- (16) Li, T.; Gu, W.; Yu, C.; Lv, X.; Wang, H.; Hao, E.; Jiao, L. Syntheses and Photophysical Properties of Meso-Phenylene Ridged Boron Dipyrrromethene Monomers, Dimers and Trimer. *Chinese Journal of Chemistry* **2016**, *34* (10), 989–996. <https://doi.org/10.1002/cjoc.201600500>.

- (17) Yang, L.; Simionescu, R.; Lough, A.; Yan, H. Some Observations Relating to the Stability of the BODIPY Fluorophore under Acidic and Basic Conditions. *Dyes and Pigments* **2011**, *91* (2), 264–267. <https://doi.org/10.1016/j.dyepig.2011.03.027>.
- (18) Bessette, A.; S. Hanan, G. Design, Synthesis and Photophysical Studies of Dipyrromethene-Based Materials: Insights into Their Applications in Organic Photovoltaic Devices. *Chemical Society Reviews* **2014**, *43* (10), 3342–3405. <https://doi.org/10.1039/C3CS60411J>.
- (19) Lu, H.; MacK, J.; Yang, Y.; Shen, Z. Structural Modification Strategies for the Rational Design of Red/NIR Region BODIPYs. *Chemical Society Reviews* **2014**, *43* (13), 4778–4823. <https://doi.org/10.1039/c4cs00030g>.
- (20) Bodio, E.; Denat, F.; Goze, C. BODIPYS and Aza-BODIPY Derivatives as Promising Fluorophores for in Vivo Molecular Imaging and Theranostic Applications. *J. Porphyrins Phthalocyanines* **2019**, *23* (11n12), 1159–1183. <https://doi.org/10.1142/S1088424619501268>.
- (21) Sakamoto, R.; Iwashima, T.; Tsuchiya, M.; Toyoda, R.; Matsuoka, R.; Kögel, J. F.; Kusaka, S.; Hoshiko, K.; Yagi, T.; Nagayama, T.; Nishihara, H. New Aspects in Bis and Tris(Dipyrinato)Metal Complexes: Bright Luminescence, Self-Assembled Nanoarchitectures, and Materials Applications. *J. Mater. Chem. A* **2015**, *3* (30), 15357–15371. <https://doi.org/10.1039/C5TA02040A>.
- (22) Nakano, K.; Kobayashi, K.; Nozaki, K. Tetravalent Metal Complexes as a New Family of Catalysts for Copolymerization of Epoxides with Carbon Dioxide. *J. Am. Chem. Soc.* **2011**, *133* (28), 10720–10723. <https://doi.org/10.1021/ja203382q>.
- (23) Ghachtouli, S. E.; Wójcik, K.; Copey, L.; Szydło, F.; Framery, E.; Goux-Henry, C.; Billon, L.; Charlot, M.-F.; Guillot, R.; Andrioletti, B.; Aukauloo, A. Dipyrinphenol–Mn(III) Complex: Synthesis, Electrochemistry, Spectroscopic Characterisation and Reactivity. *Dalton Trans.* **2011**, *40* (36), 9090–9093. <https://doi.org/10.1039/C1DT10868A>.
- (24) Hennessy, E. T.; Betley, T. A. Complex N-Heterocycle Synthesis via Iron-Catalyzed, Direct C–H Bond Amination. *Science* **2013**, *340* (6132), 591–595. <https://doi.org/10.1126/science.1233701>.
- (25) King, E. R.; Betley, T. A. C–H Bond Amination from a Ferrous Dipyrromethene Complex. *Inorg. Chem.* **2009**, *48* (6), 2361–2363. <https://doi.org/10.1021/ic900219b>.
- (26) King, E. R.; Sazama, G. T.; Betley, T. A. Co(III) Imidos Exhibiting Spin Crossover and C–H Bond Activation. *J. Am. Chem. Soc.* **2012**, *134* (43), 17858–17861. <https://doi.org/10.1021/ja307699u>.
- (27) Lam, R. H.; Walker, D. B.; Tucker, M. H.; Gatus, M. R. D.; Bhadbhade, M.; Messerle, B. A. Intermolecular Hydroalkoxylation of Terminal Alkynes Catalyzed by a Dipyrinato Rhodium(I) Complex with Unusual Selectivity. *Organometallics* **2015**, *34* (17), 4312–4317. <https://doi.org/10.1021/acs.organomet.5b00561>.
- (28) Yadav, M.; Singh, A. K.; Pandey, D. S. First Examples of Heteroleptic Dipyrin/H5-Pentamethylcyclopentadienyl Rhodium/Iridium(III) Complexes and Their Catalytic Activity. *Organometallics* **2009**, *28* (16), 4713–4723. <https://doi.org/10.1021/om900349v>.
- (29) Isar, P.; Chatterjee, T.; Ravikanth, M. β -Meso Covalently Linked Novel Dipalladium(II) Bis-Dipyrin Complex. *ChemistrySelect* **2016**, *1* (6), 1220–1224. <https://doi.org/10.1002/slct.201600188>.
- (30) Treibs, A.; Kreuzer, F.-H. Difluorboryl-Komplexe von Di- und Tripyrrylmethenen. *Justus Liebigs Annalen der Chemie* **1968**, *718* (1), 208–223. <https://doi.org/10.1002/jlac.19687180119>.

- (31) Karolin, J.; Johansson, L. B.-A.; Strandberg, L.; Ny, T. Fluorescence and Absorption Spectroscopic Properties of Dipyrrometheneboron Difluoride (BODIPY) Derivatives in Liquids, Lipid Membranes, and Proteins. *J. Am. Chem. Soc.* **1994**, *116* (17), 7801–7806. <https://doi.org/10.1021/ja00096a042>.
- (32) Rasmussen, S. C. The Nomenclature of Fused-Ring Arenes and Heterocycles: A Guide to an Increasingly Important Dialect of Organic Chemistry. *ChemTexts* **2016**, *2* (4), 16. <https://doi.org/10.1007/s40828-016-0035-3>.
- (33) Loudet, A.; Burgess, K. BODIPY Dyes and Their Derivatives: Syntheses and Spectroscopic Properties. *Chemical Reviews* **2007**, *107* (11), 4891–4932. <https://doi.org/10.1021/cr078381n>.
- (34) Frath, D.; Massue, J.; Ulrich, G.; Ziessel, R. Luminescent Materials: Locking π -Conjugated and Heterocyclic Ligands with Boron(III). *Angewandte Chemie International Edition* **2014**, *53* (9), 2290–2310. <https://doi.org/10.1002/anie.201305554>.
- (35) *BODIPY Dye Series—Section 1.4 - CA*. [//www.thermofisher.com/ca/en/home/references/molecular-probes-the-handbook/fluorophores-and-their-amine-reactive-derivatives/bodipy-dye-series.html](http://www.thermofisher.com/ca/en/home/references/molecular-probes-the-handbook/fluorophores-and-their-amine-reactive-derivatives/bodipy-dye-series.html) (accessed 2021-11-19).
- (36) Campbell, J. W.; Tung, M. T.; Diaz-Rodriguez, R. M.; Robertson, K. N.; Beharry, A. A.; Thompson, A. Introducing the Tellurophene-Appended BODIPY: PDT Agent with Mass Cytometry Tracking Capabilities. *ACS Med. Chem. Lett.* **2021**, *12* (12), 1925–1931. <https://doi.org/10.1021/acsmchemlett.1c00492>.
- (37) Klifout, H.; Stewart, A.; Elkhailifa, M.; He, H. BODIPYs for Dye-Sensitized Solar Cells. *ACS Appl. Mater. Interfaces* **2017**, *9* (46), 39873–39889. <https://doi.org/10.1021/acsami.7b07688>.
- (38) Squeo, B. M.; Ganzer, L.; Virgili, T.; Pasini, M. BODIPY-Based Molecules, a Platform for Photonic and Solar Cells. *Molecules* **2020**, *26* (1), 153. <https://doi.org/10.3390/molecules26010153>.
- (39) Karlsson, J. K. G.; Harriman, A. Origin of the Red-Shifted Optical Spectra Recorded for Aza-BODIPY Dyes. *Journal of Physical Chemistry A* **2016**, *120* (16), 2537–2546. <https://doi.org/10.1021/acs.jpca.6b01278>.
- (40) Gapare, R. L.; Thompson, A. Substitution at Boron in BODIPYs. *Chem. Commun.* **2022**, *58* (53), 7351–7359. <https://doi.org/10.1039/D2CC02362H>.
- (41) Wang, Z.; Cheng, C.; Kang, Z.; Miao, W.; Liu, Q.; Wang, H.; Hao, E. Organotrifluoroborate Salts as Complexation Reagents for Synthesizing BODIPY Dyes Containing Both Fluoride and an Organo Substituent at the Boron Center. *J. Org. Chem.* **2019**, *84* (5), 2732–2740. <https://doi.org/10.1021/acs.joc.8b03145>.
- (42) Sawazaki, T.; Shimizu, Y.; Oisaki, K.; Sohma, Y.; Kanai, M. Convergent and Functional-Group-Tolerant Synthesis of B-Organic BODIPYs. *Org. Lett.* **2018**, *20* (24), 7767–7770. <https://doi.org/10.1021/acs.orglett.8b03138>.
- (43) Beh, M. H. R.; Douglas, K. I. B.; House, K. T. E.; Murphy, A. C.; Sinclair, J. S. T.; Thompson, A. Robust Synthesis of F-BODIPYs. *Organic and Biomolecular Chemistry* **2016**, *14* (48), 11473–11479. <https://doi.org/10.1039/c6ob02238c>.
- (44) Crawford, S. M.; Thompson, A. Conversion of 4,4-Difluoro-4-Bora-3a,4a-Diaza-s-Indacenes (F-BODIPYs) to Dipyrins with a Microwave-Promoted Deprotection Strategy. *Org. Lett.* **2010**, *12* (7), 1424–1427. <https://doi.org/10.1021/ol902908j>.

- (45) Lundrigan, T.; Baker, A. E. G.; Longobardi, L. E.; Wood, T. E.; Smithen, D. A.; Crawford, S. M.; Cameron, T. S.; Thompson, A. An Improved Method for the Synthesis of F - BODIPYs from Dipyrrins and Bis(Dipyrrin)s. *Organic Letters* **2012**, *14* (8), 2158–2161. <https://doi.org/10.1021/ol300681w>.
- (46) Atansi, M. I. Development and Optimization of Methodology Towards Pyrrolic Frameworks.
- (47) Plutschack, M. B.; Pieber, B.; Gilmore, K.; Seeberger, P. H. The Hitchhiker's Guide to Flow Chemistry. *Chemical Reviews* **2017**, *117* (18), 11796–11893. <https://doi.org/10.1021/acs.chemrev.7b00183>.
- (48) Salehi Marzijarani, N.; Snead, D. R.; McMullen, J. P.; Lévesque, F.; Weisel, M.; Varsolona, R. J.; Lam, Y. H.; Liu, Z.; Naber, J. R. One-Step Synthesis of 2-Fluoroadenine Using Hydrogen Fluoride Pyridine in a Continuous Flow Operation. *Organic Process Research and Development* **2019**, *23* (8), 1522–1528. <https://doi.org/10.1021/acs.oprd.9b00178>.
- (49) Zhao, C.; An, J.; Zhou, L.; Fei, Q.; Wang, F.; Tan, J.; Shi, B.; Wang, R.; Guo, Z.; Zhu, W. H. Transforming the Recognition Site of 4-Hydroxyaniline into 4-Methoxyaniline Grafted onto a BODIPY Core Switches the Selective Detection of Peroxynitrite to Hypochlorous Acid. *Chemical Communications* **2016**, *52* (10), 2075–2078. <https://doi.org/10.1039/c5cc08936k>.
- (50) Mula, S.; Ray, A. K.; Banerjee, M.; Chaudhuri, T.; Dasgupta, K.; Chattopadhyay, S. Design and Development of a New Pyrromethene Dye with Improved Photostability and Lasing Efficiency: Theoretical Rationalization of Photophysical and Photochemical Properties. *Journal of Organic Chemistry* **2008**, *73* (6), 2146–2154. <https://doi.org/10.1021/jo702346s>.
- (51) Rastogi, S.; Marchal, E.; Uddin, I.; Groves, B.; Colpitts, J.; McFarland, S. A.; Davis, J. T.; Thompson, A. Synthetic Prodigiosenes and the Influence of C-Ring Substitution on DNA Cleavage, Transmembrane Chloride Transport and Basicity. *Organic and Biomolecular Chemistry* **2013**, *11* (23), 3834–3845. <https://doi.org/10.1039/c3ob40477c>.
- (52) Dudina, N. A.; Berezin, M. B.; Semeikin, A. S.; Antina, E. V. Difluoroborates of Phenyl-Substituted Aza-Dipyrromethenes: Preparation, Spectral Properties, and Stability in Solution. *Russian Journal of General Chemistry* **2015**, *85* (12), 2739–2742. <https://doi.org/10.1134/S1070363215120130>.
- (53) Petersen, T. B. NMR Yields, [Http://Www.Organ.Su.Se/Bo/Gruppfiler/NMR Yield Calculation.Pdf](http://www.Organ.Su.Se/Bo/Gruppfiler/NMR%20Yield%20Calculation.Pdf), Accessed 21-06-2018. *NMR Yields* **2018**, *4*.
- (54) Mahajan, S.; Singh, I. P. Determining and Reporting Purity of Organic Molecules: Why QNMR. *Magnetic Resonance in Chemistry* **2013**, *51* (2), 76–81. <https://doi.org/10.1002/mrc.3906>.
- (55) Britton, J.; Jamison, T. F. The Assembly and Use of Continuous Flow Systems for Chemical Synthesis. *Nature Protocols* **2017**, *12* (11), 2423–2446. <https://doi.org/10.1038/nprot.2017.102>.
- (56) Cantillo, D.; Kappe, C. O. Halogenation of Organic Compounds Using Continuous Flow and Microreactor Technology. *Reaction Chemistry and Engineering* **2017**, *2* (1), 7–19. <https://doi.org/10.1039/c6re00186f>.
- (57) Li, X.; Russell, R. K. Using Potassium Carbonate to Scavenge Hydrogen Fluoride: A Scale-up Process for Quantitative Production of (1-Cyclopropyl-6,7-Difluoro-1,4-Dihydro-8-Methoxy-4-(OxO-KO)-3-Quinolinecarboxylato-KO3)Difluoro Boron. *Organic Process Research and Development* **2008**, *12* (3), 464–466. <https://doi.org/10.1021/op8000228>.

- (58) Mondal, R.; Mallik, A. K. Recent Applications of Potassium Carbonate in Organic Synthesis. *Organic Preparations and Procedures International* **2014**, *46* (5), 391–434. <https://doi.org/10.1080/00304948.2014.944402>.
- (59) Honeywell. Typical Alkaline Materials (Bases) for Neutralization of Hf Alkaline. **2014**, 2014.
- (60) Wynn, D. A.; Roth, M. M.; Pollard, B. D. The Solubility of Alkali-Metal Fluorides in Non-Aqueous Solvents with and without Crown Ethers, as Determined by Flame Emission Spectrometry. *Talanta* **1984**, *31* (11), 1036–1040. [https://doi.org/10.1016/0039-9140\(84\)80244-1](https://doi.org/10.1016/0039-9140(84)80244-1).
- (61) Han, J. G.; Lee, S. J.; Lee, J.; Kim, J. S.; Lee, K. T.; Choi, N. S. Tunable and Robust Phosphite-Derived Surface Film to Protect Lithium-Rich Cathodes in Lithium-Ion Batteries. *ACS Applied Materials and Interfaces* **2015**, *7* (15), 8319–8329. <https://doi.org/10.1021/acsami.5b01770>.
- (62) Saroha, R.; Panwar, A. K.; Bhardwaj, A. Synthesis and Electrochemical Properties of Low-Temperature Synthesized Li₂MnO₃/MWCNT/Super P as a High Capacity Cathode Material for Lithium Ion Batteries. *AIP Conference Proceedings* **2018**, *2009*, 2–7. <https://doi.org/10.1063/1.5052107>.
- (63) Etacheri, V.; Marom, R.; Elazari, R.; Salitra, G.; Aurbach, D. Challenges in the Development of Advanced Li-Ion Batteries: A Review. *Energy and Environmental Science* **2011**, *4* (9), 3243–3262. <https://doi.org/10.1039/c1ee01598b>.
- (64) Li, C.; Zhang, H. P.; Fu, L. J.; Liu, H.; Wu, Y. P.; Rahm, E.; Holze, R.; Wu, H. Q. Cathode Materials Modified by Surface Coating for Lithium Ion Batteries. *Electrochimica Acta* **2006**, *51* (19), 3872–3883. <https://doi.org/10.1016/j.electacta.2005.11.015>.
- (65) Zhou, R.; Huang, J.; Lai, S.; Li, J.; Wang, F.; Chen, Z.; Lin, W.; Li, C.; Wang, J.; Zhao, J. A Bifunctional Electrolyte Additive for H₂O/HF Scavenging and Enhanced Graphite/LiNi_{0.5}Co_{0.2}Mn_{0.3}O₂ Cell Performance at a High Voltage. *Sustainable Energy and Fuels* **2018**, *2* (7), 1481–1490. <https://doi.org/10.1039/c8se00064f>.
- (66) Yamane, H.; Inoue, T.; Fujita, M.; Sano, M. A Causal Study of the Capacity Fading of Li_{1.01}Mn_{1.99}O₄ Cathode at 80°C, and the Suppressing Substances of Its Fading. *Journal of Power Sources* **2001**, *99* (1–2), 60–65. [https://doi.org/10.1016/S0378-7753\(01\)00479-7](https://doi.org/10.1016/S0378-7753(01)00479-7).
- (67) Wang, H.; Ge, W.; Li, W.; Wang, F.; Liu, W.; Qu, M. Z.; Peng, G. Facile Fabrication of Ethoxy-Functional Polysiloxane Wrapped LiNi_{0.6}Co_{0.2}Mn_{0.2}O₂ Cathode with Improved Cycling Performance for Rechargeable Li-Ion Battery. *ACS Applied Materials and Interfaces* **2016**, *8* (28), 18439–18449. <https://doi.org/10.1021/acsami.6b04644>.
- (68) Guéguen, A.; Bolli, C.; Mendez, M. A.; Berg, E. J. Elucidating the Reactivity of Tris(Trimethylsilyl)Phosphite and Tris(Trimethylsilyl)Phosphate Additives in Carbonate Electrolytes - A Comparative Online Electrochemical Mass Spectrometry Study. *ACS Applied Energy Materials* **2020**, *3* (1), 290–299. <https://doi.org/10.1021/acsaem.9b01551>.
- (69) Kennedy, J. P.; Chou, R. T. Setting the Stage: A Brief Introduction to Sterically Hindered Amines in Organic Chemistry and Scouting Experiments. *Journal of Macromolecular Science: Part A - Chemistry* **1982**, *18* (1), 3–10. <https://doi.org/10.1080/00222338208056653>.
- (70) Rumyantsev, E. V.; Marfin, Y. S.; Antina, E. V. Donor-Acceptor Complexes of Dipyrrolylmethenes with Boron Trifluoride as Intermediates in the Synthesis of Bodipy. *Russian Chemical Bulletin* **2010**, *59* (10), 1890–1895. <https://doi.org/10.1007/s11172-010-0329-3>.

- (71) Fox, A.; Hartman, J. S.; Humphries, R. E. Mixed Boron Trihalide Adducts of Amines: A Multinuclear Nuclear Magnetic Resonance Study. *Journal of the Chemical Society, Dalton Transactions* **1982**, 3 (7), 1275–1283. <https://doi.org/10.1039/DT9820001275>.
- (72) Castano, A. P.; Demidova, T. N.; Hamblin, M. R. Mechanisms in Photodynamic Therapy: Part One - Photosensitizers, Photochemistry and Cellular Localization. *Photodiagnosis and Photodynamic Therapy* **2004**, 1 (4), 279–293. [https://doi.org/10.1016/S1572-1000\(05\)00007-4](https://doi.org/10.1016/S1572-1000(05)00007-4).
- (73) Wilson, B. C.; Jeeves, W. P.; Lowe, D. M. IN VIVO and POST MORTEM MEASUREMENTS OF THE ATTENUATION SPECTRA OF LIGHT IN MAMMALIAN TISSUES. *Photochemistry and Photobiology* **1985**, 42 (2), 153–162. <https://doi.org/10.1111/j.1751-1097.1985.tb01554.x>.
- (74) Szaciłowski, K.; Macyk, W.; Drzewiecka-Matuszek, A.; Brindell, M.; Stochel, G. Bioinorganic Photochemistry: Frontiers and Mechanisms. *Chemical Reviews* **2005**, 105 (6), 2647–2694. <https://doi.org/10.1021/cr030707e>.
- (75) Rudin, M.; Weissleder, R. Molecular Imaging in Drug Discovery and Development. *Nature Reviews Drug Discovery* **2003**, 2 (2), 123–131. <https://doi.org/10.1038/nrd1007>.
- (76) Tung, C. H.; Lin, Y.; Moon, W. K.; Weissleder, R. A Receptor-Targeted near-Infrared Fluorescence Probe for in Vivo Tumor Imaging. *ChemBioChem* **2002**, 3 (8), 784–786. [https://doi.org/10.1002/1439-7633\(20020802\)3:8<784::AID-CBIC784>3.0.CO;2-X](https://doi.org/10.1002/1439-7633(20020802)3:8<784::AID-CBIC784>3.0.CO;2-X).
- (77) Frangioni, J. V. In Vivo Near-Infrared Fluorescence Imaging. *Current opinion in chemical biology* **2003**, 7 (5), 626–634. <https://doi.org/10.1016/j.cbpa.2003.08.007>.
- (78) Weissleder, R.; Ntziachristos, V. Shedding Light onto Live Molecular Targets. *Nature Medicine* **2003**, 9 (1), 123–128. <https://doi.org/10.1038/nm0103-123>.
- (79) Smith, A. M.; Mancini, M. C.; Nie, S. Second Window for in Vivo Imaging. *Nature Nanotech* **2009**, 4 (11), 710–711. <https://doi.org/10.1038/nnano.2009.326>.
- (80) Cai, Y.; Wei, Z.; Song, C.; Tang, C.; Han, W.; Dong, X. Optical Nano-Agents in the Second near-Infrared Window for Biomedical Applications. *Chemical Society Reviews* **2019**, 48 (1), 22–37. <https://doi.org/10.1039/C8CS00494C>.
- (81) Sheng, W.; Wu, Y.; Yu, C.; Bobadova-Parvanova, P.; Hao, E.; Jiao, L. Synthesis, Crystal Structure, and the Deep Near-Infrared Absorption/Emission of Bright AzaBODIPY-Based Organic Fluorophores. *Org. Lett.* **2018**, 20 (9), 2620–2623. <https://doi.org/10.1021/acs.orglett.8b00820>.
- (82) Sheng, W.; Cui, J.; Ruan, Z.; Yan, L.; Wu, Q.; Yu, C.; Wei, Y.; Hao, E.; Jiao, L. [A]-Phenanthrene-Fused BF₂ Azadipyromethene (AzaBODIPY) Dyes as Bright Near-Infrared Fluorophores. *J. Org. Chem.* **2017**, 82 (19), 10341–10349. <https://doi.org/10.1021/acs.joc.7b01803>.
- (83) Ni, Y.; Wu, J. Far-Red and near Infrared BODIPY Dyes: Synthesis and Applications for Fluorescent PH Probes and Bio-Imaging. *Organic and Biomolecular Chemistry* **2014**, 12 (23), 3774–3791. <https://doi.org/10.1039/c3ob42554a>.
- (84) Zhao, W.; Carreira, E. M. Conformationally Restricted Aza-BODIPY: Highly Fluorescent, Stable near-Infrared Absorbing Dyes. *Chemistry - A European Journal* **2006**, 12 (27), 7254–7263. <https://doi.org/10.1002/chem.200600527>.
- (85) Gresser, R.; Hummert, M.; Hartmann, H.; Leo, K.; Riede, M. Synthesis and Characterization of Near-Infrared Absorbing Benzannulated Aza-BODIPY Dyes. *Chemistry - A European Journal* **2011**, 17 (10), 2939–2947. <https://doi.org/10.1002/chem.201002941>.

- (86) Bellier, Q.; Pégaz, S.; Aronica, C.; Guennic, B. L.; Andraud, C.; Maury, O. Near-Infrared Nitrofluorene Substitued Aza-Boron-Dipyrrromethenes Dyes. *Organic Letters* **2011**, *13* (1), 22–25. <https://doi.org/10.1021/ol102701v>.
- (87) Gibson, D. H.; He, H. Synthesis and Properties Of. **2001**, *40* (Scheme 1), 2082–2083.
- (88) Kamkaew, A.; Lim, S. H.; Lee, H. B.; Kiew, L. V.; Chung, L. Y.; Burgess, K. BODIPY Dyes in Photodynamic Therapy. *Chemical Society Reviews* **2013**, *42* (1), 77–88. <https://doi.org/10.1039/c2cs35216h>.
- (89) Ge, Y.; O’Shea, D. F. Azadipyrrromethenes: From Traditional Dye Chemistry to Leading Edge Applications. *Chemical Society Reviews* **2016**, *45* (14), 3846–3864. <https://doi.org/10.1039/c6cs00200e>.
- (90) Ge, Y.; O’Shea, D. F. Azadipyrrromethenes: From Traditional Dye Chemistry to Leading Edge Applications. *Chem. Soc. Rev.* **2016**, *45* (14), 3846–3864. <https://doi.org/10.1039/C6CS00200E>.
- (91) Hall, M. J.; McDonnell, S. O.; Killoran, J.; O’Shea, D. F. A Modular Synthesis of Unsymmetrical Tetraarylazadipyrrromethenes. *J. Org. Chem.* **2005**, *70* (14), 5571–5578. <https://doi.org/10.1021/jo050696k>.
- (92) Maligaspe, E.; Pundsack, T. J.; Albert, L. M.; Zatsikha, Y. V.; Solntsev, P. V.; Blank, D. A.; Nemykin, V. N. Synthesis and Charge-Transfer Dynamics in a Ferrocene-Containing Organoboryl Aza-Bodipy Donor-Acceptor Triad with Boron as the Hub. *Inorganic Chemistry* **2015**, *54* (8), 4167–4174. <https://doi.org/10.1021/acs.inorgchem.5b00494>.
- (93) Donyagina, V. F.; Shimizu, S.; Kobayashi, N.; Lukyanets, E. A. Synthesis of N,N-Difluoroboryl Complexes of 3,3'-Diarylazadiisoindolylmethenes. *Tetrahedron Letters* **2008**, *49* (42), 6152–6154. <https://doi.org/10.1016/j.tetlet.2008.08.026>.
- (94) Loudet, A.; Bandichhor, R.; Wu, L.; Burgess, K. Functionalized BF(2) Chelated Azadipyrrromethene Dyes. *Tetrahedron* **2008**, *64*, 3642–3654. <https://doi.org/10.1016/j.tet.2008.01.117>.
- (95) Jiao, L.; Wu, Y.; Ding, Y.; Wang, S.; Zhang, P.; Yu, C.; Wei, Y.; Mu, X.; Hao, E. Conformationally Restricted Aza-Dipyrrromethene Boron Difluorides (Aza-BODIPYs) with High Fluorescent Quantum Yields. *Chemistry – An Asian Journal* **2014**, *9* (3), 805–810. <https://doi.org/10.1002/asia.201301362>.
- (96) Chen, J.; Burghart, A.; Derecskei-Kovacs, A.; Burgess, K. 4,4-Difluoro-4-Bora-3a,4a-Diaza-s-Indacene (BODIPY) Dyes Modified for Extended Conjugation and Restricted Bond Rotations. *Journal of Organic Chemistry* **2000**, *65* (10), 2900–2906. <https://doi.org/10.1021/jo991927o>.
- (97) Liras, M.; Prieto, J. B.; Pintado-Sierra, M.; Arbeloa, F. L.; García-Moreno, I.; Costela, Á.; Infantes, L.; Sastre, R.; Amat-Guerri, F. Synthesis, Photophysical Properties, and Laser Behavior of 3-Amino and 3-Acetamido BODIPY Dyes. *Organic Letters* **2007**, *9* (21), 4183–4186. <https://doi.org/10.1021/ol701674b>.
- (98) Grossi, M.; Palma, A.; McDonnell, S. O.; Hall, M. J.; Rai, D. K.; Muldoon, J.; O’Shea, D. F. Mechanistic Insight into the Formation of Tetraarylazadipyrrromethenes. *J. Org. Chem.* **2012**, *77* (20), 9304–9312. <https://doi.org/10.1021/jo301972w>.
- (99) Khaghaninejad, S.; Heravi, M. M. Chapter Three - Paal–Knorr Reaction in the Synthesis of Heterocyclic Compounds. In *Advances in Heterocyclic Chemistry*; Katritzky, A. R., Ed.; Academic Press, 2014; Vol. 111, pp 95–146. <https://doi.org/10.1016/B978-0-12-420160-6.00003-3>.

- (100) Knorr, L. Synthese von Furfuranderivaten Aus Dem Diacetbernsteinsäureester. *Berichte der deutschen chemischen Gesellschaft* **1884**, *17* (2), 2863–2870. <https://doi.org/10.1002/cber.188401702254>.
- (101) Nicolaou, K. C.; Mathison, C. J. N. Synthesis of Imides, N-Acyl Vinyllogous Carbamates and Ureas, and Nitriles by Oxidation of Amides and Amines with Dess-Martin Periodinane. *Angewandte Chemie - International Edition* **2005**, *44* (37), 5992–5997. <https://doi.org/10.1002/anie.200501853>.
- (102) Jin, Z.; Xu, B.; Hammond, G. B. Copper Mediated Oxidation of Amides to Imides by Selectfluor. *Tetrahedron Letters* **2011**, *52* (16), 1956–1959. <https://doi.org/10.1016/j.tetlet.2011.02.059>.
- (103) Aginagalde, M.; Bello, T.; Masdeu, C.; Vara, Y.; Arrieta, A.; Cossío, F. P. Formation of γ -Oxoacids and 1H-Pyrrol-2(5H)-Ones from α,β -Unsaturated Ketones and Ethyl Nitroacetate. *J. Org. Chem.* **2010**, *75* (21), 7435–7438. <https://doi.org/10.1021/jo101388x>.
- (104) Orlandi, M.; Tosi, F.; Bonsignore, M.; Benaglia, M. Metal-Free Reduction of Aromatic and Aliphatic Nitro Compounds to Amines: A HSiCl₃-Mediated Reaction of Wide General Applicability. *Organic Letters* **2015**, *17* (16), 3941–3943. <https://doi.org/10.1021/acs.orglett.5b01698>.
- (105) Gopinath, R.; Haque, S. J.; Patel, B. K. Tetrabutylammonium Tribromide (TBATB) as an Efficient Generator of HBr for an Efficient Chemoselective Reagent for Acetalization of Carbonyl Compounds. *Journal of Organic Chemistry* **2002**, *67* (16), 5842–5845. <https://doi.org/10.1021/jo025701o>.
- (106) Ojeda-Porras, A.; Gamba-Sánchez, D. Recent Developments in Amide Synthesis Using Nonactivated Starting Materials. *Journal of Organic Chemistry* **2016**, *81* (23), 11548–11555. <https://doi.org/10.1021/acs.joc.6b02358>.
- (107) De Figueiredo, R. M.; Suppo, J. S.; Campagne, J. M. Nonclassical Routes for Amide Bond Formation. *Chemical Reviews* **2016**, *116* (19), 12029–12122. <https://doi.org/10.1021/acs.chemrev.6b00237>.
- (108) DAVIS, A. P.; WALSH, J. J. ChemInform Abstract: Amide Bond Formation via Pentafluorothiophenyl Active Esters. *ChemInform* **2010**, *25* (47), no-no. <https://doi.org/10.1002/chin.199447082>.
- (109) Baco, E.; Hoegy, F.; Schalk, I. J.; Mislin, G. L. A. Diphenyl-Benzo[1,3]Dioxole-4-Carboxylic Acid Pentafluorophenyl Ester: A Convenient Catechol Precursor in the Synthesis of Siderophore Vectors Suitable for Antibiotic Trojan Horse Strategies. *Organic and Biomolecular Chemistry* **2014**, *12* (5), 749–757. <https://doi.org/10.1039/c3ob41990h>.
- (110) Rabinkov, A. G.; Pozdnev, V. F.; Amontov, S. V.; Kopelevich, V. M.; Gunar, V. I. Biotinylation of Amines with the Pentafluorophenyl Ester of D-Biotin. *Chemistry of Natural Compounds* **1989**, *25* (3), 350–353. <https://doi.org/10.1007/BF00597718>.
- (111) D'Accolti, L.; Denora, N.; La Piana, G.; Marzulli, D.; Siwy, Z. S.; Fusco, C.; Annese, C. Synthesis and Biological Evaluation of a Valinomycin Analog Bearing a Pentafluorophenyl Active Ester Moiety. *Journal of Organic Chemistry* **2015**, *80* (24), 12646–12650. <https://doi.org/10.1021/acs.joc.5b02219>.
- (112) Mark, J. E. Some Interesting Things about Polysiloxanes. *Accounts of Chemical Research* **2004**, *37* (12), 946–953. <https://doi.org/10.1021/ar030279z>.
- (113) Pandarus, V.; Ciriminna, R.; Béland, F.; Pagliaro, M. Selective Hydrogenation of Functionalized Nitroarenes under Mild Conditions. *Catal. Sci. Technol.* **2011**, *1* (9), 1616–1623. <https://doi.org/10.1039/C1CY00097G>.

- (114) Guo, S.; Xie, Y.; Hu, X.; Huang, H. Highly Diastereo- and Enantioselective Tandem Reaction toward Functionalized Pyrrolidines with Multiple Stereocenters. *Organic Letters* **2011**, *13* (20), 5596–5599. <https://doi.org/10.1021/ol2023196>.
- (115) Chandrappa, S.; Vinaya, K.; Ramakrishnappa, T.; Rangappa, K. S. An Efficient Method for Aryl Nitro Reduction and Cleavage of Azo Compounds Using Iron Powder/Calcium Chloride. *Synlett* **2010**, *2010* (20), 3019–3022. <https://doi.org/10.1055/s-0030-1259067>.
- (116) Bellamy, F. D.; Ou, K. Selective Reduction of Aromatic Nitro Compounds with Stannous Chloride in Non Acidic and Non Aqueous Medium. *Tetrahedron Letters* **1984**, *25* (8), 839–842. [https://doi.org/10.1016/S0040-4039\(01\)80041-1](https://doi.org/10.1016/S0040-4039(01)80041-1).
- (117) Romero, A. H.; Salazar, J.; López, S. E. A Simple One-Pot Synthesis of 2-Substituted Quinazolin-4(3H)-Ones from 2-Nitrobenzamides by Using Sodium Dithionite. *Synthesis* **2013**, 2043–2050. <https://doi.org/10.1055/s-0033-1338854>.
- (118) Vishnumurthy, K. A.; Adhikari, A. V. Reduction of Nitro Compounds Carrying Electron Withdrawing Groups: A Convenient Approach without Metal Catalyst. *Chemical Data Collections* **2019**, *20*, 100211. <https://doi.org/10.1016/j.cdc.2019.100211>.
- (119) Bäracker, L.; Heinrich, T.; Siemeister, G.; Prechtel, S.; Stöckigt, D.; Rottmann, A. Amno-Substituted Isoxazoles, 2016.
- (120) Kelly, S. M.; Lipshutz, B. H. Chemoselective Reductions of Nitroaromatics in Water at Room Temperature. *Org. Lett.* **2014**, *16* (1), 98–101. <https://doi.org/10.1021/ol403079x>.
- (121) Liang, Y.; Dong, D.; Lu, Y.; Wang, Y.; Pan, W.; Chai, Y.; Liu, Q. One-Pot Synthesis of Substituted Δ^1 -Pyrrolines through the Michael Addition of Nitroalkanes to Chalcones and Subsequent Reductive Cyclization in Aqueous Media. *Synthesis* **2006**, No. 19, 3301–3304. <https://doi.org/10.1055/s-2006-950227>.
- (122) Zhu, Q.; Meng, B.; Gu, C.; Xu, Y.; Chen, J.; Lei, C.; Wu, X. Diastereo- And Enantioselective Synthesis of Quaternary α -Amino Acid Precursors by Copper-Catalyzed Propargylation. *Organic Letters* **2019**, *21* (24), 9985–9989. <https://doi.org/10.1021/acs.orglett.9b03894>.
- (123) Bapat, J.; Black, D. Nitrones and Oxazirans. I. Preparation of 1 -Pyrroline 1-Oxides and 1-Pyrrolines by Reductive Cyclization of γ -Nitro Carbonyl Compounds. *Aust. J. Chem.* **1968**, *21* (10), 2483. <https://doi.org/10.1071/CH9682483>.
- (124) Cheruku, S. R.; Padmanilayam, M. P.; Vennerstrom, J. L. Synthesis of 2H-Pyrroles by Treatment of Pyrrolidines with DDQ. *Tetrahedron Letters* **2003**, *44* (18), 3701–3703. [https://doi.org/10.1016/S0040-4039\(03\)00740-8](https://doi.org/10.1016/S0040-4039(03)00740-8).
- (125) Pfoertner, K.-H.; Foricher, J. Neue Wege zu 1H- und 2H-Pyrrolen. *Helv. Chim. Acta* **1980**, *63* (3), 658–663. <https://doi.org/10.1002/hlca.19800630313>.
- (126) Sibi, M. P.; Petrovic, G.; Zimmerman, J. Enantioselective Radical Addition/Trapping Reactions with α,β -Disubstituted Unsaturated Imides. Synthesis of Anti-Propionate Aldols. *J. Am. Chem. Soc.* **2005**, *127* (8), 2390–2391. <https://doi.org/10.1021/ja043371e>.
- (127) Bittner, S.; Assaf, Y.; Krief, P.; Pomerantz, M.; Ziemnicka, B. T.; Smith, C. G. Synthesis of N-Acyl-, N-Sulfonyl-, and N-Phosphinylphospha(PV)Azenes by a Redox-Condensation Reaction Using Amides, Triphenylphosphine, and Diethyl Azodicarboxylate. *J. Org. Chem.* **1985**, *50* (10), 1712–1718. <https://doi.org/10.1021/jo00210a027>.
- (128) Han, W.; Su, J.; Mo, J.-N.; Zhao, J. Photoredox Catalytic Phosphine-Mediated Deoxygenation of Hydroxylamines Enables the Construction of N - Acyliminophosphoranes. *Org. Lett.* **2022**, *24* (34), 6247–6251. <https://doi.org/10.1021/acs.orglett.2c02226>.

- (129) Diaz-Rodriguez, R. Some Aspects of the Inorganic and Organometallic Chemistry of Dipyrins. Thesis, 2020. <https://DalSpace.library.dal.ca/handle/10222/79597> (accessed 2023-05-20).
- (130) Loudet, A.; Burgess, K. BODIPY Dyes and Their Derivatives: Syntheses and Spectroscopic Properties. *Chemical Reviews* **2007**, *107* (11), 4891–4932. <https://doi.org/10.1021/cr078381n>.
- (131) West, M. J.; Fyfe, J. W. B.; Vantourout, J. C.; Watson, A. J. B. Mechanistic Development and Recent Applications of the Chan–Lam Amination. *Chem. Rev.* **2019**, *119* (24), 12491–12523. <https://doi.org/10.1021/acs.chemrev.9b00491>.
- (132) *A Simple Catalytic Method for the Conversion of Aryl Bromides to Arylamines - Guram - 1995 - Angewandte Chemie International Edition in English - Wiley Online Library.* https://onlinelibrary.wiley.com/doi/abs/10.1002/anie.199513481?casa_token=jQ2fDq9fMlcAAAAA:SrIghszCoZ2h8AhXIRh6VR7Mo9LJPBOTRt9xgf8zdactKc8ESan1rtFih-Uux9ZXpjhT2KofBy4B5f (accessed 2023-05-16).
- (133) Louie, J.; Hartwig, J. F. Palladium-Catalyzed Synthesis of Arylamines from Aryl Halides. Mechanistic Studies Lead to Coupling in the Absence of Tin Reagents. *Tetrahedron Letters* **1995**, *36* (21), 3609–3612. [https://doi.org/10.1016/0040-4039\(95\)00605-C](https://doi.org/10.1016/0040-4039(95)00605-C).
- (134) Ullmann, F. Ueber Eine Neue Bildungsweise von Diphenylaminderivaten. *Berichte der deutschen chemischen Gesellschaft* **1903**, *36* (2), 2382–2384.
- (135) *Ueber Phenylirungen bei Gegenwart von Kupfer als Katalysator - Goldberg - 1906 - Berichte der deutschen chemischen Gesellschaft - Wiley Online Library.* <https://chemistry-europe.onlinelibrary.wiley.com/doi/abs/10.1002/cber.19060390298> (accessed 2023-05-16).
- (136) Dennis, J. M.; White, N. A.; Liu, R. Y.; Buchwald, S. L. Pd-Catalyzed C–N Coupling Reactions Facilitated by Organic Bases: Mechanistic Investigation Leads to Enhanced Reactivity in the Arylation of Weakly Binding Amines. *ACS Catal.* **2019**, *9* (5), 3822–3830. <https://doi.org/10.1021/acscatal.9b00981>.
- (137) Lipshutz, B. H. *Organometallics in Synthesis: Fourth Manual*; John Wiley & Sons, 2013.
- (138) Tasker, S. Z.; Standley, E. A.; Jamison, T. F. Recent Advances in Homogeneous Nickel Catalysis. *Nature* **2014**, *509* (7500), 299–309. <https://doi.org/10.1038/nature13274>.
- (139) D'Souza, D. M.; Müller, T. J. J. Multi-Component Syntheses of Heterocycles by Transition-Metal Catalysis. *Chem. Soc. Rev.* **2007**, *36* (7), 1095–1108. <https://doi.org/10.1039/B608235C>.
- (140) Nykaza, T. V.; Cooper, J. C.; Li, G.; Mahieu, N.; Ramirez, A.; Luzung, M. R.; Radosevich, A. T. Intermolecular Reductive C–N Cross Coupling of Nitroarenes and Boronic Acids by PIII/PV=O Catalysis. *J. Am. Chem. Soc.* **2018**, *140* (45), 15200–15205. <https://doi.org/10.1021/jacs.8b10769>.
- (141) Li, G.; Nykaza, T. V.; Cooper, J. C.; Ramirez, A.; Luzung, M. R.; Radosevich, A. T. An Improved PIII/PV=O-Catalyzed Reductive C–N Coupling of Nitroaromatics and Boronic Acids by Mechanistic Differentiation of Rate- and Product-Determining Steps. *J. Am. Chem. Soc.* **2020**, *142* (14), 6786–6799. <https://doi.org/10.1021/jacs.0c01666>.
- (142) G. Hall, D. Boronic Acid Catalysis. *Chemical Society Reviews* **2019**, *48* (13), 3475–3496. <https://doi.org/10.1039/C9CS00191C>.
- (143) Cadogan, J. I. G. Oxidation of Tervalent Organic Compounds of Phosphorus. *Q. Rev. Chem. Soc.* **1962**, *16* (2), 208–239. <https://doi.org/10.1039/QR9621600208>.
- (144) Wang, S.; Wood, G.; Meades, C.; Griffiths, G.; Midgley, C.; McNae, I.; McInnes, C.; Anderson, S.; Jackson, W.; Mezna, M.; Yuill, R.; Walkinshaw, M.; Fischer, P. M. Synthesis

- and Biological Activity of 2-Anilino-4-(1H-Pyrrol-3-Yl) Pyrimidine CDK Inhibitors. *Bioorg Med Chem Lett* **2004**, *14* (16), 4237–4240. <https://doi.org/10.1016/j.bmcl.2004.06.012>.
- (145) Cadogan, J. I. G.; Todd, M. J. On the Mechanism of Reductive Cyclisation of Nitro-Compounds by Tervalent Organophosphorus Compounds. *Chem. Commun. (London)* **1967**, No. 4, 178. <https://doi.org/10.1039/c19670000178>.
- (146) Kirby, G. W. Tilden Lecture. Electrophilic C-Nitroso-Compounds. *Chem. Soc. Rev.* **1977**, *6* (1), 1–24. <https://doi.org/10.1039/CS9770600001>.
- (147) Katritzky, A. R.; Zhang, S.; Wang, M.; Kolb, H. C.; Steel, P. J. Novel Syntheses of Polysubstituted Pyrroles and Oxazoles by 1,3-Dipolar Cycloaddition Reactions of Benzotriazole-Stabilized Nitrile Ylides. *Journal of Heterocyclic Chemistry* **2002**, *39* (4), 759–765. <https://doi.org/10.1002/jhet.5570390422>.
- (148) Hall, M. J.; McDonnell, S. O.; Killoran, J.; O’Shea, D. F. A Modular Synthesis of Unsymmetrical Tetraarylazadipyrromethenes. *J. Org. Chem.* **2005**, *70* (14), 5571–5578. <https://doi.org/10.1021/jo050696k>.
- (149) Xie, C.; Smaligo, A. J.; Song, X.-R.; Kwon, O. Phosphorus-Based Catalysis. *ACS Cent. Sci.* **2021**, *7* (4), 536–558. <https://doi.org/10.1021/acscentsci.0c01493>.
- (150) Manna, K.; Ganguly, T.; Baitalik, S.; Jana, R. Visible-Light- and PPh₃-Mediated Direct C–N Coupling of Nitroarenes and Boronic Acids at Ambient Temperature. *Org. Lett.* **2021**, *23* (21), 8634–8639. <https://doi.org/10.1021/acs.orglett.1c03343>.
- (151) Tsao, M.-L.; Gritsan, N.; James, T. R.; Platz, M. S.; Hrovat, D. A.; Borden, W. T. Study of the Chemistry of Ortho- and Para-Biphenylnitrenes by Laser Flash Photolysis and Time-Resolved IR Experiments and by B3LYP and CASPT2 Calculations. *J. Am. Chem. Soc.* **2003**, *125* (31), 9343–9358. <https://doi.org/10.1021/ja0351591>.
- (152) Brooke, P. K.; Herbert, R. B.; Holliman, E. G. On the Mechanism of Deoxygenation of Aromatic Nitro and Nitroso Compounds. *Tetrahedron Letters* **1973**, *14* (10), 761–764. [https://doi.org/10.1016/S0040-4039\(01\)95705-3](https://doi.org/10.1016/S0040-4039(01)95705-3).
- (153) Nykaza, T. V.; Ramirez, A.; Harrison, T. S.; Luzung, M. R.; Radosevich, A. T. Biphilic Organophosphorus-Catalyzed Intramolecular Csp²–H Amination: Evidence for a Nitrenoid in Catalytic Cadogan Cyclizations. *J. Am. Chem. Soc.* **2018**, *140* (8), 3103–3113. <https://doi.org/10.1021/jacs.7b13803>.
- (154) Yaghoubian, A.; K. Hodgson, G.; J. Adler, M.; Impellizzeri, S. Direct Photochemical Route to Azoxybenzenes via Nitroarene Homocoupling. *Organic & Biomolecular Chemistry* **2022**, *20* (36), 7332–7337. <https://doi.org/10.1039/D2OB01247B>.
- (155) Bigelow, H. E. Azoxy Compounds. *Chem. Rev.* **1931**, *9* (1), 117–167. <https://doi.org/10.1021/cr60032a005>.
- (156) Chen, Y.-F.; Chen, J.; Lin, L.-J.; Chuang, G. J. Synthesis of Azoxybenzenes by Reductive Dimerization of Nitrosobenzene. *J. Org. Chem.* **2017**, *82* (21), 11626–11630. <https://doi.org/10.1021/acs.joc.7b01887>.
- (157) Dai, Y.; Li, C.; Shen, Y.; Lim, T.; Xu, J.; Li, Y.; Niemantsverdriet, H.; Besenbacher, F.; Lock, N.; Su, R. Light-Tuned Selective Photosynthesis of Azo- and Azoxy-Aromatics Using Graphitic C₃N₄. *Nat Commun* **2018**, *9* (1), 60. <https://doi.org/10.1038/s41467-017-02527-8>.
- (158) Chilaya, G.; Chanishvili, A.; Petriashvili, G.; Barberi, R.; Bartolino, R.; Cipparrone, G.; Mazzulla, A.; Shibaev, P. V. Reversible Tuning of Lasing in Cholesteric Liquid Crystals

- Controlled by Light-Emitting Diodes. *Advanced Materials* **2007**, *19* (4), 565–568. <https://doi.org/10.1002/adma.200600353>.
- (159) Wang, Y.; Li, S.; Li, Y.; Zhang, R.; Wang, D.; Pang, S. A Comparative Study of the Structure, Energetic Performance and Stability of Nitro-NNO-Azoxy Substituted Explosives. *J. Mater. Chem. A* **2014**, *2* (48), 20806–20813. <https://doi.org/10.1039/C4TA04716H>.
- (160) Nishiyama, Y.; Fujii, A.; Mori, H. Selective Synthesis of Azoxybenzenes from Nitrobenzenes by Visible Light Irradiation under Continuous Flow Conditions. *Reaction Chemistry & Engineering* **2019**, *4* (12), 2055–2059. <https://doi.org/10.1039/C9RE00265K>.
- (161) Huang, J. M.; Kuo, J. F.; Chen, C. Y. Studies on Mesomorphic Behaviors of Segmented Azoxy Polyester Containing Polyoxyethylene. *Journal of Applied Polymer Science* **1995**, *55* (8), 1217–1229. <https://doi.org/10.1002/app.1995.070550809>.
- (162) Chong, X.; Liu, C.; Huang, Y.; Huang, C.; Zhang, B. Potential-Tuned Selective Electrosynthesis of Azoxy-, Azo- and Amino-Aromatics over a CoP Nanosheet Cathode. *National Science Review* **2020**, *7* (2), 285–295. <https://doi.org/10.1093/nsr/nwz146>.
- (163) Liu, Z.; Huang, Y.; Xiao, Q.; Zhu, H. Selective Reduction of Nitroaromatics to Azoxy Compounds on Supported Ag–Cu Alloy Nanoparticles through Visible Light Irradiation. *Green Chemistry* **2016**, *18* (3), 817–825. <https://doi.org/10.1039/C5GC01726B>.
- (164) Herbst, W.; Hunger, K. *Industrial Organic Pigments: Production, Properties, Applications*; John Wiley & Sons, 2006.
- (165) Kucharska, M.; Grabka, J. A Review of Chromatographic Methods for Determination of Synthetic Food Dyes. *Talanta* **2010**, *80* (3), 1045–1051. <https://doi.org/10.1016/j.talanta.2009.09.032>.
- (166) Ali, Y.; Hamid, S. A.; Rashid, U. Biomedical Applications of Aromatic Azo Compounds. *Mini Rev Med Chem* **2018**, *18* (18), 1548–1558. <https://doi.org/10.2174/1389557518666180524113111>.
- (167) Thoroldrogers, M. Rogevs : 2 4-Diavyl~yrroles. Pavt I . Syathesis Of. 7.
- (168) Qu, Z.; Wang, P.; Chen, X.; Deng, G.-J.; Huang, H. Visible-Light-Driven Cadogan Reaction. *Chinese Chemical Letters* **2021**, *32* (8), 2582–2586. <https://doi.org/10.1016/j.ccllet.2021.02.047>.
- (169) *NaI/PPh3-Mediated Photochemical Reduction and Amination of Nitroarenes | Organic Letters*. <https://pubs.acs.org/doi/10.1021/acs.orglett.1c01654> (accessed 2023-03-16).
- (170) Liras, M.; Bañuelos Prieto, J.; Pintado-Sierra, M.; García-Moreno, I.; Costela, Á.; Infantes, L.; Sastre, R.; Amat-Guerri, F. Synthesis, Photophysical Properties, and Laser Behavior of 3-Amino and 3-Acetamido BODIPY Dyes. *Org. Lett.* **2007**, *9* (21), 4183–4186. <https://doi.org/10.1021/ol701674b>.
- (171) Rogers, M. a. T. Tetra-Arylazadipyromethines: A New Class of Synthetic Colouring Matter. *Nature* **1943**, *151* (3835), 504–504. <https://doi.org/10.1038/151504a0>.
- (172) CHAPTER 5 - Oxidation and Reduction of the Pyrrole Ring. In *Organic Chemistry: A Series of Monographs*; Jones, R. A., Bean, G. P., Eds.; The Chemistry of Pyrroles; Academic Press, 1977; Vol. 34, pp 209–247. <https://doi.org/10.1016/B978-0-12-389840-1.50010-3>.
- (173) Gowenlock*, B. G.; Richter-Addo*, G. B. Preparations of C-Nitroso Compounds. *Chem Rev* **2004**, *104* (7), 3315–3340. <https://doi.org/10.1021/cr030450k>.
- (174) Baeyer, A. Nitrosobenzol und Nitrosonaphtalin. *Ber. Dtsch. Chem. Ges.* **1874**, *7* (2), 1638–1640. <https://doi.org/10.1002/cber.187400702214>.

- (175) Molander, G. A.; Cavalcanti, L. N. Nitrosation of Aryl and Heteroaryltrifluoroborates with Nitrosonium Tetrafluoroborate. *J. Org. Chem.* **2012**, *77* (9), 4402–4413. <https://doi.org/10.1021/jo300551m>.
- (176) Kohlmeyer, C.; Klüppel, M.; Hilt, G. Synthesis of Nitrosobenzene Derivatives via Nitrosodesilylation Reaction. *J. Org. Chem.* **2018**, *83* (7), 3915–3920. <https://doi.org/10.1021/acs.joc.8b00262>.
- (177) Loudet, A.; Burgess, K. BODIPY Dyes and Their Derivatives: Syntheses and Spectroscopic Properties. *Chem. Rev.* **2007**, *107* (11), 4891–4932. <https://doi.org/10.1021/cr078381n>.
- (178) Jain, A.; Gupta, Y.; Jain, S. K. Azo Chemistry and Its Potential for Colonic Delivery. *CRT* **2006**, *23* (5). <https://doi.org/10.1615/CritRevTherDrugCarrierSyst.v23.i5.10>.
- (179) Becker, A. R.; Sternson, L. A. General Catalyzed Condensation of Nitrosobenzene and Phenylhydroxylamine in Aqueous Solution. *J. Org. Chem.* **1980**, *45* (9), 1708–1710. <https://doi.org/10.1021/jo01297a046>.
- (180) Merino, E. Synthesis of Azobenzenes: The Coloured Pieces of Molecular Materials. *Chemical Society Reviews* **2011**, *40* (7), 3835–3853. <https://doi.org/10.1039/C0CS00183J>.
- (181) *A Golden Boost to an Old Reaction | Science*. https://www.science.org/doi/full/10.1126/science.1131574?casa_token=5H15qO36RgEAAA:AAA:BQJFOq-Ze-QtwofNXMByTQ5PjQ805LkpSWU-x7ESGJQpRGhGZlbTJfPYqo7sDNgszBqlvHPLPDhsY2w (accessed 2023-03-23).
- (182) Hall, M. J.; McDonnell, S. O.; Killoran, J.; O’Shea, D. F. A Modular Synthesis of Unsymmetrical Tetraarylazadipyrromethenes. *J. Org. Chem.* **2005**, *70* (14), 5571–5578. <https://doi.org/10.1021/jo050696k>.
- (183) Adib, M.; Ayashi, N.; Heidari, F.; Mirzaei, P. Reaction between 4-Nitro-1,3-Diarylbutan-1-Ones and Ammonium Acetate in the Presence of Morpholine and Sulfur: An Efficient Synthesis of 2,4-Diarylpyrroles. *Synlett* **2016**, *27* (11), 1738–1742.
- (184) Cheng, G.; Lv, W.; Xue, L. Base-Promoted Ring-Closing Carbonyl–Allene Metathesis for the Synthesis of 2,4-Disubstituted Pyrroles. *Green Chem.* **2018**, *20* (19), 4414–4417.
- (185) Kucukdisli, M.; Ferenc, D.; Heinz, M.; Wiebe, C.; Opatz, T. Simple Two-Step Synthesis of 2,4-Disubstituted Pyrroles and 3,5-Disubstituted Pyrrole-2-Carbonitriles from Enones. *Beilstein J. Org. Chem.* **2014**, *10*, 466–470. <https://doi.org/10.3762/bjoc.10.44>.
- (186) Sun, Z.-W.; Peng, F.-Z.; Li, Z.-Q.; Zou, L.-W.; Zhang, S.-X.; Li, X.; Shao, Z.-H. Enantioselective Conjugate Addition of Both Aromatic Ketones and Acetone to Nitroolefins Catalyzed by Chiral Primary Amines Bearing Multiple Hydrogen-Bonding Donors. *J. Org. Chem.* **2012**, *77* (8), 4103–4110. <https://doi.org/10.1021/jo300011x>.
- (187) Davy, H. III. The Bakerian Lecture. An Account of Some New Analytical Researches on the Nature of Certain Bodies, Particularly the Alkalies, Phosphorus, Sulphur, Carbonaceous Matter, and the Acids Hitherto Undecomposed; with Some General Observations on Chemical Theory. *Philos. Trans. R. Soc. Lond.* **1809**, *99*, 39–104. <https://doi.org/10.1098/rstl.1809.0005>.
- (188) Gay-Lussac, J. L.; Thénard, L. J. Sur La Décomposition et La Recomposition de l’acide Boracique. *Ann. Chim. Phys* **1808**, *68*, 169–174.
- (189) DeFrancesco, H.; Dudley, J.; Coca, A. Boron Chemistry: An Overview. In *Boron Reagents in Synthesis*; ACS Symposium Series; American Chemical Society, 2016; Vol. 1236, pp 1–25. <https://doi.org/10.1021/bk-2016-1236.ch001>.

- (190) Leśnikowski, Z. J. Recent Developments with Boron as a Platform for Novel Drug Design. *Expert Opin. Drug Discov.* **2016**, *11* (6), 569–578. <https://doi.org/10.1080/17460441.2016.1174687>.
- (191) Leśnikowski, Z. J. Challenges and Opportunities for the Application of Boron Clusters in Drug Design. *J. Med. Chem.* **2016**, *59* (17), 7738–7758. <https://doi.org/10.1021/acs.jmedchem.5b01932>.
- (192) Song, S.; Gao, P.; Sun, L.; Kang, D.; Kongsted, J.; Poongavanam, V.; Zhan, P.; Liu, X. Recent Developments in the Medicinal Chemistry of Single Boron Atom-Containing Compounds. *Acta Pharm. Sin. B.* **2021**, *11* (10), 3035–3059. <https://doi.org/10.1016/j.apsb.2021.01.010>.
- (193) Levine, J. M. Dakin's Solution: Past, Present, and Future. *Adv. Skin Wound Care* **2013**, *26* (9), 410–414.
- (194) Baker, S. J.; Ding, C. Z.; Akama, T.; Zhang, Y.-K.; Hernandez, V.; Xia, Y. Therapeutic Potential of Boron-Containing Compounds. *Future Med. Chem.* **2009**, *1* (7), 1275–1288. <https://doi.org/10.4155/fmc.09.71>.
- (195) Fernandes, G. F. S.; Denny, W. A.; Dos Santos, J. L. Boron in Drug Design: Recent Advances in the Development of New Therapeutic Agents. *Eur. J. Med. Chem.* **2019**, *179*, 791–804. <https://doi.org/10.1016/j.ejmech.2019.06.092>.
- (196) Rothmund, P. Formation of Porphyrins from Pyrrole and Aldehydes. *J. Am. Chem. Soc.* **1935**, *57* (10), 2010–2011. <https://doi.org/10.1021/ja01313a510>.
- (197) Fischer, H.; Orth, H. *Die Chemie Des Pyrrols*; Akademische Verlagsgesellschaft: Leipzig, 1937; Vol. I–III.
- (198) Ziessel, R.; Ulrich, G.; Harriman, A. The Chemistry of BODIPY: A New El Dorado for Fluorescence Tools. *New J. Chem.* **2007**, *31*, 496–501.
- (199) Loudet, A.; Burgess, K. BODIPY Dyes and Their Derivatives: Syntheses and Spectroscopic Properties. *Chem. Rev.* **2007**, *107* (11), 4891–4932.
- (200) Wood, T. E.; Thompson, A. Advances in the Chemistry of Dipyrrens and Their Complexes. *Chem. Rev.* **2007**, *107*, 1831–1861.
- (201) Boens, N.; Leen, V.; Dehaen, W. Fluorescent Indicators Based on BODIPY. *Chem. Soc. Rev.* **2012**, *41*, 1130–1172.
- (202) Benstead, M.; Mehl, G. H.; Boyle, R. W. 4,4'-Difluoro-4-Bora-3a,4a-Diaza-s-Indacenes (BODIPYs) as Components of Novel Light Active Materials. *Tetrahedron* **2011**, *67*, 3573–3601.
- (203) Boens, N.; Verbelen, B.; Ortiz, M. J.; Jiao, L.; Dehaen, W. Synthesis of BODIPY Dyes through Postfunctionalization of the Boron Dipyrromethene Core. *Coord. Chem. Rev.* **2019**, *399*, 213024. <https://doi.org/10.1016/j.ccr.2019.213024>.
- (204) Bassan, E.; Gualandi, A.; Cozzi, P. G.; Ceroni, P. Design of BODIPY Dyes as Triplet Photosensitizers: Electronic Properties Tailored for Solar Energy Conversion, Photoredox Catalysis and Photodynamic Therapy. *Chem. Sci.* **2021**, *12* (19), 6607–6628. <https://doi.org/10.1039/D1SC00732G>.
- (205) Shi, Z.; Han, X.; Hu, W.; Bai, H.; Peng, B.; Ji, L.; Fan, Q.; Li, L.; Huang, W. Bioapplications of Small Molecule Aza-BODIPY: From Rational Structural Design to in Vivo Investigations. *Chem. Soc. Rev.* **2020**, *49* (21), 7533–7567. <https://doi.org/10.1039/D0CS00234H>.

- (206) Bessette, A.; Hanan, G. S. Design, Synthesis and Photophysical Studies of Dipyrrromethene-Based Materials: Insights into Their Applications in Organic Photovoltaic Devices. *Chem. Soc. Rev.* **2014**, *43*, 3342–3405.
- (207) Lu, H.; Mack, J.; Yang, Y.; Shen, Z. Structural Modification Strategies for the Rational Design of Red/NIR Region BODIPYs. *Chem. Soc. Rev.* **2014**, *43* (13), 4778–4823. <https://doi.org/10.1039/C4CS00030G>.
- (208) Bodio, E.; Denat, F.; Goze, C. BODIPYS and Aza-BODIPY Derivatives as Promising Fluorophores for in Vivo Molecular Imaging and Theranostic Applications. In *Porphyrin Science by Women*; WORLD SCIENTIFIC, 2020; pp 116–140. https://doi.org/10.1142/9789811223556_0008.
- (209) Sakamoto, R.; Iwashima, T.; Tsuchiya, M.; Toyoda, R.; Matsuoka, R.; Kögel, J. F.; Kusaka, S.; Hoshiko, K.; Yagi, T.; Nagayama, T.; Nishihara, H. New Aspects in Bis and Tris(Dipyrrinato)Metal Complexes: Bright Luminescence, Self-Assembled Nanoarchitectures, and Materials Applications. *J. Mater. Chem. A* **2015**, *3* (30), 15357–15371. <https://doi.org/10.1039/C5TA02040A>.
- (210) Treibs, A.; Kreuzer, F. H. Difluoroboryl Complexes of Di- and Tripyrrylmethenes. *Liebigs Ann. Chem.* **1968**, *718*, 208–223.
- (211) Frath, D.; Massue, J.; Ulrich, G.; Ziessel, R. Luminescent Materials: Locking π -Conjugated and Heterocyclic Ligands with Boron(III). *Angew. Chem. Int. Ed.* **2014**, *53* (9), 2290–2310. <https://doi.org/10.1002/anie.201305554>.
- (212) ThermoFisherScientific. *Fluorophores and Their Amine-Reactive Derivatives: BODIPY Dye Series*. <https://www.thermofisher.com/ca/en/home/references/molecular-probes-the-handbook/fluorophores-and-their-amine-reactive-derivatives/bodipy-dye-series.html> (accessed 2022-02-27).
- (213) *LysoTrackerTM Red DND-99*. <https://www.thermofisher.com/order/catalog/product/L7528> (accessed 2022-04-06).
- (214) *BODIPYTM FL C5 (4,4-Difluoro-5,7-Dimethyl-4-Bora-3a,4a-Diaza-s-Indacene-3-Pentanoic Acid)*. <https://www.thermofisher.com/order/catalog/product/D3834> (accessed 2022-04-06).
- (215) Kowada, T.; Maeda, H.; Kikuchi, K. BODIPY-Based Probes for the Fluorescence Imaging of Biomolecules in Living Cells. *Chem. Soc. Rev.* **2015**, *44*, 4953–4972.
- (216) Das, B. C.; Thapa, P.; Karki, R.; Schinke, C.; Das, S.; Kambhampati, S.; Banerjee, S. K.; Van Veldhuizen, P.; Verma, A.; Weiss, L. M.; Evans, T. Boron Chemicals in Diagnosis and Therapeutics. *Future Med. Chem.* **2013**, *5* (6), 653–676. <https://doi.org/10.4155/fmc.13.38>.
- (217) Chatterjee, S.; Tripathi, N. M.; Bandyopadhyay, A. The Modern Role of Boron as a ‘Magic Element’ in Biomedical Science: Chemistry Perspective. *Chem. Commun.* **2021**, *57* (100), 13629–13640. <https://doi.org/10.1039/D1CC05481C>.
- (218) Liu, H.-W.; Chen, L.; Xu, C.; Li, Z.; Zhang, H.; Zhang, X.-B.; Tan, W. Recent Progresses in Small-Molecule Enzymatic Fluorescent Probes for Cancer Imaging. *Chem. Soc. Rev.* **2018**, *47* (18), 7140–7180. <https://doi.org/10.1039/C7CS00862G>.
- (219) Zhang, C.; Pu, K. Molecular and Nanoengineering Approaches towards Activatable Cancer Immunotherapy. *Chem. Soc. Rev.* **2020**, *49* (13), 4234–4253. <https://doi.org/10.1039/C9CS00773C>.
- (220) Wang, S.; Liu, H.; Mack, J.; Tian, J.; Zou, B.; Lu, H.; Li, Z.; Jiang, J.; Shen, Z. A BODIPY-Based ‘Turn-on’ Fluorescent Probe for Hypoxic Cell Imaging. *Chem. Commun.* **2015**, *51* (69), 13389–13392. <https://doi.org/10.1039/C5CC05139H>.

- (221) Campbell, J. W.; Tung, M. T.; Diaz-Rodriguez, R. M.; Robertson, K. N.; Beharry, A. A.; Thompson, A. Introducing the Tellurophene-Appended BODIPY: PDT Agent with Mass Cytometry Tracking Capabilities. *ACS Med. Chem. Lett.* **2021**, *12* (12), 1925–1931. <https://doi.org/10.1021/acsmchemlett.1c00492>.
- (222) Klifout, H.; Stewart, A.; Elkhalfifa, M.; He, H. BODIPYs for Dye-Sensitized Solar Cells. *ACS Appl. Mater. Interfaces* **2017**, *9* (46), 39873–39889. <https://doi.org/10.1021/acsmami.7b07688>.
- (223) Squeo, B. M.; Ganzer, L.; Virgili, T.; Pasini, M. BODIPY-Based Molecules, a Platform for Photonic and Solar Cells. *Molecules* **2021**, *26* (1), 153. <https://doi.org/10.3390/molecules26010153>.
- (224) Karlsson, J. K. G.; Harriman, A. Origin of the Red-Shifted Optical Spectra Recorded for Aza-BODIPY Dyes. *J. Phys. Chem. A* **2016**, *120* (16), 2537–2546. <https://doi.org/10.1021/acs.jpca.6b01278>.
- (225) Laha, J. K.; Dhanalekshmi, S.; Taniguchi, M.; Ambroise, A.; Lindsey, J. S. A Scalable Synthesis of Meso-Substituted Dipyrromethanes. *Org. Process Res. Dev.* **2003**, *7* (6), 799–812. <https://doi.org/10.1021/op034083q>.
- (226) Li, T.; Gu, W.; Yu, C.; Lv, X.; Wang, H.; Hao, E.; Jiao, L. Syntheses and Photophysical Properties of Meso-Phenylene Ridged Boron Dipyrromethene Monomers, Dimers and Trimer. *Chin. J. Chem.* **2016**, *34* (10), 989–996. <https://doi.org/10.1002/cjoc.201600500>.
- (227) Yang, L.; Simionescu, R.; Lough, A.; Yan, H. Some Observations Relating to the Stability of the BODIPY Fluorophore under Acidic and Basic Conditions. *Dyes Pigm.* **2011**, *91*, 264–267.
- (228) Wang, Z.; Cheng, C.; Kang, Z.; Miao, W.; Liu, Q.; Wang, H.; Hao, E. Organotrifluoroborate Salts as Complexation Reagents for Synthesizing BODIPY Dyes Containing Both Fluoride and an Organo Substituent at the Boron Center. *J. Org. Chem.* **2019**, *84* (5), 2732–2740. <https://doi.org/10.1021/acs.joc.8b03145>.
- (229) Sawazaki, T.; Shimizu, Y.; Oisaki, K.; Sohma, Y.; Kanai, M. Convergent and Functional-Group-Tolerant Synthesis of B-Organo BODIPYs. *Org. Lett.* **2018**, *20* (24), 7767–7770. <https://doi.org/10.1021/acs.orglett.8b03138>.
- (230) Beh, M. H. R.; Douglas, K. I. B.; House, K. T. E.; Murphy, A. C.; Sinclair, J. S. T.; Thompson, A. Robust Synthesis of F-BODIPYs. *Org. Biomol. Chem.* **2016**, *14*, 11473–11479.
- (231) Crawford, S. M.; Thompson, A. Conversion of 4,4-Difluoro-4-Bora-3a,4a-Diaza-s-Indacenes (F-BODIPYs) to Dipyrins Using a Microwave-Promoted Deprotection Strategy. *Org. Lett.* **2010**, *12*, 1424–1427.
- (232) Lundrigan, T.; Baker, A. E. G.; Longobardi, L. E.; Wood, T. E.; Smithen, D. A.; Crawford, S. M.; Cameron, T. S.; Thompson, A. An Improved Method for the Synthesis of F-BODIPYs from Dipyrins and Bis(Dipyrin)s. *Org. Lett.* **2012**, *14*, 2158–2161.
- (233) Gabe, Y.; Ueno, T.; Urano, Y.; Kojima, H.; Nagano, T. Tunable Design Strategy for Fluorescence Probes Based on 4-Substituted BODIPY Chromophore: Improvement of Highly Sensitive Fluorescence Probe for Nitric Oxide. *Anal. Bioanal. Chem.* **2006**, *386*, 621–626.
- (234) Smithen, D. A.; Baker, A. E. G.; Offman, M.; Crawford, S. M.; Cameron, T. S.; Thompson, A. Use of F-BODIPYs as a Protection Strategy for Dipyrins: Optimization of BF₂ Removal. *J. Org. Chem.* **2012**, *77*, 3439–3453.

- (235) Rajeswara Rao, M.; Ravikanth, M. Boron Complexes of Oxasmaragdyrin, a Core-Modified Expanded Porphyrin. *J. Org. Chem.* **2011**, *76*, 3582–3587.
- (236) Carrano, C. J.; Tsutsui, M. Unusual Metalloporphyrins: Synthesis and Properties of a Dimetallic Boron Porphyrin Complex. *J. Coord. Chem.* **1977**, *7*, 125–130.
- (237) Tahtaoui, C.; Thomas, C.; Rohmer, F.; Klotz, P.; Duportail, G.; Mely, Y.; Bonnet, D.; Hibert, M. Convenient Method to Access New 4,4-Dialkoxy- and 4,4-Diaryloxy-Diaza-s-Indacene Dyes: Synthesis and Spectroscopic Evaluation. *J. Org. Chem.* **2007**, *72* (1), 269–272.
- (238) Cipot-Wechsler, J.; Al-Sheikh Ali, A.; Chapman, E. E.; Cameron, T. S.; Thompson, A. Synthesis and Reactivity of a Dipyrinato Lithium Complex. *Inorg. Chem.* **2007**, *46*, 10947–10949.
- (239) Al-Sheikh Ali, A.; Cipot-Wechsler, J.; Crawford, S. M.; Selim, O.; Stoddard, R. L.; Cameron, T. S.; Thompson, A. The First Series of Alkali Dipyrinato Complexes. *Can. J. Chem.* **2010**, *88*, 725–735.
- (240) Wan, W.; Silva, M. S.; McMillen, C. D.; Creager, S. E.; Smith, R. C. Highly Luminescent Heavier Main Group Analogues of Boron-Dipyrromethene. *J. Am. Chem. Soc.* **2019**, *141* (22), 8703–8707. <https://doi.org/10.1021/jacs.9b03235>.
- (241) Lundrigan, T.; Crawford, S. M.; Cameron, T. S.; Thompson, A. Cl-BODIPYs: A BODIPY Class Enabling Facile B-Substitution. *Chem. Commun.* **2012**, *48*, 1003–1005.
- (242) Ikeda, C.; Nabeshima, T. Self-Assembled Cyclic Boron-Dipyrin Oligomers. *Chem. Commun.* **2008**, No. 6, 721–723. <https://doi.org/10.1039/B716453J>.
- (243) Rausaria, S.; Kamadulski, A.; Rath, N. P.; Bryant, L.; Chen, Z.; Salvemini, D.; Neumann, W. L. Manganese(III) Complexes of Bis(Hydroxyphenyl)Dipyrromethenes Are Potent Orally Active Peroxynitrite Scavengers. *J. Am. Chem. Soc.* **2011**, *133* (12), 4200–4203. <https://doi.org/10.1021/ja110427e>.
- (244) Lundrigan, T.; Thompson, A. Conversion of F-BODIPYs to Cl-BODIPYs: Enhancing the Reactivity of F-BODIPYs. *J. Org. Chem.* **2013**, *78*, 757–761.
- (245) Lundrigan, T. Improved Synthesis and Enhanced Reactivity of X-BODIPYs (PhD Thesis), Dalhousie University, Halifax, Nova Scotia, Canada, 2017, Vol. Ph.D.
- (246) Pauling, L. *The Nature of the Chemical Bond, 3rd Ed.*; University Press: New York, 1960.
- (247) Cornet, S. M.; Dillon, K. B.; Entwistle, C. D.; Fox, M. A.; Goeta, A. E.; Goodwin, H. P.; Marder, T. B.; Thompson, A. L. Synthesis and Characterisation of Some New Boron Compounds Containing the 2,4,6-(CF₃)₃C₆H₂ (Fluoromes = Ar), 2,6-(CF₃)₂C₆H₃ (Fluoroxyl = Ar'), or 2,4-(CF₃)₂C₆H₃ (Ar'') Ligands. *Dalton Trans.* **2003**, No. 23, 4395–4405. <https://doi.org/10.1039/B309820F>.
- (248) Lundrigan, T.; Cameron, T. S.; Thompson, A. Activation and Deprotection of F-BODIPYs Using Boron Trihalides. *Chem. Commun.* **2014**, *50*, 7028–7031.
- (249) Jiang, X.-D.; Zhang, J.; Furuyama, T.; Zhao, W. Development of Mono- and Di-AcO Substituted BODIPYs on the Boron Center. *Org. Lett.* **2012**, *14* (1), 248–251. <https://doi.org/10.1021/ol2030229>.
- (250) Ray, C.; Schad, C.; Moreno, F.; Maroto, B. L.; Bañuelos, J.; Arbeloa, T.; García-Moreno, I.; Villafuerte, C.; Muller, G.; de la Moya, S. BCl₃-Activated Synthesis of COO-BODIPY Laser Dyes: General Scope and High Yields under Mild Conditions. *J. Org. Chem.* **2020**, *85* (7), 4594–4601. <https://doi.org/10.1021/acs.joc.9b03059>.
- (251) Lerrick, R. I.; Winstanley, T. P. L.; Haggerty, K.; Wills, C.; Clegg, W.; Harrington, R. W.; Bultinck, P.; Herrebout, W.; Benniston, A. C.; Hall, M. J. Axially Chiral BODIPYs. *Chem. Commun.* **2014**, *50* (36), 4714–4716. <https://doi.org/10.1039/C4CC00851K>.

- (252) Zinna, F.; Bruhn, T.; Guido, C. A.; Ahrens, J.; Bröring, M.; Di Bari, L.; Pescitelli, G. Circularly Polarized Luminescence from Axially Chiral BODIPY DYErs: An Experimental and Computational Study. *Chem. Eur. J.* **2016**, *22* (45), 16089–16098. <https://doi.org/10.1002/chem.201602684>.
- (253) Sánchez-Carnerero, E. M.; Moreno, F.; Maroto, B. L.; Agarrabeitia, A. R.; Ortiz, M. J.; Vo, B. G.; Muller, G.; Moya, S. de la. Circularly Polarized Luminescence by Visible-Light Absorption in a Chiral O-BODIPY Dye: Unprecedented Design of CPL Organic Molecules from Achiral Chromophores. *J. Am. Chem. Soc.* **2014**, *136* (9), 3346–3349. <https://doi.org/10.1021/ja412294s>.
- (254) Ray, C.; Díaz-Casado, L.; Avellanal-Zaballa, E.; Bañuelos, J.; Cerdán, L.; García-Moreno, I.; Moreno, F.; Maroto, B. L.; López-Arbeloa, Í.; de la Moya, S. N-BODIPYs Come into Play: Smart Dyes for Photonic Materials. *Chem. Eur. J.* **2017**, *23* (39), 9383–9390. <https://doi.org/10.1002/chem.201701350>.
- (255) Wang, M.; Zhang, G.; Kaufman, N. E. M.; Bobadova-Parvanova, P.; Fronczek, F. R.; Smith, K. M.; Vicente, M. G. H. Linker-Free Near-IR Aza-BODIPY-Glutamine Conjugates Through Boron Functionalization. *Eur. J. Org. Chem.* **2020**, *2020* (8), 971–977. <https://doi.org/10.1002/ejoc.201901772>.
- (256) Wang, M.; Zhang, G.; Bobadova-Parvanova, P.; Merriweather, A. N.; Odom, L.; Barbosa, D.; Fronczek, F. R.; Smith, K. M.; Vicente, M. G. H. Synthesis and Investigation of Linker-Free BODIPY–Gly Conjugates Substituted at the Boron Atom. *Inorg. Chem.* **2019**, *58* (17), 11614–11621. <https://doi.org/10.1021/acs.inorgchem.9b01474>.
- (257) Wang, M.; Zhang, G.; Bobadova-Parvanova, P.; Smith, K. M.; Vicente, M. G. H. Syntheses and Investigations of Conformationally Restricted, Linker-Free α -Amino Acid–BODIPYs via Boron Functionalization. *J. Org. Chem.* **2021**, *86* (24), 18030–18041. <https://doi.org/10.1021/acs.joc.1c02328>.
- (258) Liu, B.; Novikova, N.; Simpson, M. C.; Timmer, M. S. M.; Stocker, B. L.; Söhnle, T.; Ware, D. C.; Brothers, P. J. Lighting up Sugars: Fluorescent BODIPY–Glucose-Furanose and –Septanose Conjugates Linked by Direct B–O–C Bonds. *Org. Biomol. Chem.* **2016**, *14* (23), 5205–5209. <https://doi.org/10.1039/C6OB00726K>.
- (259) Kanyan, D.; Horacek-Glading, M.; Wildervanck, M. J.; Söhnle, T.; Ware, D. C.; Brothers, P. J. O-BODIPYs as Fluorescent Labels for Sugars: Glucose, Xylose and Ribose. *Org. Chem. Front.* **2022**, *9* (3), 720–730. <https://doi.org/10.1039/D1QO01418H>.
- (260) Maity, A.; Sarkar, A.; Bhaktha B. N, S.; Patra, S. K. Design and Synthesis of Perfluoroalkyl Decorated BODIPY Dye for Random Laser Action in a Microfluidic Device. *New J. Chem.* **2020**, *44* (34), 14650–14661. <https://doi.org/10.1039/D0NJ03108A>.
- (261) Sharma, R.; Ravikanth, M. Synthesis, Structure and Properties of the First Examples of Hexacoordinate SnIV Complexes of Pyrrolyldipyrins. *European Journal of Inorganic Chemistry* **2017**, *2017* (4), 829–834. <https://doi.org/10.1002/ejic.201601179>.
- (262) Lakshmi, V.; Chatterjee, T.; Ravikanth, M. Lewis Acid Assisted Decomplexation of F-BODIPYs to Dipyrins. *Eur. J. Org. Chem.* **2014**, *2014* (10), 2105–2110. <https://doi.org/10.1002/ejoc.201301662>.
- (263) Yu, M.; Wong, J. K.-H.; Tang, C.; Turner, P.; Todd, M. H.; Rutledge, P. J. Efficient Deprotection of F-BODIPY Derivatives: Removal of BF₂ Using Brønsted Acids. *Beilstein J. Org. Chem.* **2015**, *11*, 37–41.
- (264) Smith, C. D.; Thompson, A. Facile Deprotection of F-BODIPYs Using Methylboronic Acid. *RSC Adv.* **2020**, *10* (41), 24273–24279. <https://doi.org/10.1039/D0RA05151A>.

- (265) Panchavarnam, S.; Sengupta, R.; Ravikanth, M. Bis-Palladium Complex of α -Benzimidazole 9-Pyrrolyl Dipyrromethene: Synthesis, Structure, and Spectral and Catalytic Properties. *Inorg. Chem.* **2021**, *60* (20), 15686–15694. <https://doi.org/10.1021/acs.inorgchem.1c02353>.
- (266) Panchavarnam, S.; Pushpanandan, P.; Ravikanth, M. Synthesis, Structure, and Properties of Helical Bis-Cu(II) Complex of Linear Hexapyrrolic Ligand. *Inorg. Chem.* **2022**, *61* (3), 1562–1570. <https://doi.org/10.1021/acs.inorgchem.1c03329>.
- (267) Li, J.; Zhang, Q.; Yin, J.; Yu, C.; Cheng, K.; Wei, Y.; Hao, E.; Jiao, L. Metal-Free and Versatile Synthetic Routes to Natural and Synthetic Prodiginines from Boron Dipyrin. *Org. Lett.* **2016**, *18*, 5696–5699.
- (268) Li, F.; Yang, K.; Tyhonas, J. S.; MacCrum, K. A.; Lindsey, J. S. Beneficial Effects of Salts on an Acid-Catalyzed Condensation Leading to Porphyrin Formation. *Tetrahedron* **1997**, *53*, 12339–12360.
- (269) Liu, S.; Lin, T.-P.; Li, D.; Leamer, L.; Shan, H.; Li, Z.; Gabbai, F. P.; Conti, P. S. Lewis Acid-Assisted Isotopic ^{18}F - ^{19}F Exchange in BODIPY Dyes: Facile Generation of Positron Emission Tomography/Fluorescence Dual Modality Agents for Tumor Imaging. *Theranostics* **2013**, *3* (3), 181–189. <https://doi.org/10.7150/thno.5984>.
- (270) Diaz-Rodriguez, R. M.; Robertson, K. N.; Thompson, A. Synthesis and Reactivity of Aza-Dipyrin Alkali Metal Salts. *Chem. Commun.* **2018**, *54* (93), 13139–13142. <https://doi.org/10.1039/C8CC07101B>.
- (271) Diaz-Rodriguez, R. M.; Robertson, K. N.; Thompson, A. Classifying Donor Strengths of Dipyrinato/Aza-Dipyrinato Ligands. *Dalton Trans.* **2019**, *48*, 7546–7550.
- (272) Diaz-Rodriguez, R. M.; Burke, L.; Robertson, K. N.; Thompson, A. Synthesis, Properties and Reactivity of BCl_2 Aza-BODIPY Complexes and Salts of the Aza-Dipyrinato Scaffold. *Org. Biomol. Chem.* **2020**, *18* (11), 2139–2147. <https://doi.org/10.1039/D0OB00272K>.
- (273) Wang, Y.; Mori, S.; Furuta, H.; Shimizu, S. Bis(1,3-Dithiol-2-Ylidene)-Substituted Subtriazachlorin: A Subphthalocyanine Analogue with Redox Properties. *Angewandte Chemie International Edition* **2019**, *58* (32), 10975–10979. <https://doi.org/10.1002/anie.201905331>.

Appendix A.

This section contains a copy of the signed letter from the Royal Society of Chemistry (RSC) granting permission for the use of my paper specified below in the printed version of this thesis.

DocuSign Envelope ID: B45A5AC8-8D63-4EC7-906A-D880951D1BCD

May 3, 2023

Chemical Communications
Royal Society of Chemistry
Thomas Graham House (290)
Science Park, Milton Road
Cambridge, CB4 0WF, UK

I am preparing my doctoral thesis for submission to the Faculty of Graduate Studies at Dalhousie University, Halifax, Nova Scotia, Canada. I am seeking your permission to include a manuscript version of the following paper(s) as a chapter in the thesis:

Gapare, R. L., & Thompson, A. (2022). Substitution at boron in BODIPYs. *Chemical Communications*, 58(53), 7351-7359.

Dalhousie graduate theses are collected and stored online by Dalhousie University and Library and Archives of Canada. I am seeking your permission for the material described above to be stored online in [Dalhousie University's institutional repository](#) and in Library and Archives of Canada (LAC)'s [Theses Canada Collection](#).


Full publication details and a copy of this permission letter will be included in the thesis.

Yours sincerely,

Rosinah Liandrah Gapare

Permission is granted for:

- a) the inclusion of the material described above in your thesis.
- b) for the material described above to be included in the copy of your thesis that is sent to the Library and Archives of Canada inclusion in Theses Canada.
- c) For the material described above to be included in the copy of your thesis that is sent to Dalhousie University's institutional repository.

Name:	Becky Roberts	Title:	Contracts & Copyright Executive
Signature:		Date:	4/5/2023 11:32 AM BST

C0888C4F8FD104CA

Appendix B: X-Ray Crystallographic Analysis Data.

4-Oxo-2,4-diphenylbutanoic acid pentafluorophenyl ester, (3.31).

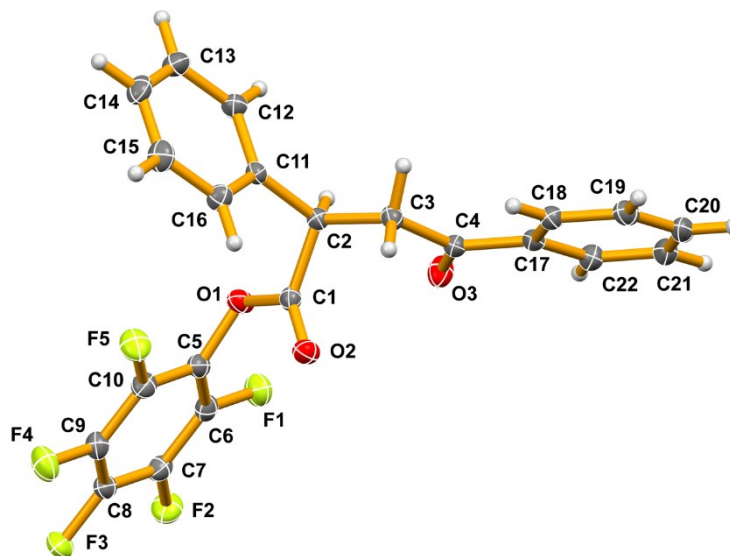


Figure 35: ORTEP diagram of ester 3.31. Thermal ellipsoids are shown at 50% probability.

Empirical formula	C ₂₂ H ₁₃ F ₅ O ₃	
Formula weight	420.32	
Temperature	125(2) K	
Wavelength	0.71073 Å	
Crystal system	Monoclinic	
Space group	P2 ₁ /c	
Unit cell dimensions	$a = 7.3358(3) \text{ \AA}$	$a = 90^\circ$
	$b = 18.2998(7) \text{ \AA}$	$b = 101.609(2)^\circ$
	$c = 13.8963(6) \text{ \AA}$	$g = 90^\circ$
Volume	1827.33(13) Å ³	
Z	4	
Density (calculated)	1.528 Mg/m ³	
Absorption coefficient	0.135 mm ⁻¹	
F(000)	856	
	183	

Crystal size	0.088 x 0.076 x 0.062 mm ³
Theta range for data collection	2.226 to 30.998°
Index ranges	-10 ≤ h ≤ 10, -26 ≤ k ≤ 26, -20 ≤ l ≤ 20
Reflections collected	129550
Independent reflections	5827 [R(int) = 0.0624]
Completeness to theta = 25.242°	99.9 %
Absorption correction	Semi-empirical from equivalents
Max. and min. transmission	0.7432 and 0.7162
Refinement method	Full-matrix least-squares on F ²
Data / restraints / parameters	5827 / 0 / 271
Goodness-of-fit on F ²	1.033
Final R indices [I > 2σ(I)]	R1 = 0.0411, wR2 = 0.0990
R indices (all data)	R1 = 0.0581, wR2 = 0.1114
Extinction coefficient	n/a
Largest diff. peak and hole	0.415 and -0.244 e.Å ⁻³

4-Nitro-1,3-diphenylbutan-1-ol, (3.32).

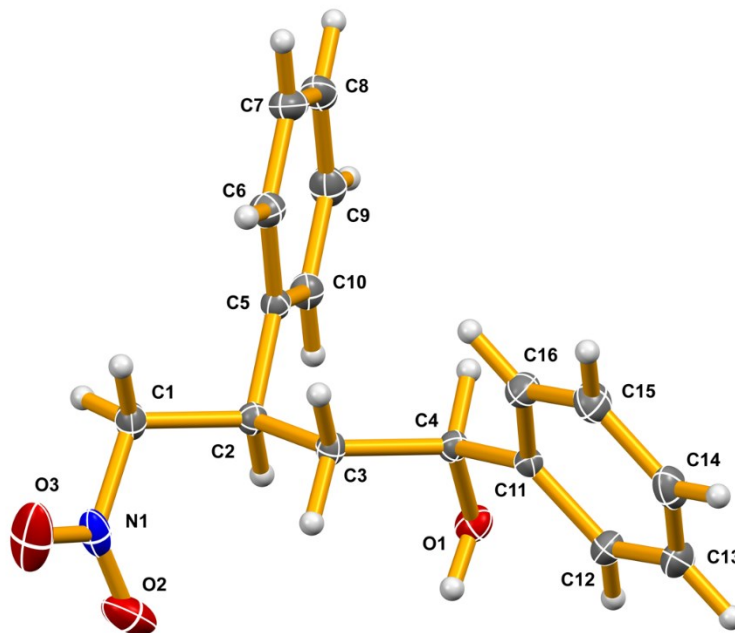


Figure 36: ORTEP diagram of alcohol 3.32. Thermal ellipsoids are shown at 50% probability.

Empirical formula	C ₁₆ H ₁₇ NO ₃	
Formula weight	271.30	
Temperature	125(2) K	
Wavelength	0.71073 Å	
Crystal system	Triclinic	
Space group	<i>P</i> -1	
Unit cell dimensions	<i>a</i> = 5.7796(2) Å	<i>a</i> = 76.2853(16)°
	<i>b</i> = 9.8634(4) Å	<i>b</i> = 88.5992(17)°
	<i>c</i> = 12.2495(5) Å	<i>g</i> = 83.5883(16)°
Volume	674.15(5) Å ³	
<i>Z</i>	2	
Density (calculated)	1.337 Mg/m ³	
Absorption coefficient	0.092 mm ⁻¹	
F(000)	288	
Crystal size	0.414 x 0.108 x 0.024 mm ³	
Theta range for data collection	1.711 to 36.316°	
Index ranges	-9 ≤ <i>h</i> ≤ 9, -16 ≤ <i>k</i> ≤ 16, -20 ≤ <i>l</i> ≤ 20	
Reflections collected	89515	
Independent reflections	6537 [R(int) = 0.0721]	
Completeness to theta = 25.242°	100.0 %	
Absorption correction	Semi-empirical from equivalents	
Max. and min. transmission	0.7489 and 0.6378	
Refinement method	Full-matrix least-squares on F ²	
Data / restraints / parameters	6537 / 0 / 185	
Goodness-of-fit on F ²	1.031	
Final R indices [I > 2σ(I)]	R1 = 0.0460, wR2 = 0.1213	
R indices (all data)	R1 = 0.0641, wR2 = 0.1359	
Extinction coefficient	n/a	
Largest diff. peak and hole	0.516 and -0.219 e.Å ⁻³	

4-Oxo-2,4 diphenylbutanamide, (3.35).

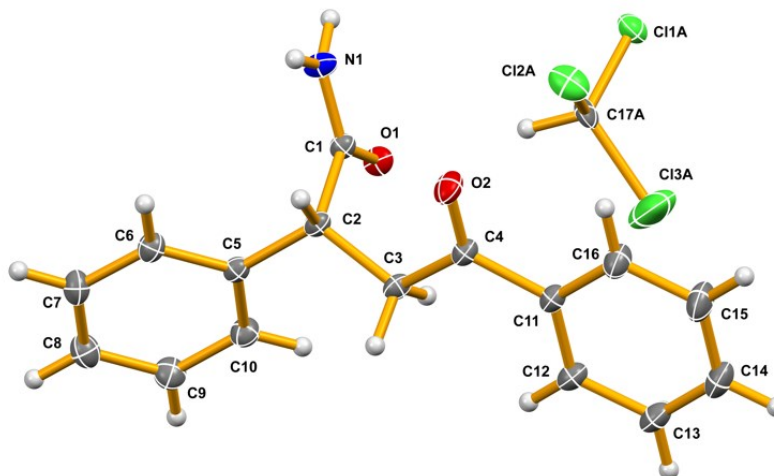


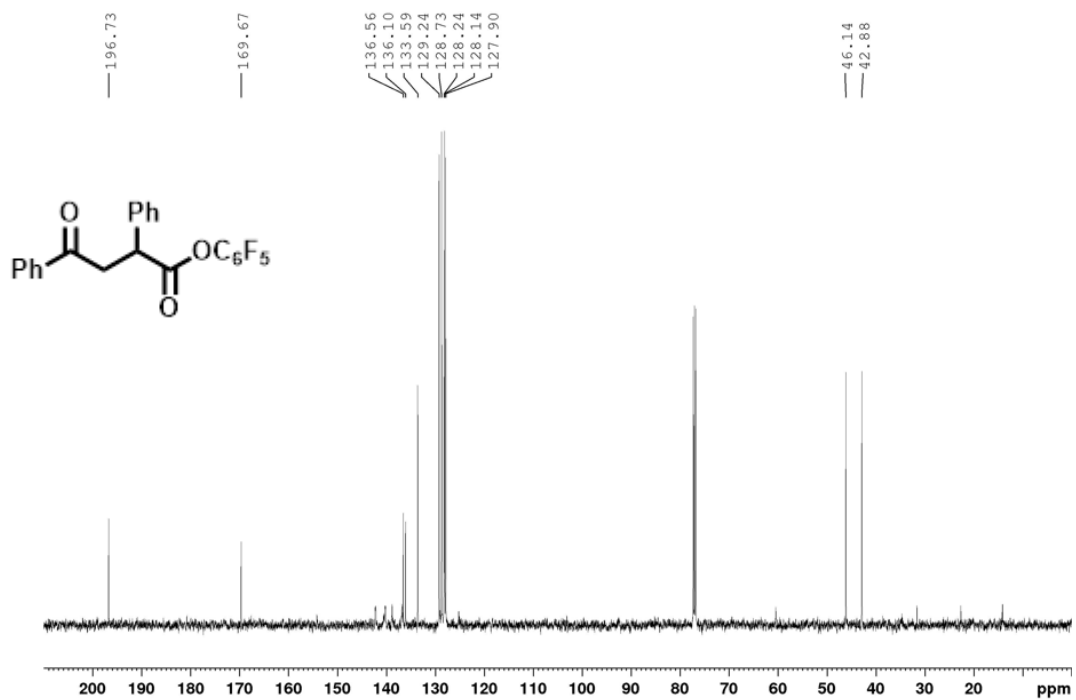
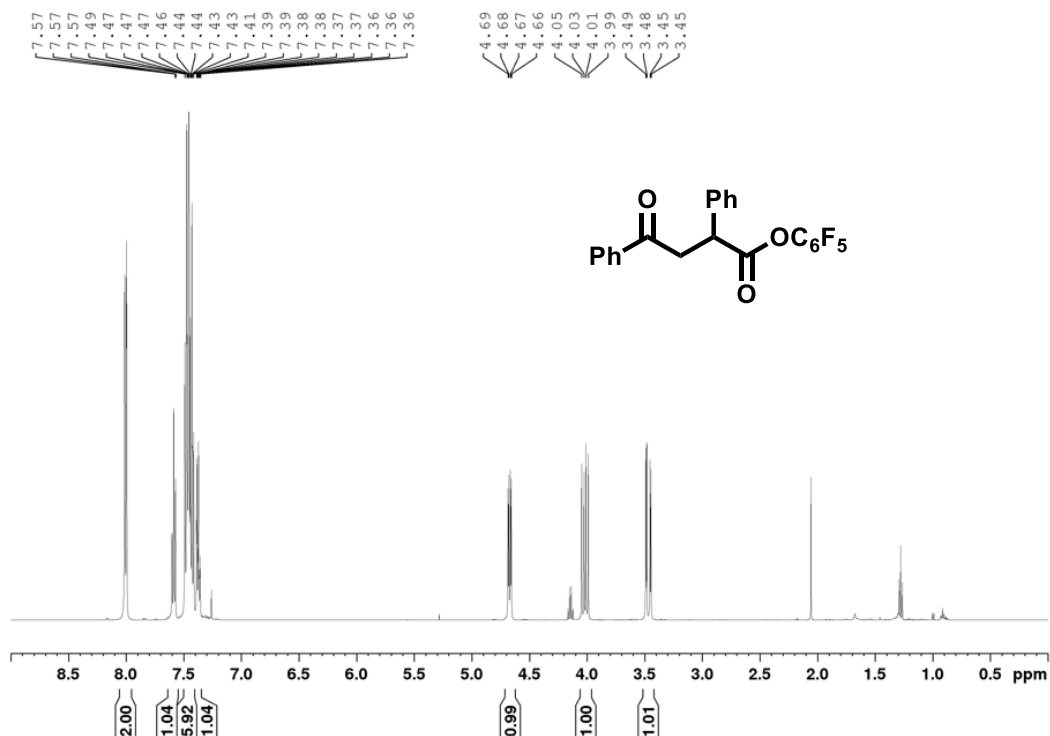
Figure 37: ORTEP diagram of amide 3.35 with solvent. Thermal ellipsoids are shown at 50% probability.

Empirical formula	C ₁₇ H ₁₆ Cl ₃ NO ₂	
Formula weight	372.66	
Temperature	125(2) K	
Wavelength	0.71073 Å	
Crystal system	Monoclinic	
Space group	P2 ₁ /c	
Unit cell dimensions	a = 10.9411(4) Å	a = 90°
	b = 20.1946(6) Å	b = 102.081(1)°
	c = 8.1906(2) Å	g = 90°
Volume	1769.64(9) Å ³	
Z	4	
Density (calculated)	1.399 Mg/m ³	
Absorption coefficient	0.525 mm ⁻¹	
F(000)	768	
Crystal size	0.180 x 0.104 x 0.085 mm ³	
Theta range for data collection	2.017 to 45.342°	
Index ranges	-21 ≤ h ≤ 21, -40 ≤ k ≤ 40, -16 ≤ l ≤ 16	

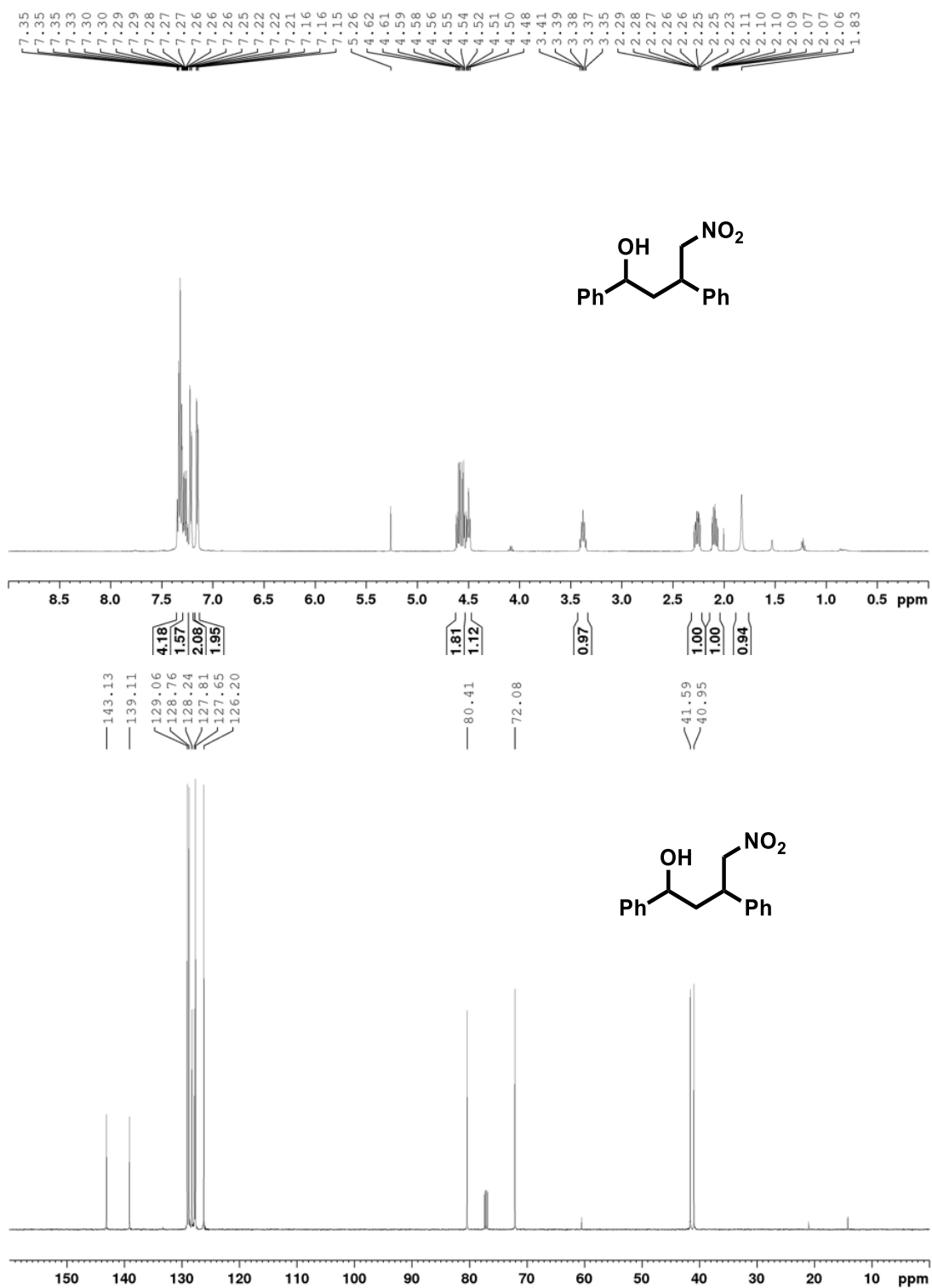
Reflections collected	244944
Independent reflections	14858 [R(int) = 0.0448]
Completeness to theta = 25.242°	99.9 %
Absorption correction	Semi-empirical from equivalents
Max. and min. transmission	0.7489 and 0.6976
Refinement method	Full-matrix least-squares on F ²
Data / restraints / parameters	14858 / 93 / 291
Goodness-of-fit on F ²	1.027
Final R indices [I > 2sigma(I)]	R1 = 0.0365, wR2 = 0.0995
R indices (all data)	R1 = 0.0566, wR2 = 0.1134
Extinction coefficient	n/a
Largest diff. peak and hole	0.523 and -0.366 e.Å ⁻³

Appendix C: NMR data for synthesized compounds.

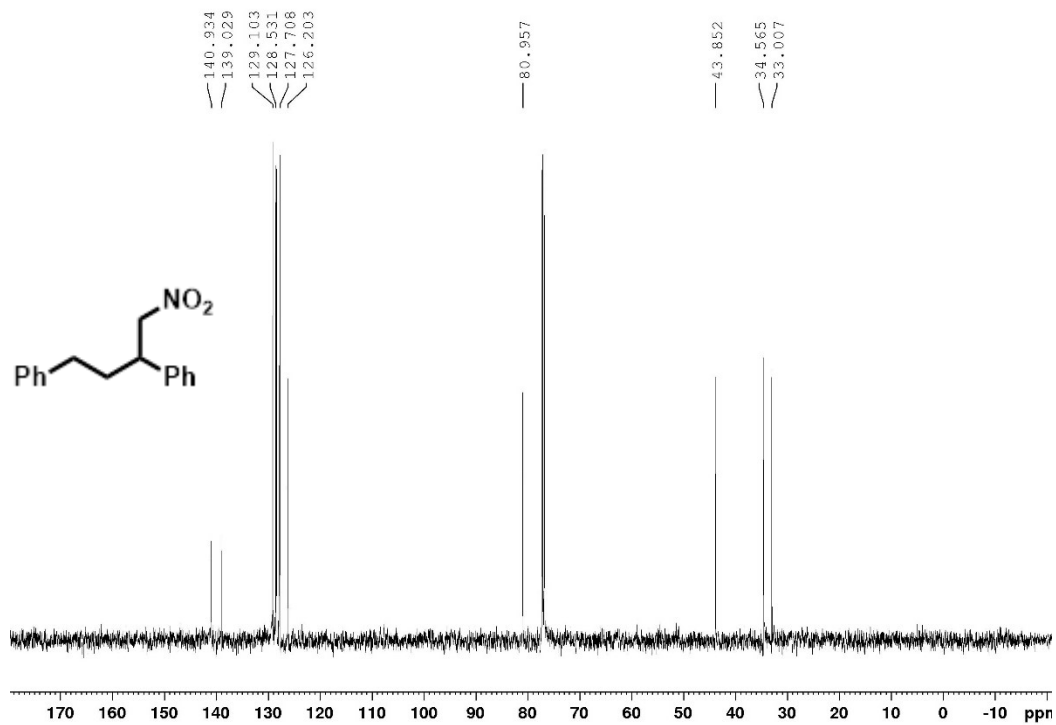
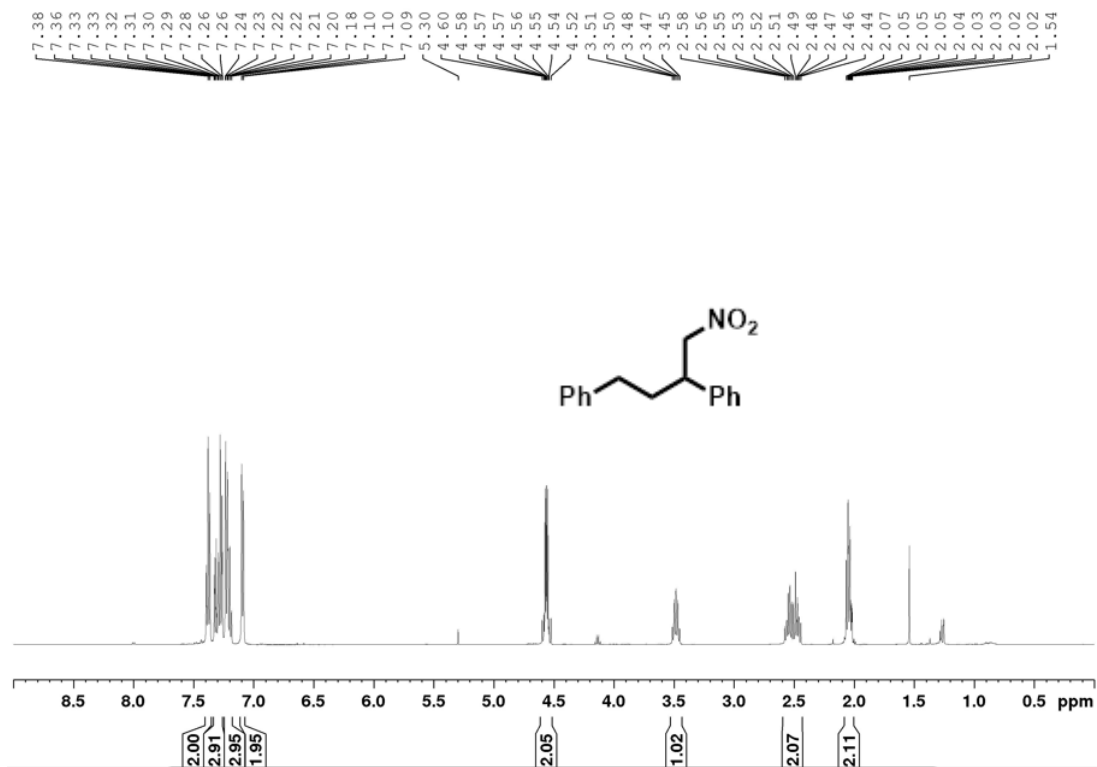
4-Oxo-2,4-diphenylbutanoic acid pentafluorophenyl ester, (3.31).



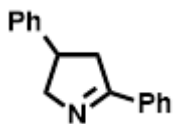
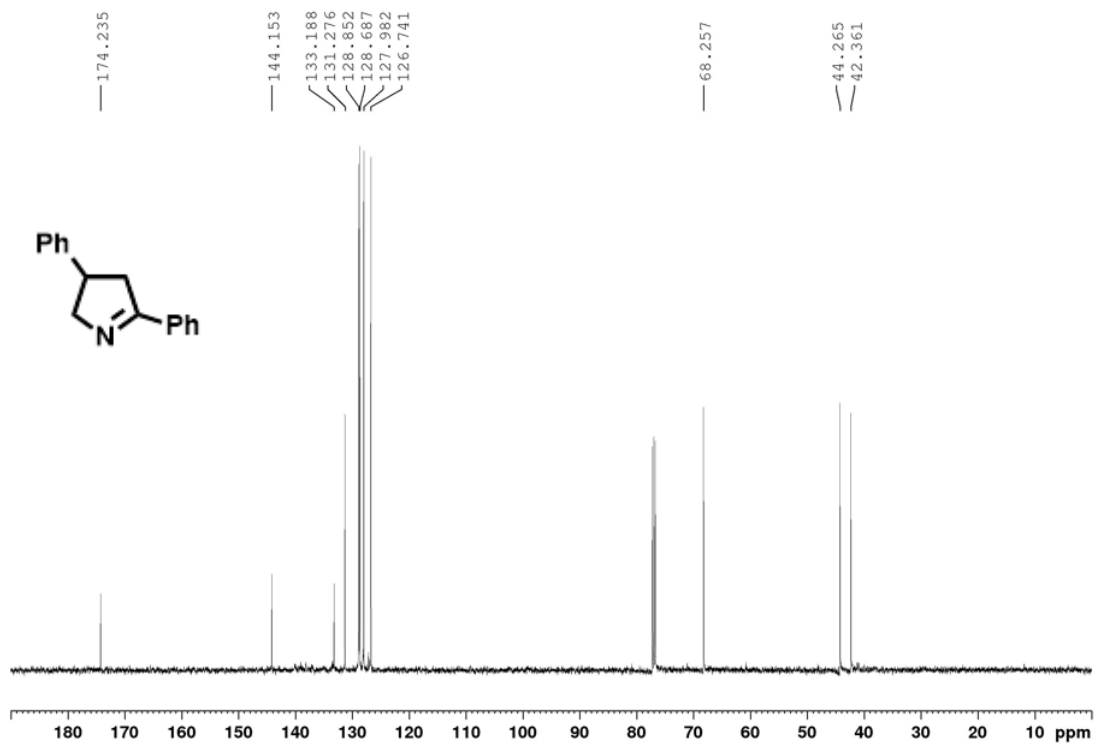
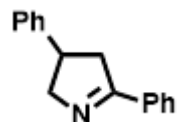
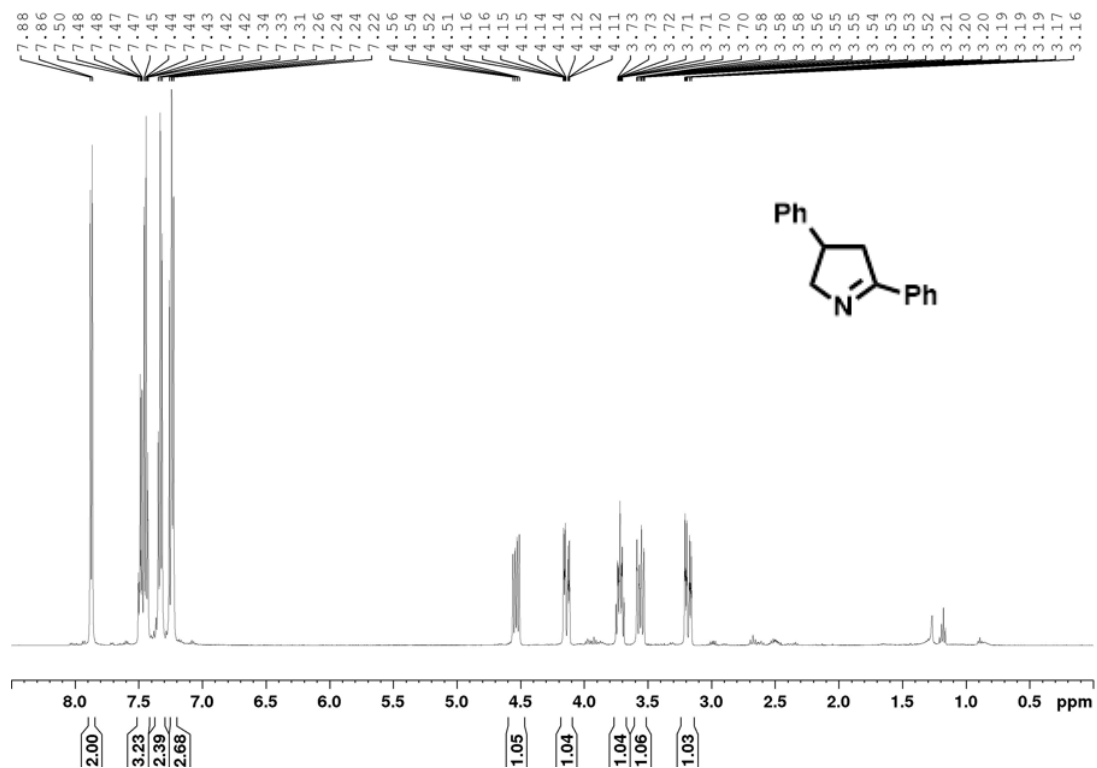
4-Nitro-1,3-diphenylbutan-1-ol, (3.32).



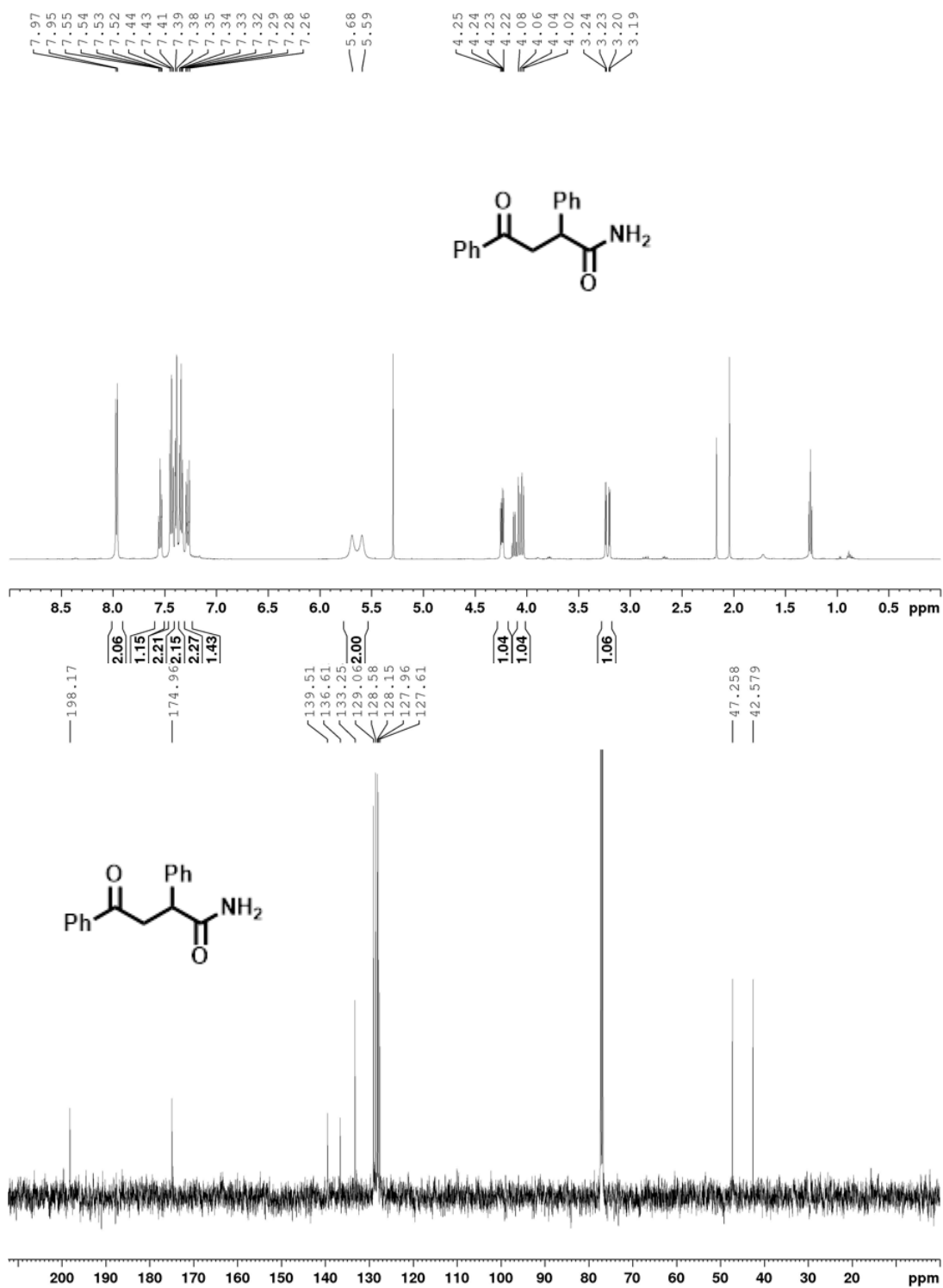
1,1'-(4-Nitrobutane-1,3-diyl)dibenzene, (3.33).



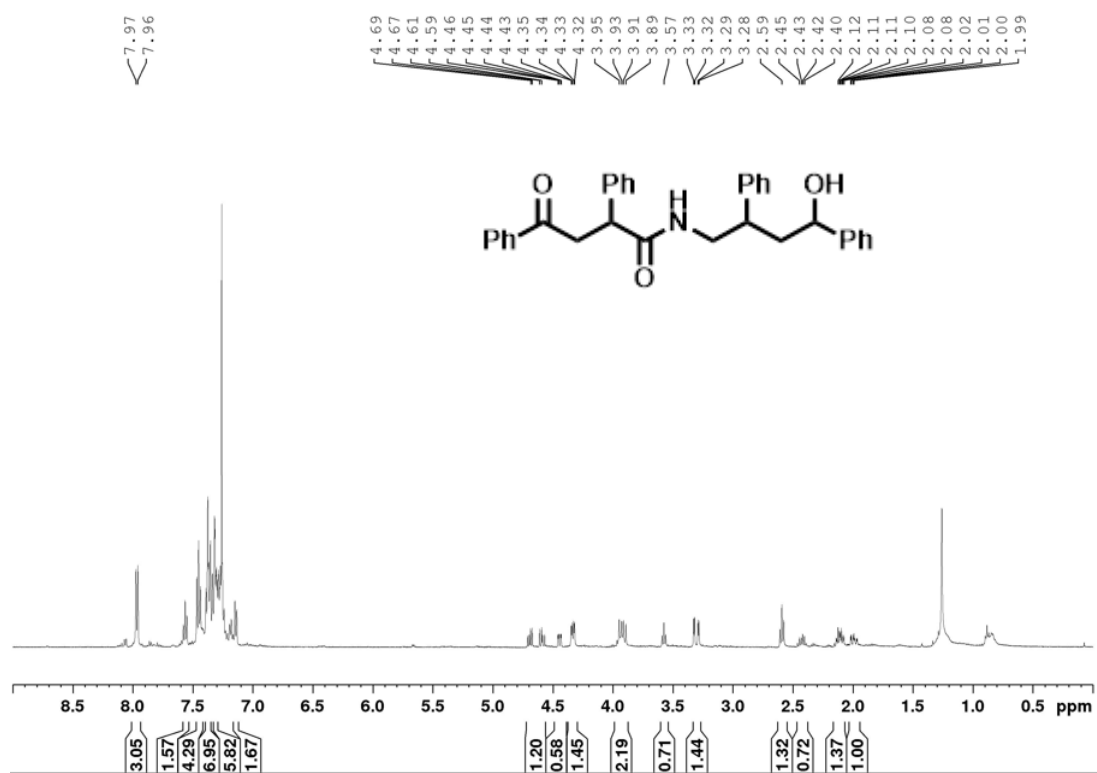
3,5-Diphenyl-3,4-dihydro-2H-pyrrole, (3.34).



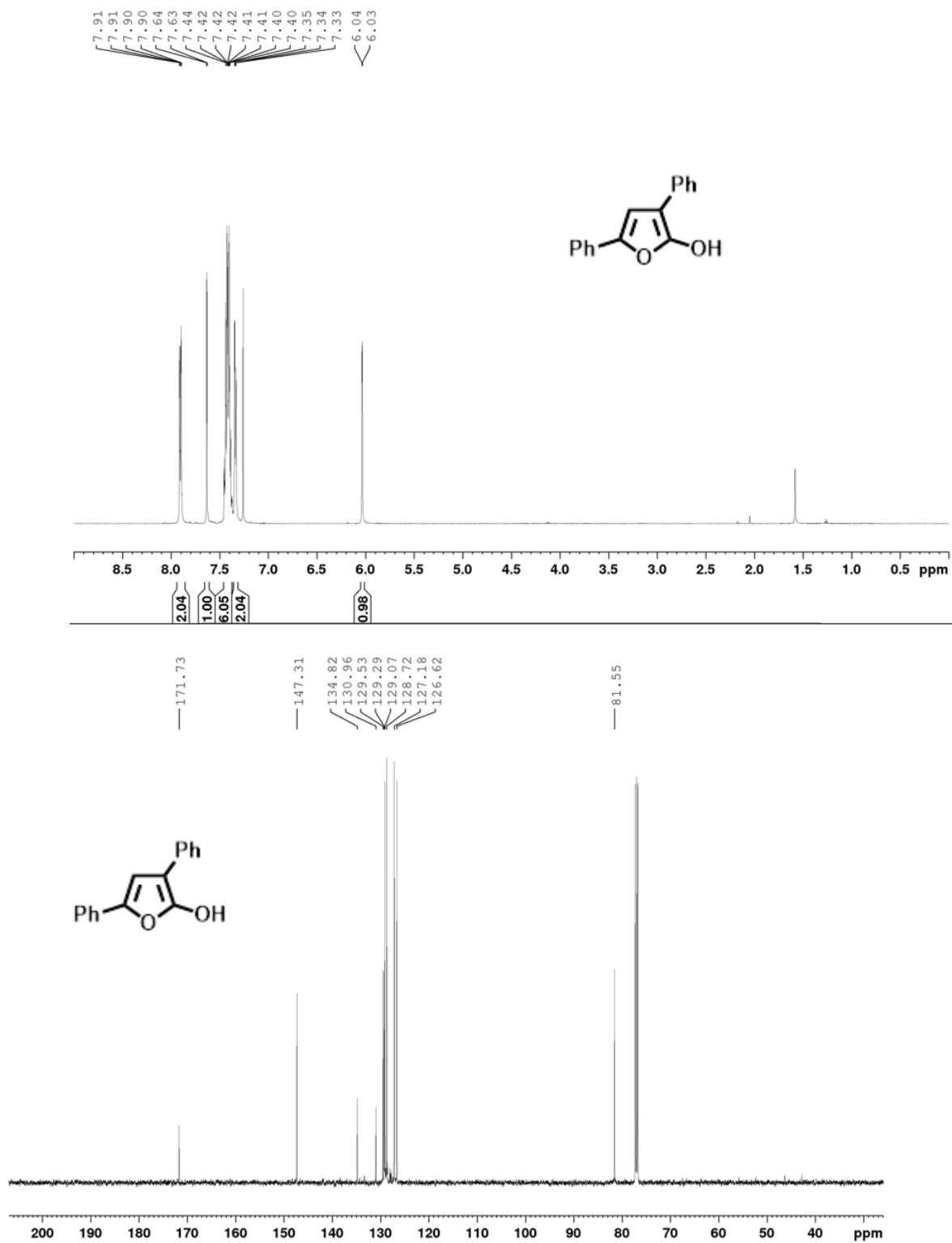
4-Oxo-2,4 diphenylbutanamide, (3.35).



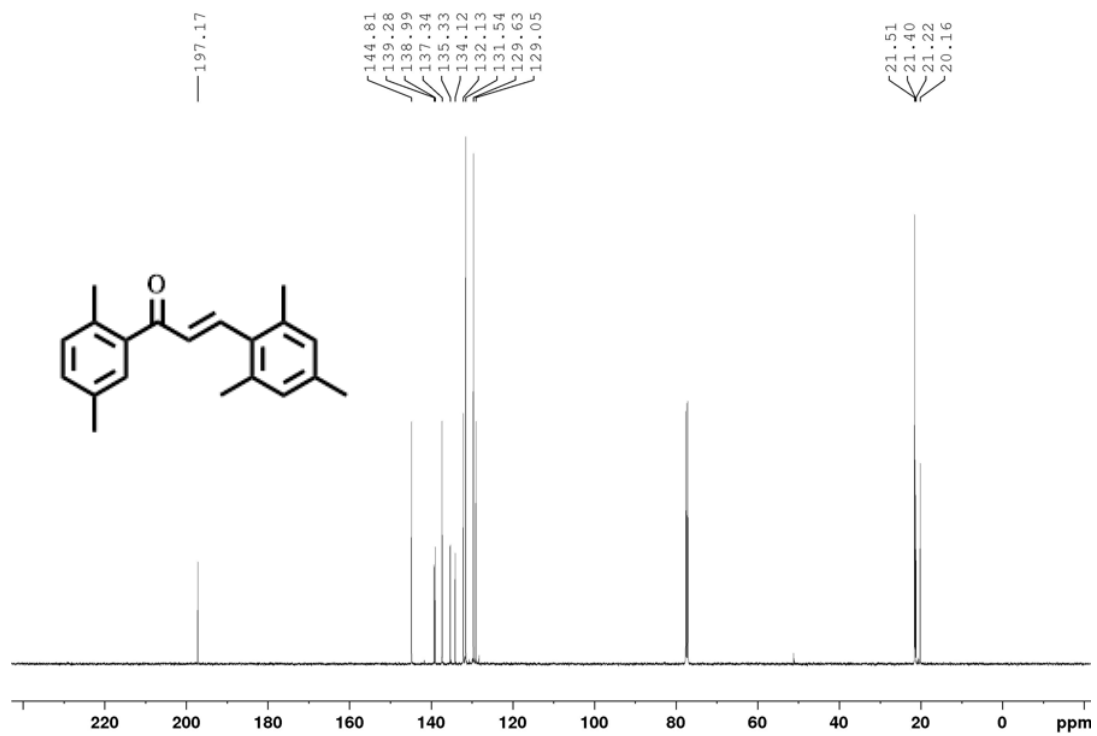
N-(2-hydroxy-4-phenylbutyl)-4-Oxo-2,4-diphenylbutanamide, (3.37).



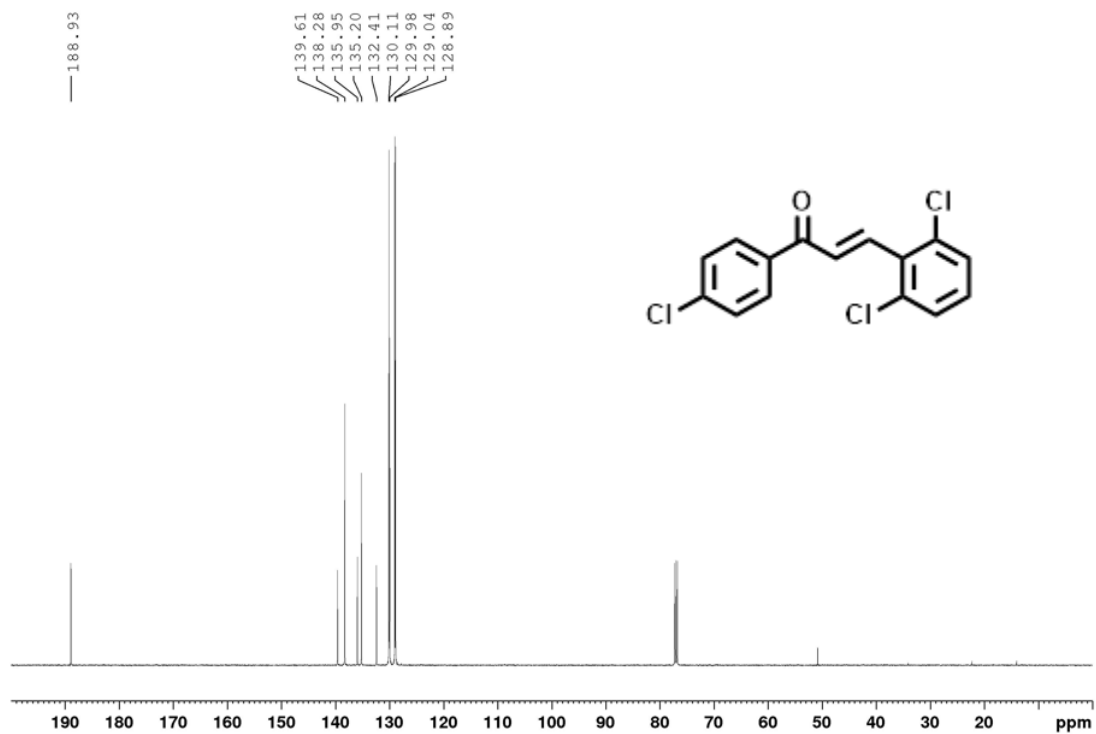
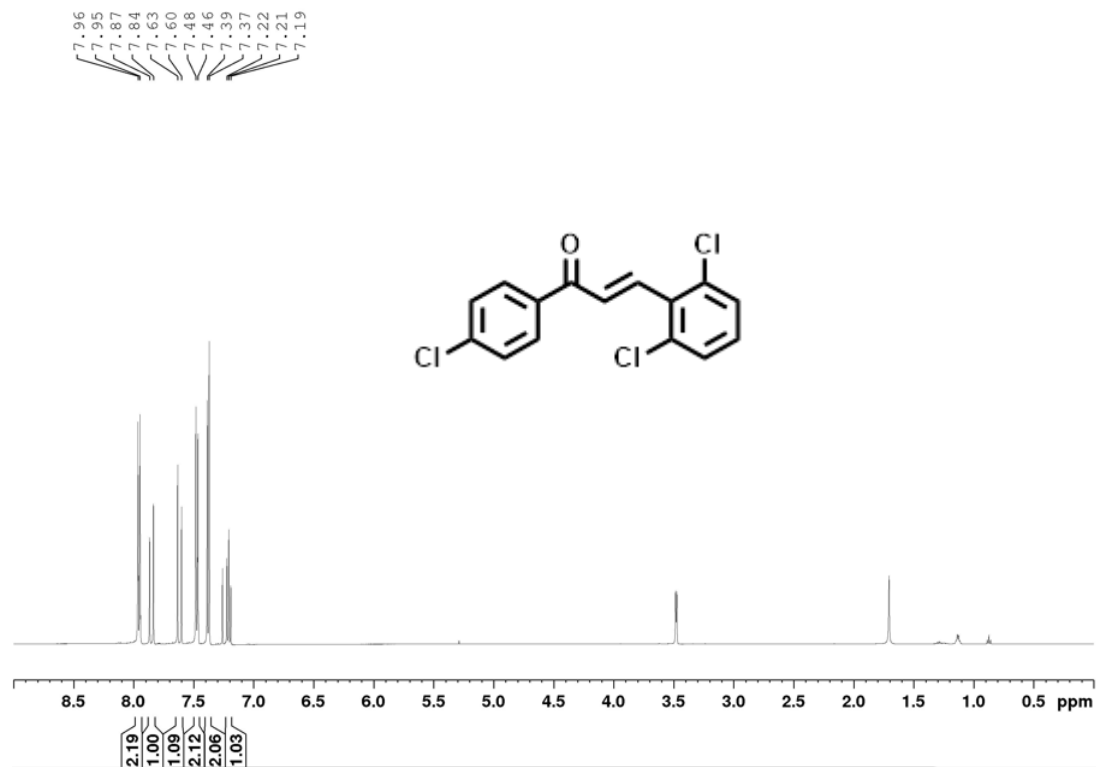
3,5-Diphenyl-2-furanol, (3.39).



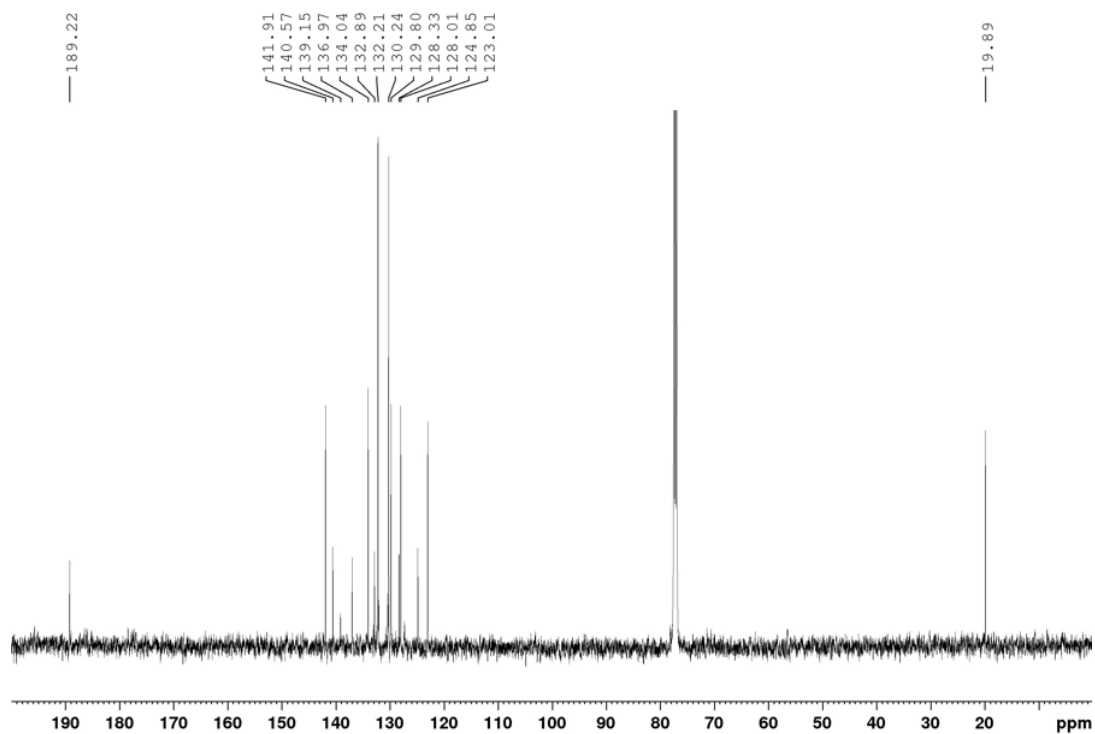
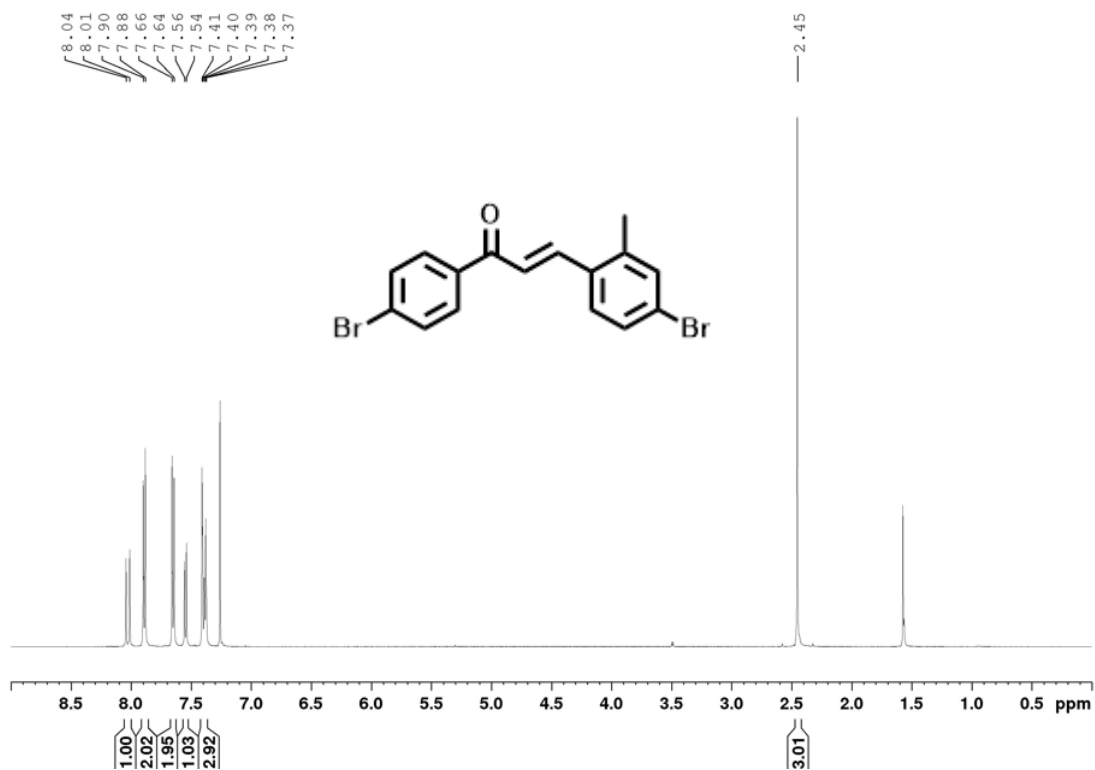
(2E)-1-(2,5-Dimethylphenyl)-3-(2,4,6-trimethylphenyl)prop-2-en-1-one, (4.42b)



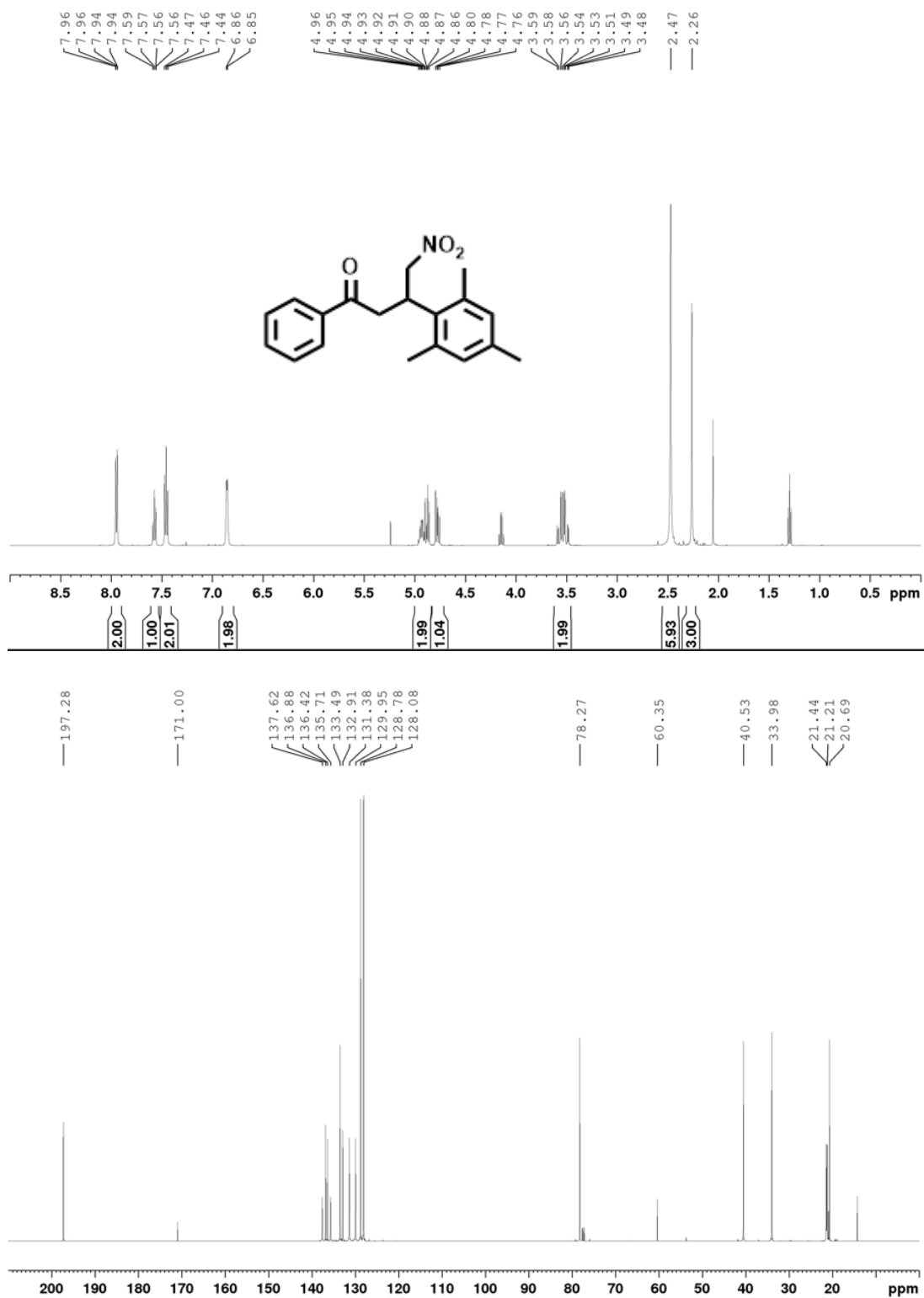
(2E)-1-(4-Chlorophenyl)-3-(2,6-dichlorophenyl)prop-2-en-1-one, (4.42c).



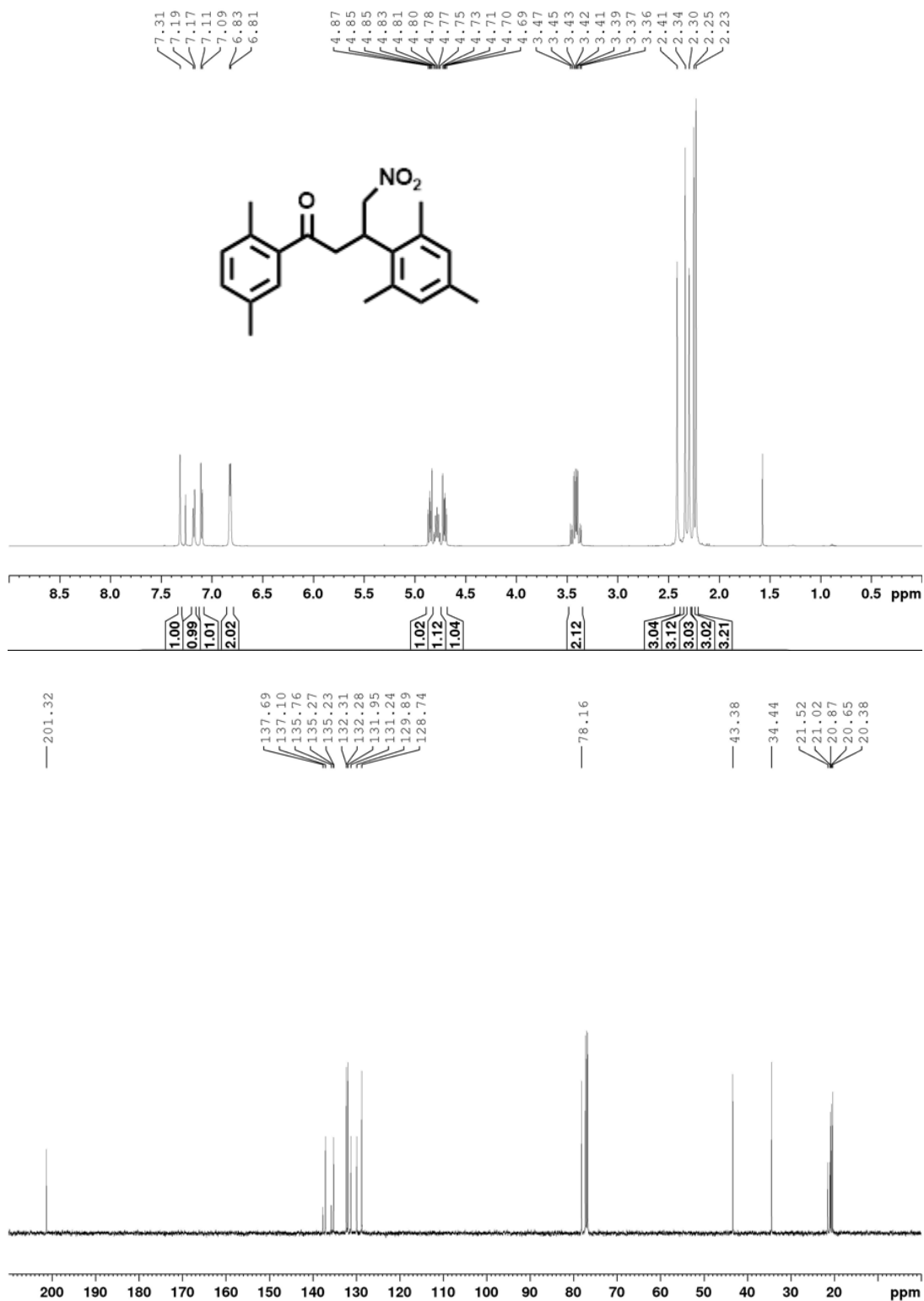
(2E)-3-(4-Bromo-2-methylphenyl)-1-(4-bromophenyl)prop-2-en-1-one, (4.42d)



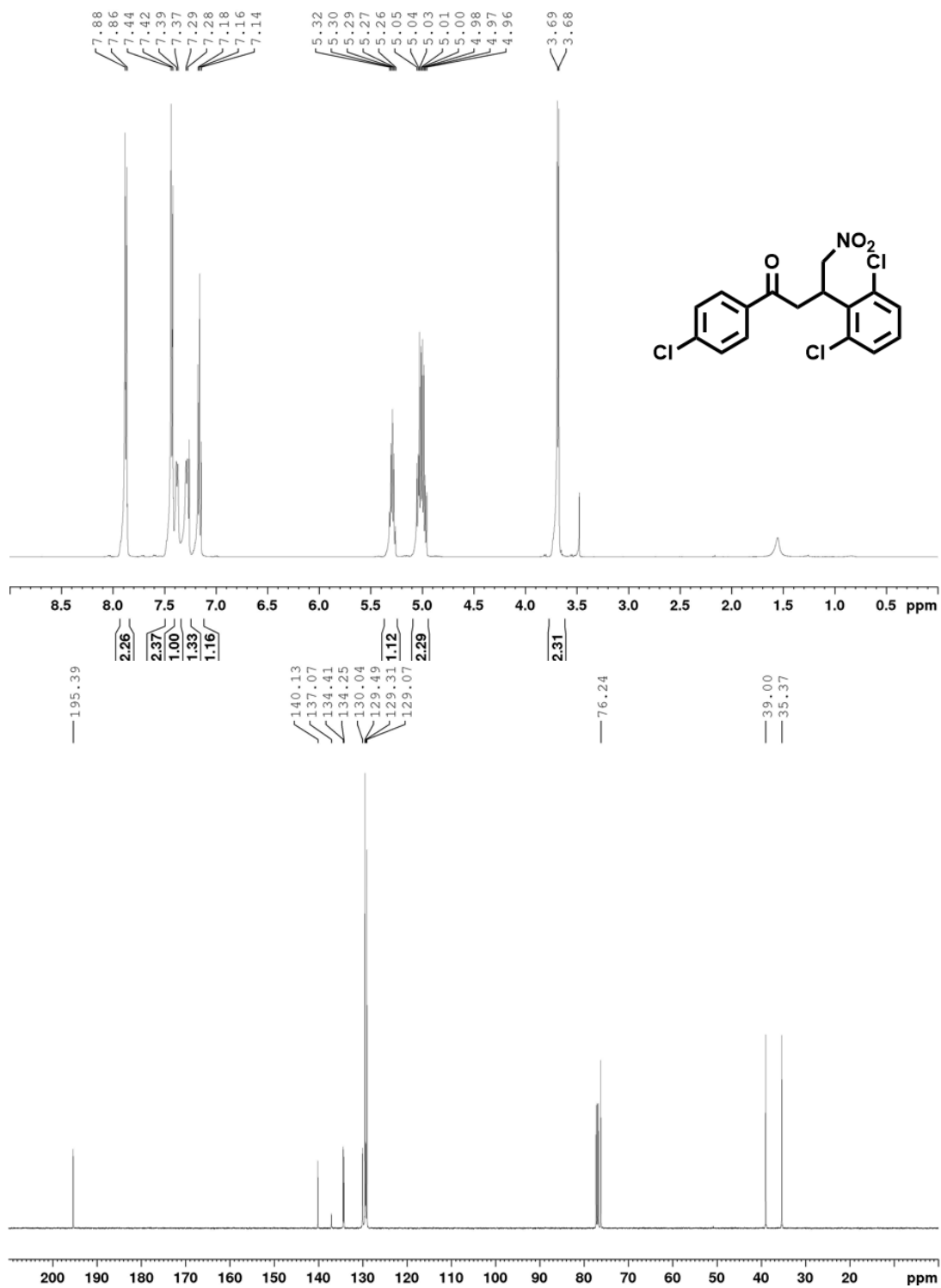
4-Nitro-1-phenyl-3-(2,4,6-trimethylphenyl)butan-1-one, (4.43a).



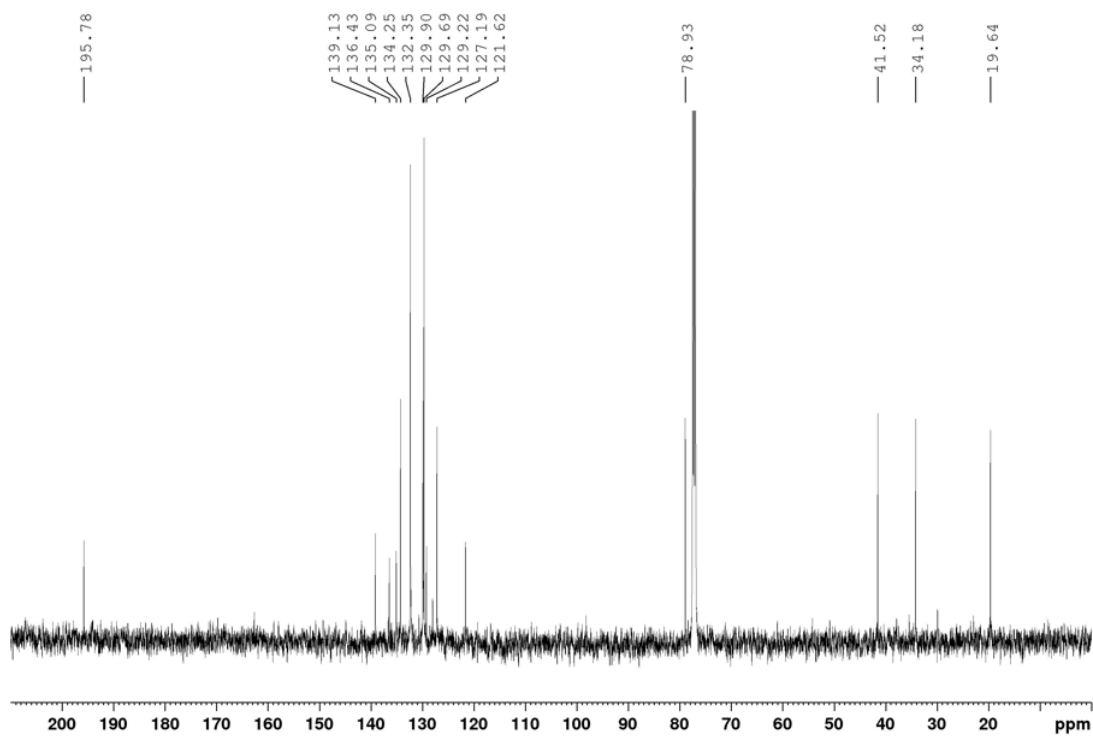
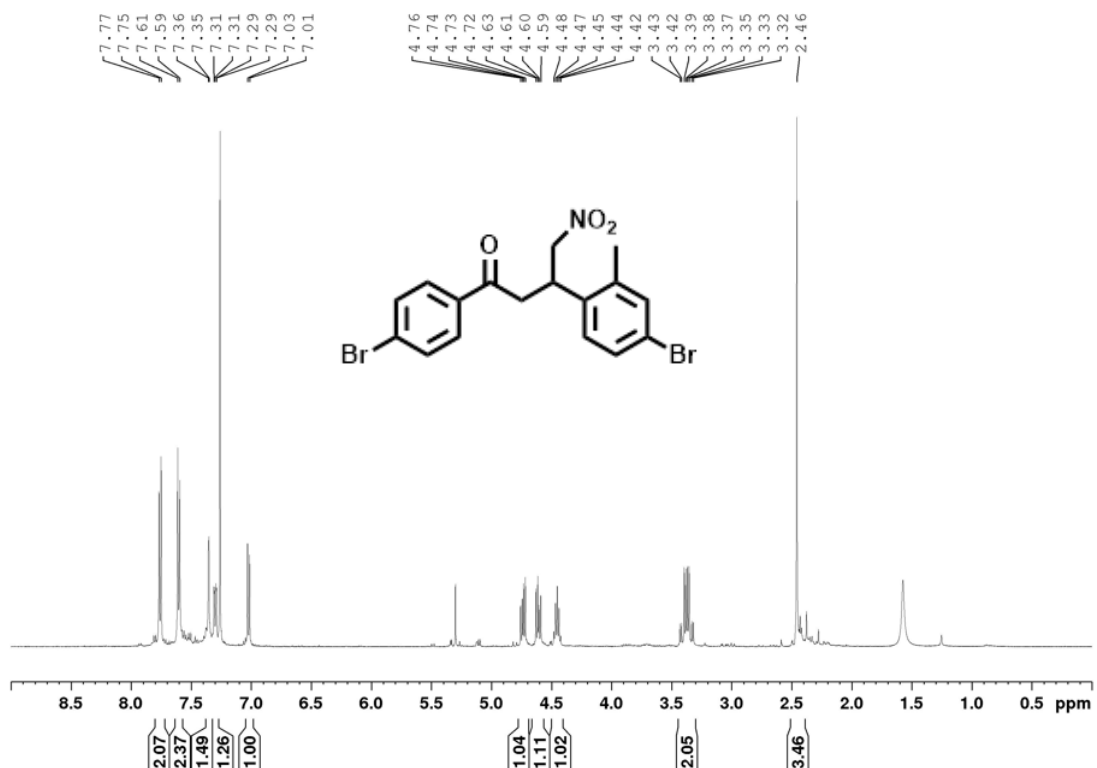
1-(2,5-Dimethylphenyl)-4-nitro-3-(2,4,6-trimethylphenyl)butan-1-one, (4.43b).



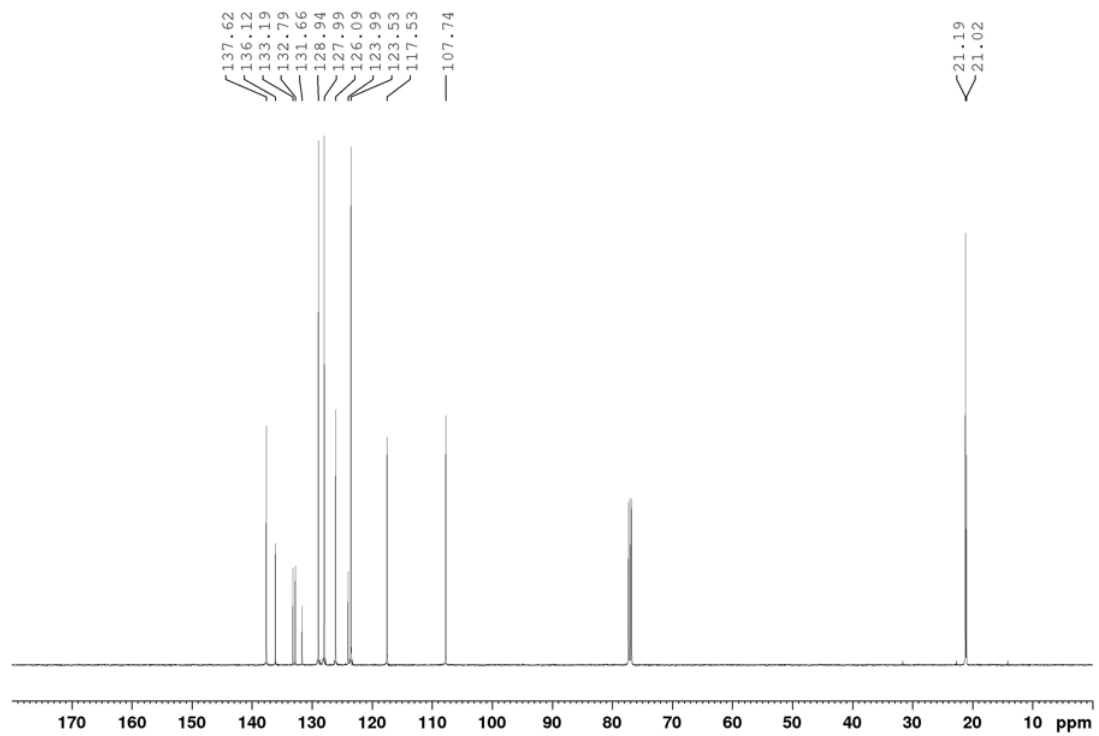
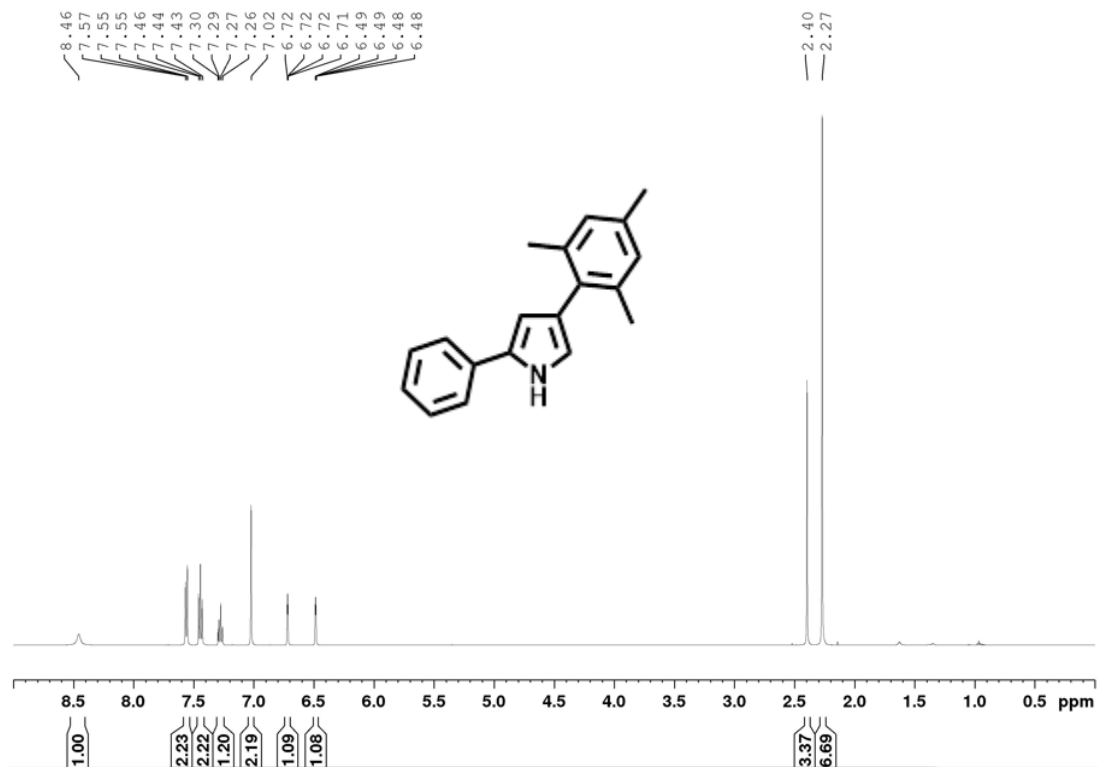
3-(2,6-Dichloro-phenyl)-4-nitro-1-(4-chloro-phenyl)-butan-1-one, (4.43c).



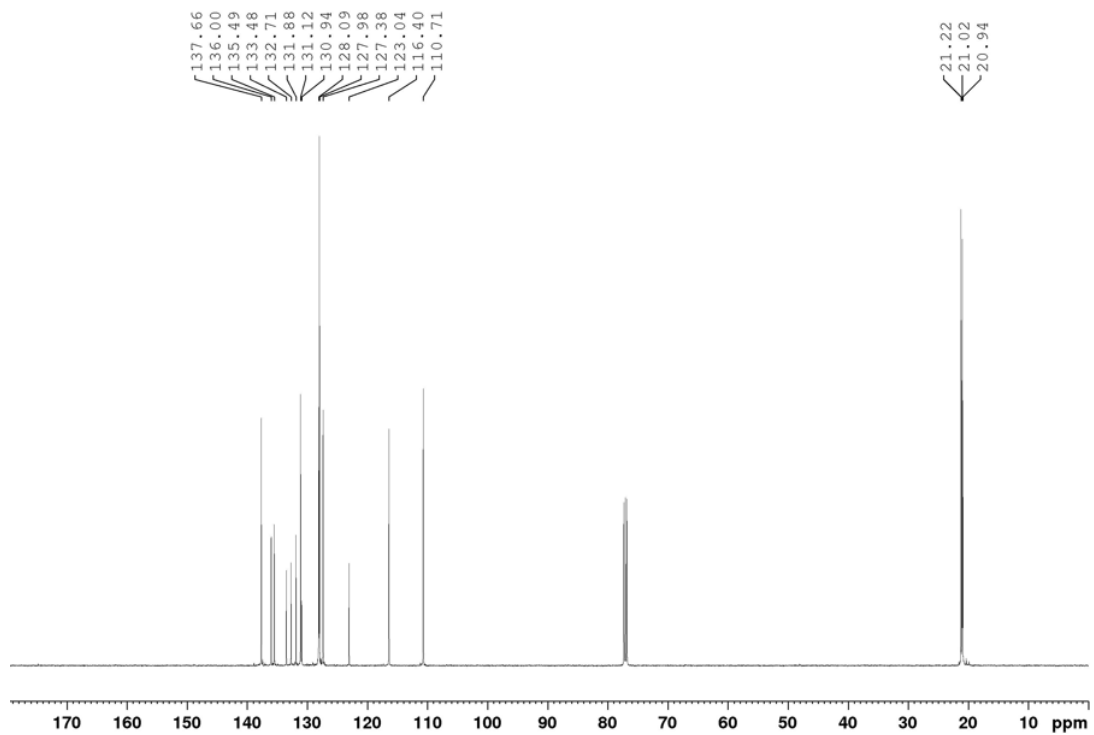
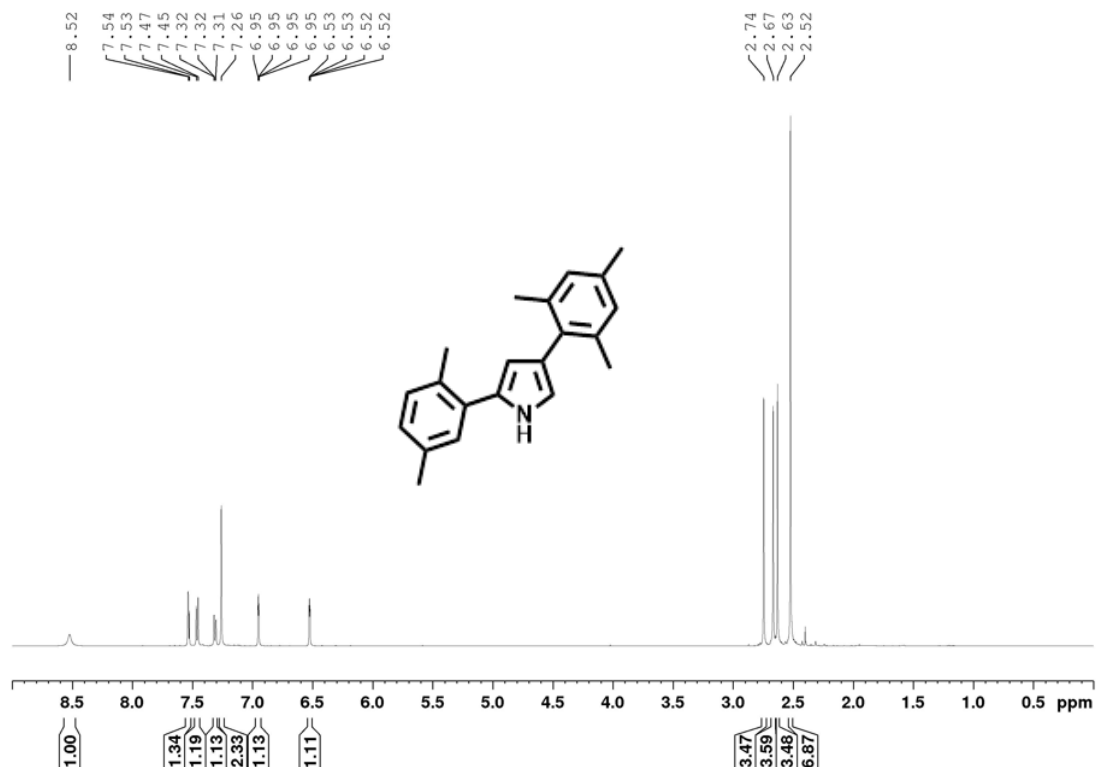
3-(2-Methyl-4-bromo-phenyl)-4-nitro-1-(4-bromo-phenyl)-butan-1-one, (4.43d).



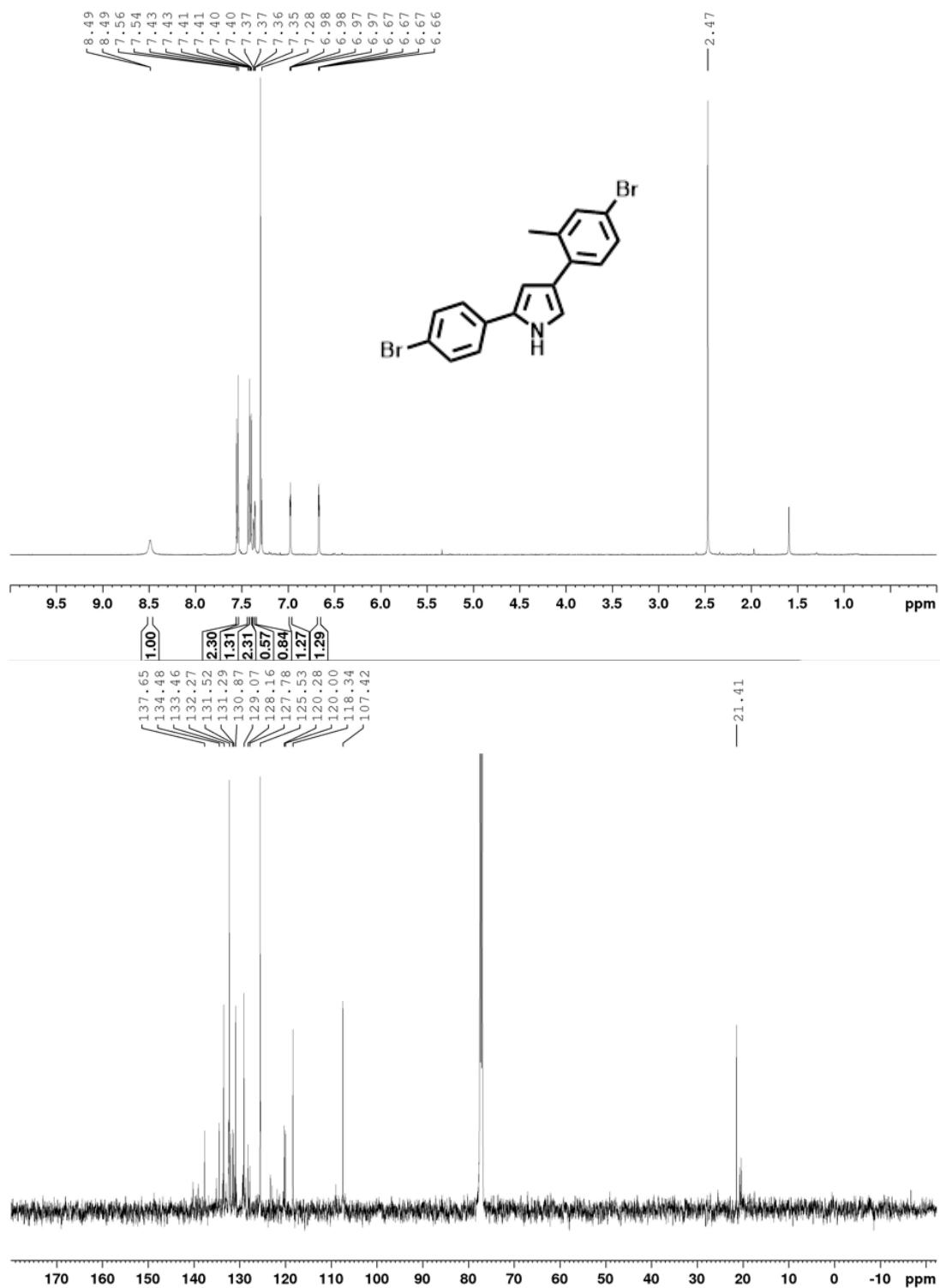
2-Phenyl-4-(2,4,6-trimethylphenyl)-1H-pyrrole, (4.44a).



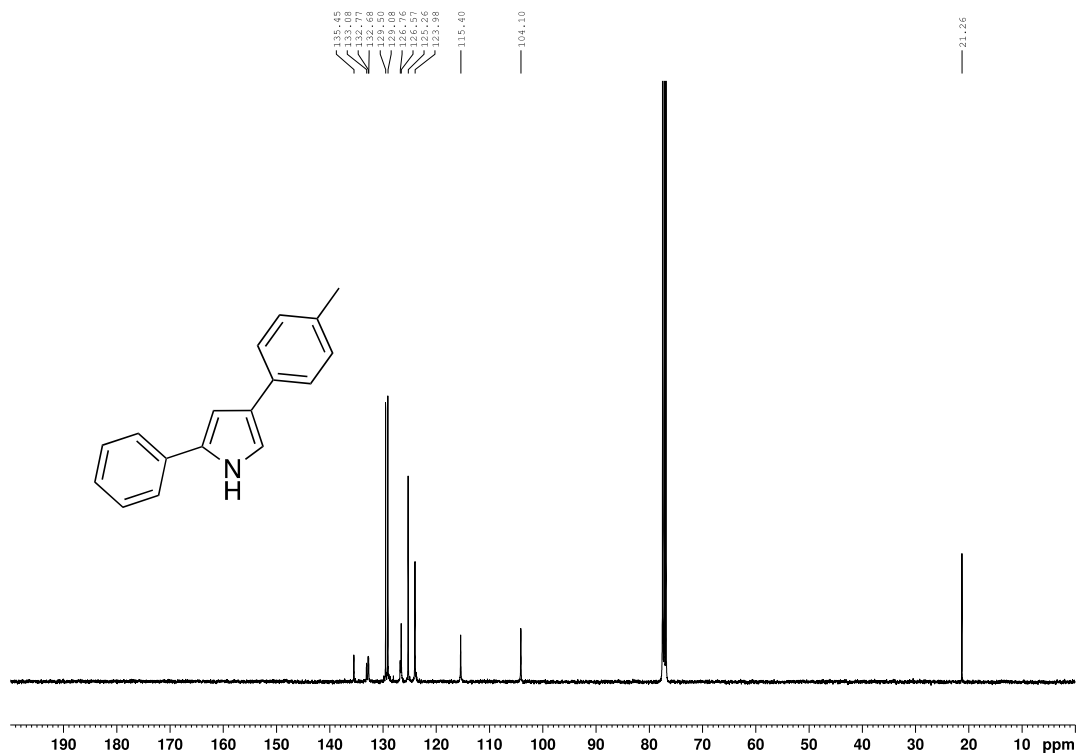
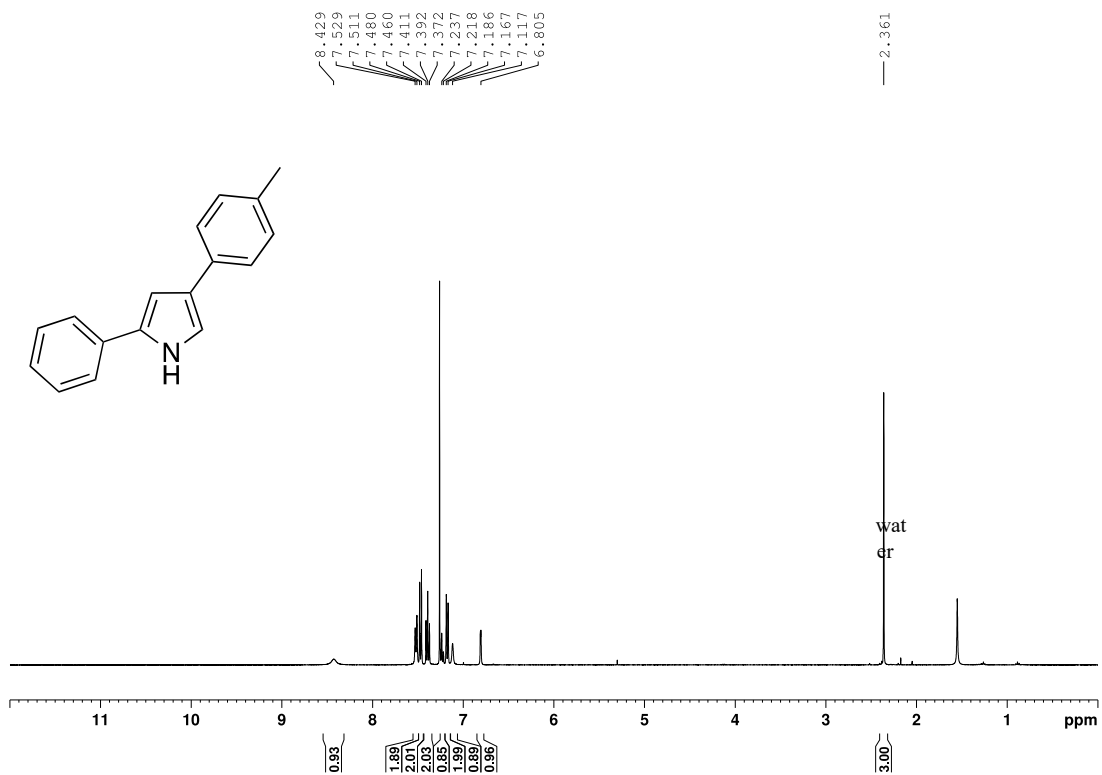
2-(2,5-Dimethylphenyl)-4-(2,4,6-trimethylphenyl)-1H-pyrrole, (4.44b).



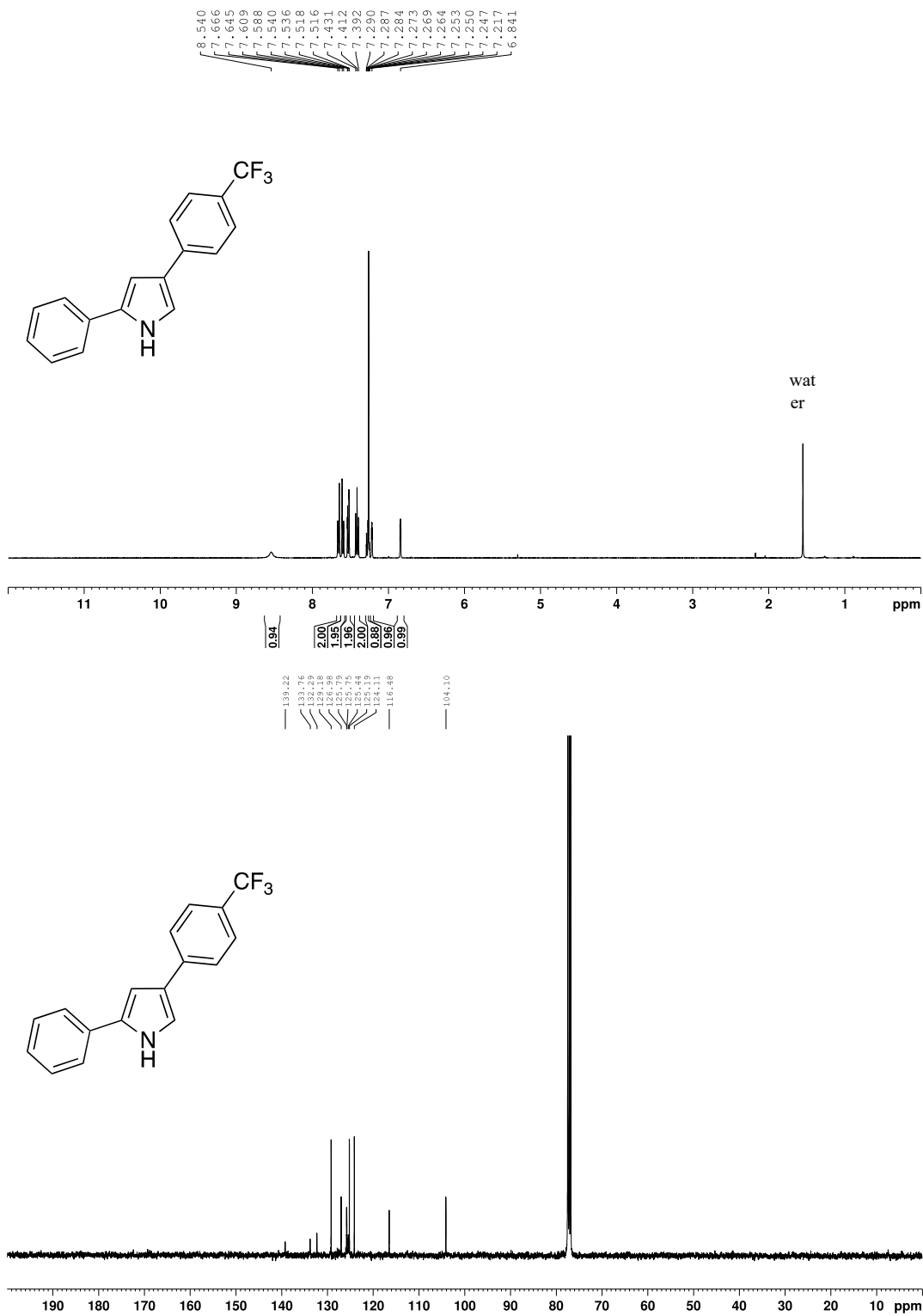
4-(4-Bromo-2-methylphenyl)-2-(4-bromophenyl)-1H-pyrrole, (4.44d).



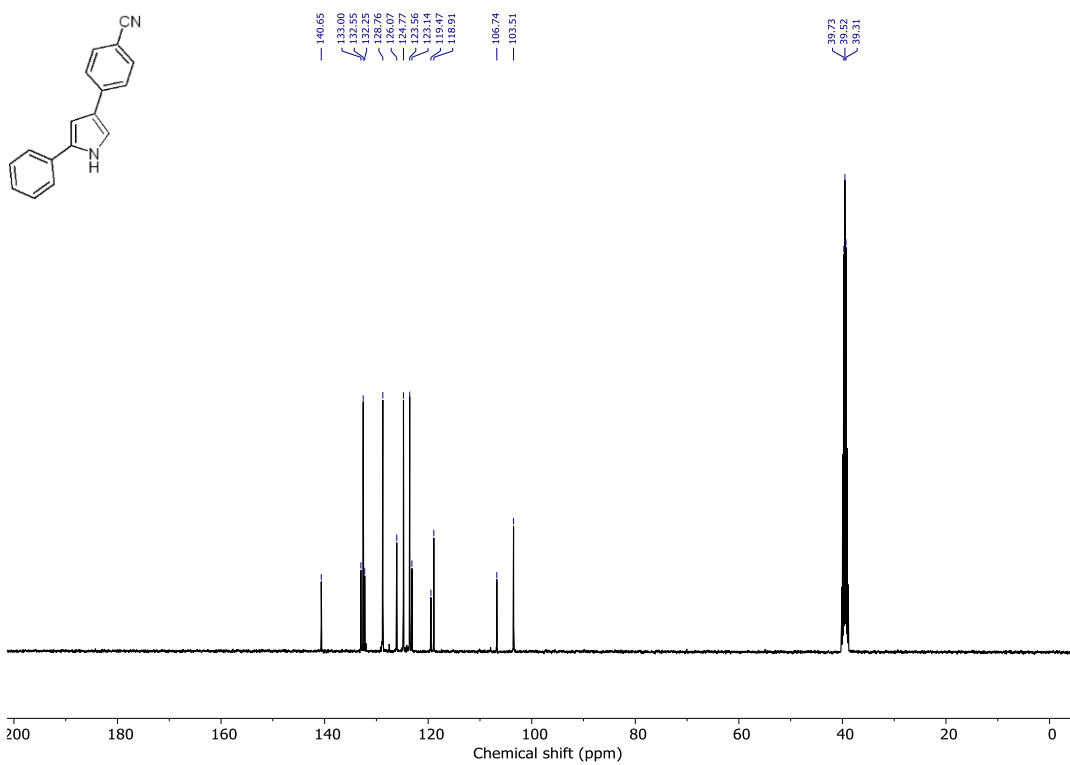
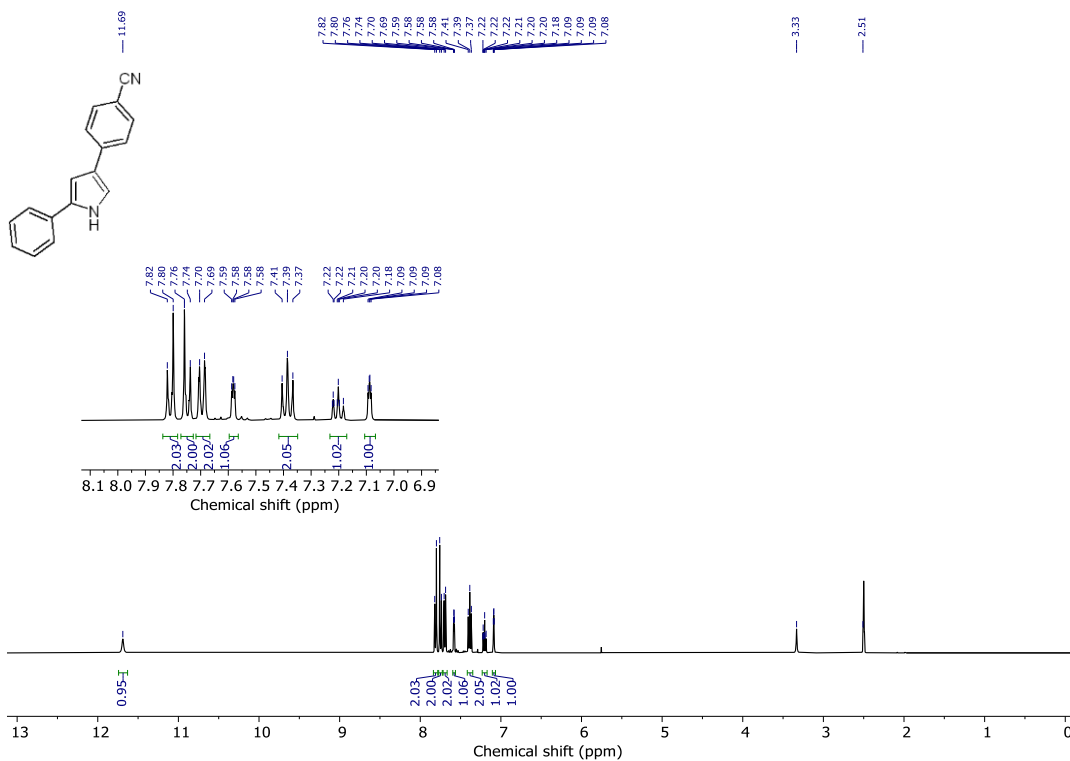
4-(4-Methylphenyl)-2-phenyl-1H-pyrrole, (4.44e).



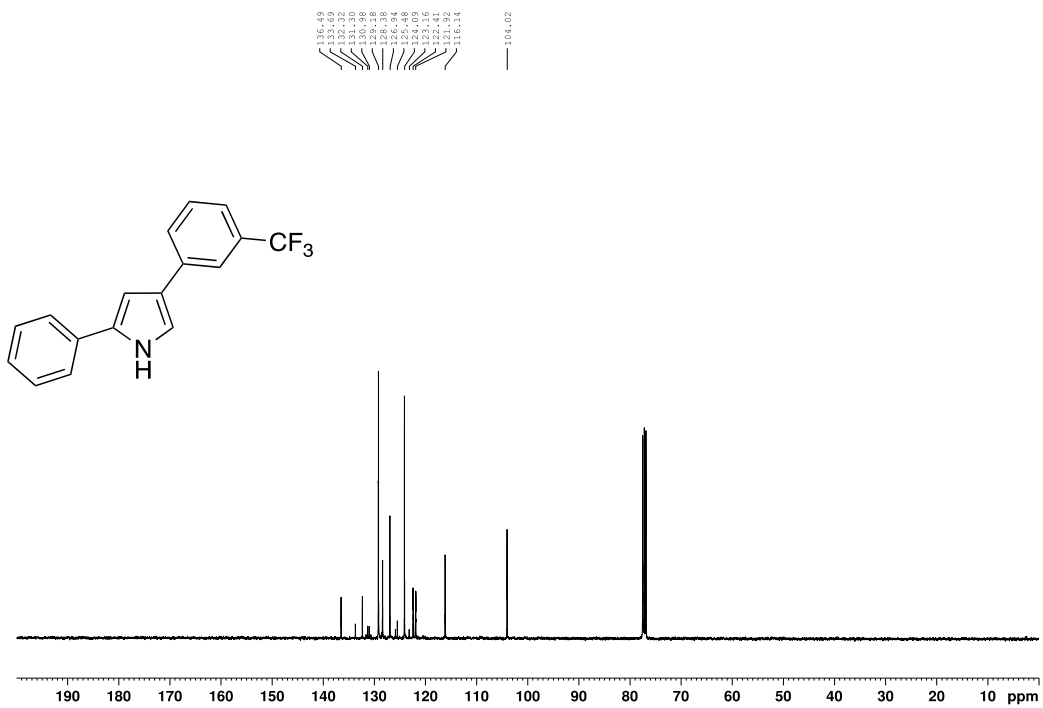
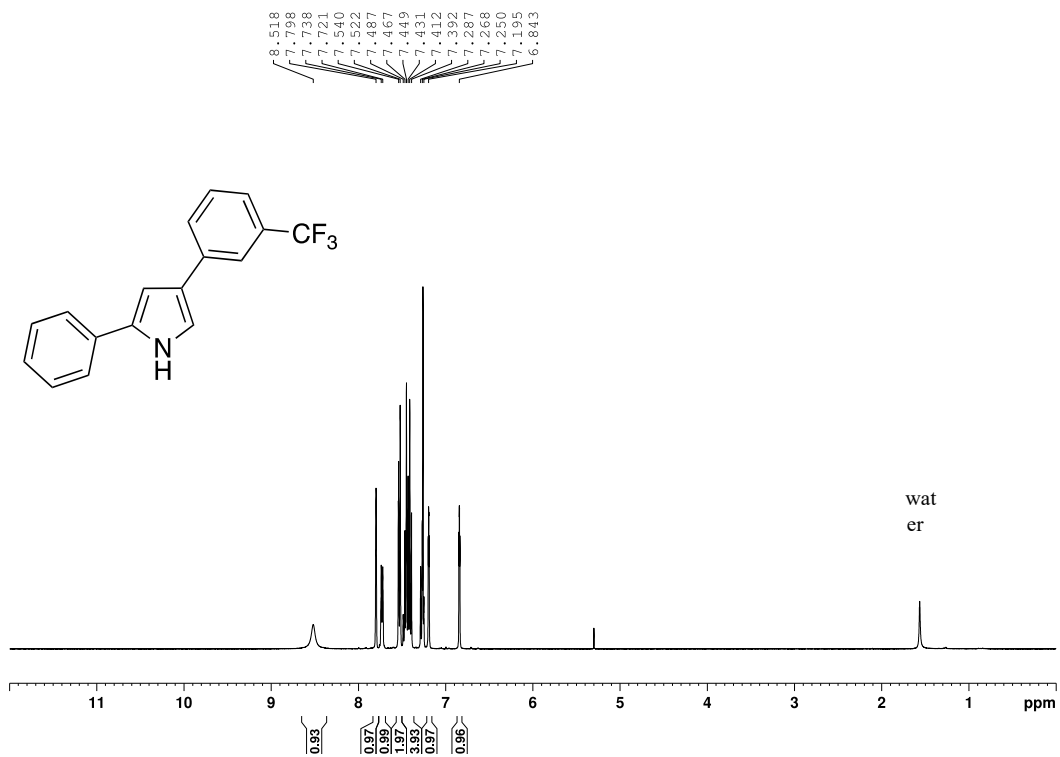
2-Phenyl-4-[4-(trifluoromethyl)phenyl]-1H-pyrrole, (4.44f).



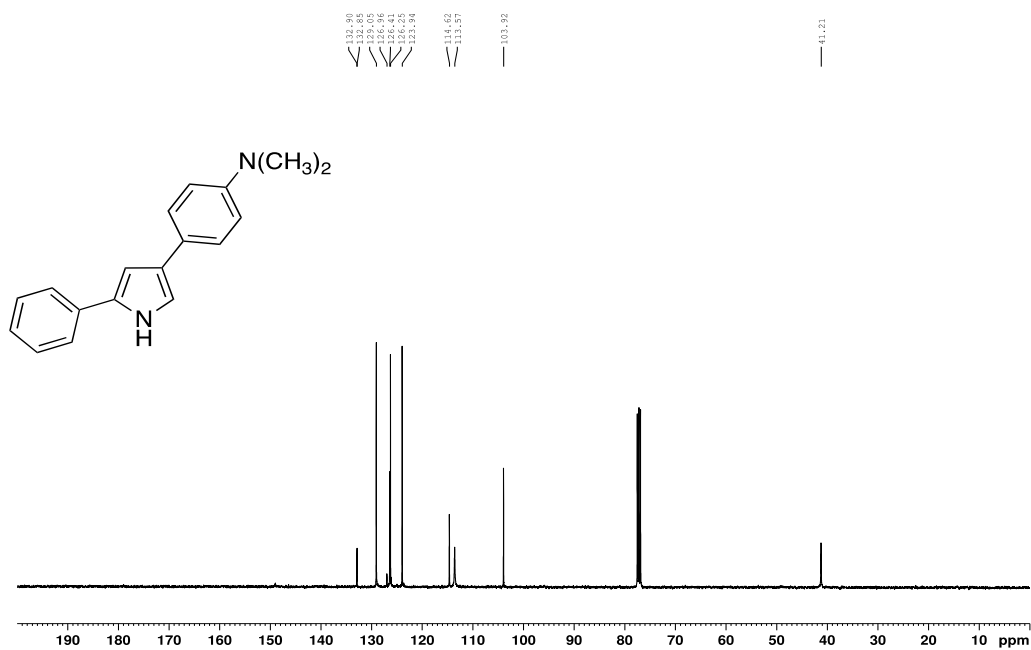
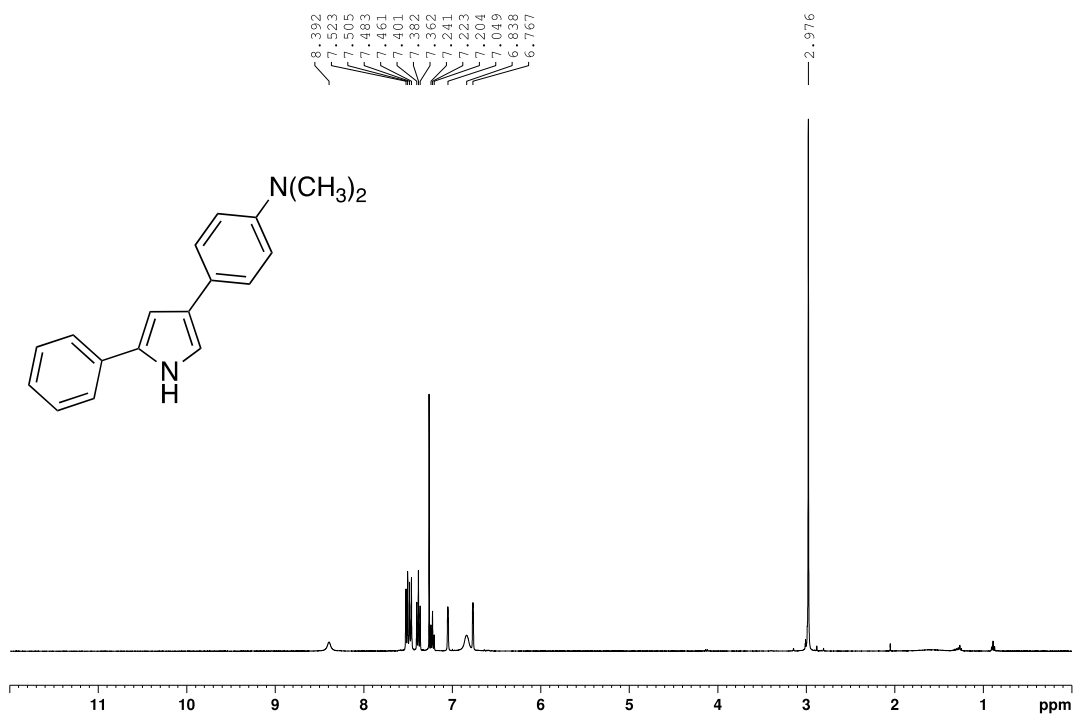
4-(4-Cyanophenyl)-2-phenyl-1H-pyrrole (4.44g).



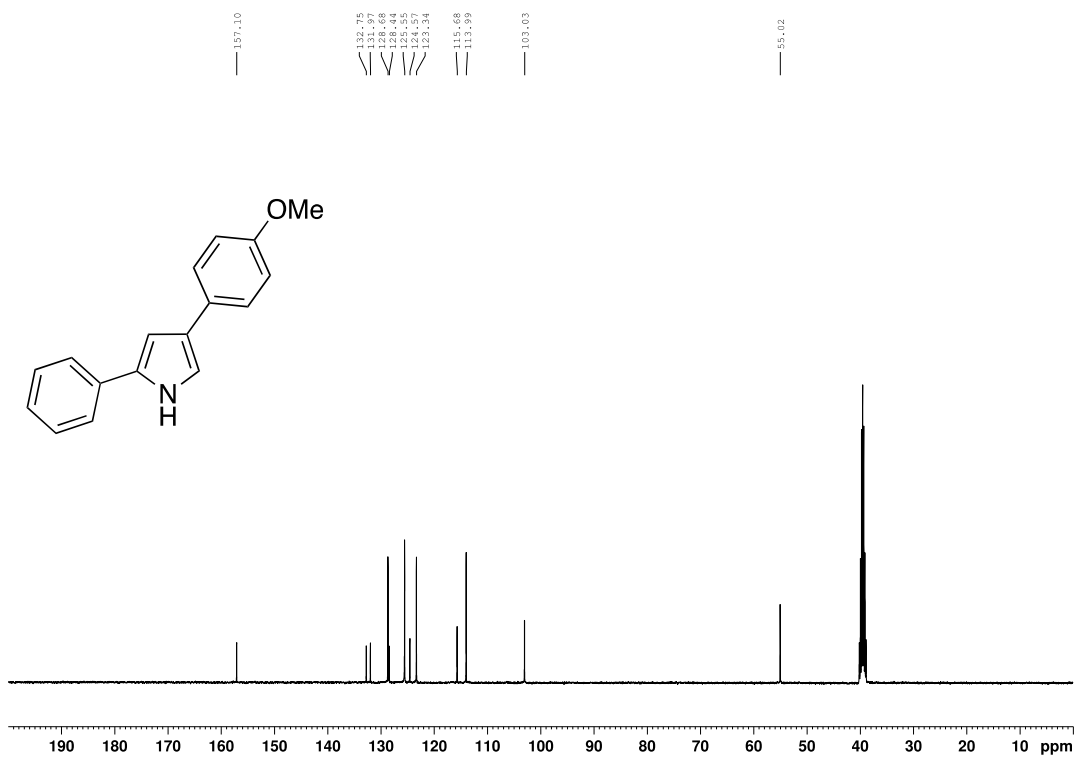
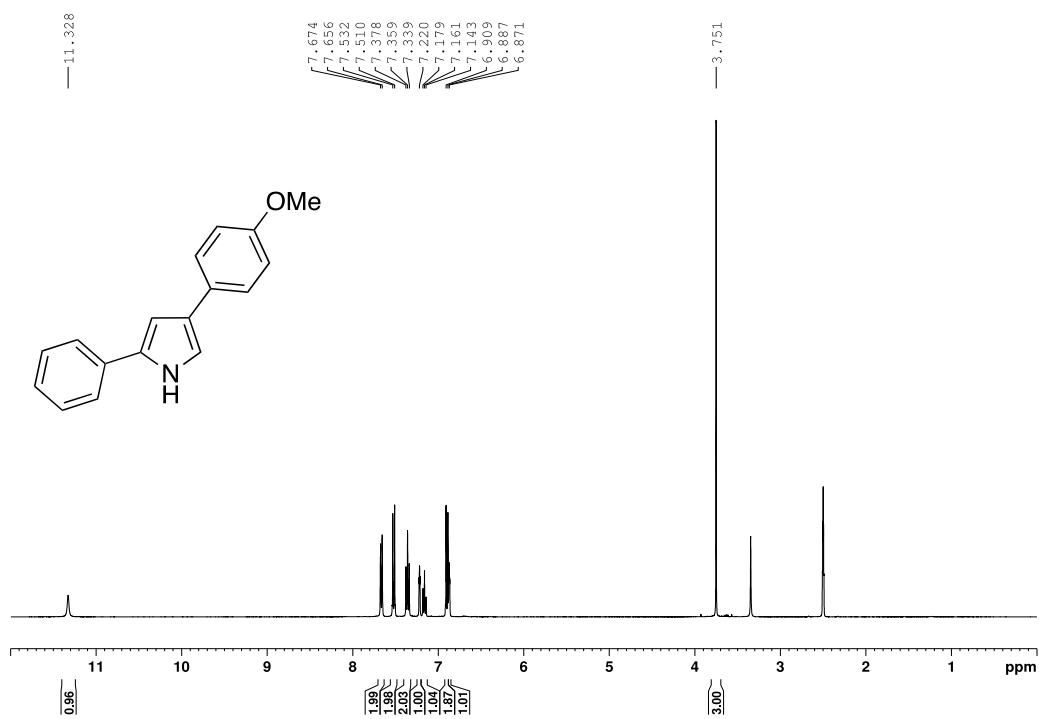
2-Phenyl-4-[3-(trifluoromethyl)phenyl]-1H-pyrrole, (4.44h).



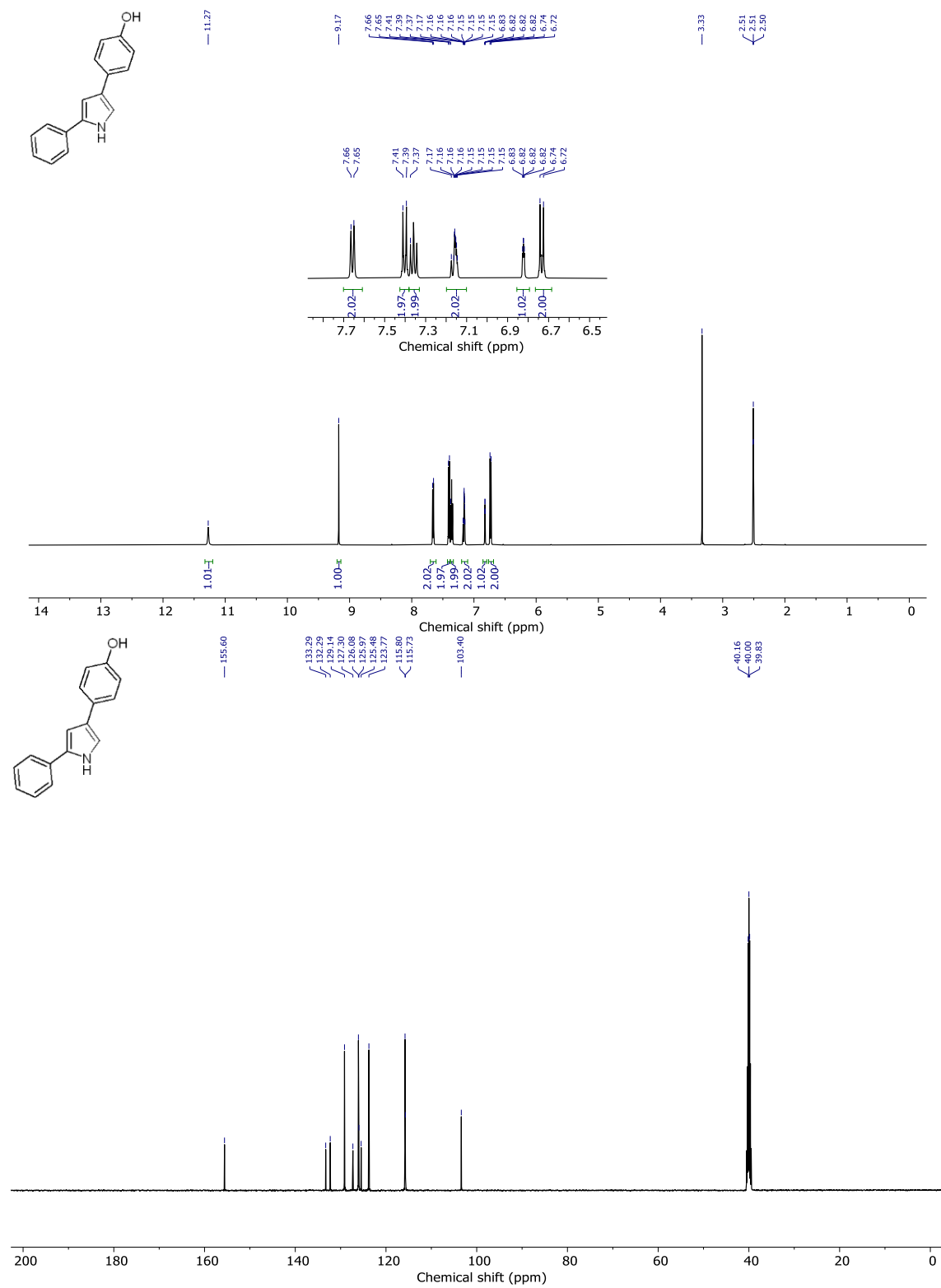
N,N-Dimethyl-4-(5-phenyl-1H-pyrrol-3-yl)benzenamine, (4.44i).



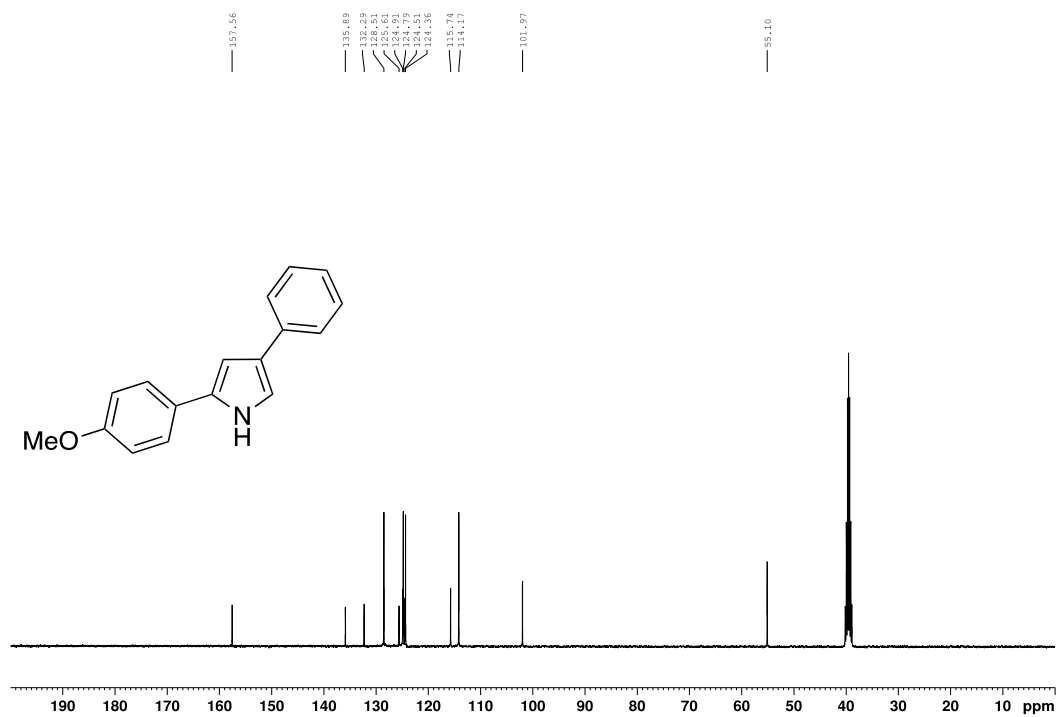
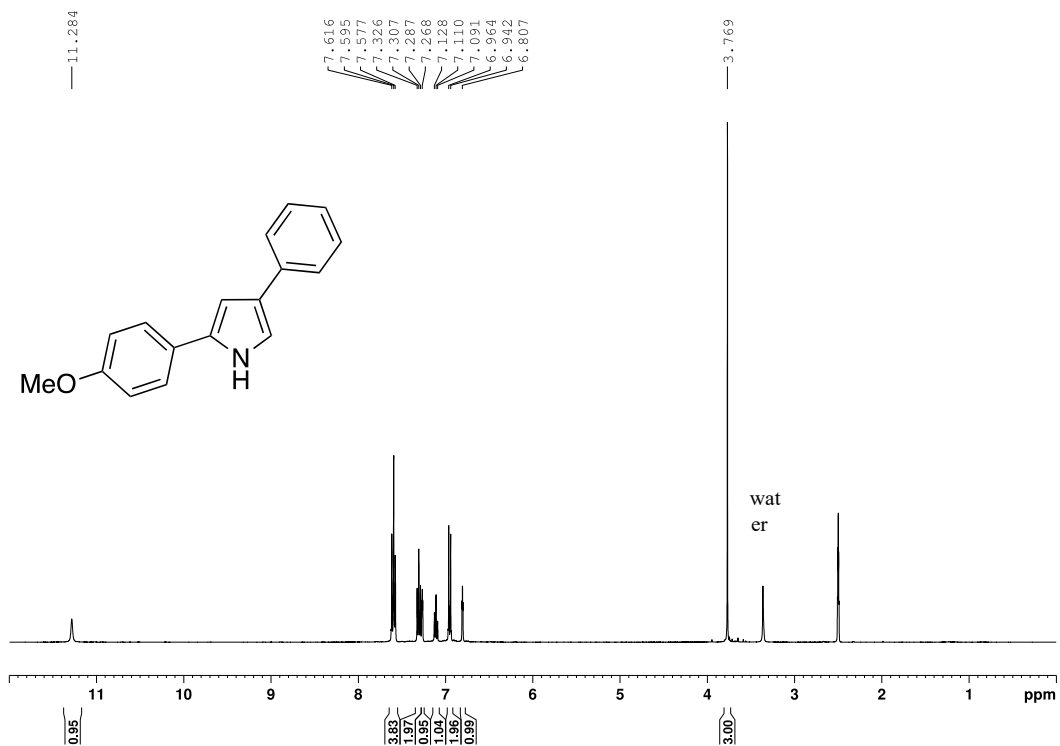
4-(4-Methoxyphenyl)-2-phenyl-1H-pyrrole, (4.44j).



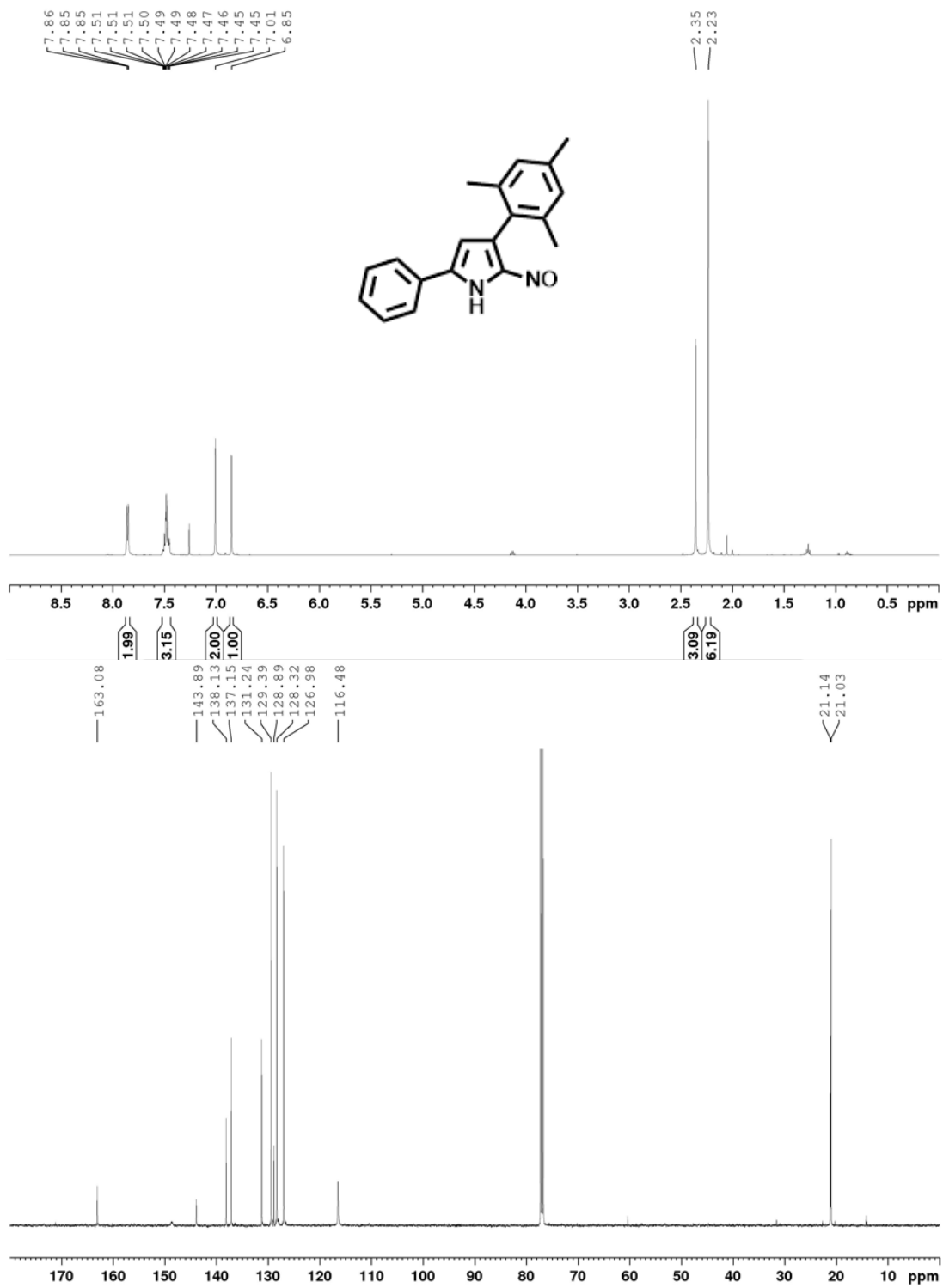
4-(4-Hydroxyphenyl)-2-phenyl-1H-pyrrole, (4.44l).



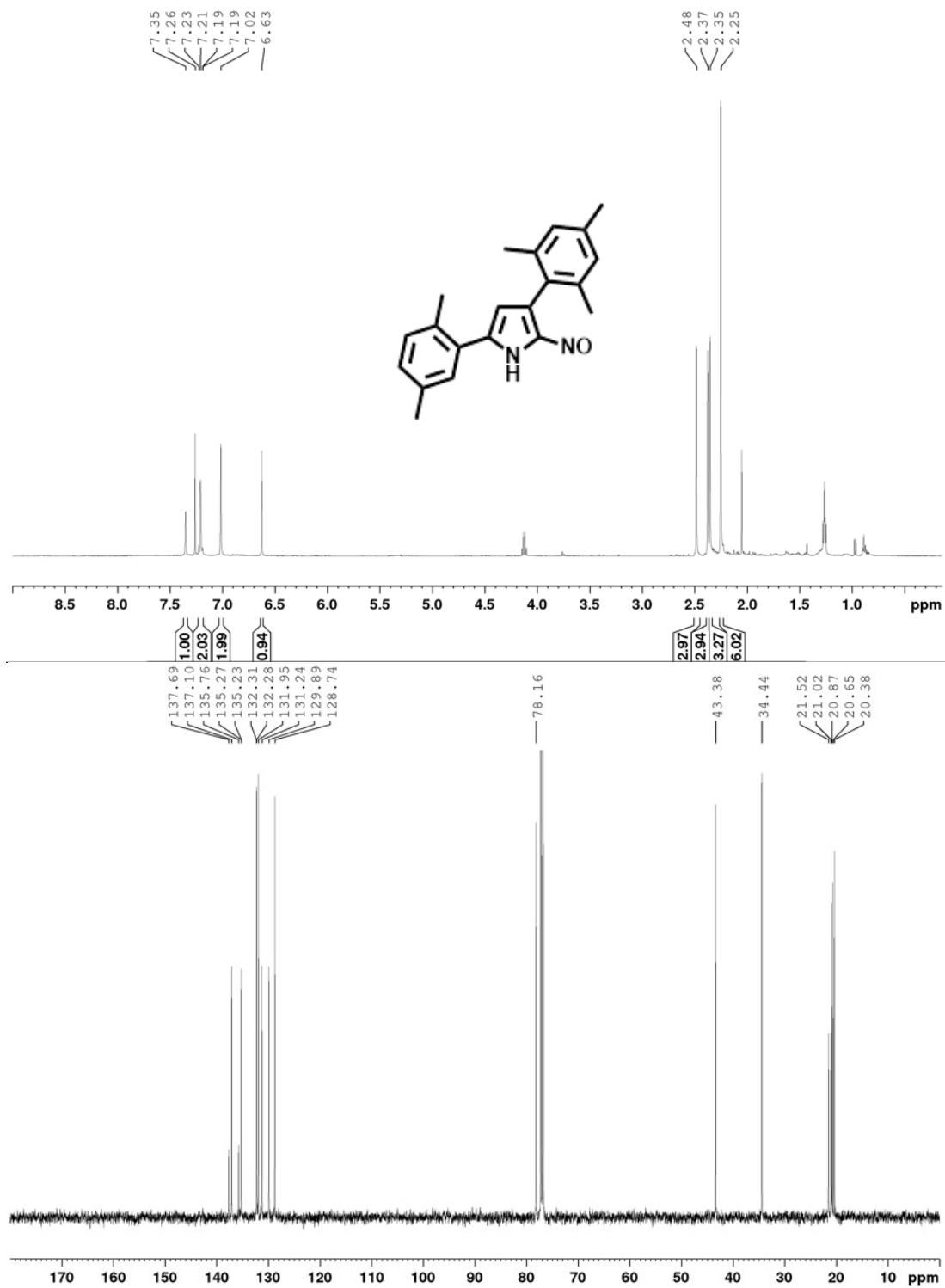
2-(4-Methoxyphenyl)-4-phenyl-1H-pyrrole, (4.44m).



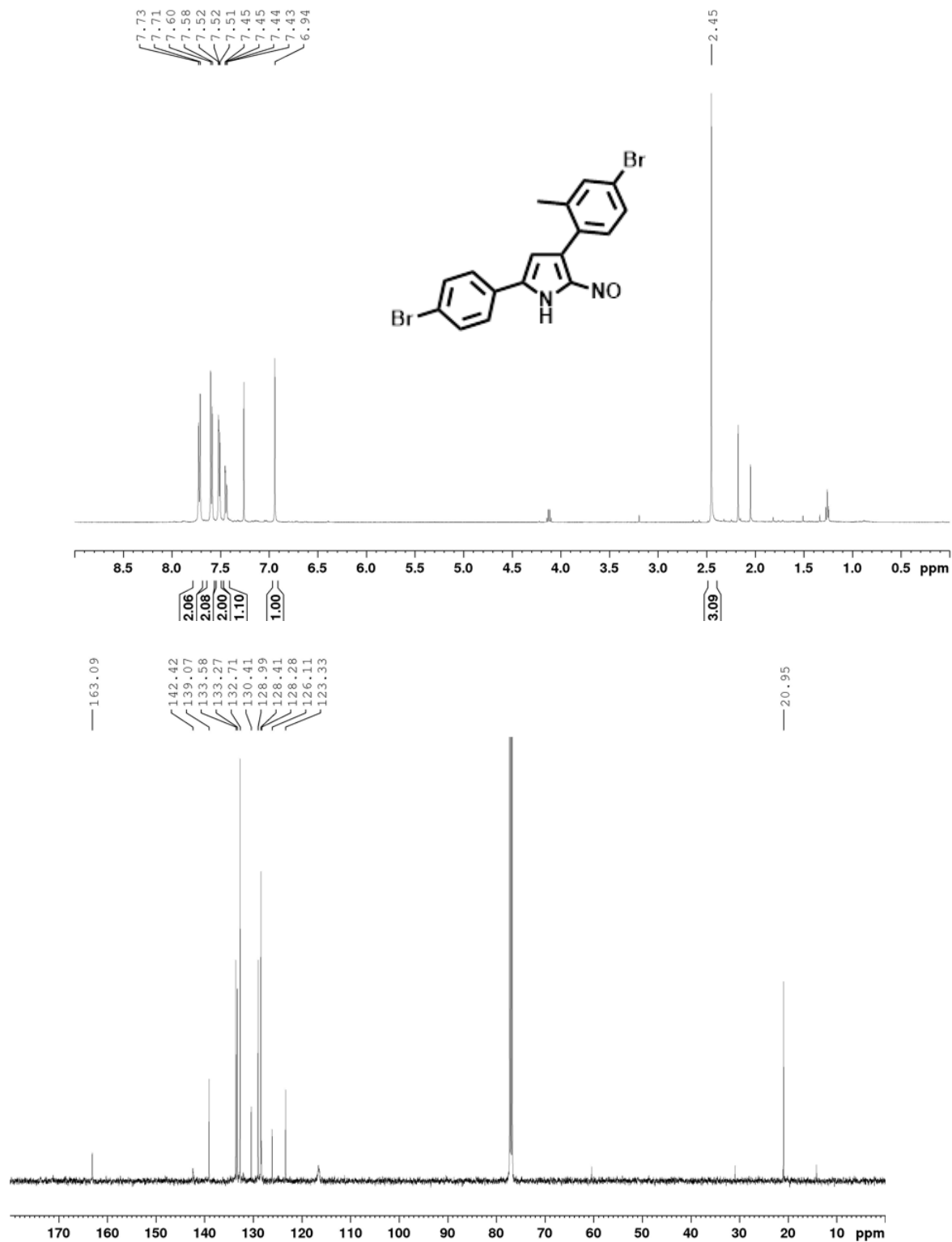
2-Nitroso-5-phenyl-3-(2,4,6-trimethylphenyl)-1H-pyrrole, (4.21a).



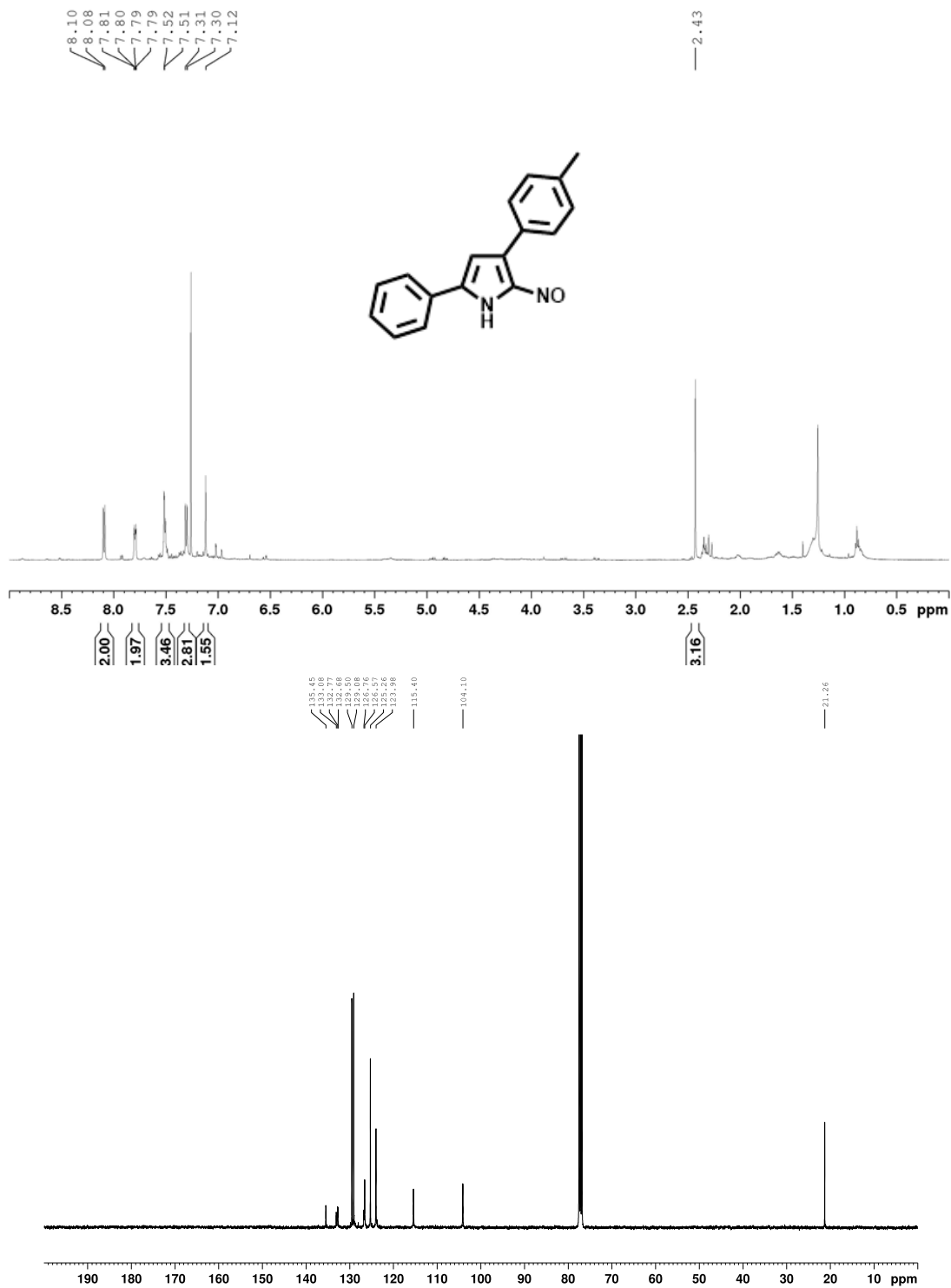
5-(2,5-Dimethylphenyl)-2-nitroso-3-(2,4,6-trimethylphenyl)-1H-pyrrole, (4.21b).



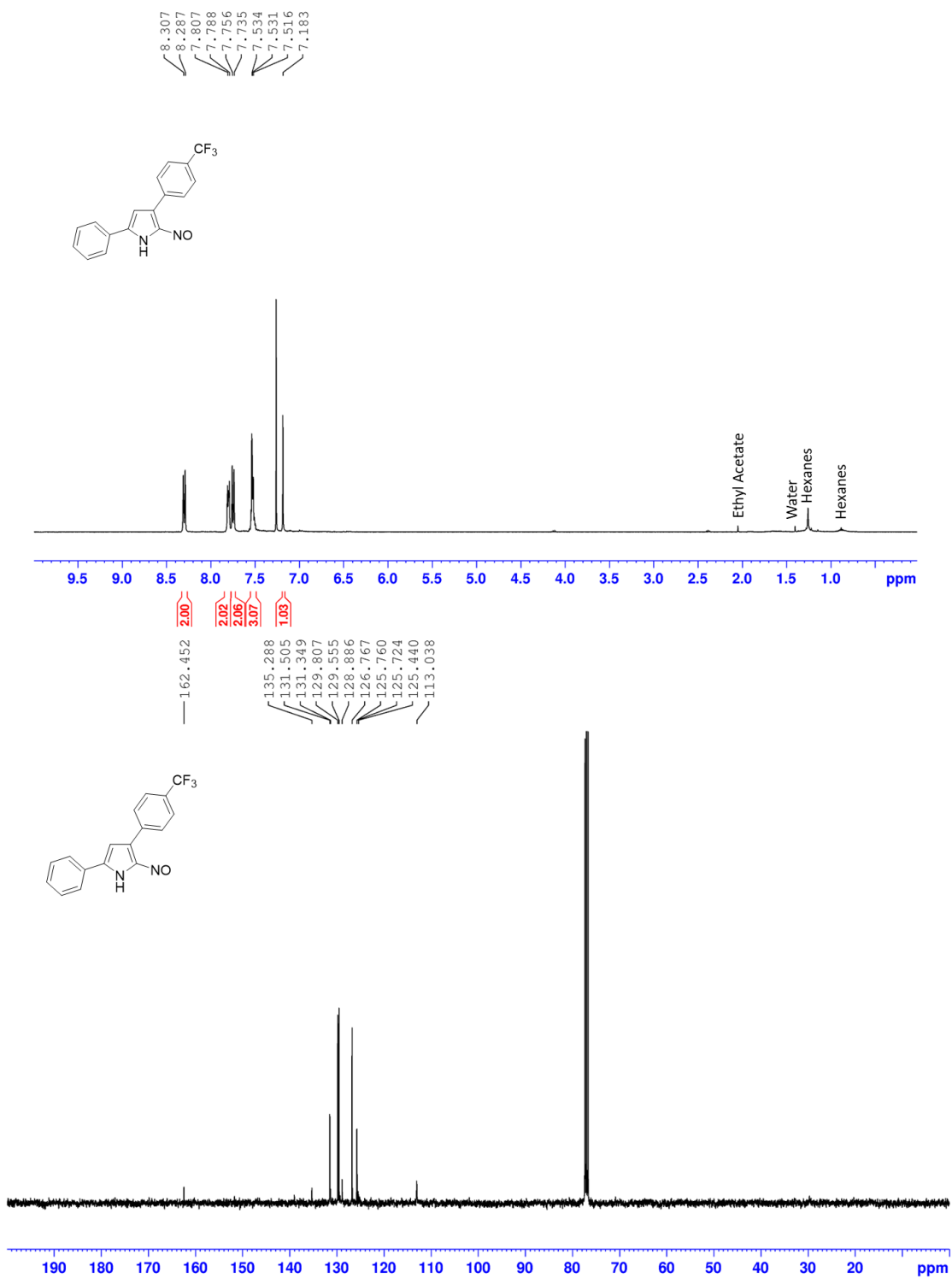
3-(4-Bromo-2-methylphenyl)-5-(4-bromophenyl)-2-nitroso-1H-pyrrole, (4.21d).



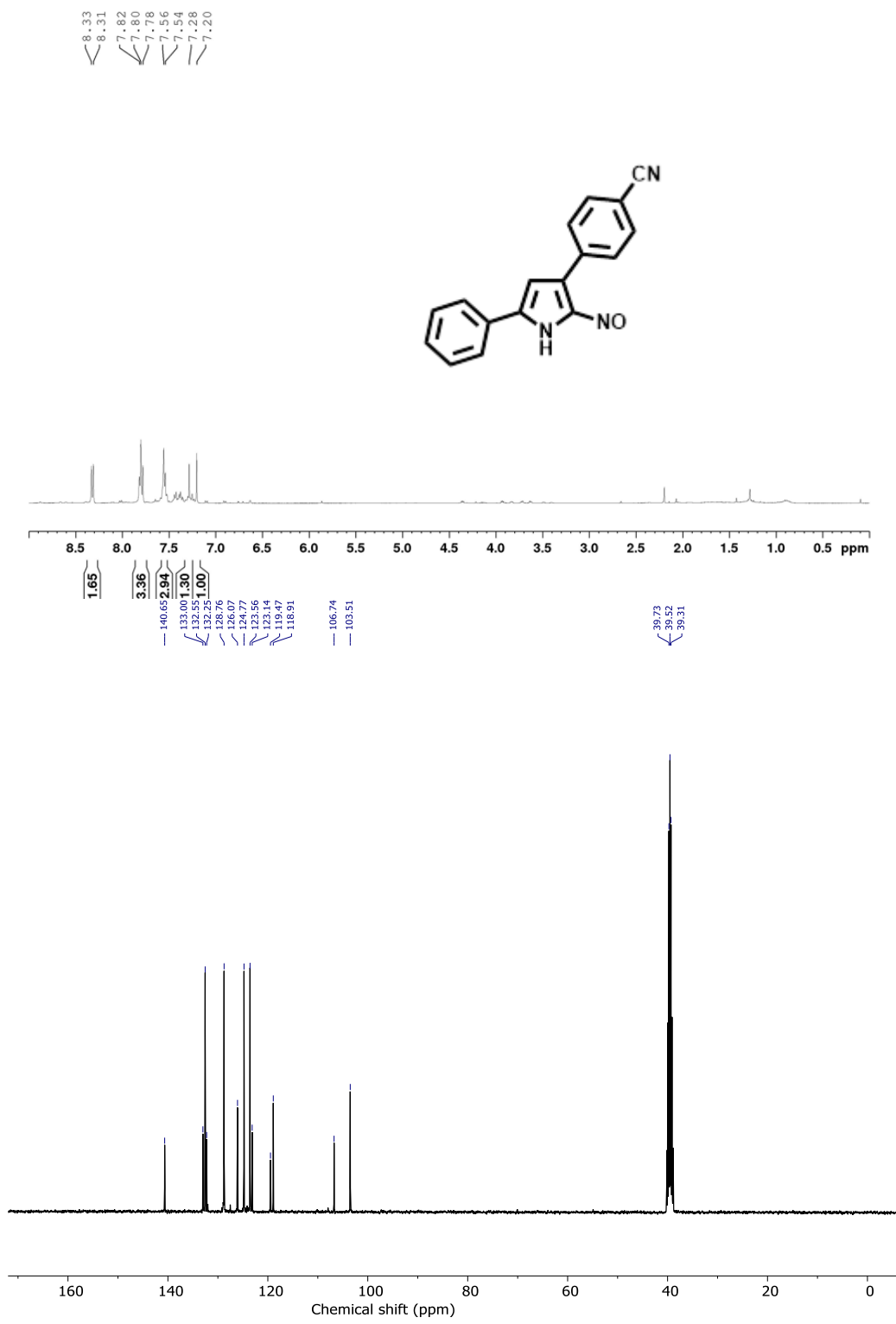
3-(4-Methylphenyl)-2-nitroso-5-phenyl-1H-pyrrole, (4.21e).



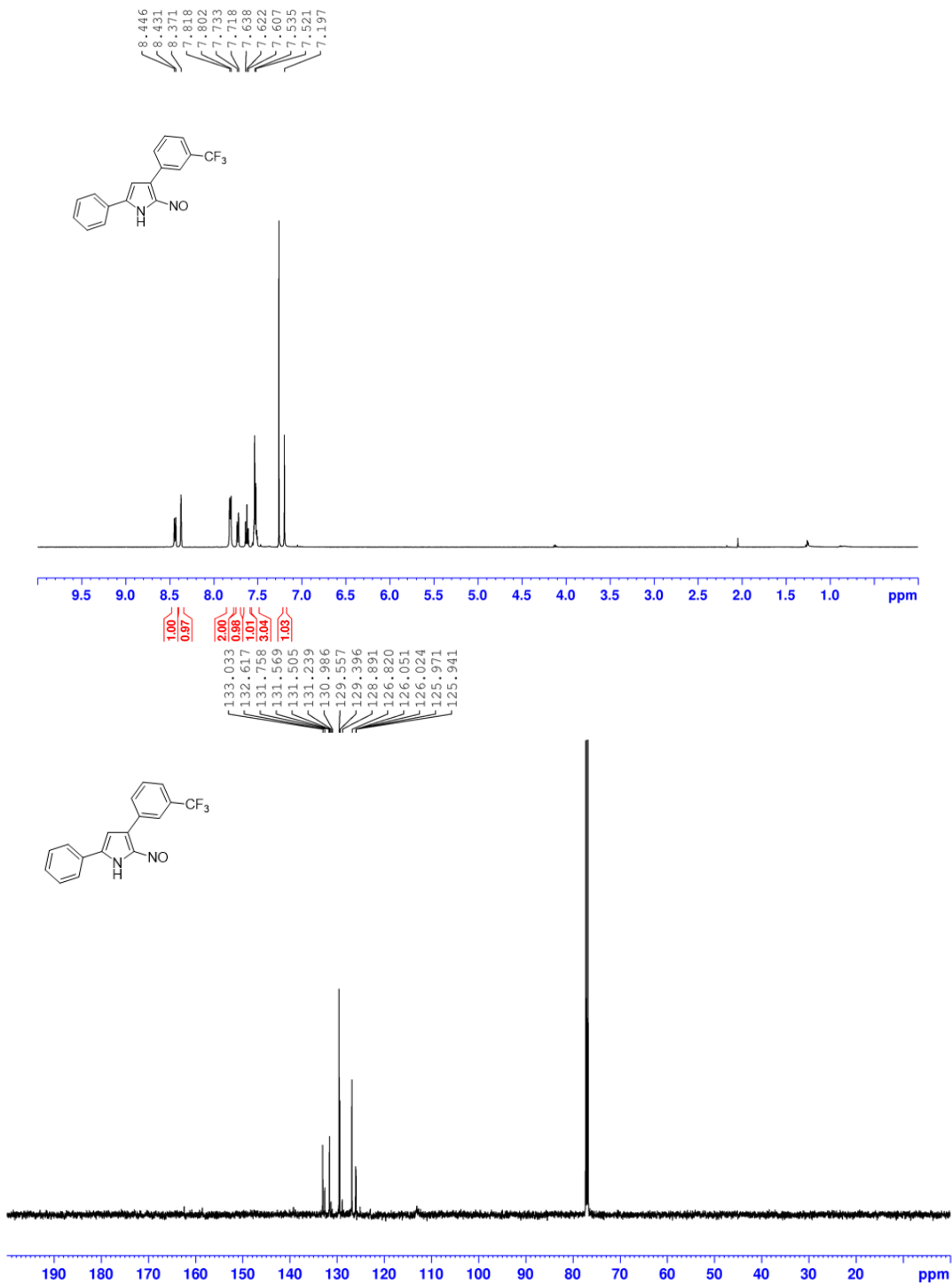
2-Nitroso-5-phenyl-3-[4-(trifluoromethyl)phenyl]-1H-pyrrole, (4.21f).



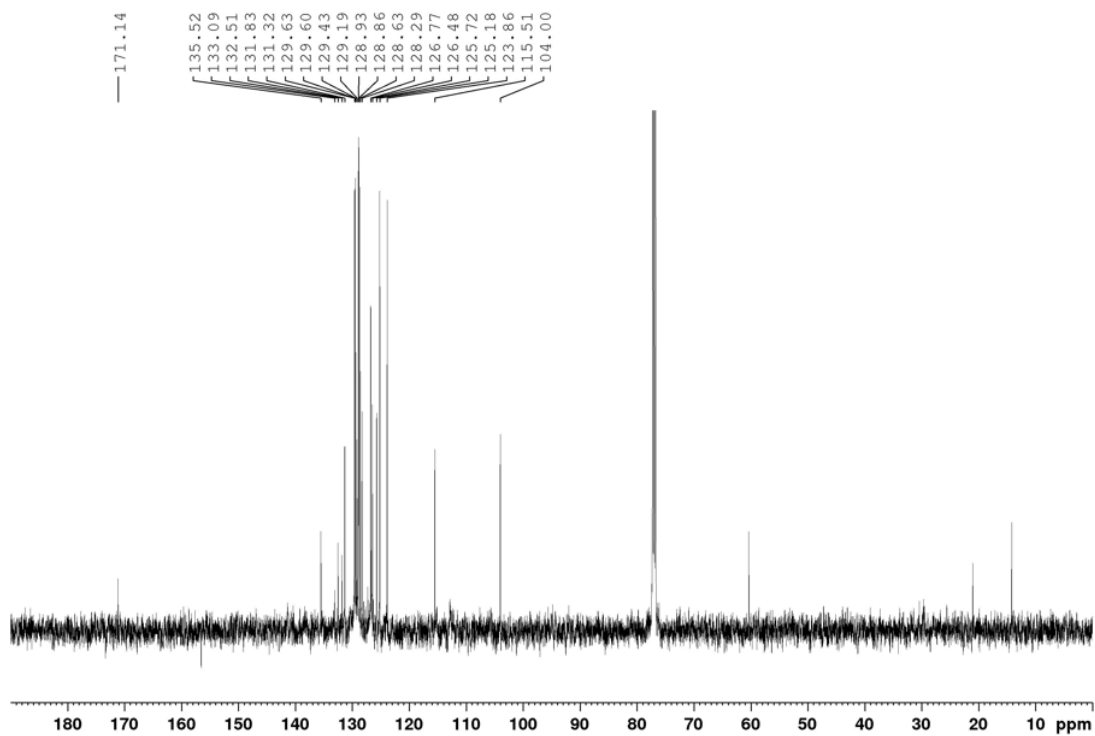
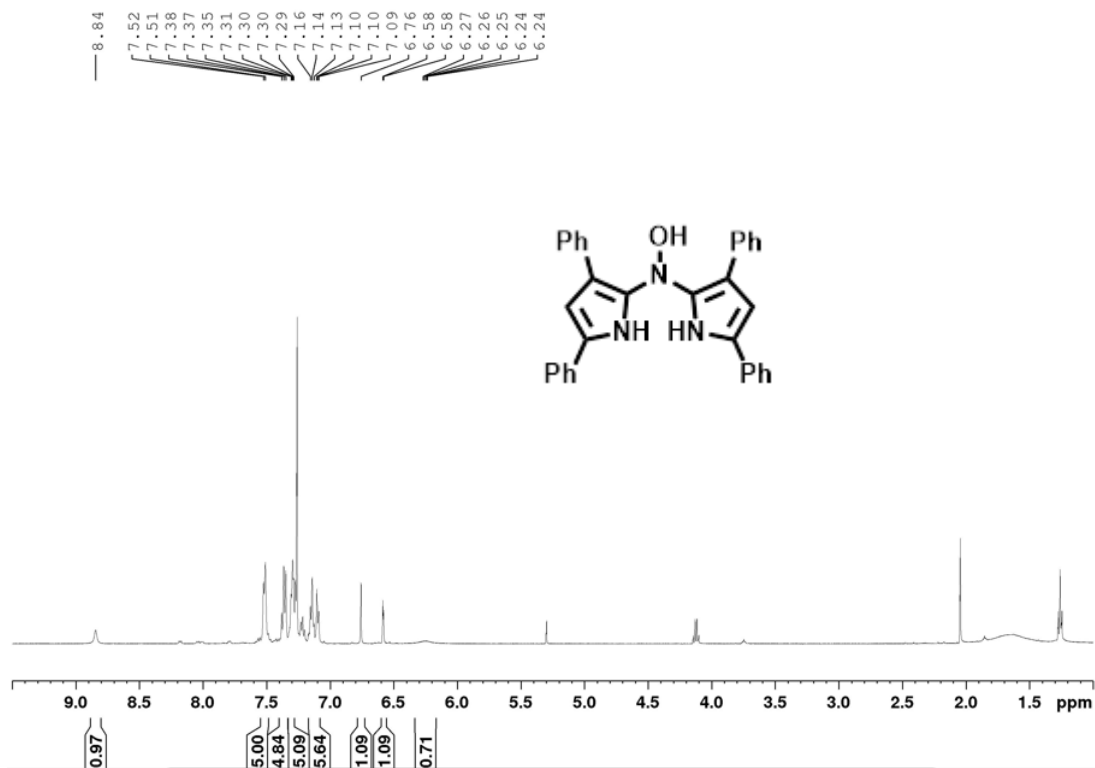
2-Nitroso 4-(4-Cyanophenyl)-2-phenyl-1H-pyrrole, (4.40g).



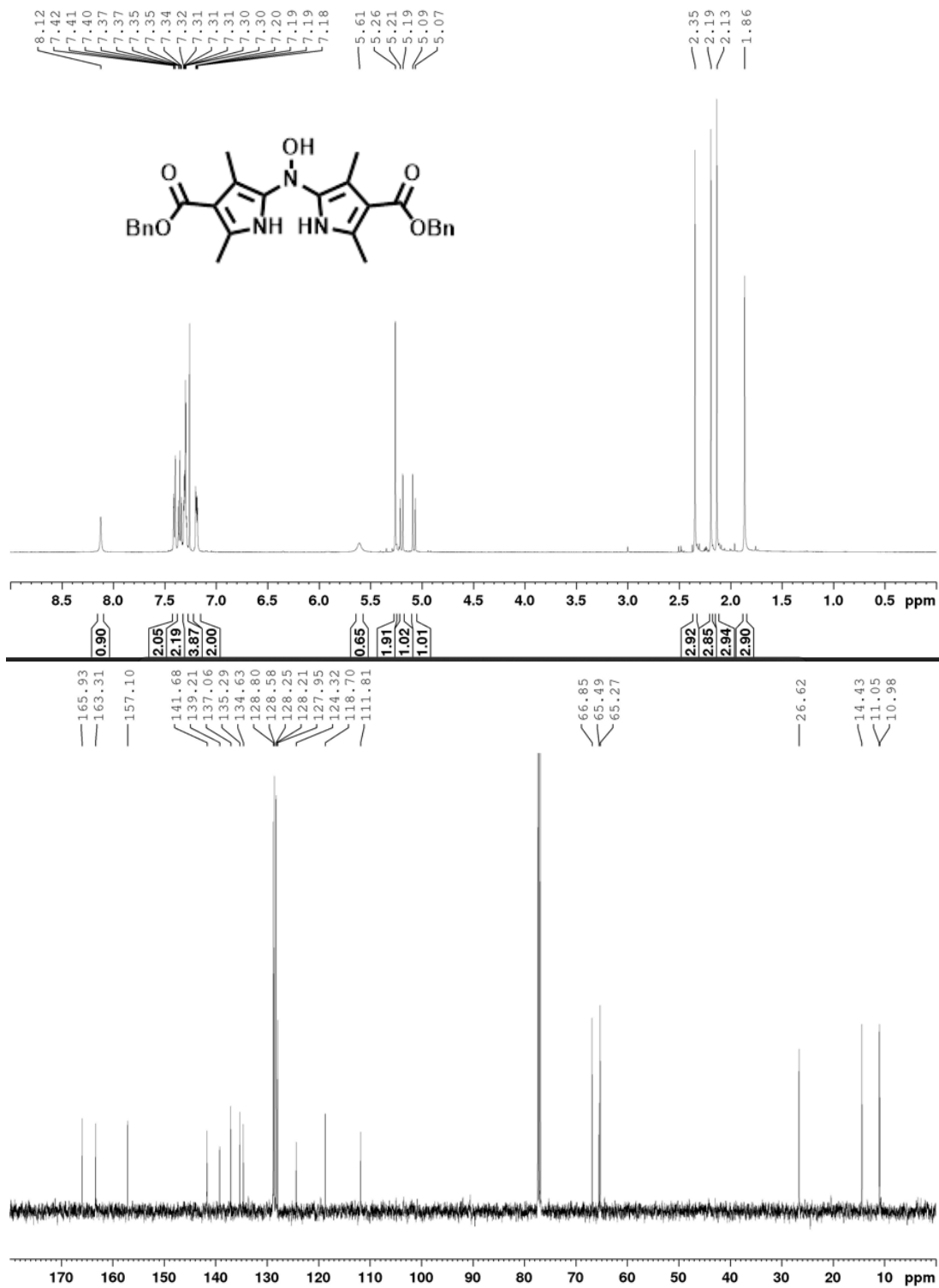
2-Nitroso-5-phenyl-3-[3-(trifluoromethyl)phenyl]-1H-pyrrole, (4.21h).



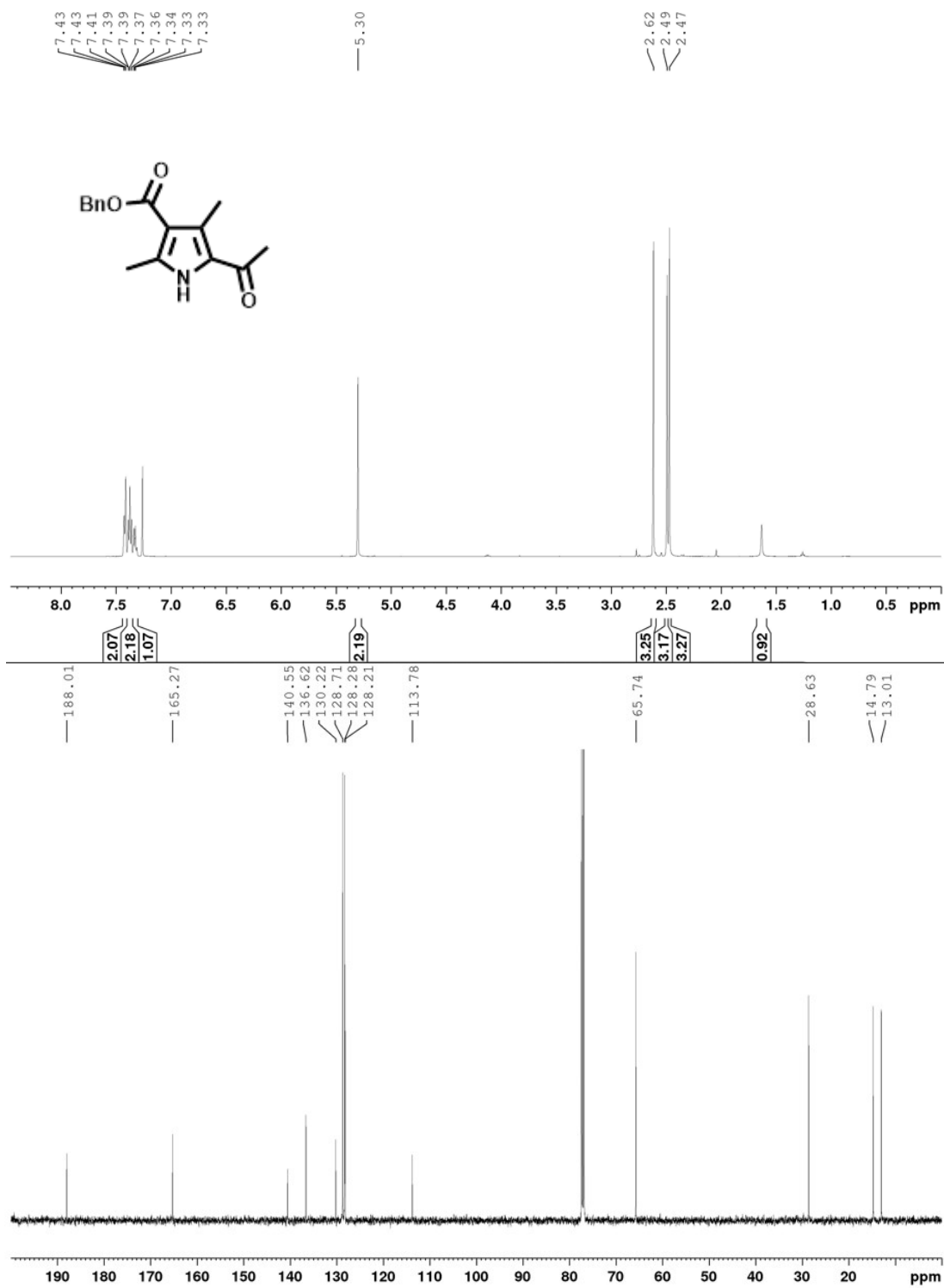
***N*-(3,5-diphenyl-1*H*-pyrrol-2-yl)-*N*-hydroxy-3,5-diphenyl-1*H*-pyrrol-2-amine, (4.41).**



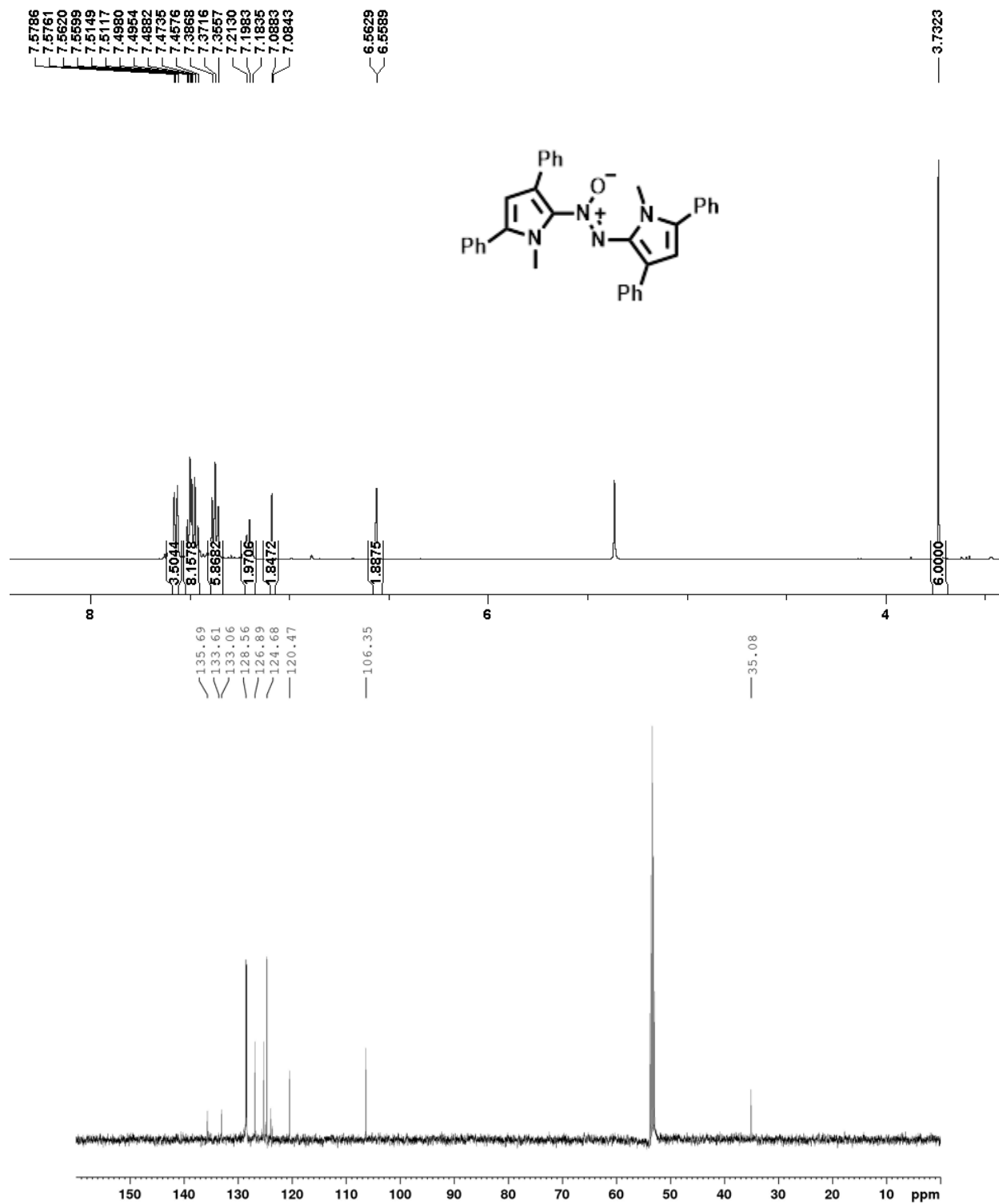
Dibenzyl 5-(hydroxyamino)-2,4-dimethyl-1*H*-pyrrole-3-carboxylate, (4.48).



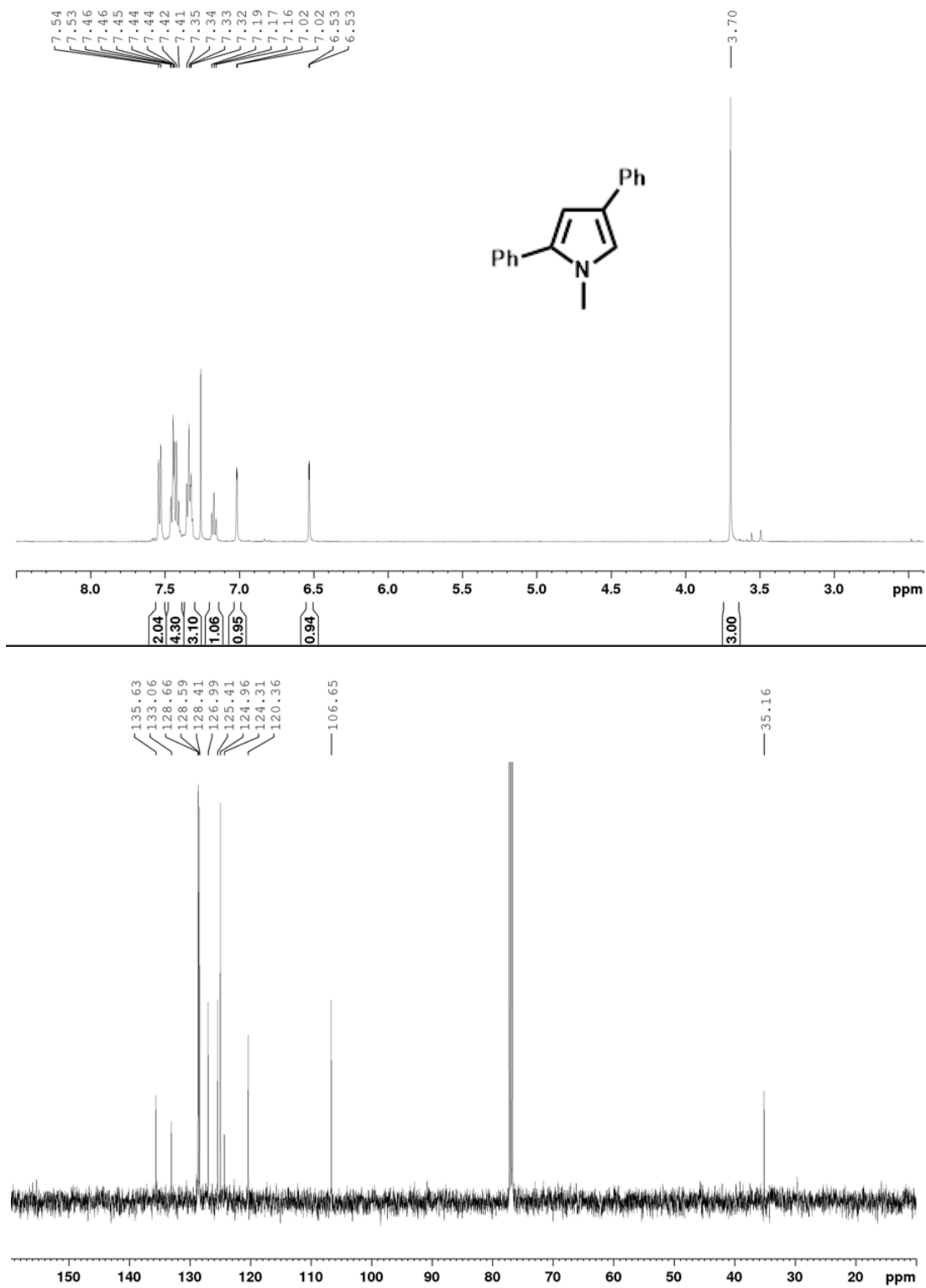
Benzyl 5-acetyl-2,4-dimethyl-1*H*-pyrrole-3-carboxylate, (4.49).



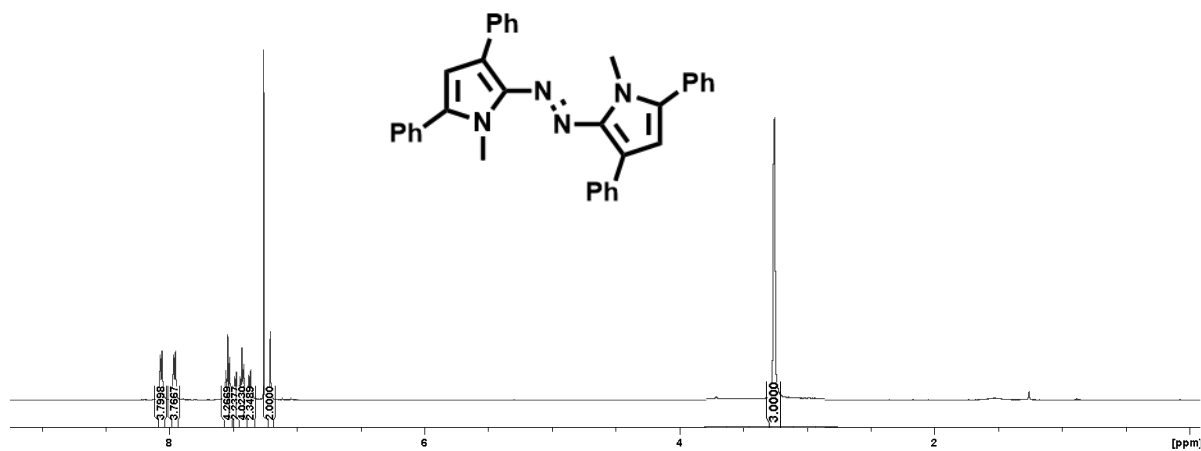
2,2'-diazenediyl-oxide-bis(3,5-diphenyl-1-methyl-pyrrole), (4.24).



1-methyl-2,4-diphenyl-1H-pyrrole, (4.20).



2,2'-diazenediyl]bis(3,5-diphenyl-1-methyl-pyrrole), (4.25).



1-methyl-2-phenyl-1,8-dihydropyrrolo[2,3-*b*]indole, (4.23).

